NATIONAL TECHNICAL UNIVERSITY OF ATHENS
SCHOOL OF NAVAL ARCHITECTURE AND MARINE ENGINEERING
DEPARTMENT OF MARINE ENGINEERING

Development of a Method for Dynamic Optimization of Integrated Energy Systems of Ships

George J. Tzortzis

Thesis submitted in partial fulfillment
of the requirements for the Ph.D. Degree

Thesis Supervisor
Prof. Em. Christos A. Frangopoulos

Athens, September 2018

ACKNOWLEDGMENTS

This work would not have been possible without the help of numerous people. Firstly, and most importantly, I wish to convey my sincere gratitude towards my advisor, Professor Ch. Fragopoulos, for having faith in my capabilities and granting me with the opportunity to conduct this interesting research. Throughout my study he has been a role model of a good researcher, whose, in–depth scientific knowledge, expertise and experience on the research fields of energy systems and optimization, combined with a logical way of approaching every problem, were of great benefit. His valuable guidance and scientific insight, as well as patience and moral support, played a decicive role in the completion of this work and are greatly appreciated.

I would also like to extend my gratitude to the members who took the time to serve on my Ph. D. studies advisory commitee, Professors N. Kyrtatos and K. Giannakoglou. Their helpful comments and advice over the course of this research were essential for the final outcome of this Thesis.

This work has been conducted as part of the project "Dynamic Optimization of Marine Energy Systems." The financial support provided by DNV-GL to the project is gratefully acknowledged.

Although the list of friends who have been there for me throughout the years is too long to write in detail, a special thanks goes to my friend, and fellow Ph.D. candidate, G. Sakalis with whom we shared the same office during our Ph. D. research. His suggestions and insights on many technical issues were always of great value and he has always been a good friend to turn to and a good diversion from work when needed.

I am deeply indebted to my family to whom I owe a great deal. My mother Maria, who has made an untold number of sacrifices for the entire family, for supporting and encouraging me to continue my pursuit of learning beyond my undergraduate degree and my sister Dimitra, for always being there when I needed her. For their unconditional love, encouragment and support over the years, I am eternally grateful.

Last but not least this dissertation is dedicated to my late father, Ioannis, who taught me to be strong and responsible but at the same time to make sure to enjoy anything I do in life. He has always been a source of inspiration for me. This is for you.

ABSTRACT

The subject of this thesis is the development of a method for the dynamic synthesis, design and operation (SDO) optimization of ship energy systems.

The common practice of synthesis, design and operation of energy systems, especially in the marine industry, is usually based on previous experience and rule-of-thumb criteria. Furthermore, the system is often designed at full load and steady state operation is assumed, while the off-design or dynamic behavior is considered only after the system is fixed.

The subject of this research activity is the determination of techno-economic optimal solutions for the SDO of marine energy systems, in order to fully cover the various energy demands for propulsion, electricity and thermal energy. Real–life dynamic elements such as time and space varying operational requirements with respect to weather conditions and time varying loads are incorporated to the performance models of the components and consequently to the performance of the integrated ship energy system, thus producing a purely dynamic optimization problem.

For the development of the appropriate methodology, special attention is given to the construction of a superconfiguration that depicts all the available synthesis options and the possible interconnections among components. A mixed integer modeling procedure that views the system as a whole is applied; integer, invariant and continuous variables are used for modeling the levels of synthesis, design and operation, respectively. The general problem is then stated using a Differential Algebraic Equation (DAE) formalism, while appropriate dynamic optimization procedures, combined with mixed integer nonlinear programming, are developed and applied. This leads to the formulation of a methodology which, in contrast to the majority of methods appearing in the literature, can be characterized as a single–level approach that treats the synthesis, design and operation levels simultaneously and requires no applicability conditions for decomposition, thus can be considered universal in the context that it can be applied to any dynamic SDO optimization problem.

Finally, the applicability and efficacy of the proposed method is demonstrated via the solution of several realistic case studies. Furthermore, the effect of certain technical and economic parameters on the optimal solution is studied via sensitivity analysis for each case study. The results provide interesting insights concerning the optimal SDO of marine energy systems and prove the suitability of the proposed modeling and optimization procedure for these types of problems.

TABLE OF CONTENTS

ABBREVIATIONS

AB	Auxiliary Boiler
BDF	Backward Differentiation Formula
BDNLSOL	Block Decomposition Nonlinear Solver
CAES	Compressed Air Energy Storage
CHP	Combined Heat and Power
COV	Calculus Of Variations
CVP	Control Vector Parameterization
DAE	Differential Algebraic Equation (Formalism)
DASOLV	Differential Algebraic Solver
DASSL	Differential Algebraic System SoLver
DE	Diesel Engine
DG	Diesel Generator
DILGO	Dynamic Iterative Local Global Optimization
DOP	Dynamic Optimization Problem
DP	Dynamic Programming
FWT	Feed Water Tank
GA	Genetic Algorithm
GT	Gas Turbine
HRSG	Heat Recovery Steam Generator
HULD	Hydro Unit Load Dispatch
IFA	Intelligent Functional Approach
ILGO	Iterative Local Global Optimization
IP	Integer Programming
LGO	Local Global Optimization
LHV	Lower Heating Value
LNG	Liquefied Natural Gas
MCR	Maximum Continuous Rating
MI	Mixed Integer
MIDO	Mixed Integer Dynamic Optimization
MINLP	Mixed Integer Non Linear Programming
MOO	Multi–Objective Optimization
NLP	Non Linear Programming
NLPSQP	Non Linear Problem Sequential Quadratic Programming
NPSOL	Nonlinear Programming Solver
NPV	Net Present Value
O&M	Operation and Maintenance
OAERAP	Outer Approximation Equality Relaxation Augmented Penalty (solver)
ORS	Optimum Response Surface
PEMFC	Proton Exchange Membrane Fuel Cell
PWC	Present Worth Cost
PWF	Present Worth Factor
SDO	Synthesis, Design and Operation
SFOC	Specific Fuel Oil Consumption
SNOPT	Sparce Nonlinear Optimizer
SOO	Single Objective Optimization
SQP	Sequential Quadratic Programming
ST	Steam Turbine
STG	Steam Turbine Generator

TFA	Thermoeconomic Functional Approach
TPBVP	Two-Point Boundary Value Problem
TSR	Traveling Salesman Problem
VRP	Vehicle Routing Problem

CHAPTER 1: INTRODUCTION

1.1 Scope of the Thesis

The objective of this thesis was the development of a method for the dynamic synthesis, design and operation (SDO) optimization of ship energy systems, under the assumption of a fixed route of the ship, while time varying operational requirements with respect to weather conditions and loads are also considered. The aforementioned three levels of optimization are defined as follows [Frangopoulos (1991a, b), Frangopoulos (1992), Frangopoulos et al (2002)]:

1. **Synthesis**: The term "synthesis" implies the components that appear in a system and their interconnections.
2. **Design**: By the word "design", the technical characteristics (specifications) of the components and the properties of the substances entering and exiting each component at the nominal load of the system are implied here. The nominal load is usually called the "design point" of the system.
3. **Operation**: With the term "operation", the operating properties of components and substances (speed, power output, mass flow rates, pressures, temperatures, composition of fluids, etc.) under specified conditions are implied.

One may argue that design includes synthesis too. However in order to distinguish the various levels of optimization and due to the lack of a better term, the word "design" will be used with the particular meaning given here. For a system, once the synthesis is specified, then, optimization is possible at the design and operation levels. If both synthesis and design characteristics are defined, the optimization is carried out at the operation level. The fact that, for marine energy systems, numerous alternatives exist in terms of synthesis and design options, as well as operational strategies, makes the SDO problem a rather complex one.

In order to cover the overall energy demands of a vessel, energy systems onboard ships are required to produce energy of several forms (e.g. mechanical, electric, thermal), while at the same time being completely autonomous and cost effective. Therefore, while searching for the optimal overall energy system for a vessel, the designer must take into account several factors such as: the need for energy efficiency in order to minimize operational costs, various safety requirements as well as legislation requirements considering emissions and operational flexibility, in order to be able to cope with the varying requirements of the mission.

Furthermore, once the time dependency of certain parameters (e.g. time varying energy demands and weather conditions along the trip) is taken into consideration and modeled accordingly in the already complex SDO problem, further complications are introduced.

Time–dependent optimization problems of energy systems can be classified as follows:

1. *Intertemporal static optimization problem*, where the time horizon of the system's operation can be divided into distinct periods of steady state operation (intervals) with conditions that differ from period to period. The periods are independent from each other and the problem can be treated as a series of static optimization problems. This

type of problem is also characterized as quasi–static or quasi–stationary in the literature [Rancruel and Spakovsky (2003), Munoz and Spakovsky (2003)].

2. *Dynamic optimization problem*, where each operating point in time affects all other operating points in time. These problems are treated with *dynamic optimization methods*. Two distinct types of problems may exist:
    a) *Intertemporal dynamic problem* where the time horizon of the system's operation can be divided into distinct periods of steady state operation (intervals) with conditions that differ from period to period. The operating point in a certain period affects and is affected by the operating points of other periods. Thus, interdependency among periods exists; the problem is then inherently dynamic.
    b) *Optimization of transients problem*, where one or more components of the system are described by transient behavior, i.e. changing from one operating point to another operating point, which is under optimization. This is characterized as a *trajectory/optimal control problem* in the dynamic optimization literature [Wozny and Li (2000), Bausa and Tsatsaronis (2001a,b), Ko et al. (2008), Saerens et al. (2008)].

Regarding the term *intertemporal*, it is used here with the following meaning: Intertemporal optimization is an optimization that takes into consideration the various operating conditions that a system encounters throughout its *life-time*, and determines the operating point at each instant of time that results in the overall optimal value of the general objective function.

Considering the case (2b), a simple example of such a problem in the area of marine engineering, could be the operation optimization of a marine diesel engine as it adapts from a certain speed of the vessel to an increase or a decrease of that speed. It is noted that, the transient operation/behavior of one or more components of the system may be included in an intertemporal static or an intertemporal dynamic problem. However, in the first case, the transient performance of a component is only simulated within each period of operation and not optimized. In the second case it can be either simulated or even optimized.

This study concerns problems of type (2a) only, where the true dynamic nature of the system is taken into account. The transients have not been considered, because they last for very small periods compared with the whole operating time of the system.

Under all the above considerations, the general (intertemporal) dynamic SDO problem can be summarized in the following question:

"What are the optimal synthesis, design characteristics and operational profiles of a system that covers all the varying energy needs of a ship (propulsion, electric, thermal) under known weather conditions along a specified route?"

In order to efficiently tackle this question, the designer must employ mathematical optimization techniques to determine the optimal system in a coherent, flexible and mathematically precise manner. Conditions changing with time affect not only the optimal operation, but also the optimal synthesis and design of the system. Thus, a dynamic – mixed integer nonlinear programming problem (MINLP) is formulated, which is solved by dynamic optimization methods.

In the past decades, static optimization methods have been successfully used for the design of land based as well as marine energy systems, although not to the same extent.

However, as will be discussed in the next section, few cases of application of dynamic SDO optimization can be found in the literature considering land based energy systems and almost none in marine energy systems. This fact has served as a main motivation for the present work.

1.2 Literature Review

1.2.1 Fundamental literature on dynamic optimization

Dynamic optimization methods have become a well-known research subject since the late 1950's with the studies of Pontryagin and Gelfand in o*ptimal control theory* [Pontryagin et al. (1962), Gelfand and Fomin (1963)] and Bellman on *dynamic programming* [Bellman (1957)] and nowadays constitute a very active field of research with many branches.

Early applications of the dynamic optimization methods had to do with locating the optimal rocket thrust profiles in atmosphere and in vacuum [Bryson and Ho (1969), Philips (1988), Philips and Drake (2000)] or to solve combinatorial or multi-stage decision optimization problems, where the goal is to find the optimal sequence of decisions so as to optimize a process based on a measure of performance, such as the Travelling Salesman Problem (TSP) [Lawler et al. (1985), Gutin and Punnen (2006)] and the Vehicle Routing Problem (VRP) [Psaraftis (1988), Toth and Vigo (2001)].

A thorough and complete presentation of dynamic optimization theory and available solution approaches is given in Chapter 2 of this thesis.

1.2.2 Setting the limits of the literature review

The literature on dynamic optimization is vast and extends to several scientific fields, thus only problems concerning energy systems are included in this literature review. Problems regarding optimal ship routing, fleet scheduling or optimal ship refueling (e.g. Norstad et al. (2011), Zhen et al. (2017)) will not be included.

Also, optimization of transients problems are not included. Examples of optimization of transients in energy systems can be found in Vassiliadis et al. (1994a, b), Bausa and Tsatsaronis (2001a, b), Rodriguez and Diaz (2006a, b), Kikkinides et al. (2006), Saerens et al. (2008).

Since in this study we are interested in SDO problems, in the next sections static SDO optimization problems for energy systems for design point only, intertemporal static SDO optimization problems for energy systems and intertemporal dynamic SDO optimization problems for energy systems are referenced. Specifically for the last category, apart from intertemporal dynamic complete SDO optimization problems, also intertemporal dynamic operation optimization and intertemporal dynamic design and operation optimization problems on energy systems are included. In Table 1.1 all the referenced papers, along with their main characteristics, are listed.

For a better understanding of the terminology used in the literature review a note on the approaches on the solution of the SDO optimization problem is first given.

1.2.3 A note on approaches to the solution of the SDO problem

A SDO optimization problem can, in general, be intractable, highly complex and highly dimensional subjected to time dependent operating conditions. In the past years, several methods\techniques have been applied in order to reformulate this initial complex problem into a tractable one. The main idea is to break up (decompose) the original –hard to solve– SDO optimization problem into a set of smaller problems, the solution of which coincides with or closely approaches the solution of the former. In general, three solution approaches of this kind can be found in the literature [for a review see Frangopoulos et al. (2002)].

The first solution approach involves the mathematical formulation of the problem in several levels based on the conceptual aspects of the optimization problem, i.e. synthesis, design, and operation. Thus, a three–level (synthesis – design – operation) [Frangopoulos (1990), Frangopoulos (1991a, b)] or a bi–level (synthesis\design – operation) [Frangopoulos (1992), Georgopoulos et al. (2002), Dimopoulos et al. (2008)] optimization problem is formulated. For each level, a set of variables (which is a sub-set of the total set of variables) is declared and an objective function (which is a part of the total objective function) is formed. Then, an appropriate three–level or bi–level algorithm is applied, which optimizes each level separately, while at the same time keeping them interrelated by setting up an iterative procedure among the several levels of optimization until the global optimum for the total objective function is found.

Another common solution approach takes advantage of the structure of the system by separating it into a set of interconnected units (subsystems, components) while at the same time considering the system as a whole [Frangopoulos (1991a, b), Frangopoulos (1992), Munoz and von Spakovsky (2001a, b), Georgopoulos et al. (2002), Munoz and von Spakovsky (2003), Oyarzabal et al. (2004)]. As in the case of the first solution approach, for each unit and for the system level a subset of the total set of variables and an appropriate objective function are declared. Then the respective sub-problem of each unit is optimized, for its respective set of variables, while the overall problem at the system level is optimized for the system level set of variables.

The final solution approach tackles the time dependent nature of the problem by dividing the time horizon of the operational optimization problem of the system into distinct periods (intervals) of steady state operation. In this way, a series of sub-problems (quasi–stationary sub-problems) is defined and an intertemporal static SDO optimization problem is formed. Then, these –independent of each other– periods of operation are optimized individually with respect to a set of operation variables and the results are summed over all intervals. [Frangopoulos (1992), Munoz and von Spakovsky (2001a, b), Rancruel and Spakovsky (2003), Dimopoulos and Frangopoulos (2008)].

It should be clarified that the aforementioned solution approaches are not always applicable to every SDO optimization problem; depending on the problem, decomposition conditions must be fulfilled in order to apply them correctly. Furthermore, it is noted that there may be cases where more than one of these techniques can be applied simultaneously in a single SDO optimization problem. In fact, in the rest of this literature review several studies where this is the case, are presented.

1.2.4 Static SDO optimization of energy systems considering design point only

Synthesis, design and operation (SDO) optimization of energy systems has grown into a research area of great interest in the past 20–30 years. The common practice of synthesis

and design of energy systems, especially in the marine industry, is usually based on previous experience and rule-of-thumb criteria of the designer and the system is often developed at full load steady state operation, while its off-design behavior is considered only after the system is fixed. However, the continuous attempt for better fuel utilization and reduction of the adverse effects on the environment leads to more and more complex and integrated systems. Past experience alone is not sufficient for the optimal design and operation of these systems, while the availability of a multitude of alternative configurations makes it rather impossible to study all of those one by one and select the best one. Thus, the formal application of mathematical optimization techniques becomes necessary.

Several methodologies have been developed [Frangopoulos et al. (2002)] and many studies of SDO optimization can be found in the literature in different scientific areas. In Pelster et al. (2001) a thermo-economic environomic methodology that facilitates synthesis and design optimization is presented and applied to a 50 MW cogeneration combined cycle power plant. A single–level approach that applies a Struggle Genetic Algorithm (Str-GA) is used for the solution of the problem. Another study in which the synthesis and design levels of optimization are treated via a single–level algorithm can be found in Mussati et al. (2004), where the synthesis and design optimization of a dual purpose desalination plant is examined. A superconfiguration[1] is used in order to model all available synthesis options and a MINLP model is developed. Another example where a superconfiguration is used can be found in Sun et al. (2017). In this study, a site utility system is optimized for cost minimization and again the SDO aspects of the system are tackled in a single level. Also time and probability based uncertainties are considered. In Calise et al. (2007) the optimal synthesis and design of a hybrid solid oxide fuel cell – gas turbine power plant is investigated. For the operation level full load is considered and again a single–level approach for the synthesis – design levels is adopted, while a genetic algorithm is used for the solution of the optimization problem.

However, not all studies utilize a single–level approach. In Tofollo (2014) the optimal synthesis and design of a set of Rankine cycles forming an energy system that absorbs/releases heat at different temperature levels and converts part of the absorbed heat into electricity is examined. For the solution of the problem a bi–level hybrid evolutionary/Sequential Quadratic Programming (SQP) algorithm is applied. The upper level is constituted of the synthesis of the system and is optimized via an evolutionary algorithm, while the lower level tackles the system design characteristics and is optimized via a traditional SQP algorithm.

A common characteristic of all these works is that only a single mode is considered for the operation of the system. Thus, optimization at the operational level is meaningless and only the synthesis and design levels are optimized. Also, since only one mode of operation is considered, the time dependency of the operation cannot modeled. In the next section several studies which have taken further steps for modeling multiple modes of operation and taking into account the time dependencies of varying loads or other time varying parameters are presented.

1.2.5 Intertemporal static SDO optimization of energy systems

The earliest publications that address in a concise mathematical manner the complete SDO optimization problem for energy systems with time dependencies can be found in

[1] The word ‘superstructure’ is usually used for land installations, but it is avoided here, because it has a different meaning on ships.

Frangopoulos, (1991a), (1991b), and (1992). In these studies the optimal SDO of a cogeneration system supplying a process plant with heat and electricity is investigated. All three solution approaches that were discussed in Section 1.2.3 are applied simultaneously.

Specifically, in Frangopoulos (1991a) the time horizon of the problem is divided into independent periods of steady state operation, while a method called Intelligent Functional Approach (IFA) is used to analyze the system as a set of interrelated units. Furthermore, for the solution of the problem a three–level algorithm is applied. At the lower level (operation), the system is optimized with respect to a set of operation variables in order to determine optimal system behavior for all time intervals. The results are then integrated over time and introduced in the intermediate (design) level, where for a fixed synthesis the system is again optimized with respect to a set of design variables. Finally, the results of this optimization are passed to the upper (synthesis) level, where a new choice of system configuration (synthesis) is made based on minimizing (or maximizing) the system's objective function with respect to a set of synthesis variables. An iterative procedure is then set up among the three levels of optimization until the global optimum for the objective function is found. The same methods are applied in Frangopoulos (1991b) with one exception; the internal economy of the system allows for the three–level procedure described previously to be simplified by combining the levels of synthesis and design into a single one.

In Frangopoulos (1992) also independent periods of steady state operation are considered and the Thermoeconomic Functional Approach (TFA) is applied in order to divide the system into a set of interrelated units. Again, a bi–level algorithm is preferred; the optimal operation is determined at the lower level while the synthesis and design are tackled simultaneously at the upper level.

Other works where all three aforementioned approaches have been used include those in which the Local Global Optimization (LGO) and Iterative Local Global Optimization (ILGO) algorithms are implemented. In LGO the system is separated into a set of units and for each unit and for the system level a subset of the total set of synthesis/design variables is declared. Then the respective sub-problem of each unit is optimized, for its respective set of variables, while the overall problem at the system level is optimized for the system level set of variables. This results in a nested set of optimizations of unit level problems within an overall system level problem. The process is repeated many times for different values of the coupling functions resulting in a set of unit level optimum response surfaces (ORSs), the combination of which results in the system level ORS. The system level optimum is then found at the lowest point (if a minimization) on this surface. Based on LGO, the ILGO algorithm uses derivative information in the form of shadow prices (derivatives of the optimal value of a function with respect to certain variables) to intelligently move along the system level ORS towards the system level optimum.

In Munoz and Spakovsky (2001a) the theory behind LGO and ILGO is discussed. In Munoz and Spakovsky (2001b) SDO optimization of a turbofan engine coupled to an environmental control system for a military aircraft is performed. For the operation of certain units of the system time is divided into independent periods of operation. The ILGO algorithm is applied. In Rancruel and Spakovsky (2003) also SDO optimization of aircraft energy systems is performed. The ILGO optimization approach combined with a bi–level optimization algorithm is implemented. Another study where the ILGO method is applied can be found in Georgopoulos et al. (2002), where SDO optimization of a stationary cogeneration proton exchange membrane fuel cell (PEMFC) based total energy system (TES) for residential/commercial applications is performed.

In Oyarzabal et al. (2004) the optimal SDO of a PEM fuel cell cogeneration system is investigated. The LGO algorithm is utilized. Also in Munoz and Spakovsky (2003) the trip

of a military aircraft that includes many phases (take-off, flight and landing) is studied under the scope of optimizing the SDO of its energy system. Transient operation of several system components is considered. Both LGO and ILGO algorithms are used for the solution of the problem.

However, not all studies involve the decomposition of the system in units via a special technique such as IFA or LGO. In Olsommer et al. (1999) the optimal SDO of a waste incineration system with cogeneration and a gas turbine topping cycle is under investigation for minimization of the total net present cost of the system over its entire economic lifetime. The time horizon is divided into independent periods of steady state operation and a bi–level (synthesis/design and operation) solution procedure is applied via a Struggle Genetic Algorithm.

Also, studies that tackle only the design and operation levels can be found. In Zheng et al. (2017) the coordinated expansion planning of the integrated natural gas and electric power systems is examined. Periods of steady state operation are assumed and a bi–level optimization procedure is formulated in order to minimize investment and operational costs. A hybrid solution approach, combining a heuristic optimization method, for the upper level of synthesis, and an analytical optimization method for the lower level of operation, is proposed.

Considering the domain of marine energy systems, noteworthy are the studies of Dimopoulos et al. and Dimopoulos and Frangopoulos. In Dimopoulos et al. (2008) the overall energy system of a cruise liner vessel, with various technological alternatives for the synthesis, is considered and optimized for cost minimization. Also, time varying operational requirements are considered. The time horizon of the ships' mission is divided into periods of steady state operation and two levels of optimization are formulated: a synthesis–design outer level and an operation inner level. In Dimopoulos and Fragopoulos, (2008) a Liquefied Natural Gas (LNG) vessel is considered and a detailed thermoeconomic model of the energy system components and the production of boil-off gas from the LNG cargo, which is used as the main fuel of the system, is developed. The same method as in Dimopoulos et al. (2008) is applied for the synthesis, design and operation optimization under the scope of maximizing the Net Present Value (NPV) of the investment.

Another study that tackles the SDO optimization of a marine energy system, specifically an organic Rankine cycle system, is performed in Kalikatzarakis and Frangopoulos (2017). The maximization of the Net Present Value (NPV) of the system is considered as the objective function. The time horizon of a year of operation is divided into periods of steady state operation and the problem is tackled by a hybrid numerical scheme that combines a Genetic Algorithm (GA) and the SQP algorithm.

A main characteristic of all the studies in the current sub-section, where the time dependencies are taken into account, is the hypothesis that the total period of operation of the energy system can be –and is– divided into a series of time intervals of steady state operation, independent of each other. However, this hypothesis is not always applicable in every SDO problem. In this case, a truly dynamic problem is formulated. In the next section several examples of intertemporal dynamic SDO optimization problems are presented.

1.2.6 Intertemporal dynamic SDO optimization of energy systems

A very fitting example of intertemporal dynamic operation optimization of an energy system can be found in Vallianou and Frangopoulos (2012). A trigeneration system, consisting of a gas engine with heat recovery, an absorption chiller, compression chillers

and two thermal storage tanks, is considered that serves the electric, thermal and cooling loads of a building complex. The operation optimization under load varying conditions is performed under the scope of minimizing costs. Also, the transient operation of certain system components is modeled and included in the problem.

In Cheng et al. (2009) the dynamic operation optimization of a large scale hydropower station is performed. Specifically the Hydro Unit Load Dispatch (HULD) problem is solved, which essentially is a question of optimal water allocation in a number of turbine generator sets, so as to maximize the plant efficiency for a time dependent load curve. The problem is solved first via dynamic programming, and then it is formulated so as to be solved by an evolutionary static optimization method, and the results are compared. Dynamic programming is also used in Marano et al. (2012), in order to solve the dynamic operation optimization of a hybrid power plant consisting of compressed air energy storage (CAES) coupled with a wind farm and a photovoltaic plant.

Considering marine energy systems, two very interesting studies of dynamic operation optimization can be found in Wang et al. (2018), Zaccone et al. (2018). Specifically, in Wang et al. a novel dynamic optimization method is proposed in order to optimize ship energy efficiency, accounting for time-varying environmental factors such as wind speed and direction and water speed and depth. The ship speeds at different time steps are set as the optimization variables and an appropriate index that models ship efficiency is set as the objective function. However, the ship energy system is considered to comprise only the propulsion engines. In the work of Zaccone et al., a 3D dynamic programming method is formulated in order to find the optimal path and speed profile for a ship voyage so as to to minimize fuel consumption. Although this example involves also weather routing, which is of no interest in this study, the ship speed optimization part is very interesting.

Moving on from only operation optimization, several studies of dynamic optimization where both the design and operation levels are considered can be found in the literature. In Mohideen et al. (1996) dynamic models and a mixed integer mathematical formulation are used to model and optimize a ternary distillation process via a suitable algorithm. The problem is solved via a single level formulation.

In Ondeck et al. (2017) the design and operating strategy of residential CHP systems is optimized in order to meet time varying energy demands. The problem is solved using a temporal Lagrangean decomposition method that was applicable due to the special scheduling nature of the problem.

Of course dynamic design and operation optimization studies where the problems are tackled in two–levels (design – operation) also exist. In Martelli et al. (2015) the optimal design and operation of combined heat and power Organic Rankine cycles is examined in order to maximize the annual profit. In Evins (2015) a multi–objective dynamic design and operation problem is solved for a building energy system. The upper (design) level contains variables for both the design of the building and the energy system and the lower (operational) level contains variables that determine the energy system operation strategy for each time step. In Barberis et al. (2016) the dynamic design and operation optimization of a real smart polygenerative grid, designed to satisfy energy demands of the University of Genoa, Campus of Savona (Italy) is investigated. Again a bi–level approach is used.

Concerning the complete dynamic SDO problem, until 2012 very few studies can be found in the literature. In Rancruel, (2005), Rancruel and Spakovsky (2005) the dynamic synthesis, design and operation optimization of a solid oxide fuel cell based auxiliary power unit is investigated using total life cycle costs of the system as the objective function. Transient operation of certain components is also considered. The solution approach is based on a decomposed optimization of individual units (components and sub-systems), which simultaneously takes into account the interactions between all the units

which make up the overall system. The DILGO algorithm –which is the dynamic version of the ILGO algorithm– is applied. A problem with three levels (based on the units of the system) and five coupling functions is formulated. DILGO is also applied in Wang (2008), where dynamic SDO optimization of a 5 kW PEMFC energy system is performed. The same system is examined in Kim et al. (2008), (2011) with the additions of a stochastic modeling and uncertainty analysis methodology for calculating the uncertainties on the system outputs.

In Arcuri et al. (2015) a dynamic SDO optimization of a small size trigeneration plant is performed. Two levels of optimization are considered and a bi–level optimization algorithm is applied. In Buoro et al. (2012) the optimal SDO for advanced energy supply system for a standard and a domotic home is investigated. The annual cost minimization is set as the objective function and the whole year of operation is modeled via 12 characteristic days of operation. A superconfiguration is used and the problem is solved on a single level. Other studies that also employ the use of a superconfiguration and formulate a single level problem can be found in Petrushke et al. (2014), where dynamic SDO optimization is performed in renewable energy systems via a hybrid method that exploits synergies between heuristic and optimization based approaches, in Goderbauer et al. (2016) where a decentralized energy supply system is optimized for an appropriate cost function via adaptive discretization algorithm and in Zhu et al. (2017), where a large scale combined cooling, heat and power (CHP) system is examined. Finally, another noteworthy study can be found in Fuentes-Cortes et al. (2015), where multi–objective dynamic SDO optimization that encompases economic, environmental and safety aspects is performed for residential CHP systems.

Considering the field of marine engineering, as aforementioned, few studies exist for the dynamic operation optimization of marine energy systems while no studies of intertemporal dynamic SDO optimization have been found.

1.3 Original Contribution of the Thesis

In the present Thesis a general methodology is proposed that is suitable for formulating and solving dynamic SDO optimization problems of ship energy systems. Based on the literature review, very few studies of dynamic SDO optimization exist in general, and none in the field of ship energy systems. Real–life dynamic elements such as time and space varying operational requirements with respect to weather conditions and time varying loads are incorporated to the performance models of the components and consequently to the performance of the integrated ship energy system, thus producing a purely dynamic optimization problem. One of the original contributions of this work is that it effectively deals with the complex problem of sub-system integration for dynamic environments as it provides a general mathematical framework, where dynamic optimization methods are successfully combined with SDO optimization of marine energy systems.

A key element of this general framework is the consideration of a superconfiguration for the energy system under optimization. This superconfiguration is a generic super–set that includes all envisaged components and their possible interconnections and is in fact the crucial concept that allows for the synthesis optimization part to be performed. This is realized via a certain modeling technique adopted by the author, which considers all possible system components initially present at the superconfiguration of the system. The existence or not of each unit is then modeled via a binary variable. Then the whole integrated system is modeled using a general mathematical formulation so as when the

optimizer chooses to exclude a specific component from the system, and thus set the corresponding binary value to 0, all accompanying equations and variables of the component are excluded from the problem. In that way no integer variables are present in the system and nested or multi–level strategies in order to tackle with the complete SDO optimization problem can now be avoided.

From the literature review it is evident that, in the very few studies of SDO optimization and dynamic SDO optimization that exist, in order to solve the problem always certain techniques are applied that lead to the formulation of a bi– level or even multi–level optimization procedure. However, in many cases, simplifications to the problems are assumed, in order for the conditions for applying these techniques to be met. This leads to severe reduction of the dimensional space of the problem and thus to sub-optimal solutions. In the specific work, especially due to the highly complex interrelations between the components of the energy system and the dynamic nature of the problem, hypotheses of decomposing the energy system in units or dividing the time horizon of the problem into independent periods of steady state operation, cannot be made. Based on the technique described in the previous paragraph, combined with specifically adapted for this work dynamic optimization methods, a single–level mathematical statement for the problem is formulated and the solution procedure is performed on a single level. The synthesis, design and operation aspects are all tackled simultaneously by the optimizer in every computational step. This means that the choices of optimal synthesis of the system, the optimal design characteristics of the components and the optimal operating state at each instant of time are all treated as interdepended to each other. This single–level approach combined with dynamic optimization methods allows for capturing the true dynamic nature of the problem and ensures a more efficient search in the optimization space, which is another contribution of this work.

Another noteworthy aspect of the modeling procedure and formulation of the optimization problem lies in the flexibility that it offers to the user. Each component model introduced in the integrated energy system is a building block that can be easily replaced with a more detailed and accurate or simpler and computationally fast model or even completely removed. The only constriction, in the case of substituting a specific model with another, is that the substitute has to follow the same computational structure as the original. The same type and number of variables should be declared as inputs and as outputs. Also, the dynamic optimization method that was developed can easily be applied to other energy systems, not necessarily related to the field of marine engineering.

It is noted that the dynamic SDO optimization method proposed in this work is applied to several realistic case studies. The results provide interesting insights concerning the optimal SDO of marine energy systems and prove the suitability of the modeling and optimization procedure for these types of problems.

1.4 Thesis Outline

The remaining of this Thesis is organized in five chapters. Also list of abbreviations and seven appendices are included.

In Chapter 2, the definition of dynamic optimization is clarified and a possible classification of dynamic optimization problems is presented. Also, a concise and complete presentation of all known dynamic optimization methods and approaches along with their advantages and disadvantages is given. Next, based on this presentation, appropriate dynamic optimization procedures, that will be used for the solution of the problems of this

Thesis, are formulated and applied in selected benchmark problems and to a trigeneration energy system.

The general formulation of the dynamic SDO problem, accompanied with a suitable mathematical framework, based on a generic marine energy system is presented in Chapter 3. Also, the concepts of the integrated energy system and the superconfiguration are discussed. In the presentation of the mathematical statement of the general problem, all synthesis, design and operation variables are formally introduced. The chapter concludes with the presentation of the appropriate dynamic optimization procedures and the related software that will be used.

The simulation models and processes for all components that comprise the overall –generic– marine energy system are presented in Chapter 4. The performance of each component is modeled for both the nominal operating state as well as for the off–design operating conditions, an essential requirement in order to properly perform design and operation optimization. Physical modeling, based on a first principles approach, as well as regression analysis based on market data, has been employed on a case by case basis, in order to derive accurate but simultaneously computationally efficient component models.

In Chapter 5 seven case studies of dynamic SDO optimization are presented and solved. For each case study, an appropriate mathematical statement of the problem and a presentation of the values of parameters (vessel characteristics, weather profile, mission parameters) are given. In all case studies, the problem is solved once for the nominal case and then sensitivity analysis is performed for several important parameters. The numerical results of each case study are presented and discussed.

Finally, in Chapter 6, concluding remarks for this Thesis are given. Also, the author's views regarding future work of the subject of dynamic synthesis, design and operation optimization of marine energy systems are presented.

Table 1.1. Aspects addressed in papers on optimization of energy systems.
(Only papers of Paragraphs 1.2.4, 1.2.5 and 1.2.6 are included)

Paper	Optimization of			Intertemporal		Transients included	Bi-level/ Multi-level	Marine
	S	D	O	Static	Dynamic			
Arcuri et al. (2015)	+	+	+		+		+	
Barberis et al. (2016)		+	+		+		+	
Buoro et al. (2012)	+	+	+		+			
Calise et al. (2007)	+	+						
Cheng et al. (2009)			+		+			
Dimopoulos and Frangopoulos (2008)	+	+	+	+			+	+
Dimopoulos et al. (2008)	+	+	+	+			+	+
Evins (2015)		+	+		+		+	
Frangopoulos (1991a)	+	+	+	+			+	
Frangopoulos (1991b)	+	+	+	+			+	
Frangopoulos (1992)	+	+	+	+			+	
Fuentes-Cortes et al. (2015)	+	+	+		+			
Georgopoulos et al. (2002)	+	+	+	+			+	
Goderbauer et al. (2016)	+	+	+		+			
Kalikatzarakis and Frangopoulos (2017)	+	+	+	+				+
Kim et al. (2011)	+	+	+		+	+	+	
Kim et al. (2008)	+	+	+		+	+	+	
Marano et al. (2012)			+		+			
Martelli et al. (2015)		+	+		+		+	
Mohideen et al. (1996)		+	+		+	+	+	
Munoz and Spakovsky (2001a)	+	+	+	+			+	
Munoz and Spakovsky (2001b)	+	+	+	+			+	
Munoz and von Spakovsky (2003)	+	+	+	+			+	
Mussati et al. (2004)	+	+						
Olsommer et al. (1999)	+	+	+	+			+	

Ondeck et al. (2017)		+	+		+		+	
Oyarzabal et al. (2004)	+	+	+	+			+	
Pelster et al. (2001)	+	+						
Petruschke et al. (2014)	+	+	+		+			
Rancruel and Spakovsky (2003)	+	+	+	+		+	+	
Rancruel and Spakovsky (2005)	+	+	+		+	+	+	
Rancruel, (2005) (PhD Thesis)	+	+	+		+	+	+	
Sun et al. (2017)	+	+	+					
Toffolo (2014)	+	+					+	
Vallianou and Frangopoulos (2012)			+		+	+		
Wang et al. (2018)			+		+			+
Wang et al. (2008)	+	+	+		+	+	+	
Zaccone et al. (2018)			+		+			+
Zeng et al. (2017) .		+	+	+			+	
Zhu et al. (2017)	+	+	+		+			

CHAPTER 2: DYNAMIC OPTIMIZATION

2.1 Introduction to Optimization

Optimization is the act of obtaining the best result under given circumstances or, expressed more formally, the process of finding the conditions that give the maximum or minimum value, under certain constraints, of a suitable function that serves as a performance criterion. Optimization has always been an integral part of the job of an engineer, although sometimes on small projects the cost of engineering time may not justify the optimization effort required. The function or functions that must be maximized or minimized are called objective functions. Those are functions of certain variables that mathematically formulate the problem and are divided into decision or independent variables and state or dependent variables. When performing optimization in a problem, we try to find the 'optimal' values of these decision variables that minimize or maximize the objective function(s). It is noted that the maximum of a function coincides with the minimum of the negative of the same function (Fig. 2.1).

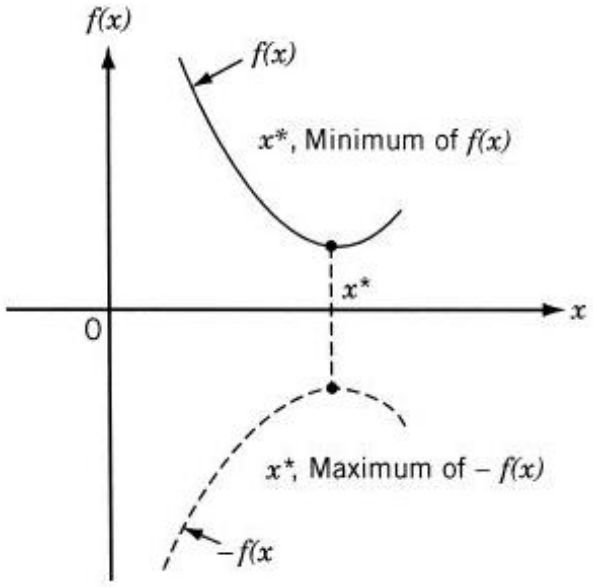

Figure 2.1. Minimum of f(x) is the same as maximum of -f(x).

The methods that seek the optimum are also known as *Mathematical Programming Techniques* and are generally considered as a branch of mathematics under the name *Operations Research*. Operations Research studies the application of scientific methods and techniques to decision making problems and attempts to locate the best or optimal solutions. Mathematical Programming Techniques are useful in finding the minimum (or maximum) of a function of several variables under a known set of constraints. Other methods that perform the same task are stochastic process techniques, that use random variables with known probability distributions, and statistical methods that analyze experimental data and build empirical models to obtain the most accurate representation of real-world phenomena or processes. Table 2.1 lists all those areas of Operations Research.

Table 2.1. Methods of Operations Research [Rao (1996)].

Mathematical programming or optimization techniques	Stochastic process techniques	Statistical methods
Calculus methods	Statistical decision theory	Regression analysis
Calculus of variations	Markov processes	Cluster analysis, pattern recognition
Nonlinear programming	Queueing theory	
Geometric programming	Renewal theory	Design of experiments
Quadratic programming	Simulation methods	Discriminate analysis (factor analysis)
Linear programming	Reliability theory	
Dynamic programming		
Integer programming		
Stochastic programming		
Separable programming		
Multiobjective programming		
Network methods: CPM and PERT		
Game theory		
Modern or nontraditional optimization techniques		
Genetic algorithms		
Simulated annealing		
Ant colony optimization		
Particle swarm optimization		
Neural networks		
Fuzzy optimization		

The general optimization problem consists in determining the extremum (minimum or maximum) of an objective function under certain constraints. Let f represent the function to be minimized (objective function). Then the problem is usually stated mathematically as follows:

$$\underset{\mathbf{x}}{\text{mininimize}}\ f(\mathbf{x}) \tag{2.1}$$

with respect to

$$\mathbf{x} = [x_1, x_2, \ldots x_n]^T \tag{2.2}$$

subject to the constraints

$$h_i(\mathbf{x}) = 0, \quad i = 1, .., p \tag{2.3}$$

$$g_j(\mathbf{x}) \leq 0, \quad j = 1, .., m \tag{2.4}$$

where:

- $\mathbf{x}$ n-dimensional vector, known as decision vector and x_1, x_2, …, x_n, the independent (decision) variables,
- h_i equality constraint functions (‘strong’ constraints), which constitute the simulation model of the system and are derived by an analysis of the system (energetic, exergetic, economic, etc.),
- g_j inequality constraint functions (‘weak’ constraints) corresponding to design and operation limits, state regulations, safety requirements, etc.

The number of variables *n* and the number of constraints *m* and *p* need not be related in the general case. The problem stated with the Eqs. (2.1) – (2.4) is called a *constrained optimization problem*. Problems that do not involve any constraints are called *unconstrained optimization problems*.

In general, engineering optimization problems can be classified in several ways, depending on the criterion. The classification is very useful from both the educational and the computational point of view, because there are many special methods available for the efficient solution of particular classes of problems. Certain ways of categorization are described in brief in the following.

Constrained or unconstrained optimization: Any optimization problem can be classified as constrained or unconstrained, depending on whether constraints are posed in the problem.

Linear, non-linear, geometric and quadratic optimization: According to the nature of equations in the objective function and/or the constraints, optimization problems can be classified as linear, non-linear, geometric and quadratic programming problems. If any of the functions is non-linear, we have a Non-Linear Programming Problem (NLP).

Integer- or real-valued optimization: Here we have integer or real-valued programming problems depending on the values permitted for the design variables. If some or all of the independent variables of an optimization problem are restricted to take on only integer (or discrete) values, then the problem is called an Integer (or Discrete) Programming (IP) problem. If all the independent variables are permitted to take any real value, then the optimization problem is called a Real-Valued Programming problem.

The existence of integer variables in linear and nonlinear programming problems leads to Mixed Integer Linear Programming (MILP) and Mixed Integer Nonlinear Programming (MINLP) problems, respectively.

Deterministic or stochastic optimization: Depending on the deterministic or stochastic nature of the variables, we have deterministic and stochastic programming problems. In a stochastic programming problem some or all the variables/parameters are probabilistic.

Separable or non-separable optimization: Optimization problems can be classified as separable or non-separable, based on whether the objective and constraint functions are *separable* functions. A function $f(\mathbf{x})$, $\mathbf{x} = (x_1, x_2, \ldots, x_n)$, is called *separable*, if it can be expressed as the sum of *n* single-variable functions:

$$f(\mathbf{x}) = \sum_{i=1}^{n} f_i(x_i) \tag{2.5}$$

Single-Objective or Multi-Objective optimization: Depending on whether there is only one or more than one objective functions, optimization problems can be classified as single (SOO) or multi-objective (MOO) optimization problems.

Static and Dynamic optimization: Depending on the nature of the problem, optimization problems can be classified as static or dynamic.

A static optimization problem has already been mathematically stated above in Eqs (2.1) – (2.4). The optimal values of the decision/optimization variables are single numbers/points. To the contrary, in a dynamic optimization problem, the objective function

and/or the constraints, thus the values of the decision/optimization variables, are continuous or discrete functions of time. These types of problems are called *Dynamic Optimization Problems* (DOP) and are solved by dynamic optimization methods as will be thoroughly presented in the rest of this chapter.

2.2 Definition and Mathematical statement of the Dynamic Optimization Problem (DOP)

As previously mentioned, optimization problems can be divided into static and dynamic. In dynamic optimization problems, the variables, objective functions, parameters or the constraint functions may be time-dependent. However this is not sufficient in order for an optimization problem to be characterized as dynamic. There are cases where a seemingly dynamic or time-dependent problem can be treated as a static one and tackled by static optimization methods. For example, we may have an energy system where the period of operation can be decomposed into time intervals of steady-state operation, independent of each other [Munoz and Spakovsky (2003), Dimopoulos et al. (2008), Dimopoulos and Frangopoulos (2008)]. In that case, this 'pseudo-dynamic' optimization problem can be solved relatively easily, since it can be decomposed into a series of static, independent of each other, optimization problems. A more complete definition of a Dynamic optimization Problem is the following:

Dynamic optimization problems (DOPs) are those whose specifications change over time during the optimization procedure, thus resulting in the change over time of the global optimal values of the independent variables [Xin et al. (2010)].

The dependence over time can be continuous or discrete, based on the nature of the problem. The most important point to take away from the previous discussion over static optimization problems is that the choice of the optimal input combination is made just once: there is no planning for the future, nor are there future decisions to be made. This is exactly as the static framework of the problem dictates. In contrast, given the parameters of a dynamic optimization problem, its solution is a *sequence* of optimal decisions in discrete-time, or a *time path* or *curve* of optimal decisions in continuous-time, over the relevant *planning period* or *planning horizon*.

The optimal time path or curve is, by definition, the one that optimizes an objective function. The type of objective function in dynamic problems however is quite different from that in static problems. To clarify the form of the objective function in dynamic problems, let us consider Fig. 2.2. Here three typical time paths of a function or curve $y(t)$ are displayed, along with the resulting value of the objective function associated with each time path $J[y(t)]$, the latter of which we refer to as a *path value*. Notice that all time paths or curves begin at time $t = t_0$ at the point $y = y_0$, and end at time $t = t_1$ at the point $y = y_1$, all four of which are given or fixed, thereby requiring that the paths being compared begin and end at the same position and time. The typical problem in dynamic optimization seeks to find a time path or curve $y(t)$, or equivalently a function $y(.)$ that minimizes the objective function $J[.]$. Thus to each time path or curve $y_i(t)$, $i = a, b, c$, or function $y_i(.)$, $i = a, b, c$, there is a corresponding value of the objective function $J[y_i(t)]$, $i = a, b, c$.

$J[y(t)]$ represents a mapping from paths or curves to real numbers, or equivalently, from functions to real numbers, and therefore is not a mapping from real numbers to real numbers as in the case of functions. Such a mapping from paths or curves to path values, or from functions to real numbers, is what Fig. 2.2 depicts, and is called a *functional*.

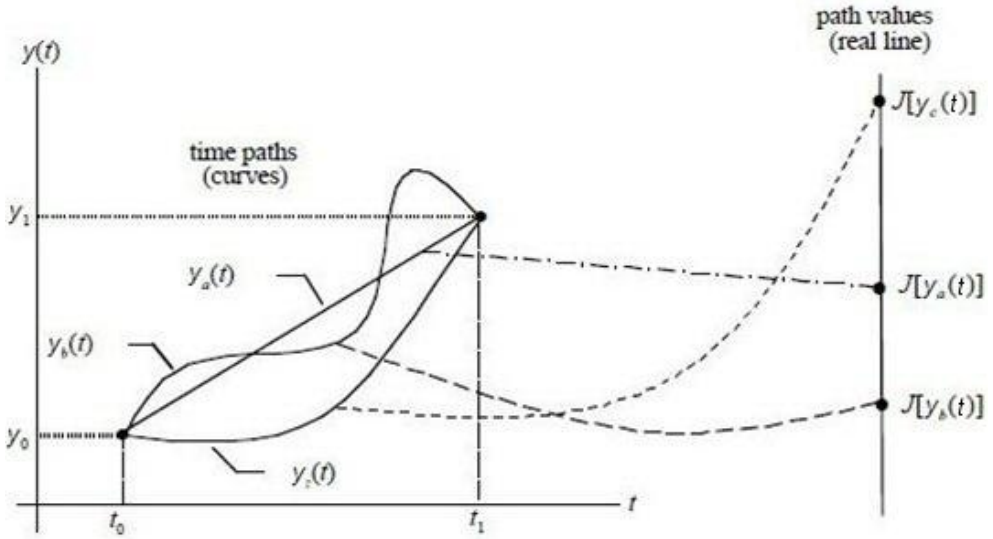

Figure 2.2. Values of the objective function $J[y_i(t)]$ for curves $y_i(t)$, $i = a, b, c$ [Caputo (2005)].

The general notation we shall employ for such a mapping from functions to real numbers is $J[y(t)]$. This notation emphasizes that the functional $J[.]$ depends on the *function* $y(t)$, or equivalently, on the *entire curve* $y(t)$. Moreover, it highlights the fact that it is a change in the position of the entire path or curve $y(t)$, that is, the *variation* in the path or curve $y(t)$, rather than the change in t, that results in a change in the path value or functional $J[.]$. Thus, a dynamic optimization problem in continuous time seeks to find a path or curve $y(t)$, or equivalently, a function $y(t)$, that optimizes the objective functional $J[y(t)]$. Now, that a proper definition has been given we can proceed to the formal mathematical statement of a DOP.

A dynamic optimization problem can be formulated using a Differential-Algebraic Equation (DAE) formulation. The DAE system consists of differential equations that describe the behavior of the system, such as mass and energy balances, and algebraic constraints that ensure thermodynamic consistency or other physically meaningful relations-limits imposed on the problem. A general DAE optimization problem can be stated in implicit form as follows [Allgor and Barton (1997), Biegler et al. (2002), Biegler and Grossman (2004), Biegler (2010)]:

$$\underset{\mathbf{z}(t),\mathbf{y}(t),\mathbf{u}(t),t_f,\mathbf{p}}{\text{mininimize}} \; J[\mathbf{z}(t_f),\mathbf{y}(t_f),\mathbf{u}(t_f),t_f,\mathbf{p}] \tag{2.6}$$

subject to

$$\mathbf{F}(\dot{\mathbf{z}}(t),\mathbf{z}(t),\mathbf{y}(t),\mathbf{u}(t),t,\mathbf{p}) = 0 \tag{2.7}$$

$$\mathbf{G}(\dot{\mathbf{z}}(t),\mathbf{z}(t),\mathbf{y}(t),\mathbf{u}(t),t,\mathbf{p}) \le 0 \tag{2.8}$$

with initial conditions

$$\mathbf{z}(0) = \mathbf{z}^0 \tag{2.9}$$

point conditions

$$\mathbf{H}_s(\mathbf{z}(t_s), \mathbf{y}(t_s), \mathbf{u}(t_s), t_s, \mathbf{p}) = 0, \quad t_s \in [t_0, t_f] \tag{2.10}$$

and bounds

$$\mathbf{z}^L \le \mathbf{z}(t) \le \mathbf{z}^U \tag{2.11}$$
$$\mathbf{y}^L \le \mathbf{y}(t) \le \mathbf{y}^U \tag{2.12}$$
$$\mathbf{u}^L \le \mathbf{u}(t) \le \mathbf{u}^U \tag{2.13}$$
$$\mathbf{p}^L \le \mathbf{p} \le \mathbf{p}^U \tag{2.14}$$
$$t_f{}^L \le t_f \le t_f{}^U \tag{2.15}$$

where:

J	scalar objective functional
F	differential-algebraic equality constraints
G	differential-algebraic inequality constraints
$\mathbf{H}_s$	additional point conditions at times t_s (including t_f)
z	differential state profile vector
$\mathbf{z}^0$	initial values of **z**(t)
y	algebraic state profile vector
u	control (independent variables) profile vector
p	time-independent parameters vector
t_f	final time.

As a simple illustration of a dynamic optimization, consider the brachistochrone problem that was proposed in 1696 by John Bernoulli to challenge the mathematicians of Europe (Fig. 2.3).

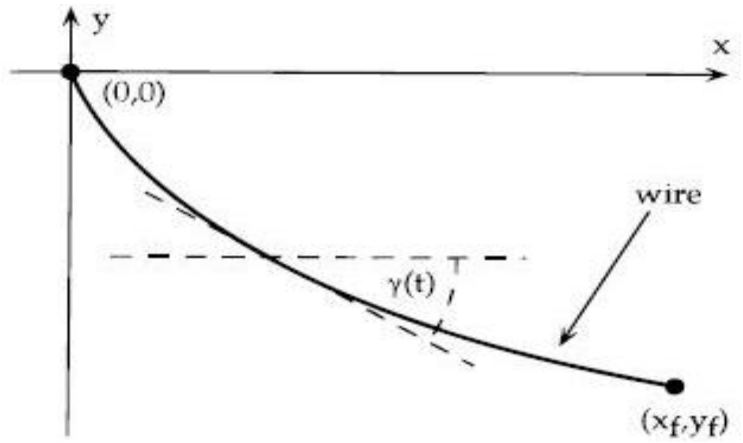

Figure 2.3. Schematic of the Brahistochrone problem [Barton et al. (1998)].

The objective of the brachistochrone problem is to find (in two dimensions) the shape of a frictionless wire that causes a bead, initially at rest, to move under the force of gravity

between the origin and a specified final point in minimum time. This can be formulated as a dynamic optimization problem in the following way [Kraft (1994)]:

$$\min_{\gamma(t)} t_f \tag{2.16a}$$

subject to

$$\dot{x} = w \cdot \cos(\gamma(t)) \tag{2.16b}$$
$$\dot{y} = -w \cdot \sin(\gamma(t)) \tag{2.16c}$$
$$\dot{w} = g \cdot \sin(\gamma(t)) \tag{2.16d}$$

with initial conditions

$$x(0) = 0 \tag{2.16e}$$
$$y(0) = 0 \tag{2.16f}$$
$$w(0) = 0 \tag{2.16g}$$

and final conditions

$$x(t_f) = x_f \tag{2.16h}$$
$$y(t_f) = y_f \tag{2.16i}$$

where:

w	the velocity tangential to the wire
g	the gravitational acceleration (a given constant)
γ	the angle of the wire to horizontal.

Equation (2.16a) defines the objective function for the optimization, which in this case is to minimize the time required to reach the final point. The motion of the bead in a gravity field is described by a set of differential equations, Eqs. (2.16b) – (2.16d), that constitute the dynamic model of the system. In this case the control (or forcing function) for the dynamic system is $\gamma(t)$, the angle of the wire to horizontal, which defines the shape of the wire as a function of time. Hence, the decision variable in this problem is the control *profile* $\gamma(t)$. The purpose of the optimization is to find, out of all the possible functions $\gamma(t)$/shapes of the wire, the function/shape that minimizes the final time.

In order to complete the formulation of the brachistochrone problem, it is necessary to include the *point constraints*, Eqs. (2.16e) – (2.16i). The initial point constraints, Eqs. (2.16e) – (2.16g), require the bead to be at rest at the origin at the initial time, and the final point constraints, Eqs. (2.16h), (2.16i), require the bead to be at a certain point in the two-dimensional space at the final time.

Of course the statement given by Eqs. (2.6) – (2.15) is the most general statement of a DAE optimization problem (containing first order derivatives), including equality and inequality constraints for the differential, state and control variables. It must be noted here that in the area of dynamic optimization of energy systems that is examined in this study, differential inequality constraints are rarely imposed, so Eq. (2.8) may, in some cases, be replaced with the following:

$$\mathbf{G}(\mathbf{z}(t), \mathbf{y}(t), \mathbf{u}(t), t, \mathbf{p}) \leq 0 \tag{2.17}$$

where ***G*** now stands for only the algebraic inequality constraints. On the other hand, in most problems, Eq. (2.7) can be written in separable form considering the differential and algebraic variables as:

$$\frac{d\mathbf{z}(t)}{dt} = \mathbf{F}(\mathbf{z}(t), \mathbf{y}(t), \mathbf{u}(t), t, \mathbf{p}) \tag{2.18}$$

In this case, the dynamic optimization problem may be treated by *optimal control theory*. Furthermore, special cases of the inequality constraints may be considered (only the bounds of the variables described by Eqs. (2.11) – (2.15)), in which case Eq. (2.17) would be re-stated as an equality constraint:

$$\mathbf{G}(\mathbf{z}(t), \mathbf{y}(t), \mathbf{u}(t), t, \mathbf{p}) = 0 \tag{2.19}$$

thus formulating an even simpler statement of the DAE optimization problem that can, in general, describe the majority of the dynamic optimization problems examined in studies of energy systems.

The scalar functional J that represents the objective function of the minimization problem can have various forms. In Eq. (2.6) it is stated in Mayer form. Another general form for continuous time commonly used in our field of research of energy systems, is the one known as Bolza form:

$$J[\mathbf{z}(t_f), \mathbf{y}(t_f), \mathbf{u}(t_f), t_f, \mathbf{p}] = P(\mathbf{z}(t_f), \mathbf{y}(t_f), t_f, \mathbf{p}) + \int_{t_0}^{t_f} L(\mathbf{z}(t), \mathbf{y}(t), \mathbf{u}(t), t, \mathbf{p}) dt \tag{2.20}$$

that consists of the function P at the end of the time interval t_f and the integral of the function L over the time horizon. Both forms can be proven to be mathematically equivalent.

Of course, the same problem can be stated in discrete form too, in order to cover optimization problems in discrete time. The time period $[t_0, t_f]$ can be considered as consisting of N time intervals of length Δt_n, so that $t_f - t_0 = N \cdot \Delta t_n$ and the integral in Eq. (2.20) is replaced by a summation over the N time intervals, while the variables are discrete vector sequences (e.g. $\mathbf{u} = \{\mathbf{u}_1, \mathbf{u}_2, ..., \mathbf{u}_N\}$). The analogous discrete problem is stated as follows:

$$\underset{\mathbf{z},\mathbf{y},\mathbf{u},t_f,\mathbf{p}}{\text{minimize}}\, J[\mathbf{z}, \mathbf{y}, \mathbf{u}, t_f, \mathbf{p}] \tag{2.21}$$

with

$$J[\mathbf{z}, \mathbf{y}, \mathbf{u}, t_f, \mathbf{p}] = P(\mathbf{z}_N, \mathbf{y}_N, N, \mathbf{p}) + \sum_{n=1}^{N} L(\mathbf{z}_n, \mathbf{y}_n, \mathbf{u}_n, n, \mathbf{p}) \tag{2.22}$$

subject to

$$\mathbf{z}_{n+1} = \mathbf{F}(\mathbf{z}_n, \mathbf{y}_n, \mathbf{u}_n, n, \mathbf{p}), \qquad 1 \le n \le \mathrm{N} \tag{2.23}$$

$$\mathbf{G}(\mathbf{z}_n, \mathbf{y}_n, \mathbf{u}_n, n, \mathbf{p}) \le 0, \qquad 1 \le n \le \mathrm{N} \tag{2.24}$$

with initial conditions

$$\mathbf{z}_0 = \mathbf{z}^0 \tag{2.25}$$

point conditions

$$\mathbf{G}_s(\mathbf{z}_s, \mathbf{y}_s, \mathbf{u}_s, s, \mathbf{p}) = 0, \qquad 1 \le \mathrm{s} \le \mathrm{N} \tag{2.26}$$

and bounds

$$\mathbf{z}_n{}^L \le \mathbf{z}_n \le \mathbf{z}_n{}^U, \qquad 1 \le \mathrm{n} \le \mathrm{N} \tag{2.27}$$

$$\mathbf{y}_n{}^L \le \mathbf{y}_n \le \mathbf{y}_n{}^U, \qquad 1 \le \mathrm{n} \le \mathrm{N} \tag{2.28}$$

$$\mathbf{u}_n{}^L \le \mathbf{u}_n \le \mathbf{u}_n{}^U, \qquad 1 \le \mathrm{n} \le \mathrm{N} \tag{2.29}$$

$$\mathbf{p}^L \le \mathbf{p} \le \mathbf{p}^U \tag{2.30}$$

Furthermore, the general DAE formulation of a DOP that is given by Eqs. (2.6) – (2.15) can be re-stated in order to include DOPs of multi–modal systems. Very characteristic problems of this kind are those of energy systems described by dynamic models that, during their period of service, include different modes of the system and need to be optimized for the whole period of service. In this case, the system characteristics (state equations, constraints, etc.) may vary from mode to mode, and this type of variation may be formulated as a mixture of continuous and discrete functions of time. Thus, the operation of the whole system must be described as a sequence of different sets of DAEs (multimodal systems) with the objective to find the duration and operating conditions of each stage in order to achieve an overall optimal result for the whole system.

As an example, a real-life engineering problem of this type may be that of the trip of an aircraft that includes the phases of take-off, flight and landing, where each phase is described by a different DAE system and the optimization must be performed for the whole trip [Munoz and Spakovsky (2003)]. Another very characteristic example is the voyage of a ship that can be decomposed in many different phases [loaded trip, ballast trip, ports], [Dimopoulos (2008), Dimopoulos and Frangopoulos (2008)], where in each phase the synthesis of the system, and thus the system of equations that describe its characteristics, may change while the cost minimization or the revenue maximization must be performed for the whole voyage.

A mathematical statement of such a multi–modal problem must be given. So an energy system is considered, the operation of which consists of N modes, and $\mathbf{z}(t)$, $\mathbf{y}(t)$, $\mathbf{u}(t)$, $\mathbf{p}$, t_n, t_f for $n = 1, ..., N$ need to be calculated for the dynamic optimization problem:

$$\underset{\mathbf{z}(t),\mathbf{y}(t),\mathbf{u}(t),t_f,t_k,\mathbf{p}}{\text{mininimize}} \; J[\mathbf{z}(t_f), \mathbf{y}(t_f), \mathbf{u}(t_f), t_f, \mathbf{p}] \tag{2.31}$$

subject to

$$\mathbf{F}_n(\dot{\mathbf{z}}(t), \mathbf{z}(t), \mathbf{y}(t), \mathbf{u}(t), t, \mathbf{p}) = 0 \tag{2.32}$$

$$\mathbf{G}_n(\mathbf{z}(t), \mathbf{y}(t), \mathbf{u}(t), t, \mathbf{p}) \le 0 \tag{2.33}$$

where $t \in [t_{n-1}, t_n]$ with $n = 1, ..., N$,

with initial conditions

$$\mathbf{Q}_0(\dot{\mathbf{z}}(t_0), \mathbf{z}(t_0), \mathbf{y}(t_0), \mathbf{u}(t_0), t_0, \mathbf{p}) = 0 \tag{2.34}$$

junction conditions (that ensure that the values of the variables at the beginning of each mode are related to the values at the end of the previous mode)

$$\mathbf{Q}_n(\dot{\mathbf{z}}(t_n), \mathbf{z}(t_n), \mathbf{y}(t_n), \mathbf{u}(t_n), \dot{\mathbf{z}}(t_{n-1}), \mathbf{z}(t_{n-1}), \mathbf{y}(t_{n-1}), \mathbf{u}(t_{n-1}), t_n, \mathbf{p}) = 0 \tag{2.35}$$

point conditions

$$\mathbf{H}_s(\mathbf{z}(t_s), \mathbf{y}(t_s), \mathbf{u}(t_s), t_s, \mathbf{p}) = 0, \quad t_s \in [t_{n-1}, t_n], \quad \text{for } n = 1, \ldots, N \tag{2.36}$$

and bounds

$$\mathbf{z}^L \le \mathbf{z}(t) \le \mathbf{z}^U \tag{2.37}$$
$$\mathbf{y}^L \le \mathbf{y}(t) \le \mathbf{y}^U \tag{2.38}$$
$$\mathbf{u}^L \le \mathbf{u}(t) \le \mathbf{u}^U \tag{2.39}$$
$$\mathbf{p}^L \le \mathbf{p} \le \mathbf{p}^U \tag{2.40}$$
$$t_f{}^L \le t_f \le t_f{}^U \tag{2.41}$$
$$t_n{}^L \le t_n \le t_n{}^U, \quad \text{for } n = 1, \ldots, N \tag{2.42}$$

where the functional J can have the form

$$J[\mathbf{z}(t_f), \mathbf{y}(t_f), \mathbf{u}(t_f), t_f, \mathbf{p}] = P(\mathbf{z}(t_f), \mathbf{y}(t_f), t_f, \mathbf{p}) + \int_{t_0}^{t_f} L(\mathbf{z}(t), \mathbf{y}(t), \mathbf{u}(t), t, \mathbf{p}) dt \tag{2.43}$$

Several methods can be proposed for the solution of such problems. In certain simple cases, the problem can be stated in an appropriate mathematical form, where calculus of variations or dynamic programming can be applied. However, in the general case only *direct approach* solution methods can be successfully applied. Their main characteristic (as will be presented in the following Section 2.4) is the transformation of the original dynamic optimization problem into a NLP problem through discretization that can be solved using a non-linear programming optimization method. Of course evolutionary optimization methods modified suitably for dynamic optimization can be applied successfully too.

2.3 Classification of Dynamic Optimization Problems

As mentioned before, the research trends in optimization for the past decade have evolved from a focus on static problems to complex cases with dynamic aspects. This swift of interest in dynamic optimization problems was inevitable, as it was becoming more and more evident that static approaches could not always model reality accurately. However, dynamic optimization problems have proved extremely complex and hard to solve. It is very important how dynamic changes in the input variables affect the results in the

objective functions' space, therefore it is clear that a classification of dynamic problems is needed as a first step, in order to understand the effects of the dynamic factors on the optimal solution of each problem.

Studies regarding the structural view on dynamic optimization problems have been provided by many authors in the past. A first approach was given in Branke (2001). Another recent approach that provides a formal framework on the classification of dynamic optimization problems is given in Tantar et al. (2010, 2011). This study is based on classifying the problems based on the different dynamic elements that appear in the problem, or equivalently by specifying the basic time-dependent components. In more detail, Tantar classifies the problems in four categories as follows:

- First order: time-dependent parameter evolution, dynamic transformation of the input variables.
- Second order: time-dependent function evolution of the objective function values.
- Third order: time-depended state dependency, parameter or function state time-dependency (the parameters or the function is defined by accounting for not only the current moment but also the previous states).
- Fourth order: time-dependent environment, parts of or the whole integral environment evolves with time.

Other notable studies are those of [Weicker (2002)], which outline the role of classification as a tool for systematic research in dynamic optimization, and the works of [Bu and Zheng (2010), Mehnen et al. (2006)].

2.4 Solution Approaches for the Dynamic Optimization Problem

Along with growing application and acceptance of large-scale dynamic simulation in chemical, mechanical and marine engineering, much attention was also given to the research regarding possible methods of solution of optimization problems (DOPs) around these dynamic systems. Specifically, DOPs gained much publicity in 1960's with the development of *optimal control theory* and several solution techniques have been investigated since (for a fairly complete review see Longsdon and Biegler (1989), Longsdon and Biegler (1992)). In general, the several solution approaches are divided in two main categories, the *Indirect Methods* and the *Direct Methods*. Figure 2.4 depicts the various possible solution approaches.

In the category of Indirect Methods belong *Calculus of Variations* (COV) and *Dynamic Programming* (DP).

Calculus of variations belongs to the general group of *variational methods* that were developed and introduced in the 1960's by the Russian Mathematician Lev Pontryagin (*Pontryagin's Maximun Principle*) [Pontryagin et al. (1962)]. In this approach, the problem is transformed into a two-point boundary value problem (TPBVP) and solved likewise. Variational methods work fairly well for unconstrained problems, but the solution of the TPBVP is still difficult to be achieved especially with the addition of profile inequalities/path constraints. The general idea behind variational methods is the use of the necessary mathematical conditions for optimality in order to find an optimal solution.

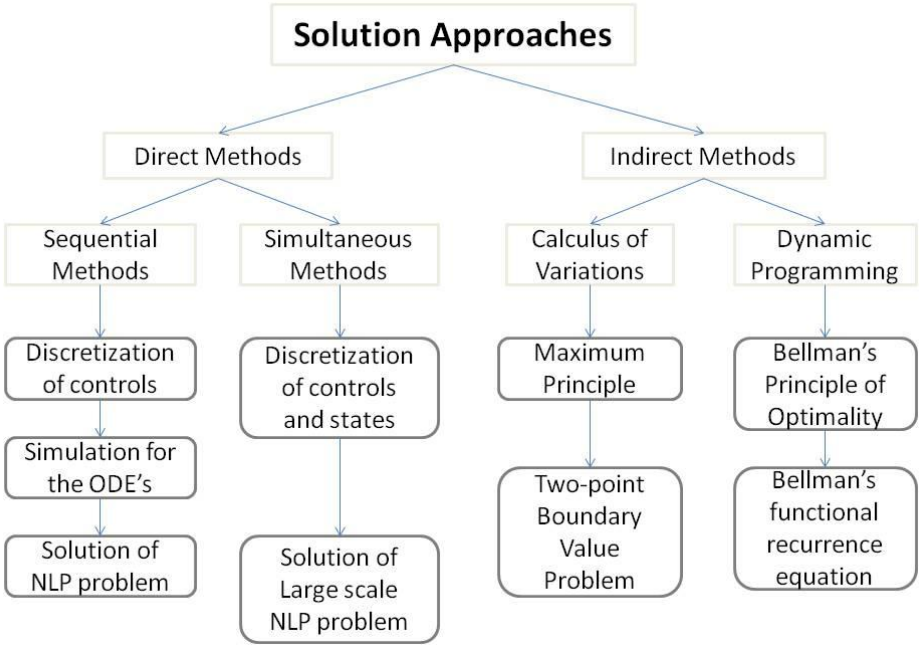

Figure 2.4. Solution approaches for dynamic optimization problems.

Dynamic Programming (DP) was developed at the same time as Calculus of Variations by the American mathematician Richard Bellman [Bellman (1957)]. The primary goal of Bellman was to invent a method to tackle decision/optimization problems with discrete characteristics. In general, Dynamic Programming is suitable for solving complicated and multi-stage decision problems by tracing the optimal strategy. It is based on the concept that, if the current state and the planned decision of a system are known, an optimal policy formed in the future will be independent of the past policy already formed. It is noted that this method is mostly applied to multi-stage sequential decision problems, where the objective function equations are non-differentiable mainly due to the fact that they are in discrete form (the functional J in Eq. (2.22) contains summations of terms over time). The key idea behind this method lies in the famous *Bellman's recursive equation*, which in essence restates the original DOP in recursive form.

In the category of Direct Methods, the DOP is approached by applying a certain level of discretization that converts the original continuous time problem into a discrete one. The key idea behind Direct Methods is the conversion of the original DOP into a Non-Linear Programming Problem (NLP). As it is shown in Figure 2.4, Direct Methods can be divided into two sub-categories, the *Sequentia*l and the *Simultaneous* Methods, according to the level of discretization applied.

In the first sub-category, there is discretization of only the independent variables profiles (control variables). These methods are known as *sequential* or *decomposed* methods, because the system under optimization is decomposed into the control and state variables and only the control variables are discretized and treated as optimization variables. The problem is solved by non-linear programming (NLP) methods (e.g. steepest descent, Quasi-Newton methods, Successive Quadratic Programming, SQP), whereas the state variables are determined by integration of the system of DAE's via computer software solvers, simulation tools, etc. In certain cases, Dynamic Programming can be used too, but it is generally not recommended.

In the second sub-category, we have the *simultaneous* methods, where full discretization is performed in both the control and state variables and a large scale NLP problem is formulated. Different NLP methods and full discretization techniques can be used, but their basic characteristic is that they solve the DAE system only once, at the optimum, in contrast to the sequential methods approach, where the differential system is integrated in each iteration of the optimization procedure.

An early comment that can be made here is that the full discretization methods (simultaneous) have the advantage of better stability properties than the partial discretization methods (sequential), however they generate bigger and more computationally expensive problems. Furthermore, in the sequential approach the solution is always feasible and only the guess profiles of the independent (control) variables are required to initiate the optimization, unlike the simultaneous methods where guess profiles for the controls and the states must be provided in advance. Another comment should be that direct methods are commonly used in practical applications since, unlike indirect methods, they can be applied to large scale complicated problems and are typically easier to use. However the fact that usually all direct methods utilize gradient approaches poses a main drawback, since the global optimum cannot be ensured, except for cases where the system is convex.

In general, we can say that there are two broad categories of algorithms that can be used in order to solve the resulting NLP problem that originates from the discretization of a dynamic optimization problem: *Evolutionary* and *Gradient-based* Algorithms.

Evolutionary algorithms (EAs) are a class of stochastic search and optimization methods that are based on stochastic search, social metaphors and principles of natural biological evolution. Genetic algorithms, evolutionary programming, evolution strategies, genetic programming, and their variants [Michalewicz (1996)] are some of the examples included in the broad category of Evolutionary algorithms, that have received considerable and increasing interest over the past decade. Several engineering optimization problems have been solved by EAs [Androulakis and Venkatasubramanian (1991), Dakev et al. (1996), Morimoto et al. (1996), Moros et al. (1996), Chen and Zalzala (1997), McKay et al. (1997)], because EAs are robust and suitable for effectively obtaining optima. Furthermore, their main advantage lies in the fact that they have a smaller probability than other algorithms of falling into local optima, thus being characterized as global optimization tools.

Gradient based algorithms require the evaluation of the first order (and in certain cases the second order) gradient of the objective function plus an estimation of the initial point of the independent variables must be provided in order to solve the problem. Thus, gradient based algorithms suffer from dependence on the initial point value and can be "trapped" in local optima in cases of non-convex objective functions. In addition, the gradients must be calculated in each iteration so an additional computation burden is introduced in the problem.

For the rest of this Section, a more detailed mathematical presentation of both the Indirect and Direct methods is given.

2.4.1 Indirect methods: calculus of variations

The Calculus of Variations is a method associated with the problem of extremum seeking for functionals of the type

$$S = \int_{t_0}^{t_f} L(\mathbf{y}, \mathbf{u}, t)dt \tag{2.44}$$

while the state equations have the special form

$$\frac{d\mathbf{y}}{dt} = \mathbf{u} \tag{2.45}$$

and satisfy an initial condition. For simplicity we consider here the initial state:

$$\mathbf{y}(t_0) = \mathbf{y}^0 \tag{2.46}$$

In this type of problem, for functional equations of the form given by Eq. (2.44) subject to Eq. (2.45), the control variables **u** are equal in number with the state variables of vector **y**. Since the control vector can then be replaced by the derivative of the state vector, the typical problem of variational calculus can be stated by the maximization or the minimization of the integral

$$S = \int_{t_0}^{t_f} L(\mathbf{y}, \dot{\mathbf{y}}, t)dt \tag{2.47}$$

subject to the initial condition given by Eq. (2.46) and a final condition

$$\mathbf{y}(t_f) = \mathbf{y}^f \tag{2.48}$$

This is called the fixed end problem.
In variational analysis the meaning of variation is fundamental. The variation of the argument $\mathbf{y}(t)$ is the difference between two functions

$$\delta\mathbf{y} = \mathbf{y}(t) - \hat{\mathbf{y}}(t) \tag{2.49}$$

while the variation of the functional

$$\Delta S = S(\hat{\mathbf{y}} + \delta\mathbf{y}) - S(\hat{\mathbf{y}}) \tag{2.50}$$

is called the *accretion* of the functional S. For the functional of Eq. (2.47) the variation δS is

$$\delta S = \int_t^{t_f} \sum_{i=1}^{I} \left\{ \frac{\partial L}{\partial y_i}\delta y_i + \frac{\partial L}{\partial \dot{y}_i}\delta \dot{y}_i \right\} dt \tag{2.51a}$$

The fundamental theorem of variational calculus states that the vanishing of variation δS along the extremal curve $\hat{\mathbf{y}}(t)$ is the necessary condition for the extremum of the functional, Eq. (2.47). Using differentiation by parts

$$\frac{d}{dt}\left(\frac{\partial L}{\partial \dot{y}_i}\delta y_i\right) = \delta y_i \frac{d}{dt}\left(\frac{\partial L}{\partial \dot{y}_i}\right) + \frac{\partial L}{\partial \dot{y}_i}\delta \dot{y}_i \tag{2.51b}$$

and combining Eqs. (2.51a) and (2.51b), we obtain the following expression for δS

$$\delta S = \int_{t_0}^{t_f} \sum_{i=1}^{I} \left\{ \frac{\partial L}{\partial y_i}\delta y_i + \frac{d}{dt}\left(\frac{\partial L}{\partial \dot{y}_i}\delta y_i\right) - \delta y_i \frac{d}{dt}\left(\frac{\partial L}{\partial \dot{y}_i}\right)\right\} dt \tag{2.52}$$

where the middle term does not contribute to the extremum of S when the end points of the extremal are fixed. This results in the necessary extremum conditions satisfied along the extremal curve $\hat{\mathbf{y}}(t)$ in the form of I differential equations:

$$\frac{\partial L}{\partial y_i} - \frac{d}{dt}\left(\frac{\partial L}{\partial \dot{y}_i}\right) = 0, \qquad i = 1, 2, ..., I \tag{2.53}$$

These equations are called the *Euler-Lagrange equations* of variational calculus. The extremum condition describes the disappearance of the so-called *variational derivative* $\partial L/\partial y_i$ defined as the left hand side of Eq. (2.53).

The Euler-Lagrange equation is also valid when the right end of the trajectory is fixed, as in Eq. (2.48). Of course, there is also the case where the right end of the trajectory moves along a surface or a line. In that case the form of the final condition depends on the manifold along which the end of the trajectory moves. For the motion along a curve described by the equations

$$x_i = \varphi_i(t_f), \qquad i = 1, 2, ..., I \tag{2.54}$$

a necessary condition for the vanishing of the first variation must be satisfied

$$\sum_{i=1}^{I} \left\{ \frac{\partial L^f}{\partial \dot{y}_i^f} (\dot{\varphi}(t_f) - \dot{y}_i^f) \right\} + L^f = 0 \tag{2.55}$$

Equation (2.55) is called the *transversality condition.*

Solving the set of Euler-Lagrange equations, with initial and final conditions defined by Eqs. (2.46) and (2.48), leads to the determination of the extremal trajectory. The nature of the functional extremum (maximum, minimum or saddle point) is determined by the investigation of *sufficient conditions*. More information about Calculus of Variations can be found in many sources [Gelfand and Fomin (1963), Moiseiwitsch (1966), Rund (1966)]. Also, important generalizations of the Euler-Lagrange equations to cases with many independent variables and for functional containing derivatives of higher order exist, but they will not be presented here.

The application of the aforementioned method in the DAE optimization problem stated by Eqs (2.6), (2.9) – (2.15), (2.17) and (2.18) requires the formulation of the necessary conditions of optimality that are obtained from Potryagins Maximum Principle [Potryagin et al. (1962)] as a set of differential-algebraic equations:

$$\frac{d\mathbf{z}}{dt} = \frac{\partial H}{\partial \boldsymbol{\lambda}} = \mathbf{F}(\mathbf{z}(t), \mathbf{y}(t), \mathbf{u}(t), \mathbf{p}) \tag{2.56a}$$

$$\mathbf{z}(0) = \mathbf{z}_0 \tag{2.56b}$$

$$\frac{d\boldsymbol{\lambda}}{dt} = -\frac{\partial H}{\partial \mathbf{z}} \tag{2.57a}$$

$$\boldsymbol{\lambda}(t_f) = \frac{\partial J}{\partial \mathbf{z}} + \frac{\partial \mathbf{G}_f}{\partial \mathbf{z}_f} \nu_f \tag{2.57b}$$

$$\frac{dH}{d\mathbf{y}} = \frac{\partial \mathbf{F}}{\partial \mathbf{y}} \boldsymbol{\lambda} + \frac{\partial \mathbf{G}}{\partial \mathbf{y}} \boldsymbol{\mu} = 0 \tag{2.58}$$

$$\frac{dH}{d\mathbf{u}} = 0 \tag{2.59}$$

$$\int_{t_0}^{t_f} \frac{\partial H}{\partial \mathbf{p}} dt = 0 \tag{2.60}$$

$$\mathbf{G}(\mathbf{z}(t), \mathbf{y}(t), \mathbf{u}(t), t, \mathbf{p}) = 0 \tag{2.61}$$

where, the Hamiltonian H is a scalar function of the form

$$H(t) = \boldsymbol{\lambda}^T(t)\mathbf{F}(t) + \boldsymbol{\mu}^T(t)\mathbf{G}(t) \tag{2.62}$$

$\boldsymbol{\lambda}$, $\boldsymbol{\mu}$ are vectors of the adjoint variables and ν_f is the multiplier associated with the final time constraint

$$\mathbf{G}_f(\mathbf{z}(t_f), \mathbf{y}(t_f), \mathbf{u}(t_f), t_f, \mathbf{p}) = 0 \tag{2.63}$$

The main difficulty in obtaining a solution to these equations is due to the boundary conditions. The state variables are given as initial conditions and the adjoint variables as final conditions. This procedure leads to a two-point boundary value problem (TPBVP) that can be solved with various approaches, including single shooting, invariant embedding, multiple shooting or a discretization method such as collocation of finite elements or finite differences.

In the single shooting methods the missing initial conditions values are guessed. Then, an initial value solver is used to integrate Eqs. (2.7) and (2.8) and Newton iteration is applied to adjust the guessed initial conditions so that the final conditions are equal to the given values. The main disadvantage of this method is that in most cases the problem is infeasible for a given set of guessed initial conditions. The difficulty is with the non-linearities and instabilities of the DAE system.

Invariant embedding is a procedure for converting the TPBVP to an initial value problem (IVP). It is based on assuming the structure of the solution, and results in solution

procedures analogous to the Ricatti matrix differential equation. The main disadvantage here is the high dimensionality of the resulting problem.

Multiple shooting methods follow the same idea as single shooting, but with the integration horizon divided into smaller sub-intervals. State variable values are not only guessed at initial time, but also at several points in between. Then the system of equations is decomposed by either solving a collocation system for each region or using a direct integrator along the nominal trajectory on each sub-interval. Newton iteration is also needed to enforce the continuity between sub-intervals.

The discretization methods are known as the most stable. The solution to the TPBVP is obtained simultaneously for the whole horizon, so the initial conditions do not need to be guessed.

For the multiple shooting and discretization methods, special decomposition strategies are usually used to decompose the structured linear algebraic system that is obtained, in each iteration, of the solution procedure. Efficient factorization schemes, based on structured Gaussian elimination and structured orthogonal factorization can be used in order to minimize the computational effort. Although these methods work well for problems without bounds, handling inequality constraints is difficult, unless a priori information about the active constraints is known.

2.4.2 Indirect methods: dynamic programming

The term *Dynamic Programming* was originally used in the 1940s by Richard Bellman to describe the process of solving problems where one needs to find the best decisions one after another. By 1953, he refined this to the modern meaning, referring specifically to nesting smaller decision problems inside larger decisions, and the field was thereafter recognized by the IEEE as a systems analysis and engineering topic. Bellman's contribution is remembered in the name of the Bellman equation, a central result of dynamic programming, which restates an optimization problem in recursive form [Bellman (1957)].

The word *dynamic* was chosen by Bellman to capture the time-varying aspect of the problems and also because it sounded impressive. The word *programming* referred to the use of the method to find an optimal program, e.g. a military schedule for training or logistics. This usage is the same as that in the terms *linear programming* and *mathematical programming*, a synonym for mathematical optimization.

The method of dynamic programming is based on Bellman's Principle of optimality:

"An optimal policy has the property that whatever the initial state and decisions are, the remaining decisions must constitute an optimal policy with regard to the state resulting from the first decision" [Bellman, (1957)].

Essentially, the principle of optimality states that the optimal path for the control variable in a problem will be the same whether we solve the problem over the entire time interval of interest or solve for future periods as a function of the initial conditions given by past optimal solutions. We can break the problem up into two bits, solving only for the current optimal path, taking the fact that the future path will also be optimal as a given.

More specifically let's consider the following discrete problem:

$$\underset{\{x_t\},\{u_t\}}{\text{minimize}} V = \sum_{t=0}^{T} P(x_t, u_t), \qquad t = 0,1,...,\text{T} \tag{2.64}$$

subject to

$$x_{t+1} = f(x_t, u_t) \tag{2.65}$$

with lower and upper bounds

$$x_0 = \bar{x}_0 \tag{2.66}$$

$$x_{T+1} = \bar{x}_{T+1} \tag{2.67}$$

In this problem, both P and f are functions of the current period's state and control variables and not of their past or future values. In addition, the function V is time additive with the same functional form P[.] for any time period. Using these two properties, Bellman found the solution properties called the *principle of optimality*. Let a feasible solution be u(0,T) which is decomposed into two time segments: u(0,t-1) and u(t,T). The principle of optimality says that the optimal solution u^*(0,T) must be such that at any stage t the remaining decisions u^*(t,T) must be optimal with regard to the new starting state x_t^* which results from the first period t=0, and evolves under the earlier decisions u^*(0,t-1). Since V has an additive form, we can write:

$$V(0,T) = V(0,t-1) + V(t,T) \tag{2.68}$$

Formally, the principle of optimality is stated as follows:

"u^*(0,T) minimizes V(0,T) with starting initial state $\bar{x}_0$ if and only if u^*(t,T) minimizes V(t,T) with starting state $\bar{x}_0$ for any t, t+1,..., T."

The optimal solution u^*(t,T) from stage t is determined only by x_t^* and the past values u^*(0,t-1) and the corresponding $x^*(0,t-1) = (x_0^*, x_1^*, ..., x_{t-1}^*)$ are irrelevant because they are all summarized in x_t^*. The state variable at time t already contains all the relevant information for planning the remaining horizon. If we start the planning horizon from time t instead of time 0, we can rewrite Eq. (2.68) as

$$V(t,T) = V(t,t+1) + V(t+1,T) \tag{2.69}$$

which can be expressed as

$$U(x_t) = \min_{u_t}[P(x_t, u_t) + U(x_{t+1})] \tag{2.70}$$

by setting $U(x_t) = V$(t,T). Using Eq. (2.65) we write Eq. (2.70) as:

$$U(x_t) = \min_{u_t}[P(x_t, u_t) + U(f(x_t, u_t))] \tag{2.71}$$

which is known as Bellman's functional recurrence equation. This equation is solved by backward induction, meaning that from the last period T, we proceed to $\min_{u_T} P(x_T, u_T)$ subject to $x_{T+1} = f(x_T, u_T)$ with $x_{T+1} = \bar{x}_{T+1}$ and x_T a known parameter. Once u_T^* is

obtained, the resulting $P(x_T, u_T)$ is only a function of x_T which is expressed as $V(x_T)$. Proceeding one period backward, we solve the problem:

$$U(x_{T-1}) = \min_{u_{T-1}}[P(x_{T-1}, u_{T-1}) + U(f(x_{T-1}, u_{T-1}))] \tag{2.72}$$

where x_{T-1} is treated as a known parameter. The first order condition is given by:

$$P(x_{T-1}, u_{T-1}) + U'(x_T) f_{u_{T-1}}(x_{T-1}, u_{T-1}) = 0 \tag{2.73}$$

which can be solved for u_{T-1}^* as a function of x_{T-1}. By proceeding to solve successively backward to the initial period 0, the sequence u_t^* is generated as a function of x_t. But it is $x_1 = f(x_0, u_0) = f(x_0, u_0^*) = f^*(x_0)$ so x_1^* can be obtained and u_1^* can be determined and so on. Repeating the process forward to the last period, all x_t^* are determined and the optimized value of *V*(0,T) is obtained.

However, the use of iterative dynamic programming for the solution of large scale DOPs has been limited, largely because of the high dimensionality issues associated with it. Usually, the phrase "curse of dimensionality" is used to describe this limitation and what is essentially meant by it, is, that the augmentation of the number (dimension) of variables leads to an exponential augmentation of all the "paths" that need to be calculated and stored, thus leading to major memory and computational time demands.

2.4.3 Direct methods: the sequential approach

In the sequential approach, optimization is carried out in the space of the control variables only while the values of the state variables emerge from the integration of the DAE system of equations at each iteration. The control variables **u**(*t*) are discretized using a well-known discretization scheme and the differential equations, Eq. (2.7), are integrated using standard integration algorithms while both the objective function *J*, the values of the constraints and the required gradients are evaluated (Figs. 2.5, 2.7). This method corresponds to a 'feasible' path approach since the differential equations are satisfied at each step of the optimization. A piecewise constant, piecewise linear or piecewise polynomial approximation of the inputs is often utilized (Fig. 2.6).

The basic procedure is as follows:

a) Parameterize the control variables using a finite number of decision/optimization variables (typically piecewise constant or piecewise polynomial). The vector of decision variables also includes t_f.
b) Choose an initial guess for the decision/optimization variables.
c) Integrate the system states to the final time and compute the objective function *J* and the constraints.
d) Use an optimization algorithm to update the values of the decision variables.
e) Repeat Steps c and d until the objective function is minimized.

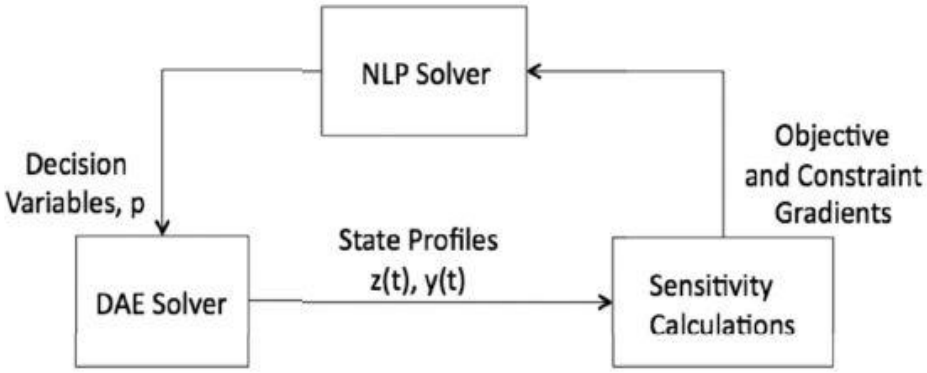

Figure 2.5. Sketch of sequential approach of a DOP [Biegler (2010)].

Often, in the case where a piecewise constant discretization over equally spaced intervals is selected for the control variables, the method is referred to in the literature as *Control Vector Parameterization* (CVP) [Ray (1981), Edgar and Himmelblau (1988)]. This approach has been extended to DAE systems of *index 1* [Vassiliadis et al. (1994a,b)], where the term "index 1" refers to the fact that only first derivatives of variables are included in the system model. Utilization of the CVP approach can be found in many engineering applications e.g. trigeneration systems [Vallianou and Frangopoulos (2012)], electric arc furnace systems [MacRosty and Swartz (2007)], hydrogen storage beds [Kikkinides et al. (2006)] as well as many chemical engineering applications, e.g. reactive distillation [Sargent and Sullivan (1979), Sorensen et al. (1996)], industrial batch processes [Srinivasan et al. (2003a,b)], and batch distillation systems [Furlonge et al. (1999)]. The CVP method is also employed in the current work by the author as it will be presented in the following chapters.

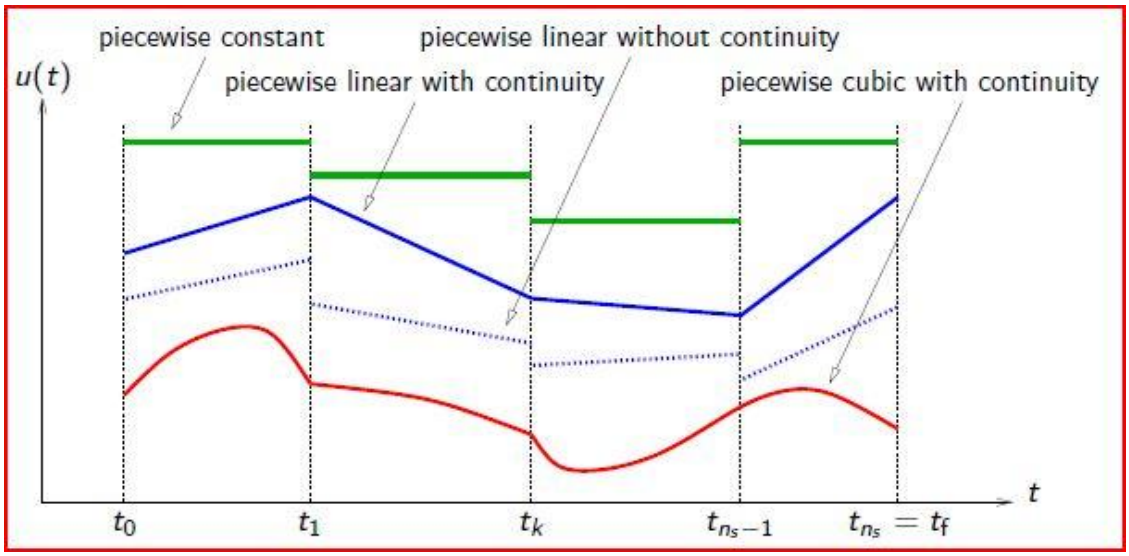

Figure 2.6. Constant, linear and polynomial approximations [Chachuat (2009)].

In order to apply the sequential method to a Dynamic Optimization Problem, the time horizon is divided into *N* time stages and at each stage the control variables are represented with a piecewise constant, linear or polynomial approximation [Biegler (2010), Feehery and Barton (1998), Vassiliadis (1993)]. A very common method is to use a set of Lagrange polynomials, as follows. In each stage *i*, the control variables can be written as

$$u_i(t) = \sum_{k=1}^{Ncol} \ell_k \left(\frac{t - t_{i-1}}{L_i} \right) u_{i,k} \tag{2.74}$$

where $u_{i,k}$ represents the values of control variables in stage *i* at collocation point *k* and ℓ_k can be a Lagrange polynomial of order N_{col} satisfying the condition

$$\psi_k(x_r) = \begin{Bmatrix} 1, \text{ if k = r} \\ 0, \text{ if k} \neq \text{r} \end{Bmatrix} \tag{2.75}$$

While the CVP approach is straightforward to implement, it tends to be slow, especially in dealing with inequality path constraints [Bell et al. (1996)]. This is mainly due to the fact that this feasible path method requires repeated and expensive solution of the differential equations. Furthermore, the quality of the solution is strongly dependent on the parameterization of the control profile [Logsdon and Biegler (1989)].

Concerning the required gradients, they can be calculated by three different strategies: *perturbation*, *direct sensitivity* or *adjoint sensitivity (*Fig. 2.7). Perturbation is the easiest way to implement but may lead to significant errors in the values of the gradients as perturbation methods are often plagued by truncation and round-off errors [Biegler (2010)]. The key idea behind perturbation is the application of a forward difference perturbation to the vector of the optimization variables,

$$\mathbf{u}_j = \mathbf{u} + \delta e_j \tag{2.76}$$

where the *j*th element of vector e_j is 1 and the other elements are zero, and δ is a small perturbation size. Then, the DAE system is solved for the new point and the approximate gradient is calculated:

$$\frac{1}{\delta} \cdot (J(\mathbf{u}_j) - J(\mathbf{u})) = \nabla_{\mathbf{u}_j} J(\mathbf{u}) \tag{2.77}$$

Unlike perturbation, direct and adjoint sensitivity methods can provide gradients with the same level of accuracy as the state profiles. Direct and adjoint sensitivity methods calculate the required gradients by solving the sensitivity equations, which are derived by differentiating the DAE system with respect to the discretized control variables **u**.

In direct sensitivity methods [Caracotsios and Steward (1985), Feehery et al. (1997), Biegler (2010)], gradients are calculated using the sensitivity equations, which are found by differentiating the DAE system after the control vector has been discretized with a parameter set (here we take θ for example)

$$\frac{\partial \frac{d\mathbf{z}}{zt}}{\partial \theta} = \frac{d\frac{\partial \mathbf{z}}{zt}}{\partial \theta} = \left(\frac{\partial F}{\partial \mathbf{z}}\right)\left(\frac{\partial \mathbf{z}}{\partial \theta}\right) + \left(\frac{\partial F}{\partial \mathbf{y}}\right)\left(\frac{\partial \mathbf{y}}{\partial \theta}\right) + \left(\frac{\partial F}{\partial \theta}\right) \tag{2.78}$$

and

$$\left(\frac{\partial G}{\partial \mathbf{z}}\right)\left(\frac{\partial \mathbf{z}}{\partial \theta}\right) + \left(\frac{\partial G}{\partial \mathbf{y}}\right)\left(\frac{\partial \mathbf{y}}{\partial \theta}\right) + \left(\frac{\partial G}{\partial \theta}\right) = 0 \tag{2.79}$$

These equations can be solved, and once the sensitivities of the states with respect to the parameters are known, the gradient of the objective function can be calculated:

$$\frac{dJ}{d\theta} = \left(\frac{\partial J}{\partial \theta}\right) + \left(\frac{\partial J}{\partial \mathbf{z}}\right)\left(\frac{\partial \mathbf{z}}{\partial \theta}\right) + \left(\frac{\partial J}{\partial \mathbf{y}}\right)\left(\frac{\partial \mathbf{y}}{\partial \theta}\right) = 0 \tag{2.80}$$

Because of their desired properties, BDF methods are often applied for the solution of the combined state – sensitivity system. However, in cases where the number of discretization points, and thus the number of variables, becomes very large, direct sensitivity methods may be inefficient. A complementary approach that copes with many optimization variables can be derived based on the combination of variational methods and sensitivity equations, and that approach constitutes the adjoint sensitivity method.

In adjoint sensitivity, the sensitivity equations of the objective function and constraint functions are calculated separately and in cases where the number of variables is greater than the number of equations, this approach is much more efficient than the direct sensitivity approach.

In the first case, the DAE adjoint equations are determined by the Hamiltonian given by Eq. (2.62). The adjoint profiles $\boldsymbol{\lambda}$ and $\boldsymbol{\mu}$ form a semi-explicit DAE that can be solved. Once the system is solved, the gradients are obtained from:

$$\delta J = \int_{t_0}^{t_f} \left(\frac{\partial F}{\partial \mathbf{u}}\boldsymbol{\lambda} + \frac{\partial G}{\partial \mathbf{u}}\boldsymbol{\mu}\right)\delta \mathbf{u}\,\delta t \tag{2.81}$$

If the control profile is discretized into piecewise constants u_i, the gradient can be expressed as

$$\delta J = \int_{t_0}^{t_1} \left(\frac{\partial F}{\partial \mathbf{u}}\boldsymbol{\lambda} + \frac{\partial G}{\partial \mathbf{u}}\boldsymbol{\mu}\right) dt du_1 + \ldots + \int_{t_{N-1}}^{t_N} \left(\frac{\partial F}{\partial \mathbf{u}}\boldsymbol{\lambda} + \frac{\partial G}{\partial \mathbf{u}}\boldsymbol{\mu}\right) dt du_N \tag{2.82}$$

so that

$$\frac{dJ}{du_i} = \int_{t_{i-1}}^{t_i} \left(\frac{\partial F}{\partial \mathbf{u}}\boldsymbol{\lambda} + \frac{\partial G}{\partial \mathbf{u}}\boldsymbol{\mu}\right) dt \tag{2.83}$$

Of course, adjoint methods require the storage of the state profiles for the calculations. Another difficulty is that the state variables boundaries cannot be treated directly. Usually,

when state constraints are imposed, a separate adjoint system is developed for each constraint.

Although there have been a lot of advances in solving sensitivity equations more efficiently [Feehery et al. (1997)], the computational effort remains an expensive part of the optimization algorithm, because the cost of solving the equations is strongly dependent on the number of the variables. As with adjoint methods, direct sensitivity methods too cannot treat directly the bounds on state variables. Also different techniques have been developed for dealing with inequality constraints by penalty functions or by the introduction of slack variables [Jacobson et al. (1971)].

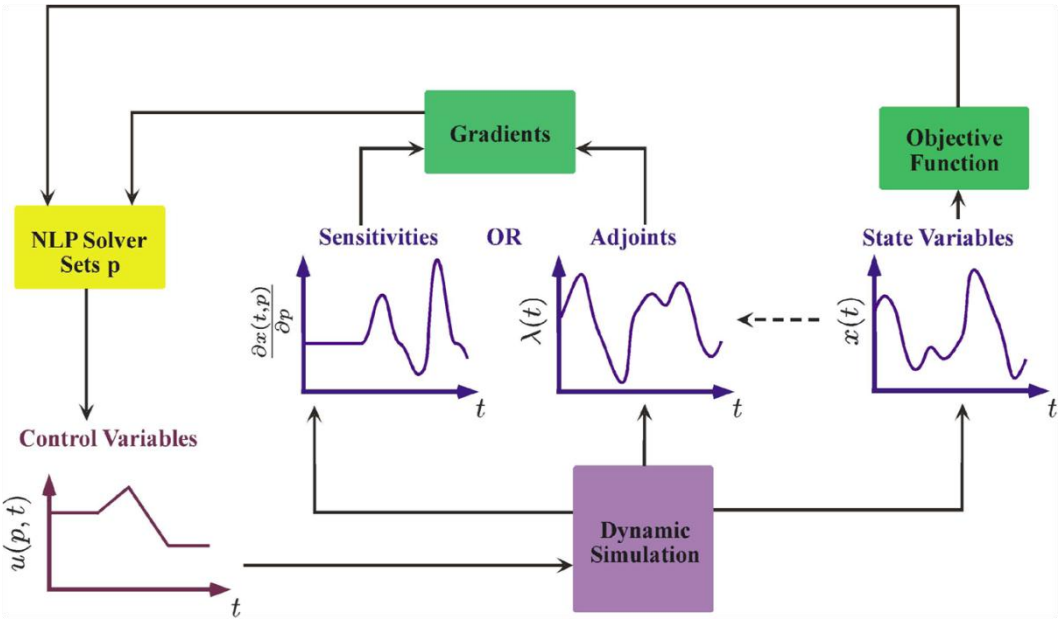

Figure 2.7. Sequential approach of a DOP [Chachuat (2009)].

Before moving on to the simultaneous approach, two important topics must be highlighted. In general the sequential approach produces methods that can be easy to implement and can prove to be very efficient in terms of both computational time and accuracy. However, they suffer from the disadvantage that they are too dependent on the efficiency of the embedded DAE solver that integrates the underlying DAE system. This may pose a real problem in cases where the DAE system suffers of instabilities or in cases where the DAE system is highly non-linear and consists of numerous equations and state variables thus making its integration computationally intensive.

2.4.4 Direct methods: the simultaneous approach

As we have seen above, one of the most important disadvantages of the sequential approach is the fact that the computational intensive integration of the DAE system is performed in each iteration of the optimization procedure, even when the optimization variables are far from the optimal solution. In the simultaneous approach an approximation - discretization of the system of equations is introduced, along with the discretization of the controls, in order to avoid explicit integration for each input profile, thereby reducing the computational burden. Optimization is carried out in the full space of discretized control

and state variables. Thus, in general, the differential equations are satisfied only at the solution of the optimization problem [Vassiliadis et al. (1994a)]. This is therefore called an '*infeasible path*' approach. Simultaneous methods are also known as *direct transcription* methods, as the original dynamic optimization problem is fully transcribed into a, usually, large scale Non-linear Programming Problem (NLP) and solved with an efficient NLP solver.

The basic procedure is as follows [Neuman and Sen (1973), Tsang et al. (1975), Srinivasan et al. (2003a,b)]:

a) Parameterize both the control and the state variables using a finite number of decision/optimization variables (typically piecewise polynomials). The vector of control variables also includes t_f.
b) Discretize the differential equations, Eq. (2.7), i.e. the differential equations are satisfied only at a finite number of time instants (typically via orthogonal collocation). These two steps transform the dynamic optimization problem into a nonlinear programming problem (NLP).
c) Choose an initial guess for the decision variables.
d) Iteratively solve for the optimal set of decision/optimization variables using an NLP code.

Since the above procedure typically leads to a large NLP, efficient numerical methods are necessary to solve this problem [Gill et al. (1981)]. With the development of Successive Quadratic Programming (SQP), reduced space SQP, the interior-point approach and the conjugate gradient methods, the NLP's resulting from the simultaneous approach can be solved efficiently [Biegler (1984), Renfro et al. (1987), Cervantes and Biegler (1998), Biegler et al. (2002)]. The role of finite elements in terms of node locations and breakpoints in order to account for control profile discontinuities is studied in Cuthrell and Biegler (1987), Cuthrell and Biegler (1989) and Logsdon and Biegler (1989).

The use of simultaneous methods requires awareness of the tradeoff between approximation and optimization [Srinivasan et al. (1995)]. It could turn out that a less accurate approximation of the integration gives a better value of the objective function. Thus, since the goal in Step d is merely the optimization of the objective function, the solution obtained could correspond to an inadequate state approximation. Improvement of the integration accuracy requires either introducing accuracy as a constraint or increasing the number of collocation points. Especially when the system is stiff, a very fine grid, which translates into a large number of decision variables, is needed.

As can be seen in Fig. 2.6, the discretization of the control and the state variables can be in a piecewise constant, linear or polynomial fashion. There are mainly two different methods for discretizing the state variables, *multiple shooting* and *collocation on finite elements*.

The direct multiple shooting method [Bock and Platt (1984)] is a hybrid between the sequential and simultaneous methods discussed in the preceding. In this approach, the time interval $[t_0, t_f]$ is divided into N stages. Except for the first stage, the initial conditions of the various stages are considered as decision variables along with continuity constraints stating that the initial states of every stage should match the final ones of the preceding stage. This procedure is an 'infeasible' path method as in simultaneous approaches, while the integration is accurate as in sequential approaches.

More specifically, the control variables are approximated by suitable parameterizations using only a finite set of control parameters. Usually, a constant or linear representation is used. In each stage $i = 0, 1, \ldots, N$ a time transformation is used

$$\theta_i(\tau,\upsilon) = t_i + \tau h_i \tag{2.84}$$

$$t_i = t_0 + \sum_{k=0}^{i-1} h_i \tag{2.85}$$

with τ belonging to [0,1] and $\upsilon = (t_0, d_0, d_1, ...d_{N-1})$ with a dimensionless discretization grid

$$0 = \tau_{i,0} < \tau_{i,1} < ... < \tau_{i,m_i} = 1 \tag{2.86}$$

such that $\theta_i(\tau_i, 0, \upsilon) = t_i$ and $\theta_i(\tau_i, m_i, \upsilon) = t_i + 1$. An approximation of the control u_i is then defined by

$$\hat{u}_i(\tau) = \varphi_{i,j}(\tau, q_{ij}) \tag{2.87}$$

using the local control parameters q_{ij}. For the functions $\varphi_{i,j}$, basic forms are selected, e.g. polynomials. If a constant approximation is selected, we have the form $\varphi_{i,j}(\tau, q_{ij}) = q_{ij}$, while for a linear approximation, the form

$$\varphi_{i,j}(\tau, q_{ij}) = q_{ij}^1 + \frac{\tau - \tau_{ij}}{\tau_{i,j+1} - \tau_{ij}}\left(q_{ij}^2 - q_{ij}^1\right) \tag{2.88a}$$

$$q_{ij} = \begin{bmatrix} q_{ij}^1 \\ q_{ij}^2 \end{bmatrix} \tag{2.88b}$$

is constructed by linear interpolation between the values q_{ij}^1 and q_{ij}^2 at the endpoints of the stage. Using this representation, a continuous approximation can be obtained by imposing continuity equations between the stages. After this, the DAE system is explicitly discretized in each stage i at the points τ_{ij} of the discretization grid using multiple shooting. At each grid point, the values of the state variables $s_{ij} = (s_{ij}^z, s_{ij}^y)$ are chosen as additional unknowns and a set of decoupled initial value problems (IVP) is formulated:

$$\frac{dz_i}{d\tau} = f_i(z_i(\tau), y_i(\tau), \varphi_{i,j}(\tau, q_{ij}), p, \theta_i(\tau,\upsilon))h_i \tag{2.89}$$

$$\begin{aligned} &g_i(z_i(\tau), y_i(\tau), \varphi_{i,j}(\tau, q_{ij}), p, \theta_i(\tau,\upsilon)) - \\ &g_i(s_{ij}^z, s_{ij}^y, \varphi_{i,j}(\tau_{ij}, q_{ij}), p, \theta_i(\tau_{ij},\upsilon)) = 0 \end{aligned} \tag{2.90}$$

with initial conditions

$$z_i(\tau_{ij}) = s_{ij}^z, y_i(\tau_{ij}) = s_{ij}^y \tag{2.91}$$

By including the continuity conditions for the differential variables into the NLP and the consistency conditions

$$g_i(s_{ij}^z, s_{ij}^y, \varphi_{i,j}(\tau_{ij}, q_{ij}), p, \theta_i(\tau_{ij}, \upsilon)) = 0 \tag{2.92}$$

as equality constraints, the final solution satisfies the DAE system. With this approach, the inequality constraints for the states and controls can be imposed directly at the grid points.

The resulting NLP is solved using an SQP-type method that requires the gradient of the objective function and the constraints Jacobians at each iteration. For almost all the different explicit functions, the corresponding derivatives can be easily calculated. Further extensions of the direct multiple shooting methods to DAE systems are described in Schulz et al. (1998).

Another method of discretization of the state variables and the DAE system is collocation on finite elements. In this method, the time horizon is divided into intervals (finite elements) and the continuous time problem is converted into an NLP problem by approximating the profiles to a family of polynomials on each finite element. Different polynomial representations are used in the literature. Due to their accuracy, formulations based on *orthogonal collocation methods* are generally preferred [Carey and Finlayson (1974), Biegler (2010)]. Orthogonal collocation methods are a special class of the Implicit Runge-Kutta (IRK) methods, where orthogonal polynomials are used to approximate the state profiles in each finite element. The resulting large scale NLP allows a great deal of sparsity and structure. Moreover, difficulties related to the efficiency of the embedded DAE solver are avoided and sensitivity calculations for the derivatives are replaced by direct gradient and Hessian evaluations within the NLP formulation. Furthermore, in more advanced formulations, the length of the finite elements themselves can be treated as optimization variables, thus making the method more efficient in problems with instabilities. Here a monomial basis representation [Bader and Ascher (1987)] for the differential profiles is used as an example.

$$z(t) = z_{i-1} + h_i \sum_{k=1}^{Ncol} \Omega_k \left(\frac{t - t_{i-1}}{h_i} \right) \frac{dz}{dt_{i,k}} \tag{2.93}$$

where z_{i-1} is the value of the differential variable at the beginning of element i, h_i is the length of the element i, $dz/dt_{i,k}$ is the value of its first derivative in element i at the collocation point k, and Ω_k is a polynomial of order N_{col} satisfying the conditions

$$\Omega_k(0) = 0 \text{ for } q = 1, ..., N_{col} \tag{2.94a}$$

$$\frac{d}{dt}\Omega_k(\rho_r) = \begin{Bmatrix} 1, \text{ if k = r} \\ 0, \text{ if k} \neq \text{r} \end{Bmatrix} \text{ for } q = 1, ..., N_{col} \tag{2.94b}$$

with ρ_r, the collocation point within each element. This representation is recommended because of smaller rounding errors. One disadvantage of the above representation is that state path constraints can only be enforced directly at the mesh points dividing each element. However the problem can be solved by adding bounded algebraic variables. The control and state variables are approximated using Lagrange polynomials of the form

$$y(t) = \sum_{k=1}^{Ncol} \ell_k \left(\frac{t - t_{i-1}}{h_i} \right) y_{i,k} \tag{2.95}$$

$$u(t) = \sum_{k=1}^{Ncol} \ell_k \left(\frac{t - t_{i-1}}{h_i} \right) u_{i,k} \tag{2.96}$$

with

$$\psi_k(\rho_r) = \begin{Bmatrix} 1, \text{ if k = r} \\ 0, \text{ if k} \neq \text{r} \end{Bmatrix} \tag{2.97}$$

Many authors also prefer to use low order Lagrange polynomials for the differential variables as well. Orthogonal collocation on finite elements will also be discussed in more detail in the next section.

Indirect methods are of no specific interest in this text, thus the next Section focuses on the formulation and implementation of Direct methods, in order to gain a better understanding of the sequential and the simultaneous approach and examine the advantages and drawbacks of each by implementing them to several "simple" examples of DOPs selected from the literature.

2.5 Formulation of Customized Direct Methods

In the present Section, a method based on the sequential approach, which we will from now on refer to as *Control Vector Parameterization (CVP)*, and a method based on the simultaneous approach, which we will from now on refer to as *Radau Collocation*, are developed and stated mathematically in more detail. Next, both of these methods will be applied in five, selected from the literature, dynamic optimization problems. The results are presented in comparison with the original literature results in Section 2.6. Several conclusions are drawn from this procedure and valuable insight considering the pros and cons of each approach and the correct ways of implementing them is gained.

2.5.1 Formulation of a sequential approach: the CVP method

A dynamic optimization method based on the sequential approach, and more specifically based on the Control Vector Parameterization (CVP) scheme is developed. As in all sequential methods, also in CVP, the control variables are discretized and each variable at each time step is treated as an optimization variable, whereas the state variables are calculated at each iteration by solving the system of differential equations that describe the problem. The necessary gradients are calculated by the NLP optimization software. Discretization is performed via a piecewise constant discretization scheme over equally spaced time intervals which, as presented in the previous Section, is the main characteristic of all CVP methods.

The system of differential equations that constitute the model of the system of each problem can be solved with the help of a variety of integration methods that exist in the literature. For reasons of simplicity the *first order Euler Method for integration* is used as a first approach.

The Euler Method is a first-order numerical procedure for solving ordinary differential equations (ODEs) with a given initial value. It is the most basic explicit method for numerical integration of ordinary differential equations and is the simplest Runge–Kutta method. The Euler method is named after Leonhard Euler, who treated it in his book Institutionum Calculi Integralis [Kentall (1989)]. The Euler method is a first-order method, which means that the local error (error per step) is proportional to the square of the step size, and the global error (error at a given time) is proportional to the step size. It also suffers from stability problems. For these reasons, the Euler method is not often used in practice. It serves as the basis to construct more complicated methods. Here, however, we apply the Euler method to solve relatively simple systems of ODEs and of course it is expected that a more sophisticated method should be applied in order to tackle with more complicated problems.

The Euler method can be summarized as follows: suppose that we want to approximate the solution to the first order initial value problem:

$$y'(t) = f(y(t), t) \tag{2.98}$$

with initial value

$$y(t_0) = y_0 \tag{2.99}$$

We choose a value h for the size of the time step and set

$$t_n = t_0 + n \cdot h \tag{2.100}$$

One step of the Euler method from t_n to $t_{n+1} = t_n + h$ is

$$y_{n+1} = y_n + h \cdot f(y_n, t_n) \tag{2.101}$$

Thus knowing the initial value y_0 at $n = 0$ the profile of y(t) can be constructed.

Finally, the resulting NLP static optimization problem is solved with the SNOPT [Gill et al. (1997)] version 7.0 software. A schematic of the algorithm of the method is depicted in Figure 2.8.

SNOPT is a set of Fortran subroutines designed to minimize a linear or nonlinear function subject to bound on the variables and sparse linear or nonlinear constraints. SNOPT uses a sequential quadratic programming (SQP) algorithm. Search directions are obtained from QP subproblems that minimize a quadratic model of the Lagrangian function subject to linearized constraints. An augmented Lagrangian merit function is reduced along each search direction to ensure convergence from any starting point.

SNOPT requires relatively few evaluations of the problem functions. Hence it is especially effective if the objective or constraint functions (and their gradients) are expensive to evaluate.

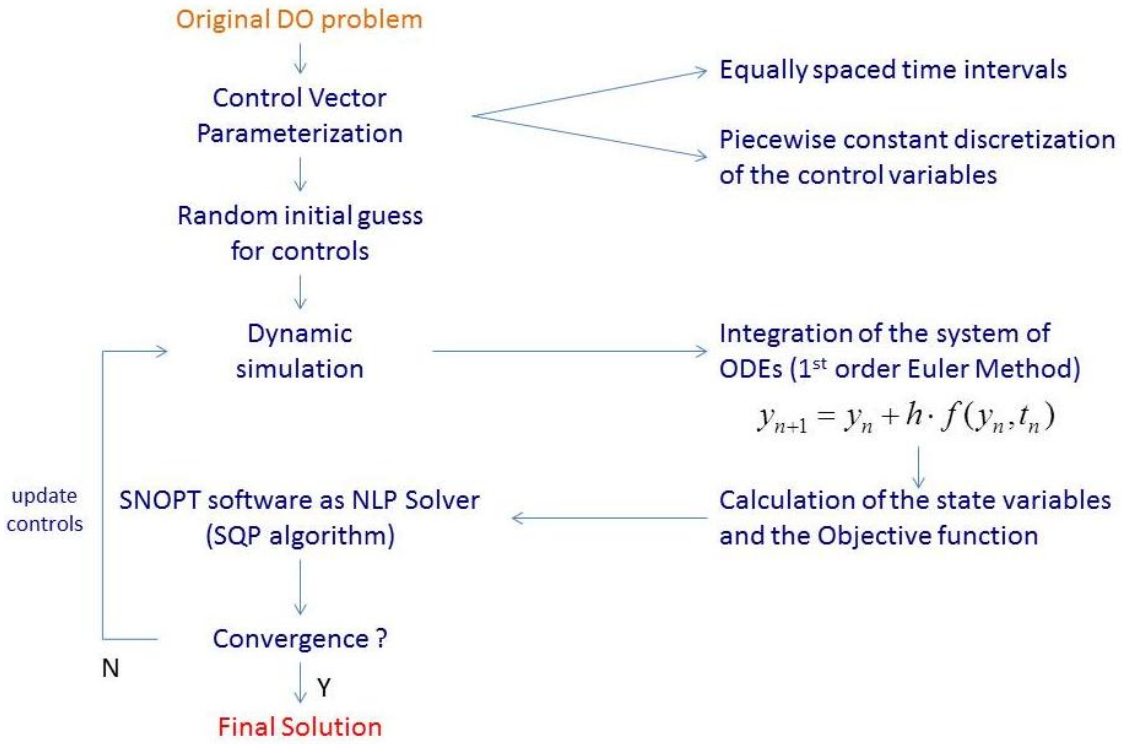

Figure 2.8. The algorithm of the Control Vector Parameterization method.

2.5.2 Formulation of a simultaneous approach: the Radau collocation method

In the same way as in the previous section, a simultaneous approach is now chosen to be developed. As has been explained earlier, the simultaneous approach belongs to the family of direct methods, where the original DOP is fully transcribed into a large scale NLP problem and the resulting static optimization problem is treated via a static optimization algorithm/large scale NLP solver.

Here the simultaneous approach based on orthogonal collocation methods over finite elements will be applied [Biegler (2010), Carey and Finlayson (1974)]. These methods can also be considered as a special class of the Implicit Runge-Kutta (IRK) methods [Suli and Mayers (2003)]. The main idea behind orthogonal collocation methods is the use of piecewise polynomial representations for the representation of the control and the state variables in each finite element. Thus, the system of differential equations is solved exactly at selected points in time. To be more specific, we consider the polynomial representation/ approximation of a state variable, i.e $z(t)$ over a single finite element of length h_i as shown in Fig. 2.9.

The polynomial that approximates $z(t)$ is denoted as $z^K(t)$ and is in essence a polynomial of order K+1. A number of various ways can be selected for the representation of this polynomial (power series, Newton divided differences or B-splines) [Ascher et al. (1995), Betts (2010)], however representations based on Lagrange interpolation [Hazewinkel (2001)] are in general selected in order to incorporate the same bounds and constraints of the variables to the polynomial coefficients as well.

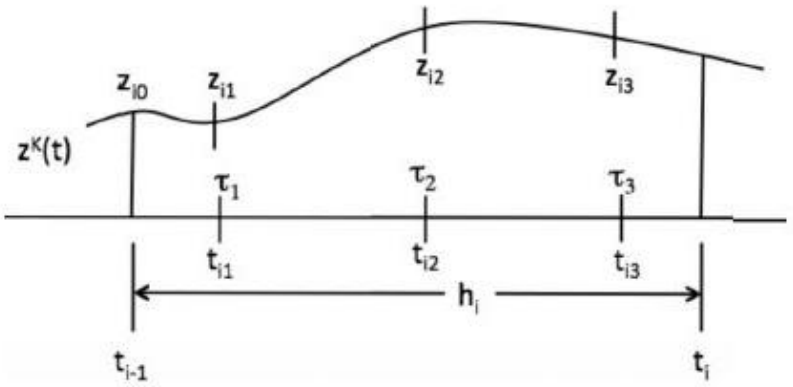

Figure 2.9. Polynomial approximation for a state profile across a finite element [Biegler (2010)].

In this work, K+1 interpolation points in each element *i* are chosen and the state variable *z*(t) is represented as

$$z^K(t) = \sum_{j=0}^{K} \ell_j(\tau) \cdot z_{ij} \tag{2.102}$$

with

$$t = t_{i-1} + h_i \cdot \tau, \text{with } \tau \in [0,1] \text{ and } t \in [t_{i-1}, t_i] \tag{2.103}$$

where $\ell_j(t)$ are the Lagrange polynomials denoted as

$$\ell_j(\tau) = \prod_{\substack{k=0 \\ k \neq j}}^{K} \frac{(\tau - \tau_k)}{(\tau_j - \tau_k)} \tag{2.104}$$

h_i is the length of each element and τ_j are the selected collocation points with $\tau_0 = 0, \tau_j < \tau_{j+1}, j = 0,...,K-1$. This polynomial representation is specifically chosen due to its very desirable property that the value of the polynomial in each selected collocation point is in fact the value of its respective coefficient. In mathematical terms this is denoted as follows:

Let $\tau = \tau_j$, then time t is

$$t_{ij} = t_{i-1} + h_i \cdot \tau_j, \text{with } \tau_j \in [0,1] \text{ and } t_{ij} \in [t_{i-1}, t_i] \tag{2.105}$$

and by substituting in Eq. (2.102) and performing the necessary algebra we have

$$z^K(t_{ij}) = \sum_{j=0}^{K} \ell_j(\tau_j) \cdot z_{ij} = z_{ij} \tag{2.106}$$

due to the following property of the Lagrange polynomials:

$$\ell_j(\tau_i) = \prod_{\substack{k=0 \\ k\neq j}}^{K} \frac{(\tau_i - \tau_k)}{(\tau_j - \tau_k)} = \begin{Bmatrix} 0, & i \neq j \\ 1, & i = j \end{Bmatrix} \tag{2.107}$$

As concerning the time derivatives, they can be represented as sums of the derivatives of the Lagrange polynomials simply by applying the derivative in Eq. (2.102):

$$\frac{dz^K(t)}{dt} = \sum_{j=0}^{K} \ell'_j(\tau) \cdot z_{ij} \tag{2.108}$$

The point of this procedure is the determination of the coefficients z_{ij} that approximate the solution to the DAE system. To achieve this, the formulas given by Eqs. (2.102) and (2.108) are substituted to the corresponding differential equation of the state z(t), Eq. (2.109), and the resulting algebraic equations are enforced in the interpolation points τ_k as it is shown in Eq. (2.110). Here we chose a simple but fairly general differential equation for z(t) in order to facilitate the presentation:

$$\frac{dz(t)}{dt} = f(z(t), t) \tag{2.109}$$

$$\frac{dz^K(t_{ik})}{dt} = f(z^K(t_{ik}), t_{ik}), \quad \text{k=1, ..., K} \tag{2.110}$$

which results in

$$\sum_{j=0}^{K} \ell'_j(\tau_k) \cdot z_{ij} = f(z_{ij}, t_{ik}), \quad \text{k=1, ..., K} \tag{2.111}$$

after the necessary substitutions. The K equations that are given by the formula of Eq. (2.111) are known as *collocation equations* and are merely algebraic equations that can be incorporated directly into the NLP formulation of the dynamic optimization problem.

In order for the presentation of our simultaneous approach to be complete, there are two remaining issues that need to be addressed: the determination of the collocation points τ_k and the expression for the derivatives of the Lagrange Polynomials $\ell'_j(\tau_k)$.

Gauss-Radau collocation

The determination of the collocation points τ_k plays an important role in order to obtain the most accurate approximation of the control/state variables. So the question of how we shall determine the collocation points instantly arises. The answer to this question is given by a theorem known as theorem of Accuracy of Gaussian Quadrature [Abramowitz and Stegun (1965), Laurie (2001), Stoer and Bulirsch (2002)], which in short states that the method of orthogonal collocation gives an exact solution to the differential equation, Eq. (2.109), if $f(z(t), t)$ is a polynomial of order 2K and τ_j are the roots of a Kth degree polynomial, P_K(t), with the property

$$\int_0^1 P_j(\tau)\cdot P_{j'}(\tau)d\tau = 0, \quad \text{j=0,...K-1, j'=1,...K for j} \neq \text{j'} \tag{2.112}$$

The proof of this theorem is of no direct importance in this text, so it is not presented here. The polynomial $P_K(t)$ is known as the Gauss-Legendre polynomial with the orthogonality property denoted by Eq. (2.112). Several choices of $P_K(t)$ are known in the literature that of course give different values for τ_k. In this work we focus on Gauss-Radau collocation [Wang and Guo (2012), Biegler (2010), Garg et al. (2010)], which means that the Gauss-Radau roots as given in Table 2.2 are utilized as collocation points. The choice of Gauss-Radau collocation was made due to many reasons. The first one is the fact that the τ_K 'th Radau root is always equal to 1, thus the point that determines the end of each element is a collocation point itself, a fact that simplifies a lot the necessary algebra. Another reason is the fact that Gauss-Radau collocation is compatible with the NLP formulation and has, always according to the literature, decent stability properties. More specifically, Gauss-Radau collocation is said to be *AN-stable* or equivalently algebraically stable, which results in no stability limitation for h_i in stiff problems (a definition of A-stability and AN-stability can be found in Appendix A). Finally, a very important reason lies in the fact that Radau collocation is among the highest order methods. The truncation error is evaluated as $O(h^{2K-1})$, of course only for the collocation points z_{ij} and **not** for the intermediate points.

Table 2.2. Gauss-Radau roots as collocation points [Biegler (2010)].

Degree K	Radau Roots
1	1.000000
2	0.333333 1.000000
3	0.155051 0.644949 1.000000
4	0.088588 0.409467 0.787659 1.000000
5	0.057104 0.276843 0.583590 0.860240 1.000000

Derivatives of the Lagrange Polynomials

Another important issue that needs to be addressed is the calculation of the derivatives of the states/controls in the collocation points which, as we showed earlier, Eq. (2.108), is deduced from the calculation of the derivatives of the Lagrange polynomials at those points. For the calculation of the derivatives of the Lagrange polynomials we analyze the multiple:

$$\ell_j(t)=\prod_{\substack{i=0\\ i\neq j}}^{K}\frac{t-t_i}{t_j-t_i}=\frac{t-t_0}{t_j-t_0}\cdot\frac{t-t_1}{t_j-t_1}\cdots\frac{t-t_{j-1}}{t_j-t_{j-1}}\cdot\frac{t-t_{j+1}}{t_j-t_{j+1}}\cdots\frac{t-t_K}{t_j-t_K} \tag{2.113}$$

By differentiating we have:

$$\ell'_j(t)=\left(\frac{t-t_0}{t_j-t_0}\cdot\frac{t-t_1}{t_j-t_1}\cdots\frac{t-t_{j-1}}{t_j-t_{j-1}}\cdot\frac{t-t_{j+1}}{t_j-t_{j+1}}\cdots\frac{t-t_K}{t_j-t_K}\right)'=$$

$$\sum_{n=0}^{K}\left(\left(\frac{t-t_n}{t_j-t_n}\right)'\cdot\prod_{\substack{i=0\\ i\neq j,n}}^{K}\left(\frac{t-t_i}{t_j-t_i}\right)\right)=\sum_{n=0}^{K}\left(\left(\frac{1}{t_j-t_n}\right)\cdot\prod_{\substack{i=0\\ i\neq j,n}}^{K}\left(\frac{t-t_i}{t_j-t_i}\right)\right)\Rightarrow$$

$$\ell'_j(t)=\sum_{\substack{m=0\\ m\neq i,j}}^{K}\left(\frac{1}{t_j-t_m}\cdot\prod_{\substack{i=0\\ i\neq j}}^{K}\frac{t-t_i}{t_j-t_i}\right) \tag{2.114}$$

Equation (2.114) provides us with a subtle formula to calculate $\ell'_j(t_k)$ at the collocation points.

Of course, the above formulation can be used in the case of one single element as well as for multiple elements. A final detail that needs to be clarified is what happens with the continuity of the controls/states across the element boundaries in case we use multiple elements. The answer to this question is simple: continuity is forced in the state profiles (and some cases in control profiles too, as has been done in this work). In the case of N elements, this is written as

$$z_{i+1,0}=\sum_{j=0}^{K}\ell_j(\tau_K)\cdot z_{ij}=\sum_{j=0}^{K}\ell_j(1)\cdot z_{ij}=z_{i,K},\ \text{for i=1, ..., N-1} \tag{2.115}$$

with the initial value

$$z_{1,0}=z(0) \tag{2.116}$$

and maybe the final value

$$z_{N,K}=z_f \tag{2.117}$$

Whether continuity should be enforced on the control profiles too depends on the problem at hand. For example, considering the DOPs examples solved in the next chapter of this text, there is no reason why the control variables profiles should not be (enforced to be) continuous across elements. In those problems control and state variables are expected to be continuous likewise. However, DOPs exist where control profiles should be allowed to be discontinuous at the beginning point of each element (τ=0). Typical examples of these are DOPs on systems that involve multistage/multiphase processes. In this case, each

element may be set to represent a different stage/phase, so it is not necessary to enforce continuity between elements, as this will prevent the NLP solver to capture with accuracy an interesting and possibly correct solution of the problem at hand.

The resulting NLP static optimization problem is solved with the SNOPT version 7.0 software. Details about the SNOPT software have been given in Section 2.5.1. In the next section, simple examples of DOPs chosen from the literature are selected and solved utilizing the two approaches that have been described above.

2.6 Application of the Customized Direct Methods to Example Problems

A series of dynamic optimization problems are selected from the literature and solved by implementation of the direct methods that have been presented in the previous section. Many dynamic optimization problems are available as "simple examples" or even "benchmarks" in the literature. In the following, five relatively simple or, to be more exact, not very complicated dynamic optimization problems are presented. All five problems can be categorized as "optimal trajectory" problems based on the categorization proposed in Section 2.3. Each example is solved by the two direct methods described in Section 2.5 of this chapter.

The five dynamic optimization problems that have been selected to serve as examples in order to evaluate the performance of the Control Vector Parameterization (CVP) and the Radau Collocation methods are: the Van der Pol oscillator problem, the Car optimization problem, the Batch reactor problem, the Continuously Stirred Tank Reactor (CSTR) problem and a Mathematical example problem with no known real-life problem relation. In the following of this chapter, each problem will be stated and then solved first by CVP and then by Radau Collocation, followed by relative comments upon the results. However, before we proceed, two important issues must be noted.

Considering the CVP method, an important parameter of the algorithm is the number of discretization points that the user selects for the control variables. All five problems have been solved for N=20, 50, 100 and 200 discretization points for each control variable. However only the results with N=100 points are presented, as they were found to produce smoother plots for the state and control variables and more accurate values for the objective function and the constraints than the cases with N=20 and N=50 points. The case with N=200 points, practically adds no more accuracy in the results, while it costs more on computational time and memory.

For the Radau collocation method, it is clarified that different combinations of collocation points and elements have been used in order to study the functionality of this method. The related results are however presented only in the first example, the Van der Pol oscillator. In the remaining examples only the results of the best combination are presented and compared to the results from the literature and from the CVP method. A useful aspect that the reader must keep in mind in order to better comprehend the results given by the Radau Collocation method, is that accuracy in the solution of the DAE system is promised **only** in the collocation points and not the intermediate ones, that are calculated by the formula of the polynomial expression of Eq. (2.102).

2.6.1 Van der Pol oscillator problem

The van der Pol oscillator problem in various alternative statements has been solved by many authors [Vassiliadis V. S. (1993), Tanartkit and Biegler (1995), Banga et al. (1998)]. The problem tackled here is set with two inequality constraints and one equality constraint. The system with the integral term of the cost function is described with the following set of differential equations and the aim of the optimization is to minimize the cost function in a fixed final time $t_F = 5$:

$$\min_u J_0 = x_3(t_F) \tag{2.118}$$

subject to

$$\dot{x}_1 = (1 - x_2^2)x_1 - x_2 + u \tag{2.119}$$

$$\dot{x}_2 = x_1 \tag{2.120}$$

$$\dot{x}_3 = x_1^2 + x_2^2 + u^2 \tag{2.121}$$

$$-0.4 \le x_1(t) \le 0 \tag{2.122}$$

$$-0.3 \le u \le 1 \tag{2.123}$$

with initial conditions,

$$\begin{aligned} x_1(0) &= 0 \\ x_2(0) &= 1 \\ x_3(0) &= 0 \\ u(0) &= 0.7 \end{aligned} \tag{2.124}$$

and final conditions:

$$x_2(t_F) = -0.1 \tag{2.125}$$

The importance of this problem lies in the fact that, although it is not a very complex system, it poses some difficulty due to non-linearity, Eq. (2.119) and the presence of a final time constraint for the variable x_2, Eq. (2.125).

Solution with the CVP method

The time step is set in 0.05 and 101 discretization points were used. The calculation was completed in 0.94 seconds and the optimal objective function value was found at 3.0106587, whereas the best objective function value from the literature is found to be 2.96099523. In Figs. 2.10 and 2.11 the optimal control and states plots are presented in comparison to the plots taken from the literature.

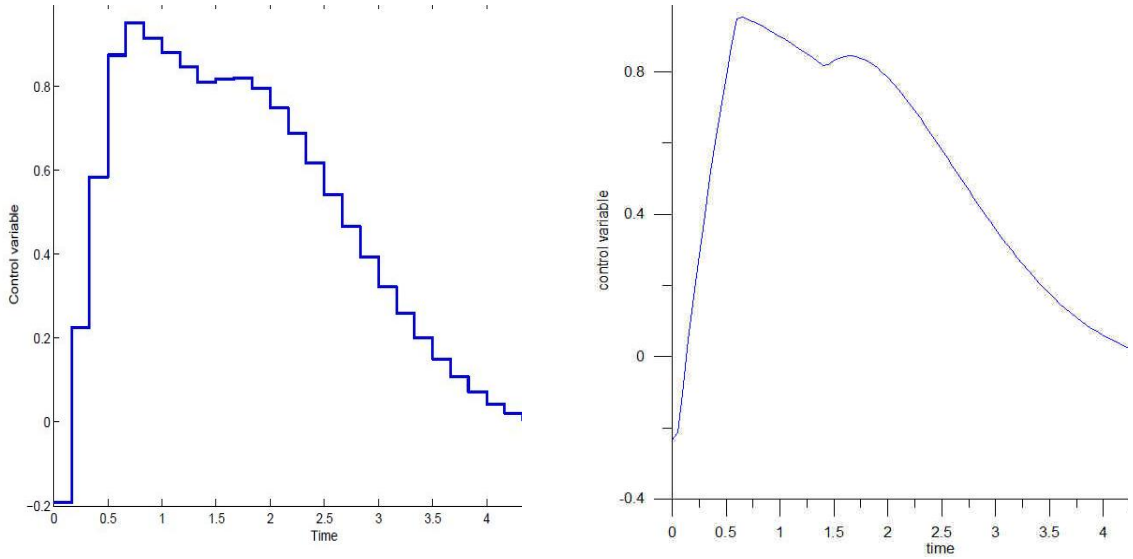

(a) (b)

Figure 2.10. Optimal trajectory of control variable from (a) literature (b) CVP method.

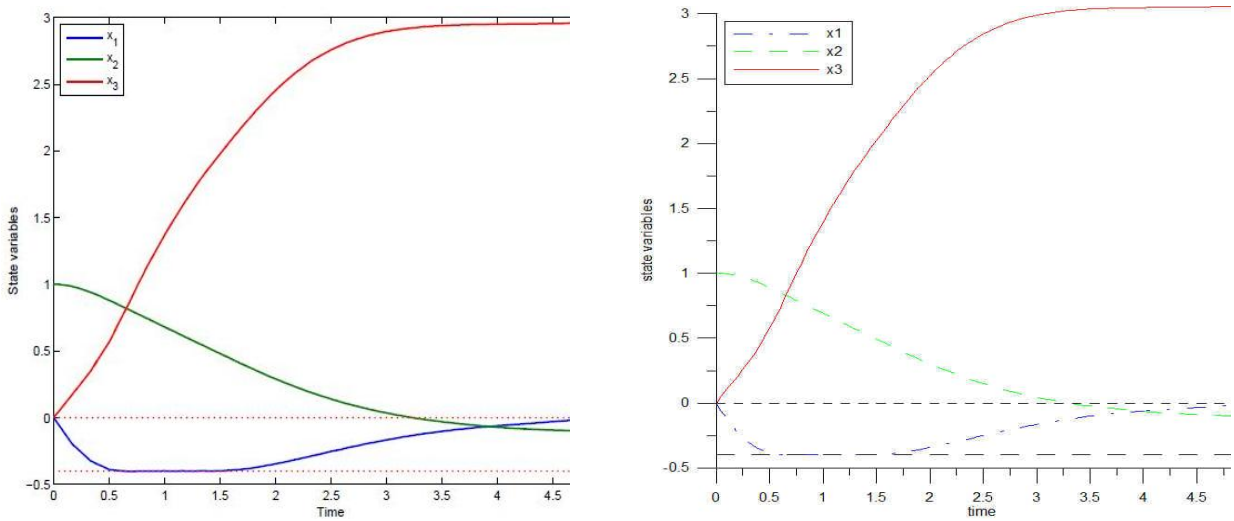

(a) (b)

Figure 2.11. Optimal trajectory of state variables from (a) literature (b) CVP method.

It is noted that the results from the CVP method are in good agreement with the best known results from the literature.

Solution with the Radau Collocation method

In Figs. 2.12 and 2.13, the plots for the control and the states found in the literature in comparison with the plots produced by the various combinations of number of elements and collocation points via the Radau Collocation method are presented.

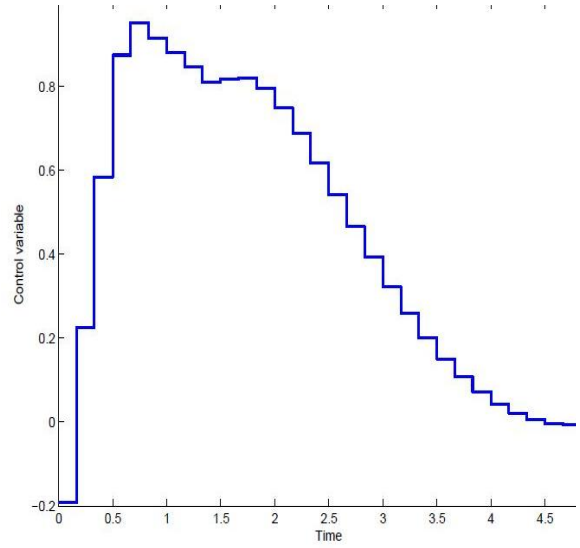

(a)

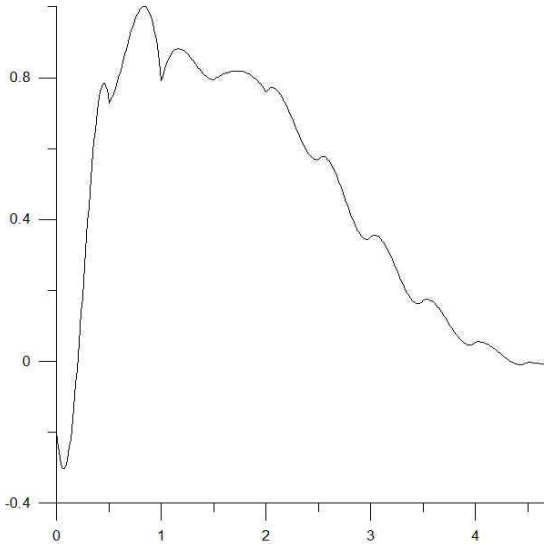

(b)

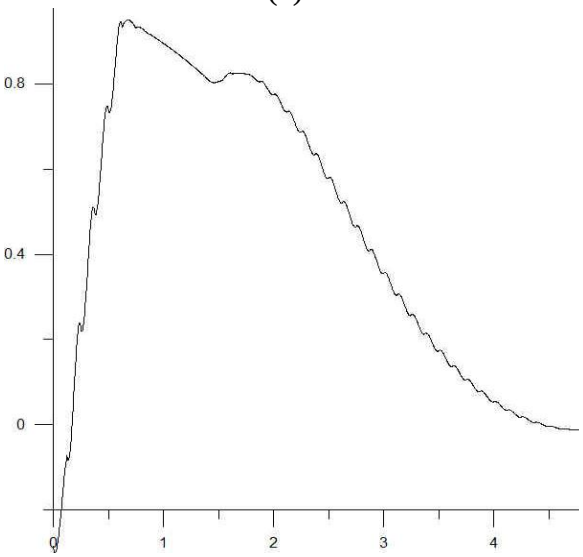

(c)

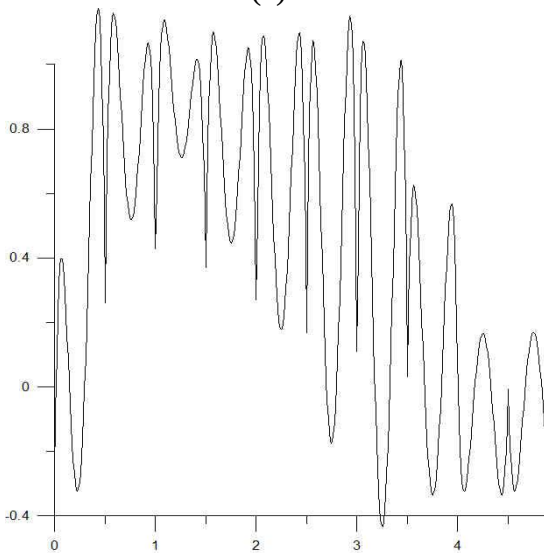

(d)

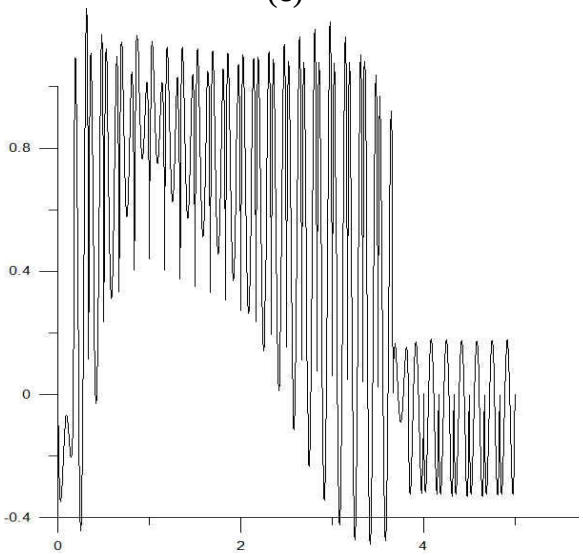

(e)

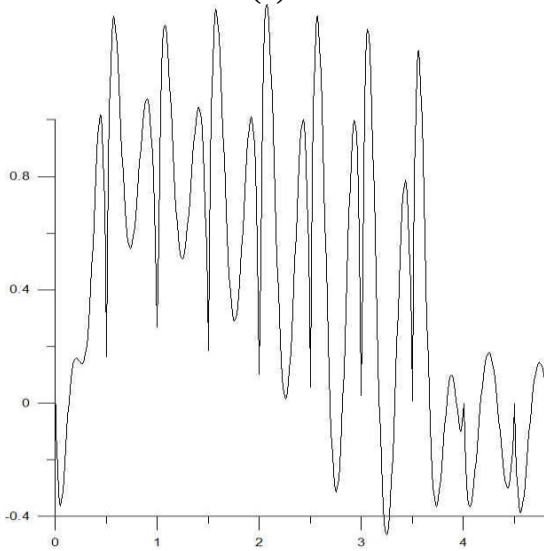

(f)

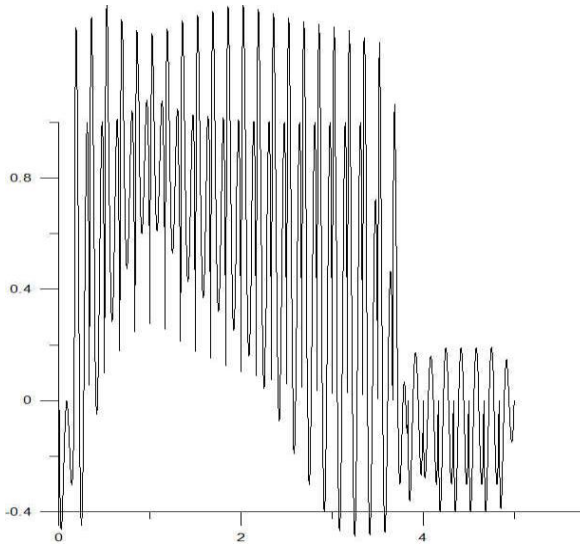

(g)

Figure 2.12. Optimal trajectory of control variable from (a) literature, and with Radau method with (b) K=3, N=10; (c) K=3, N=40; (d) K=4, N=10; (e) K=4, N=30; (f) K=5, N=10;(g) K=5, N=30.

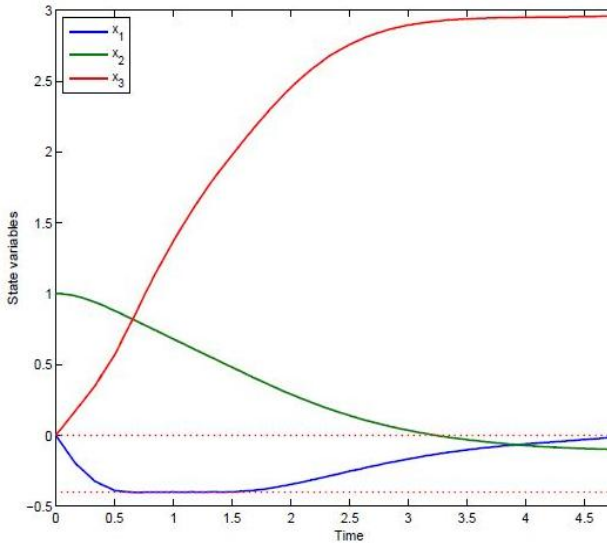

(a)

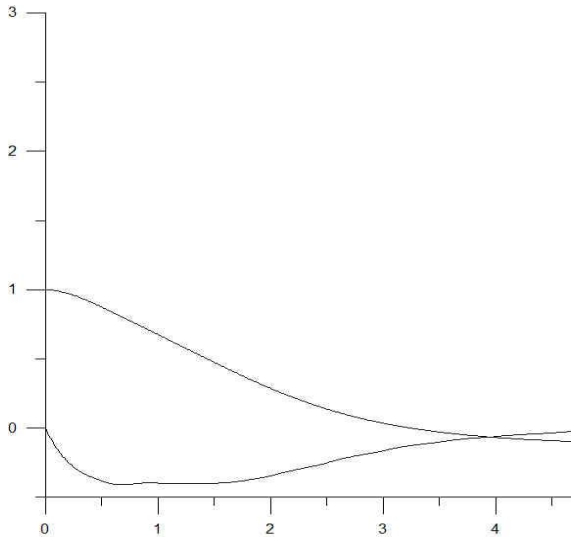

(b)

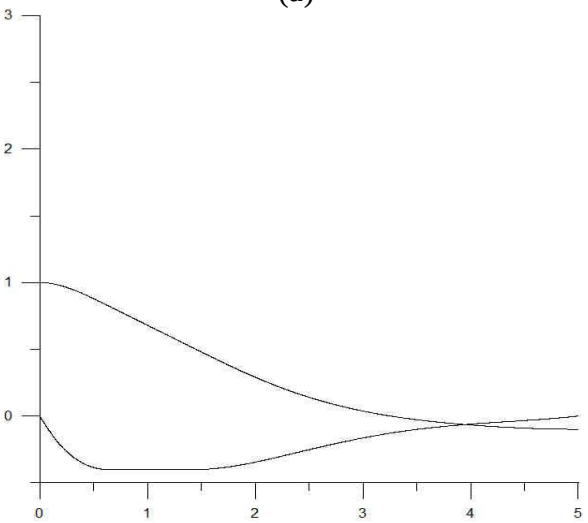

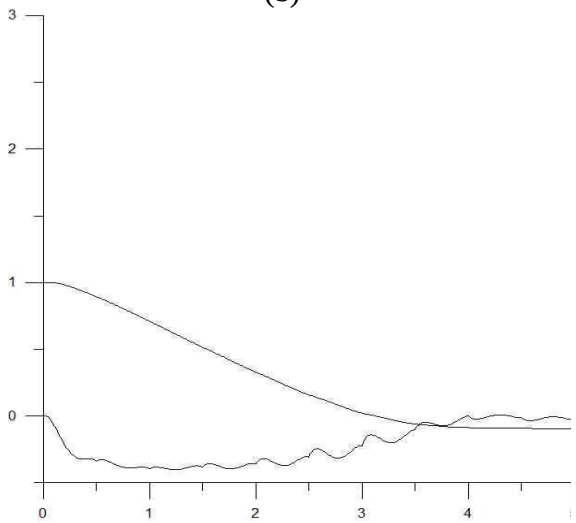

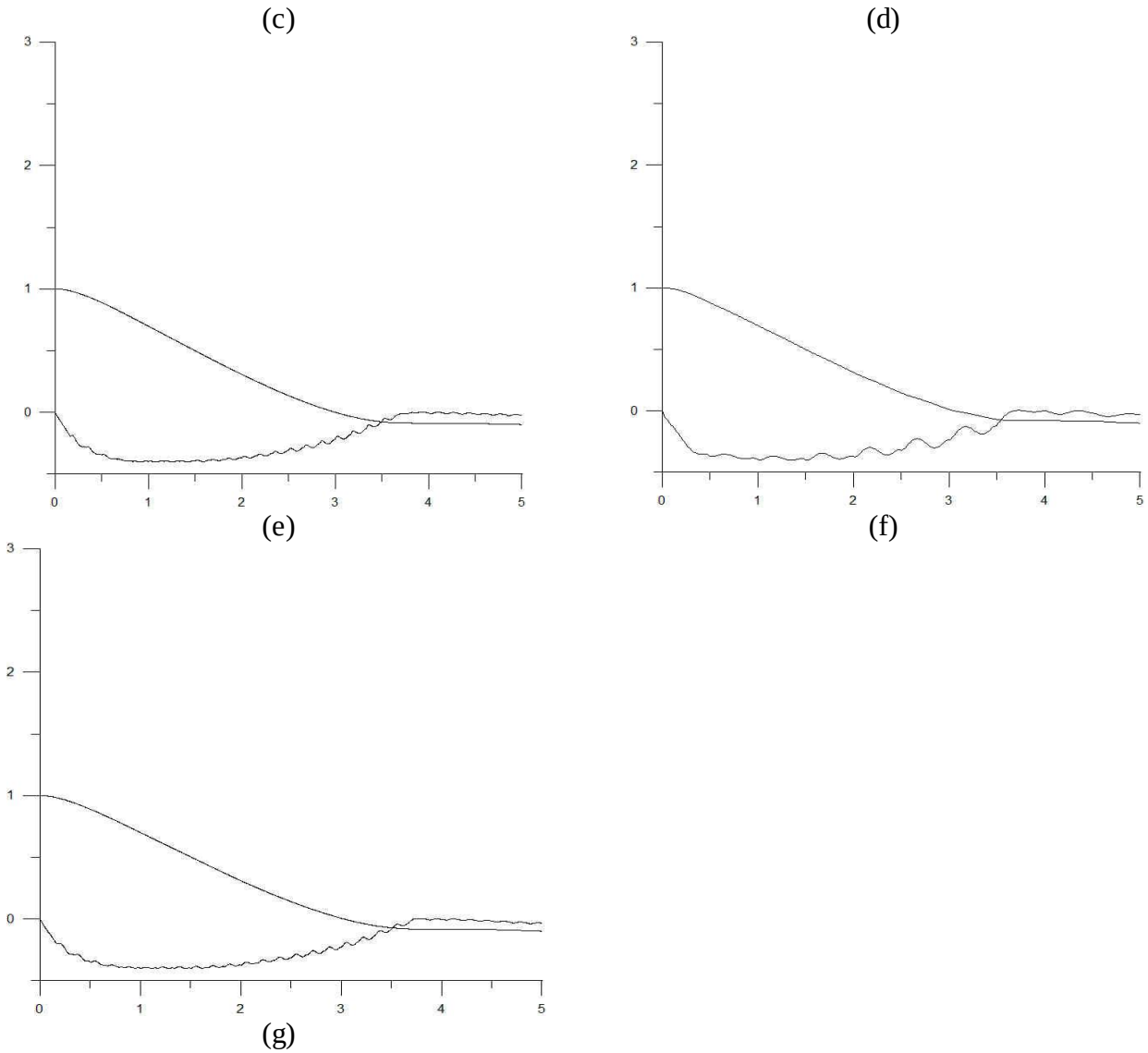

Figure 2.13. Optimal trajectory of state variables from (a) literature, and with Radau method with (b) K=3, N=10; (c) K=3, N=40; (d) K=4, N=10; (e) K=4, N=30; (f) K=5, N=10; (g) K=5, N=30.

It can be deduced from Figures 2.12 and 2.13 that the most accurate results are obtained with K=3 collocation points with accuracy increasing while the number of elements is increased, which is expected. The results with K=4 and K=5 collocation points are not in fact as disappointing as they seem. This can be explained by the comment stated earlier, which claims that the method used to solve the differential system of equations promises very good accuracy at the collocation points, but not at the intermediate ones. The intermediate points are calculated via the use of the polynomial expression, and can easily deviate from reality if few elements and many collocation points are used. Furthermore, the more collocation points we use, the more the dimension of the problem per element is increased thus leading to inability of the NLP solver to operate efficiently. More about this aspect of Radau Collocation will be explained later in this section.

In the case K=3 and N=40 (where the best result is observed) the calculation was completed in 0.79 seconds and the optimal objective function value was found equal to 2.9615007.

In the next examples, although all the above combinations have been calculated too, only the best one (which is also the case with K=3 collocation points and N=40 elements) is plotted in comparison with the literature results.

2.6.2 Car optimization problem

A broadly referred dynamic optimization problem is that of starting and stopping a car in minimum time for a fixed distance (300 units) [Longsdon and Biegler (1989), Dadebo and McAuley (1995), Rajesh et al. (2001)]:

$$\min_u J_0 = t_F \tag{2.126}$$

subject to

$$\dot{x}_1 = u \tag{2.127}$$

$$\dot{x}_2 = x_1 \tag{2.128}$$

$$-2 \le u \le 1 \tag{2.129}$$

with initial conditions

$$\begin{aligned} x_1(0) &= 0 \\ x_2(0) &= 0 \end{aligned} \tag{2.130}$$

and final conditions

$$\begin{aligned} x_1(t_F) &= 0 \\ x_2(t_F) &= 300 \end{aligned} \tag{2.131}$$

where

$x_1(t)$ velocity,

$x_2(t)$ distance,

$u(t)$ acceleration (control variable).

The main interest in this problem lies in the fact that it is an open-ended dynamic optimization problem, where the value of the final time is unknown and in fact an optimization variable too.

Solution with the CVP method

In Figs. 2.14-2.16, the plots for acceleration, distance and velocity found in the literature are presented in comparison to the plots produced by the CVP method. Moreover, the best value for the objective function found in the literature is 30 (time units) which also comes in agreement with our calculations with a minor numerical error of 0.1%.

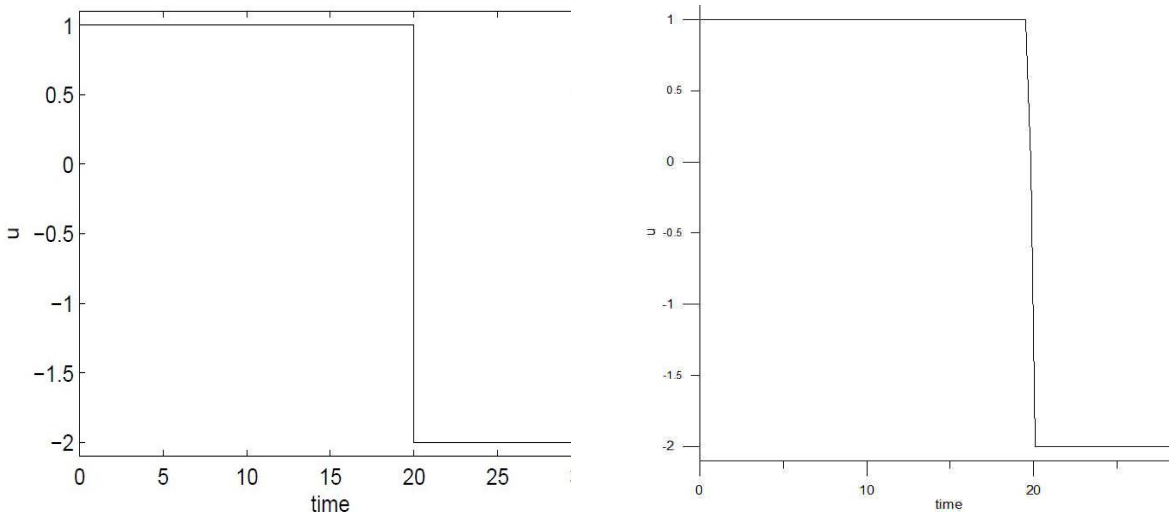

(a) (b)

Figure 2.14. Optimal trajectory of acceleration from (a) literature (b) CVP method.

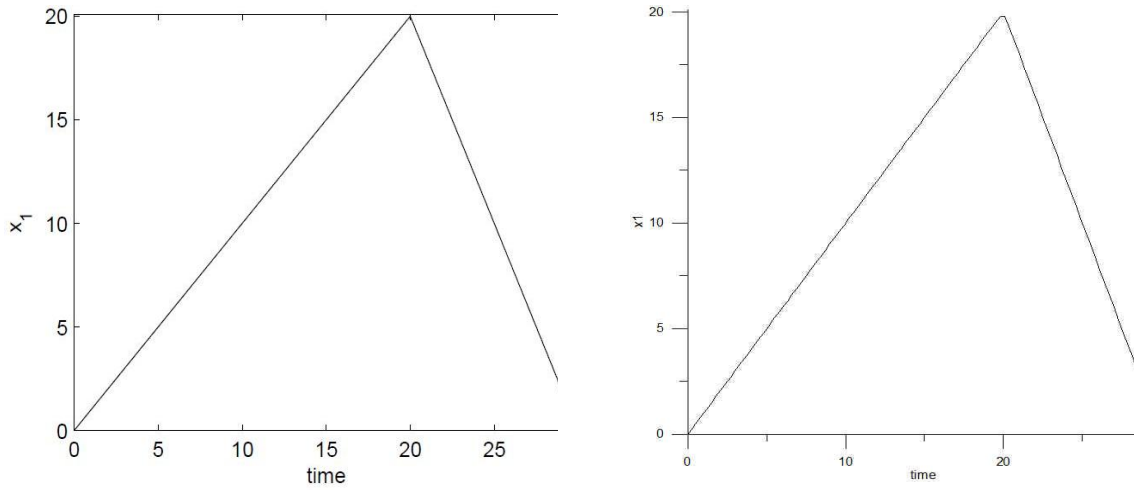

(a) (b)

Figure 2.15. Optimal trajectory of distance from (a) literature (b) CVP method.

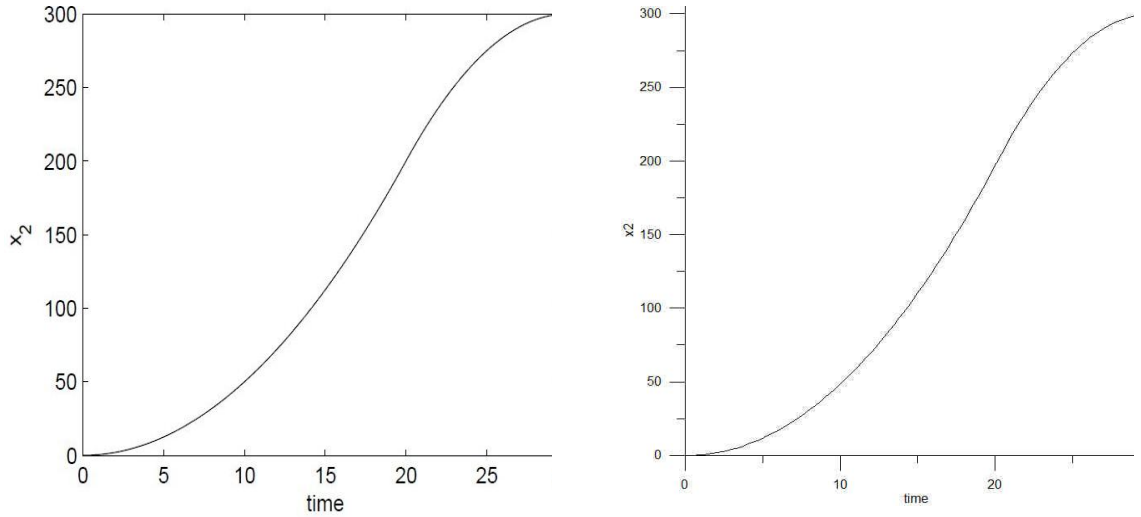

(a) (b)

Figure 2.16. Optimal trajectory of velocity from (a) literature (b) CVP method.

The calculation was performed for 100 discretization points and was completed in 0.17 seconds.

Solution with the Radau Collocation method

In Figs. 2.17-2.19, the plots for acceleration, distance and velocity found in the literature are presented in comparison with the best plots produced by the Radau collocation method with K=3 collocation points and N=40 elements. The best value for the objective function found in the literature is 30 (time units) which also comes in agreement with our calculations with a minor numerical error of 0.05%. The calculation was completed in 0.31 CPU seconds.

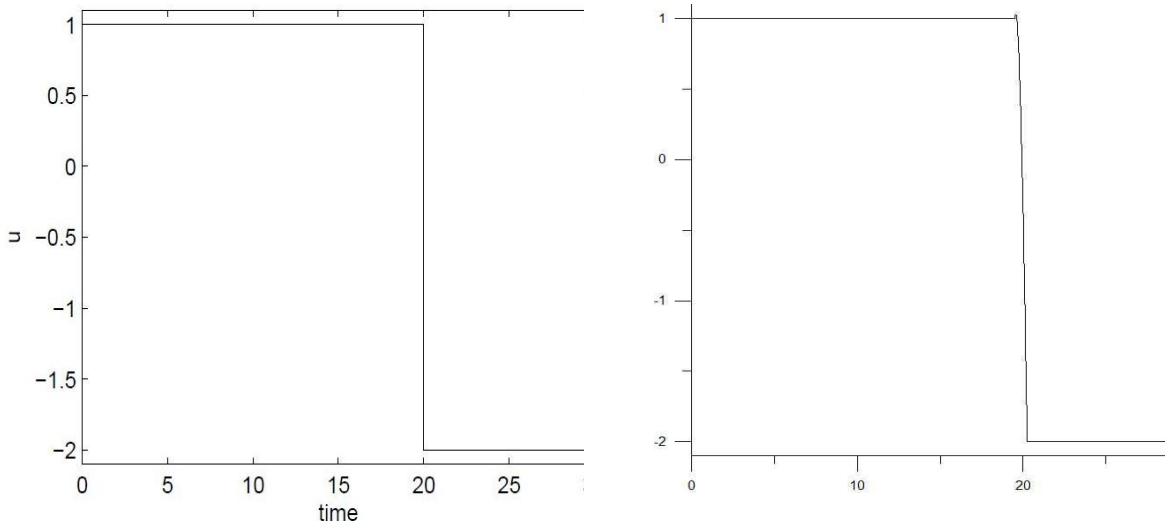

(a) (b)

Figure 2.17. Optimal trajectory of acceleration from (a) literature, (b) Radau method with K=3, N=40.

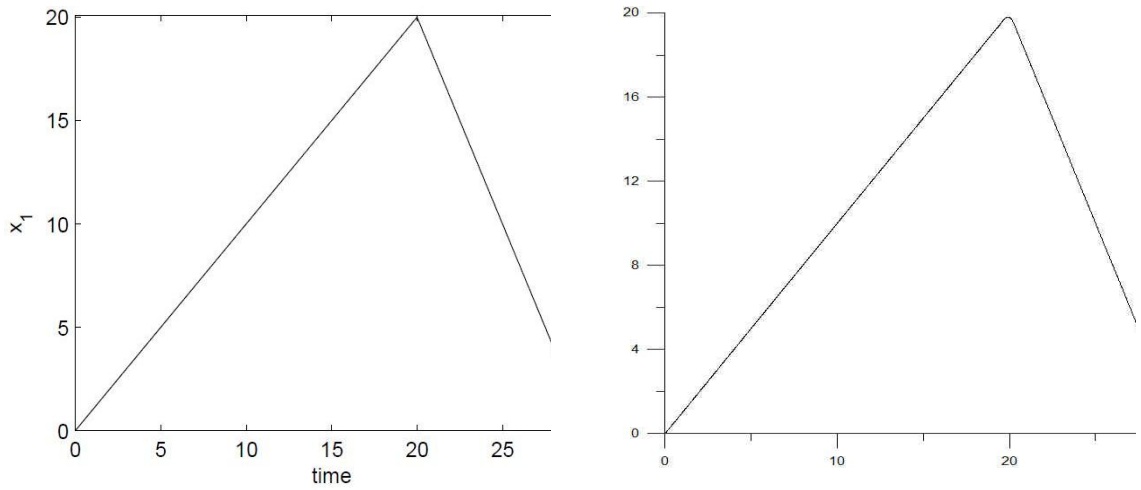

(a) (b)

Figure 2.18. Optimal trajectory of distance from (a) literature, (b) Radau method with K=3, N=40.

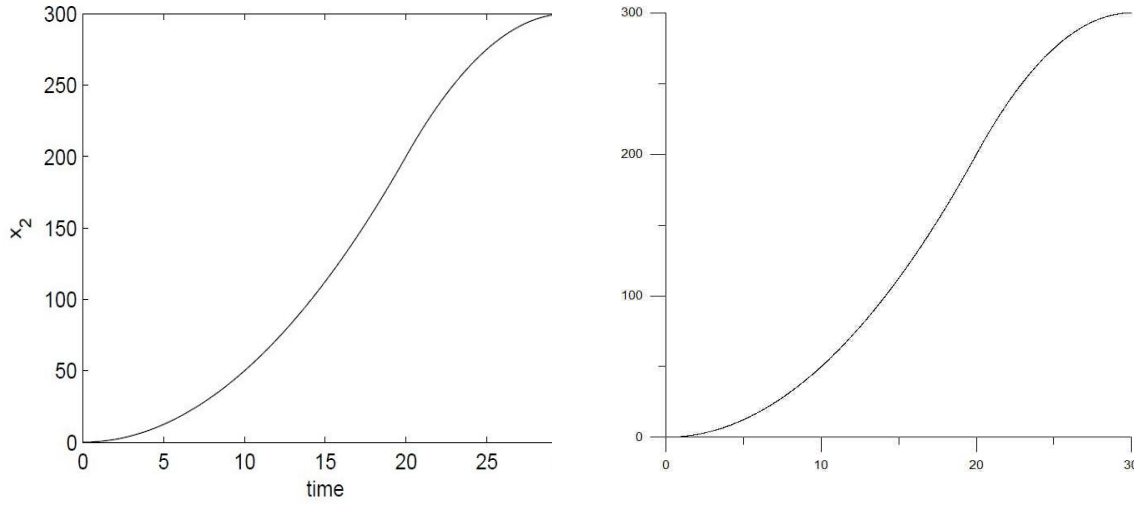

(a) (b)

Figure 2.19. Optimal trajectory of velocity from (a) literature, (b) Radau method with K=3, N=40.

2.6.3 Batch reactor problem

The simple batch reactor [Crescitelli and Nicoletti (1973)] is considered with the following chemical reaction: A → B → C. The parameters of the reactor for the two reactant species are: activation energy e_1 = 18000 cal·mol^{-1} and e_2 = 30000 cal·mol^{-1}, frequency factors k_{10} = 0.535x10^{11} min^{-1} and k_{20} = 0.461x10^{18} min^{-1}, initial concentration β_1 = 0.53 mol l^{-1} and β_2 = 0.43 mol·l^{-1}, constants α and c defined as $\alpha = e_1/e_2$, $c = k_{20}/k_{10}^{\alpha}$ and final time t_F = 8.0 min. The objective of the optimization is to maximize the amount of the product B at the final time:

$$\max_u J_0 = x_2(t_F) \tag{2.132}$$

s.t.

$$\dot{x}_1 = -ux_1 \tag{2.133}$$

$$\dot{x}_2 = ux_1 - cu^{\alpha}x_2 \tag{2.134}$$

$$1 \le u \le 2 \tag{2.135}$$

with initial conditions

$$\begin{aligned} x_1(0) &= \beta_1 \\ x_2(0) &= \beta_2 \\ u(0) &= 0.5 \end{aligned} \tag{2.136}$$

The importance of this problem lies in the presence of Eq. (2.134), which introduces high non-linearity in the DAE system.

Solution with the CVP method

In Figs. 2.20 and 2.21, the plots for the control and the states found in the literature are presented in parallel with the best plots produced by the CVP method.

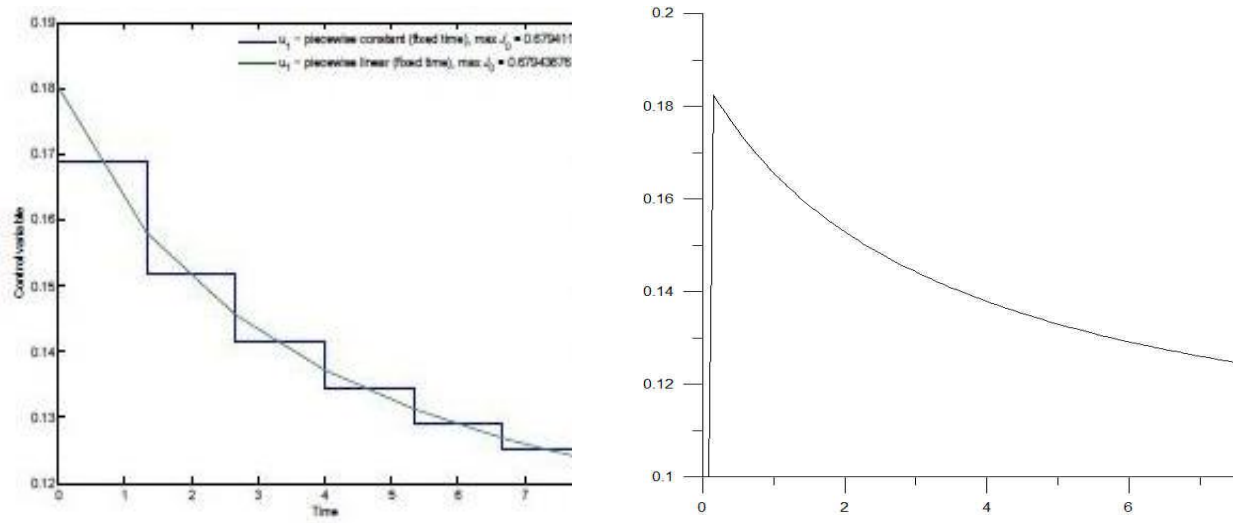

(a) (b)

Figure 2.20. Optimal trajectory of control variable from (a) literature, (b) CVP method.

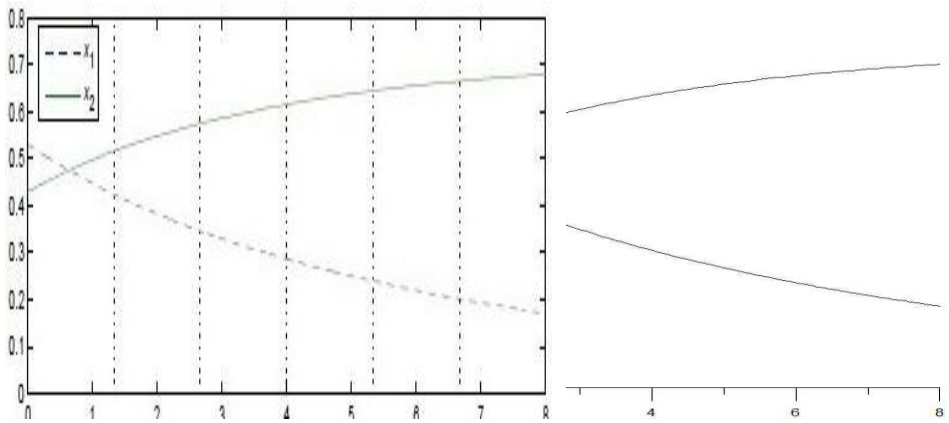

(a) (b)

Figure 2.21. Optimal trajectory of state variables from (a) literature, (b) CVP method.

The calculation was completed in 0.77 seconds and the optimal objective function value was found equal to 0.678939, whereas the best objective function value from the literature is found to be 0.679436. 100 discretization points were used.

Solution with the Radau Collocation method

In Figs. 2.22 and 2.23, the plots for the control and the states found in the literature are presented in parallel with the best plots produced by the Radau collocation method with K=3 collocation points and N=40 elements.

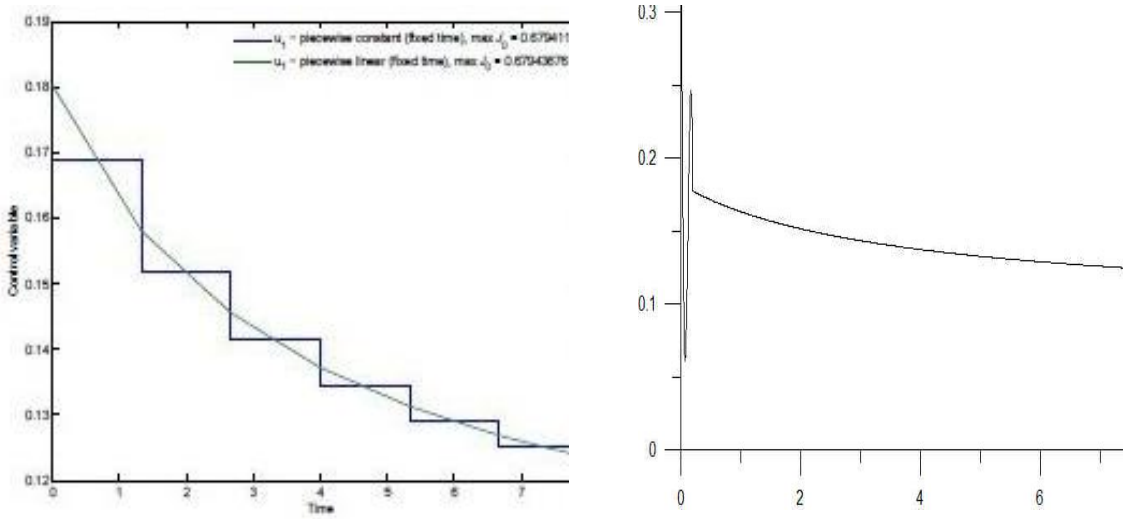

(a) (b)

Figure 2.22. Optimal trajectory of control variable from (a) literature, (b) Radau method with K=3, N=40.

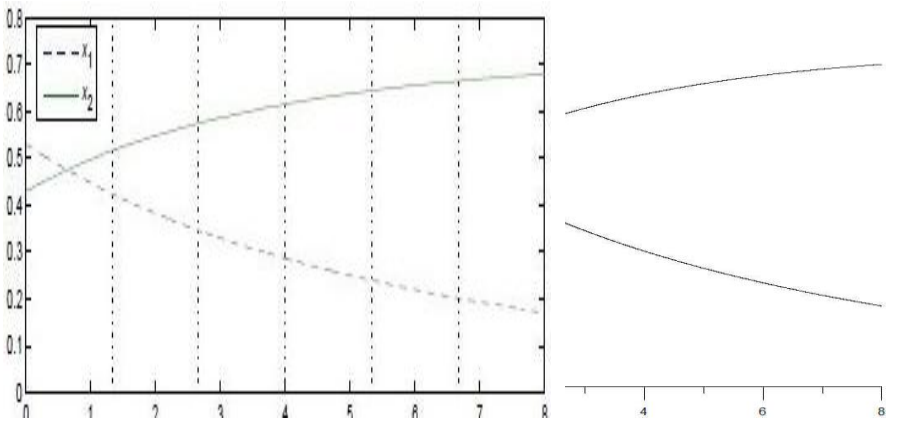

(a) (b)

Figure 2.23. Optimal trajectory of state variables from (a) literature, (b) Radau method with K=3, N=40.

Calculation was completed in 1.63 seconds and the optimal objective function value was found equal to 0.67943837.

It can be easily observed that in both methods the plots of the control variable *u* have a minor inaccuracy in comparison with the literature results. In CVP method this happens in the very first point (t=0.0) and in Radau Collocation in the first element (Δt=0.2). This result can be explained by the observation that in its discretized formulation, the differential system, Eqs. (2.133), (2.134), does not produce any equation containing $u(0)$, that can be programmed in the form of a constraint in the NLP solver in order to correctly calculate the first point $u(0)$ of the control variable profile. Thus $u(0)$ remains at its initial value, as this is set by the user in the initialization of the NLP algorithm.

2.6.4 CSTR problem

The following problem of a continuously stirred tank reactor (CSTR) [Balsa-Canto et al. (2001), Fikar and Latifi (2002), Luus (1990)] is considered, in which four control variables of a chemical reactor are optimized, in order to obtain maximum economic benefit for the time horizon of $t_f = 0.2$ sec:

$$\max_u J_0 = \int_0^{0.2} (5.8(qx_1 - u_4) - 3.7u_1 - 4.1u_2 + q(23x_4 + 11x_5 + 28x_6 + 35x_7) - 5.0u_3^2 - 0.099)dt \tag{2.137}$$

s.t.

$$\dot{x}_1 = u_4 - qx_1 - 17.6x_1x_2 - 23x_1x_6u_3 \tag{2.138}$$
$$\dot{x}_2 = u_1 - qx_2 - 17.6x_1x_2 - 146x_2x_3 \tag{2.139}$$
$$\dot{x}_3 = u_2 - qx_3 - 73x_2x_3 \tag{2.140}$$
$$\dot{x}_4 = -qx_4 + 35.2x_1x_2 - 51.3x_4x_5 \tag{2.141}$$
$$\dot{x}_5 = -qx_5 + 219x_2x_3 - 51.3x_4x_5 \tag{2.142}$$
$$\dot{x}_6 = -qx_6 + 102.6x_4x_5 - 23x_1x_6u_3 \tag{2.143}$$
$$\dot{x}_7 = -qx_7 + 46x_1x_6u_3 \tag{2.144}$$

$$0 \le u_1 \le 20 \tag{2.145}$$
$$0 \le u_2 \le 6 \tag{2.146}$$
$$0 \le u_3 \le 4 \tag{2.147}$$
$$0 \le u_4 \le 20 \tag{2.148}$$

with initial conditions

$$\mathbf{x}(0) = [0.1883; 0.2507; 0.0467; 0.0899; 0.1804; 0.1394; 0.1046] \tag{2.149}$$

where

$$q = u_1 + u_2 + u_4 \tag{2.150}$$

The difficulty in this problem is due to the fact that it is not a single control dynamic optimization problem, but has 4 control variables, thus quadrupling the number of optimization variables. Moreover, the DAE system consists of 7 state variables and 7 highly nonlinear equations thus making the problem highly complex.

Solution with the CVP method

In Figs. 2.24 - 2.27, the plots for the four control variables found in the literature are presented in parallel with the best plots produced by the CVP method. 100 discretization points were used.

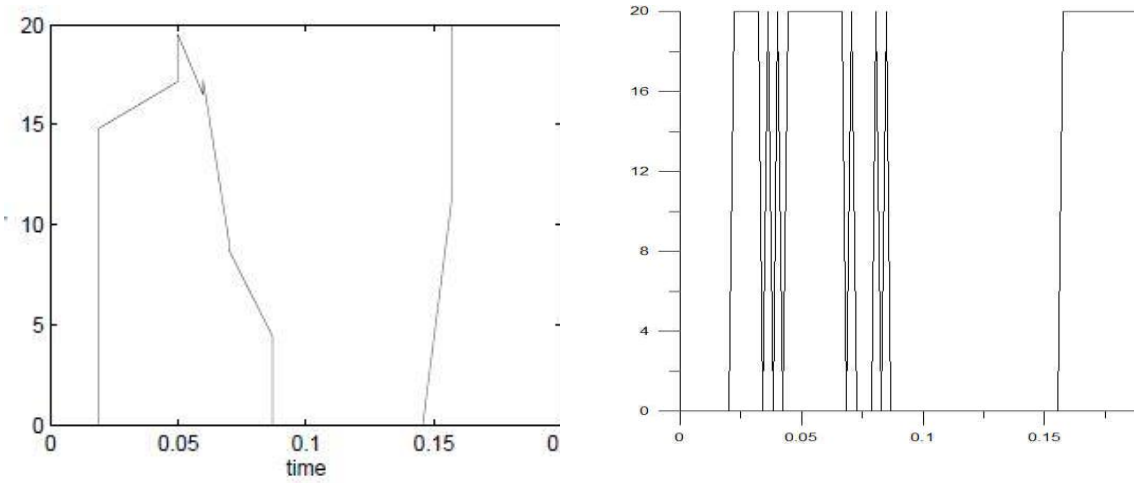

(a) (b)

Figure 2.24. Optimal trajectory of control variable u_1 from (a) literature, (b) CVP method.

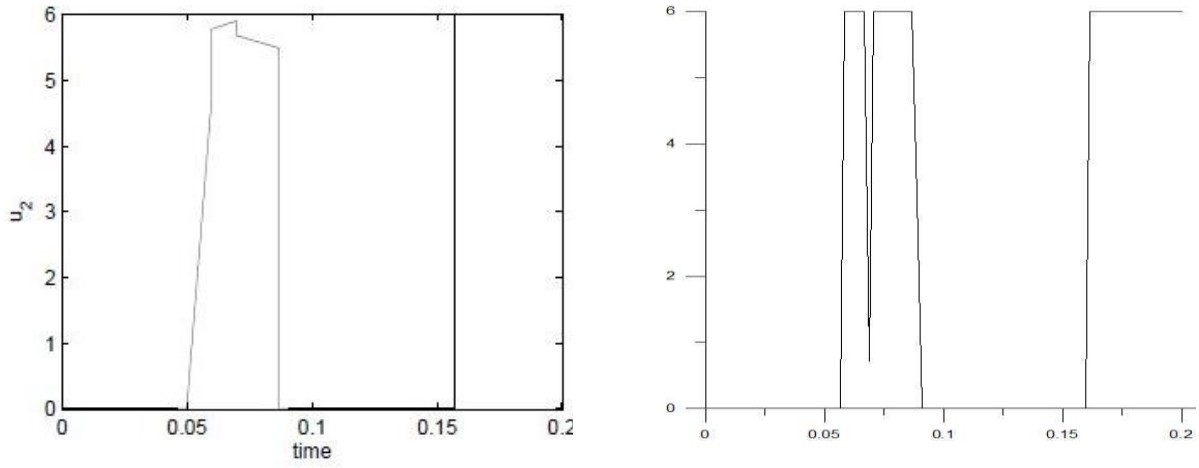

(a) (b)

Figure 2.25. Optimal trajectory of control variable u_2 from (a) literature, (b) CVP method.

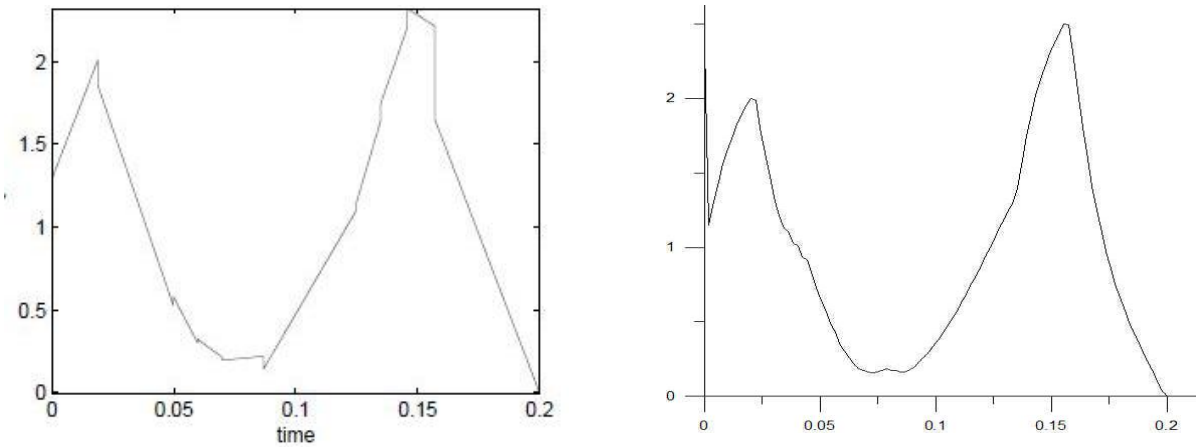

(a) (b)

Figure 2.26. Optimal trajectory of control variable u_3 from (a) literature, (b) CVP method.

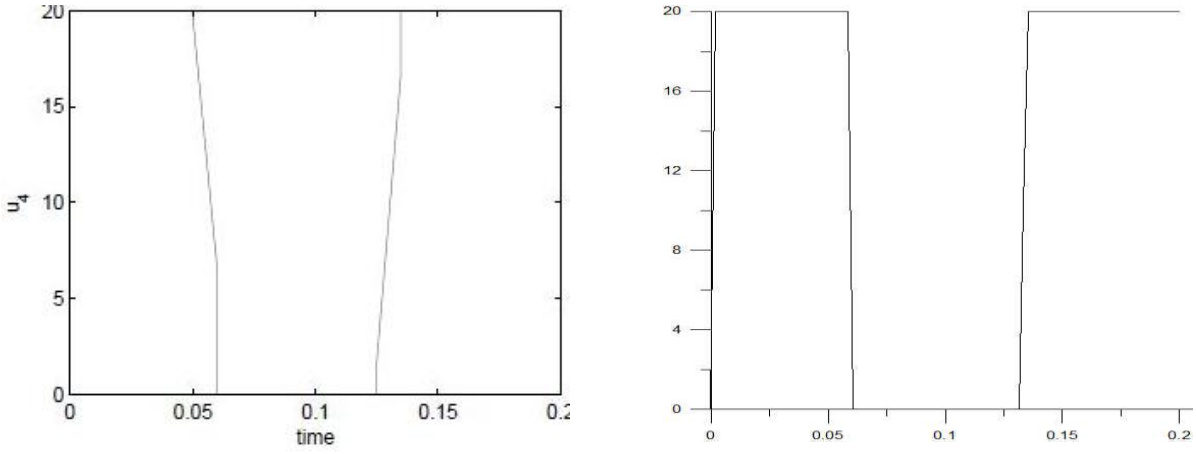

(a) (b)

Figure 2.27. Optimal trajectory of control variable u_4 from (a) literature, (b) CVP method.

The calculation was completed in 7.45 seconds and the optimal objective function value was found at 22.1135, while the best objective function value from the literature is found to be at 21.8003.

From the figures several discrepancies for the calculated optimal solutions of the control variables u_1 and u_2 in comparison with the literature results are observed, although the values of the objective function and constraints are accurate. By observing the figures more closely we can understand that the general shape of the curves is correct, while several points are not predicted correctly, thus disfiguring the final result. This can be only explained by the inefficiency of the NLP solver to correctly and accurately calculate the values of the optimization variables corresponding to these specific points. This result is not, in general, unexpected. As has been mentioned before, this specific problem has 4 control variables, thus by using 100 discretization points per variable, a 400 variable problem is produced. Several errors are to be expected even from the most efficient NLP solver.

Furthermore, it is also natural that the 1st order Euler integration scheme used here is not adequate to tackle with the highly complex and non-linear nature of the system of differential equations, Eqs. (2.138) - (2.144). A smaller time-step must be used, but smaller time step means shorter time intervals, thus, more discretization points per variable. This in turn leads to a higher dimension NLP problem, so once again the question of the efficiency of the NLP arises.

Solution with the Radau Collocation method

In Figs. 2.28 - 2.31, the plots for the four control variables found in the literature are presented in parallel with the best plots produced by the Radau collocation method with K=3 collocation points and N=40 elements.

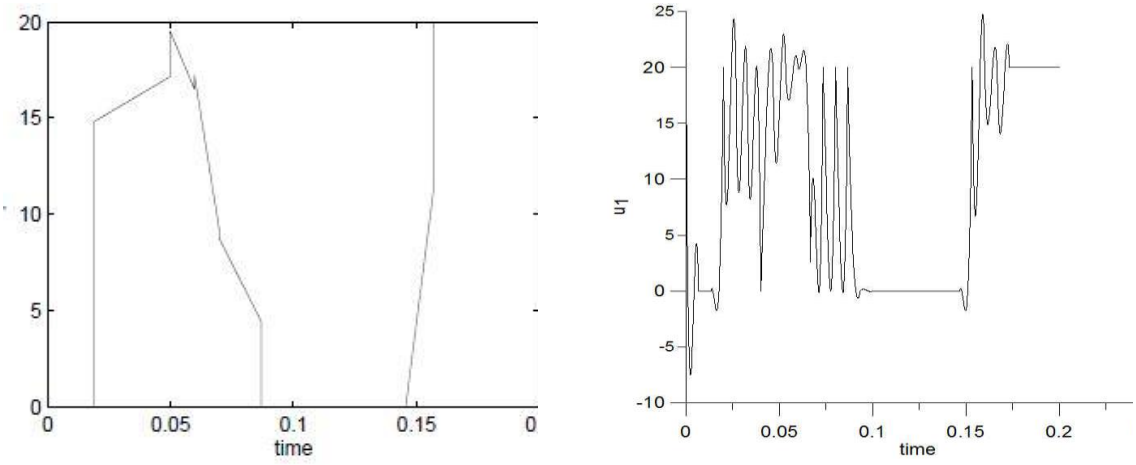

(a) (b)

Figure 2.28. Optimal trajectory of control variable u_1 from (a) literature, (b) Radau method with K=3, N=30.

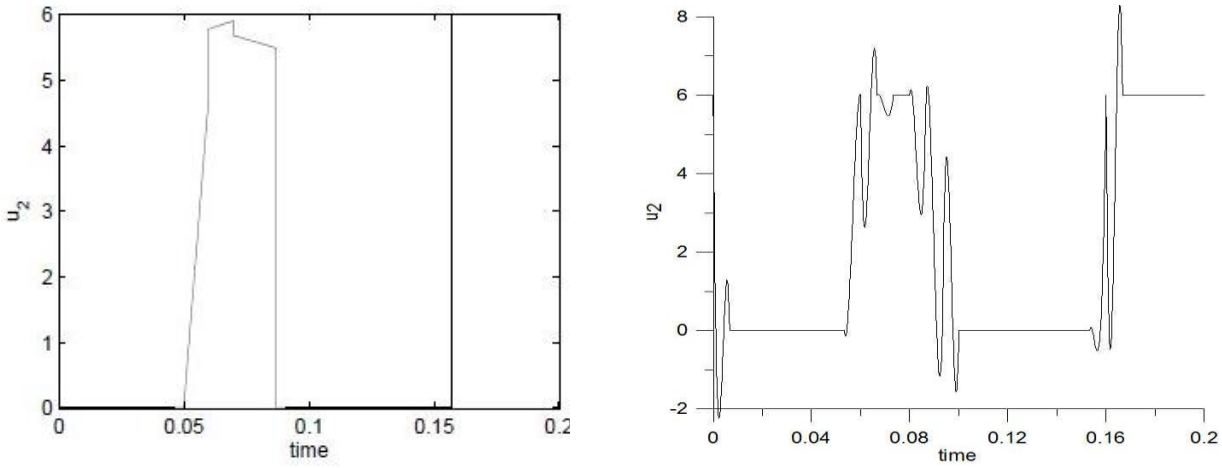

(a) (b)

Figure 2.29. Optimal trajectory of control variable u_2 from (a) literature, (b) Radau method with K=3, N=40.

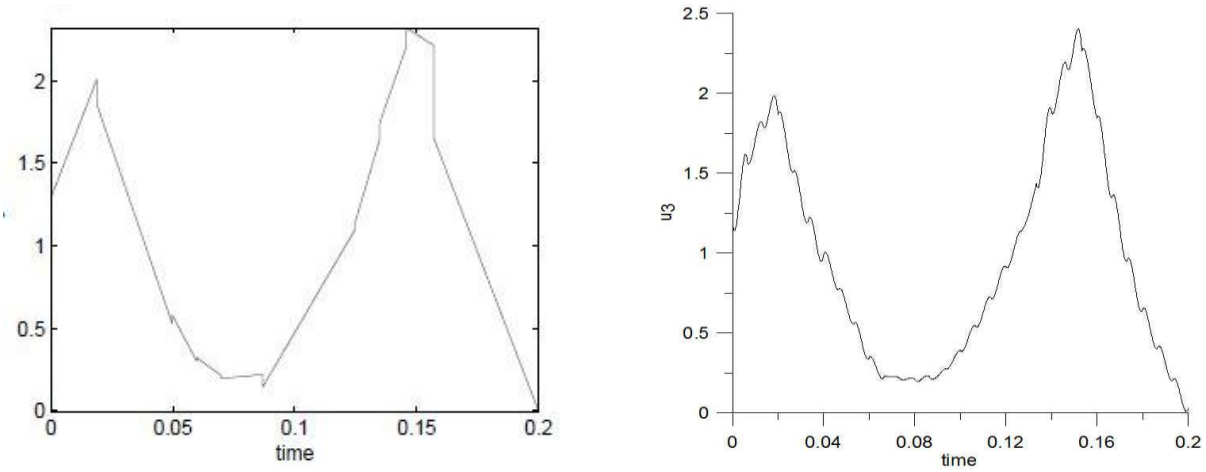

(a) (b)

Figure 2.30. Optimal trajectory of control variable u_3 from (a) literature, (b) Radau method with K=3, N=40.

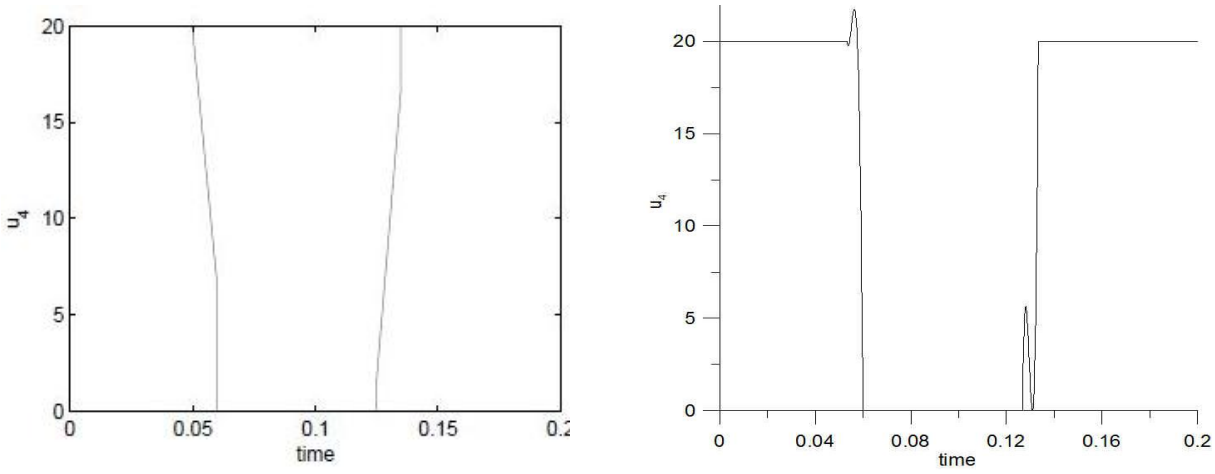

(a) (b)

Figure 2.31. Optimal trajectory of control variable u_4 from (a) literature, (b) Radau method with K=3, N=30.

Figures 2.28 and 2.29 are a clear example of the comment stated previously that only the collocation points, and not the intermediate, are an exact solution of the DAE system. This can explain why there is so much deviance between the Radau Collocation method solution and the solution from the literature as concerning the control variables u_1 and u_2. In essence, the profiles of u_1 and u_2 calculated by the Radau collocation method are found to be very accurate in comparison to the literature results only at the collocation points, while all the intermediate points, calculated by the polynomial formula of Eq. (2.102), are observed to deviate. Furthermore, this method also suffers from the problem described in the previous paragraph: the presence of 4 control variables quadruples the total number of optimization variables thus leading to inaccuracies of the NLP solver in certain points.

The calculation was completed in 247.19 seconds and the optimal objective function value was found at 21.8536179.

The solution presented above can be partially improved by using a greater number of elements, but not too many. Too many elements would produce a problem of too many variables and the inefficiency of the NLP solver would be cataclysmic for the results. In Figs. 2.32 - 2.35, the plots for the four control variables found in the literature are presented in parallel with the best plots produced by the Radau collocation method with K=3 collocation points and N=80 elements. We must note that by nearly doubling the number of elements, the time of calculation has severely augmented (749.31 seconds), while the optimal objective function value was found at 21.837459.

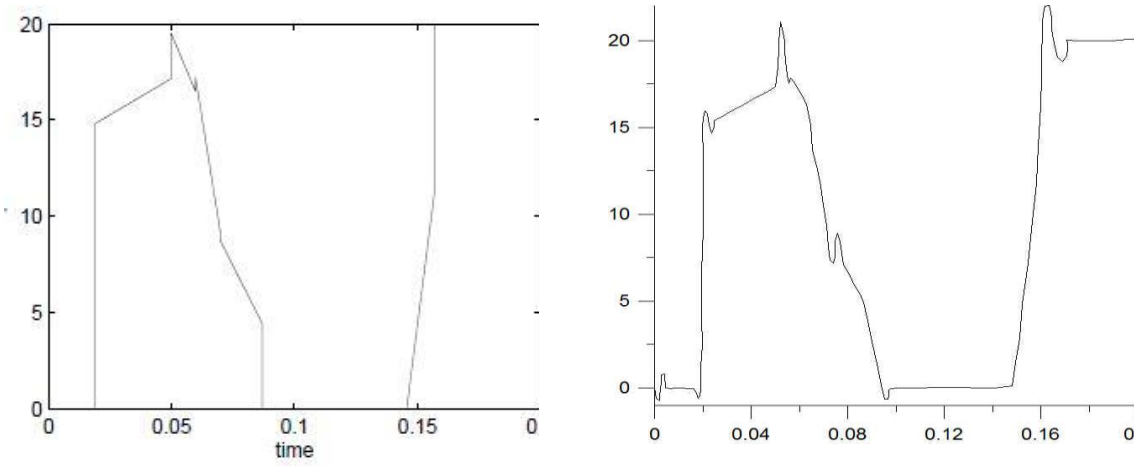

(a) (b)

Figure 2.32. Optimal trajectory of control variable u_1 from (a) literature, (b) Radau method with K=3, N=80.

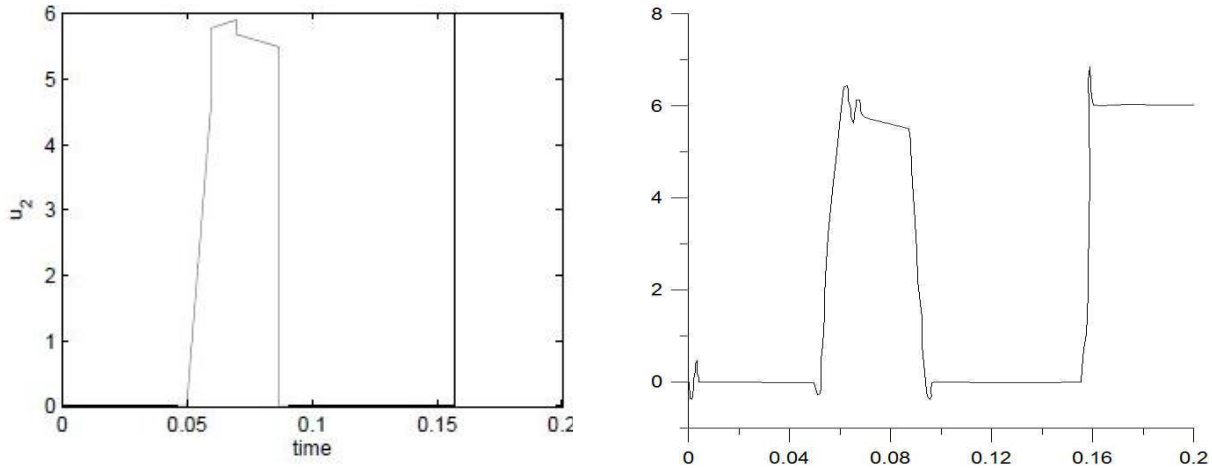

(a) (b)

Figure 2.33. Optimal trajectory of control variable u_2 from (a) literature, (b) Radau method with K=3, N=80.

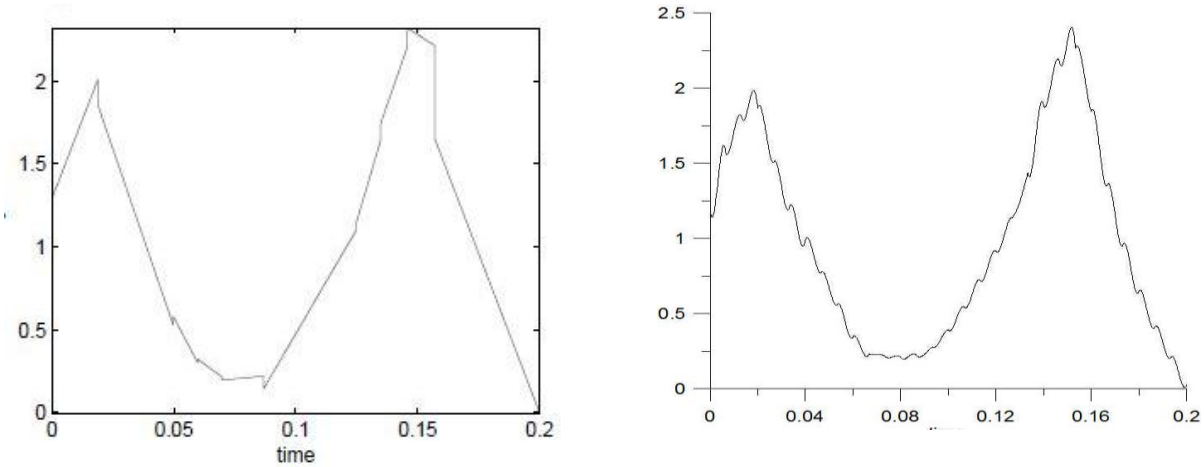

(a) (b)

Figure 2.34. Optimal trajectory of control variable u_3 from (a) literature, (b) Radau method with K=3, N=80.

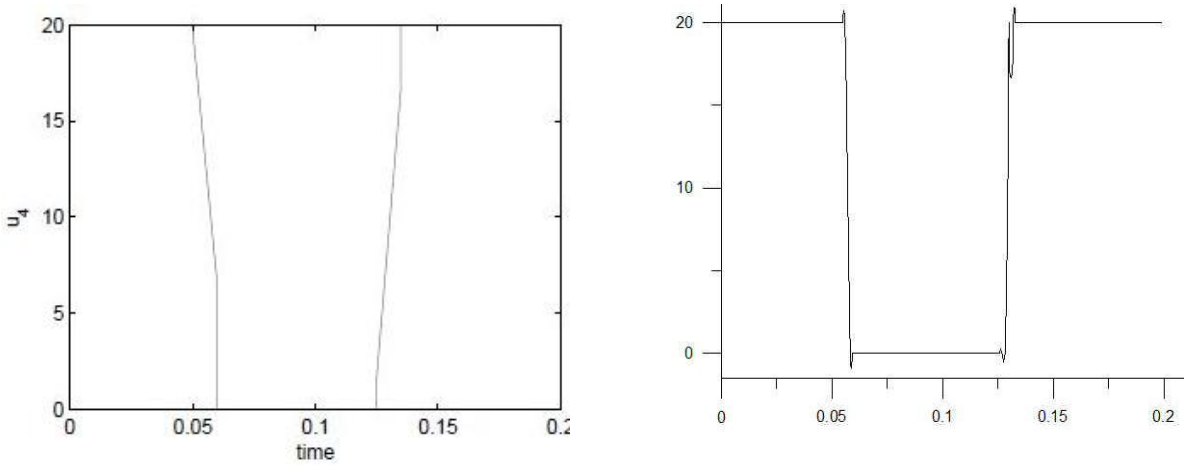

(a) (b)

Figure 2.35. Optimal trajectory of control variable u_4 from (a) literature, (b) Radau method with K=3, N=80.

It can be observed that the use of more elements has provided more accurate (in accordance with the literature) and more "smooth" curves for the control variables.

In conclusion, the aforementioned results concerning the application of the CVP method and the Radau collocation method for the solution of the CSTR problem, are to be expected. The utilization of a simultaneous approach based on orthogonal collocation is far superior (in terms of solving a highly complex highly non-linear system of differential equations) than a sequential approach based on control vector parameterization, which integrates the differential system of equations utilizing a 1st order Euler integration scheme.

2.6.5 Purely mathematical example problem

Consider the following DOP [Feehery (1998), Luus (1990), Rajesh et al. (2001)] with one inequality state path constraint:

$$\min_u J_0 = \int_0^1 (x_1^2 + x_2^2 + 0.005u^2)dt \tag{2.151}$$

subject to:

$$\dot{x}_1 = x_2 \tag{2.152}$$

$$\dot{x}_2 = -x_2 + u \tag{2.153}$$

$$x_2 - 8(t-0.5)^2 + 0.5 \le 0 \tag{2.154}$$

with initial conditions

$$\begin{aligned} x_1(0) &= 0 \\ x_2(0) &= -1 \end{aligned} \tag{2.155}$$

and final time $t_F = 1$.

This problem is considered as a relatively simple optimal control problem with one control variable *u* and two state variables x_1 and x_2. The main interest of this problem lies in the presence of one inequality state path constraint described by the non-autonomous Eq. (2.154), where time t is introduced explicitly.

Solution with the CVP method

From Figures 2.36 and 2.37 it can be verified that the literature results are in agreement with our results as concerning the plots of control and state variables versus time. Best objective function value found in the literature was 0.1701564, while the optimal value calculated with the CVP method was 0.1695485. For the calculation, 101 discretization points were used with a time step of 0.01 and the calculations were completed in 0.96 seconds.

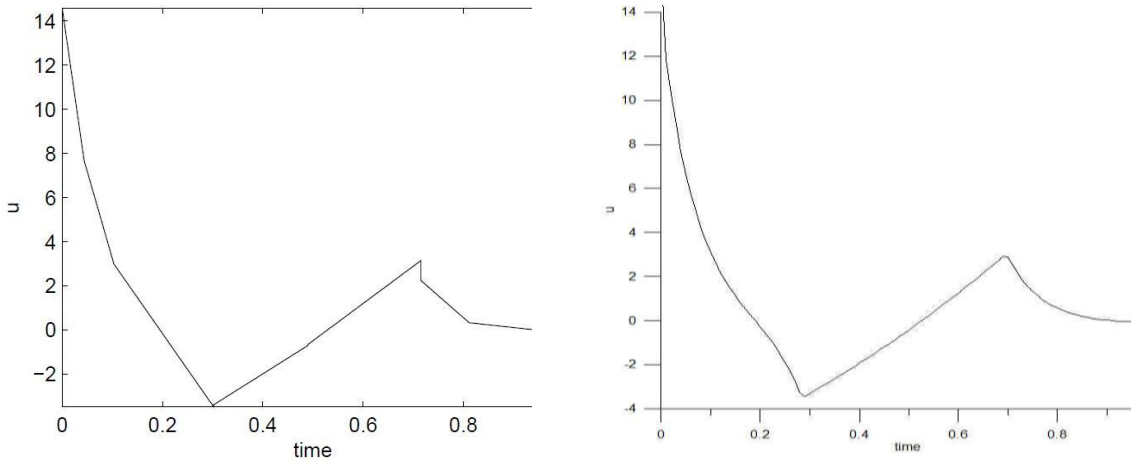

(a) (b)

Figure 2.36. Optimal trajectory of the control variable u from (a) literature, (b) CVP method.

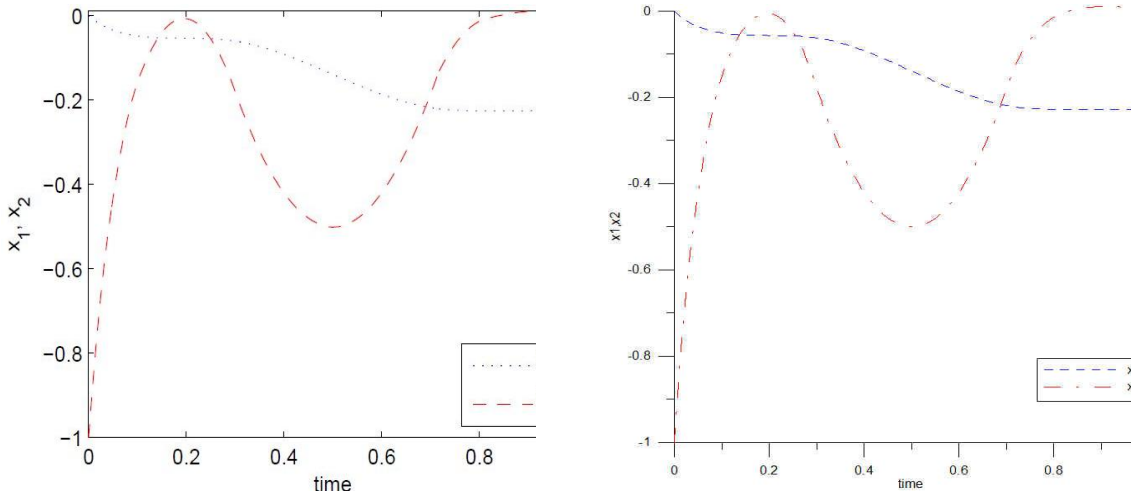

(a) (b)

Figure 2.37. Optimal trajectory of the state variables x_1, x_2 from (a) literature, (b) CVP method.

Solution with the Radau Collocation method

In Figs. 2.38 - 2.39, the plots for the control variable and the two state variables found in the literature are presented in parallel with the best plots produced by the Radau collocation method with K=3 collocation points and N=40 elements. The minimum objective function value was found to be 0.169685 and the optimization was completed in 1.12 seconds

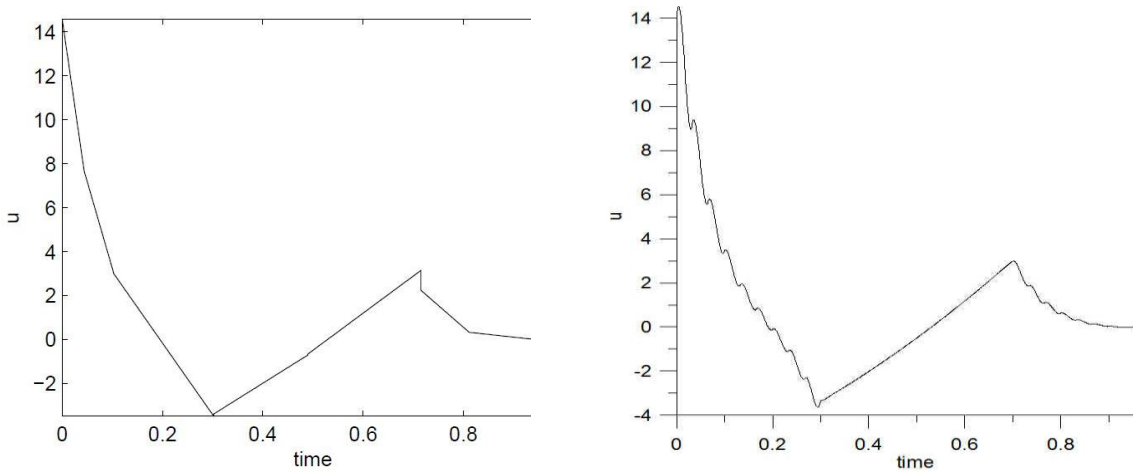

(a) (b)

Figure 2.38. Optimal trajectory of control variable u from (a) literature, (b) Radau method with K=3, N=40.

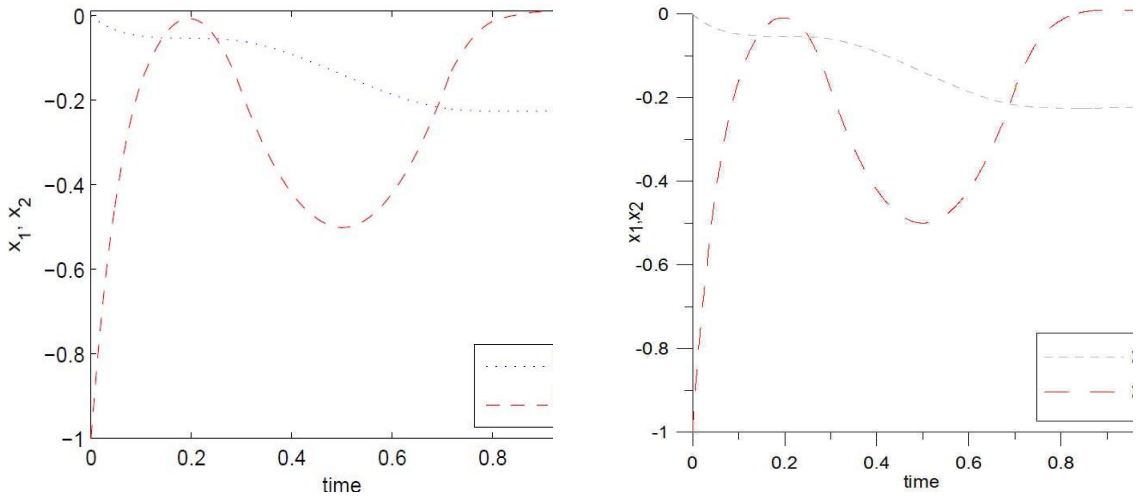

(a) (b)

Figure 2.39. Optimal trajectory of the state variables x_1, x_2 from (a) literature, (b) Radau method with K=3, N=40.

The "tricky" part about the application of the Radau Collocation method (or any simultaneous method) in this problem lies in the way the path constraint, Eq. (2.154), will be handled. The problem with the path constraint lies in the fact that it is *non-autonomous*, which means that it contains time t in explicit form. Thus, if the discretized equivalent of Eq. (2.154) is declared as extra constraint equations in our NLP software, the values of

their gradients (given that they are automatically calculated by the NLP solver) may be wrong. In order to perform the correct transcription of the particular problem into a NLP problem and reach the correct solution, the path constraint must be "declared" in the form of bounds on the x_2 variable.

2.6.6 Comparative and general comments

Application of the CVP method at the selected example problems has revealed that, although CVP is a relatively simple method that relies on the -not extremely accurate- 1st order Euler scheme in order to integrate the DAE system of equations, the results are rather satisfactory. The required computational times were observed to be very short and the method was implemented in a computer code of no more than 700-1000 lines in each problem. In the case of dynamic optimization problems with few control variables and with relatively stable dynamic systems, the CVP method works extremely well and can be considered as a better choice than the Radau Collocation method. However, CVP method is expected to be strongly affected by non-linearity, as happens in the case of the Continuously Stirred Tank Reactor (CSTR) problem.

Considering the Radau Collocation method, judging by the corresponding results derived for the CSTR problem, it can be stated that, indeed as a basic representative of simultaneous methods, it can handle unstable dynamic systems with success. The method also works fairly well in the simpler dynamic optimization problems and its results can be compared with those of the CVP method both in terms of accuracy and computational time. Of course, due to the fact that Radau Collocation is a far more complex method to be applied than CVP, the generated computer code necessary was at the levels of 1500-2500 lines, depending of the problem. Another important fact proved by the application of the method to the aforementioned problems is that the method promises, and indeed produces, arithmetical accuracy of 10^{-5} but only at the collocation points, and not the intermediate ones. Finally, what must be kept in mind is that this specific method is a trade-off between the number of collocation points and the number of elements to be used in order to reach the best results. As it can be observed by the figures provided in the solution of the Van der Pol Oscillator problem, the use of too many collocation points and elements as well as the use of too few collocation points and elements is not correct. An "optimal" combination of these two parameters exists and must be specified in order for the method to work best.

Finally, a more general observation that can be applied to both methods is that they both highly depend on the efficiency of the gradient-based NLP solver that is chosen to solve the resulting optimization problem after the discretization, especially in cases of dynamic optimization problems with many variables where the original problem, after discretization is performed, is translated to a static optimization problem of -perhaps- thousands of variables.

2.7 Dynamic Optimization of a Trigeneration System

A trigeneration system is a system that produces electric (or mechanical) energy, while its thermal energy is used to cover heating loads directly or cooling loads by means of an absorption chiller. This feature proves to be very important for the economic feasibility of such units in areas like Greece, where mild winters and long hot summers are observed, thus making the heating period short.

Dynamic optimization has been performed on such a system installed in a complex of buildings in the past [Vallianou and Frangopoulos (2012)]. This system has been selected for further study in this work, as a good application example of dynamic optimization in energy systems.

2.7.1 Description of the Trigeneration system

An important feature of the trigeneration system at hand is the presence of storage tanks for hot and cold water. Storage tanks are used in order to deal with the fact that the peak of thermal and cooling loads are not, in general, expected to coincide with the peak of the electric load. So the option of being able to store the produced thermal and cooling energy seems, if not necessary, at least very reasonable.

A simplified diagram of the supply lines of hot and cold water is depicted in Figure 2.40.

The energy needs of the building complex are covered by the trigeneration system at hand and by electricity coming from the local network. The basic components that constitute the trigeneration system are: a gas-engine cogeneration unit, natural gas boilers, one hot water tank with its own natural gas burner, one cold water storage tank, an absorption chiller driven by thermal energy and electrically driven compression chillers.

The boilers and compression chillers are designed to have sufficient capacity in order to fully cover the energy needs of the building, if needed, without the aid of the cogeneration unit or any other component. As it can be observed in Figure 2.40, hot water from the cogeneration unit and the boilers is stored in the hot water tank and then supplied to the absorption chiller and, of course the building. In the same way, cold water from the compression chillers and the absorption chiller is stored in the cold water tank and then supplied to the building. Both tanks are connected to closed circuits, thus the mass of water in them remains constant. A natural gas burner is installed on the hot water tank in order to compensate for thermal losses.

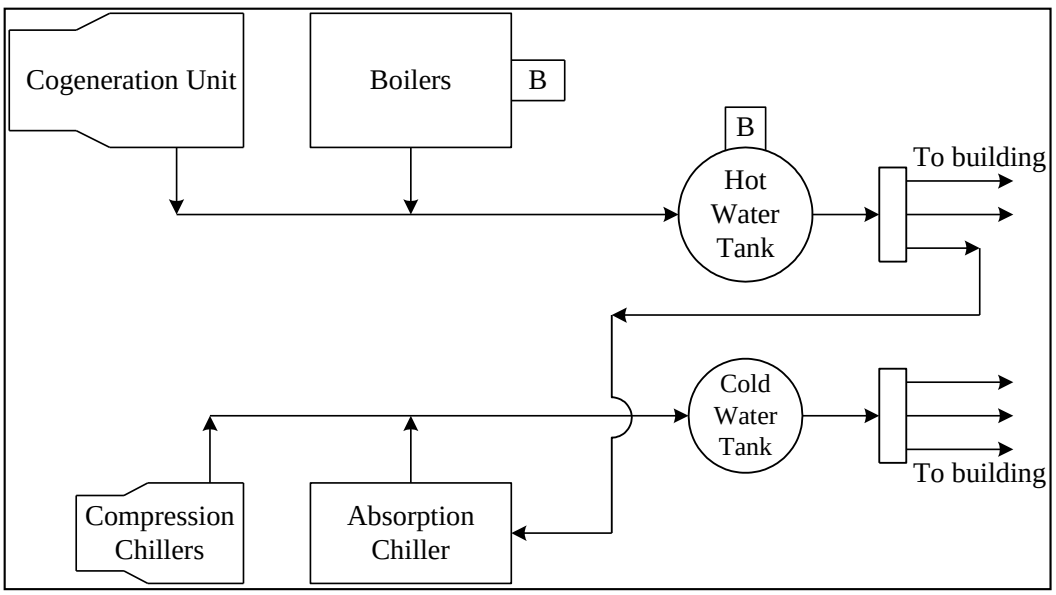

Figure 2.40. Simplified diagram of the trigeneration energy system [Vallianou and Frangopoulos (2012)].

Another important feature that needs to be mentioned is that the building operates for a five-day week (Monday through Friday). This means that during the weekend only the storage tanks operate and bridge the gap between Friday and Monday.

Further details about the technical characteristics of the components of the system and about the energy loads of the building complex can be found in the work of Vallianou and Frangopoulos (2012). General details considering the simulation, optimization, performance evaluation and complexities of trigeneration systems can be found in the literature [Cardona and Piacentino (2007), Kavvadias and Maroulis (2010), Carvalho et al. (2011)].

2.7.2 Modeling of the Trigeneration system

The complete model can be obtained from the original publication [Vallianou (2009), Vallianou and Frangopoulos (2012)]. Here, for brevity, only selected important elements of the model used for the simulation of the trigeneration system are presented.

Although storage of thermal and cooling energy exists, no storage for electric energy is present. Thus the electric energy produced by the cogeneration system and the electric energy provided by the grid must be equal to the total electric load (including the compression chillers). This is stated by Eq. (2.156) as

$$\dot{W}_{cog} + \dot{W}_b = \dot{W}_{cons} + \dot{W}_{chel} \tag{2.156}$$

where $\dot{W}_{cog}$ is the electric power from the cogeneration unit, $\dot{W}_b$ is the power bought from the grid, $\dot{W}_{cons}$ is the power consumed by the building, and $\dot{W}_{chel}$ is the electric power consumed by the compression chillers.

For the boilers and the auxiliary burner of the hot water tank a constant efficiency is assumed. The coefficient of performance at nominal load for the compression chillers is assumed to be constant at partial load and is given as a function of the ambient temperature:

$$COP_{chel} = \sum_{i=0}^{2} c_{chel,i} \cdot T_{amb}{}^{i} \tag{2.157}$$

Considering the cogeneration unit, the energy flow rate of the fuel consumed $\dot{H}_{fcog}$ is given as a function of the electric power output:

$$\dot{H}_{fcog} = \sum_{i=0}^{2} c_{fcog,i} \cdot \dot{W}_{cog}{}^{i} \tag{2.158}$$

A similar expression is used for the useful heat produced, $\dot{Q}_{fcog}$:

$$\dot{Q}_{fcog} = \sum_{i=0}^{2} c_{Qcog,i} \cdot \dot{W}_{cog}{}^{i} \tag{2.159}$$

In order to simulate the transient behaviour of the hot and cold water storage tanks, differential equations are used. Specifically, the energy balance for the hot water tank is given as:

$$m_{hwt} c_p \frac{dT_{hwt}}{dt} = \dot{Q}_{cog} + \dot{Q}_B - \dot{Q}_{abs} - \dot{Q}_{cons} - (UA)_{hwt}(T_{hwt} - T_r) \tag{2.160}$$

with m_{hwt} the water mass of the hot water tank, $\dot{Q}_{cog}$ the useful thermal power output of the cogeneration unit, $\dot{Q}_B$ the thermal power output of the boilers and the burner, $(UA)_{hwt}$ the product of overall heat transfer coefficient and external surface area of the hot water tank, T_{hwt} the temperature of the hot water tank, and T_r the room temperature. The energy balance for the cold water tank is given by Eq. (2.161)

$$m_{cwt} c_p \frac{dT_{cwt}}{dt} = \dot{\Psi}_{cons} - \dot{\Psi}_{abs} - \dot{\Psi}_{chel} - (UA)_{cwt}(T_{cwt} - T_r) \tag{2.161}$$

with m_{cwt} the water mass of the cold water tank, $\dot{\Psi}_{cons}$ the cooling power output to the building, $\dot{\Psi}_{abs}$ the cooling power of the absorption chiller, $\dot{\Psi}_{chel}$ the cooling power output of the compression chillers, $(UA)_{cwt}$ the product of overall heat transfer coefficient and external surface area of the cold water tank, T_{cwt} the temperature of the cold water tank, and T_r the room temperature.

Finally the model for the transient operation of the absorption chiller is discussed in brief. The operation of the absorption chiller can be described by the Gompertz function (Figs. 2.41, 2.42).

Two equations are used, one for the load increase from zero to nominal load

$$G_{incr}(t) = ab^{c^t} - ab \tag{2.162}$$

and one for the load decrease from nominal to zero load

$$G_{decr}(t) = 1 - ab^{c^{1.75t}} + ab \tag{2.163}$$

where α=1.228455, b=0.000128 and c=0.810818. The cooling power of the absorption chiller is thus given as a function of time

$$\dot{\Psi}_{abs}(t) = G(t) \cdot \dot{\Psi}_{Dabs} \tag{2.164}$$

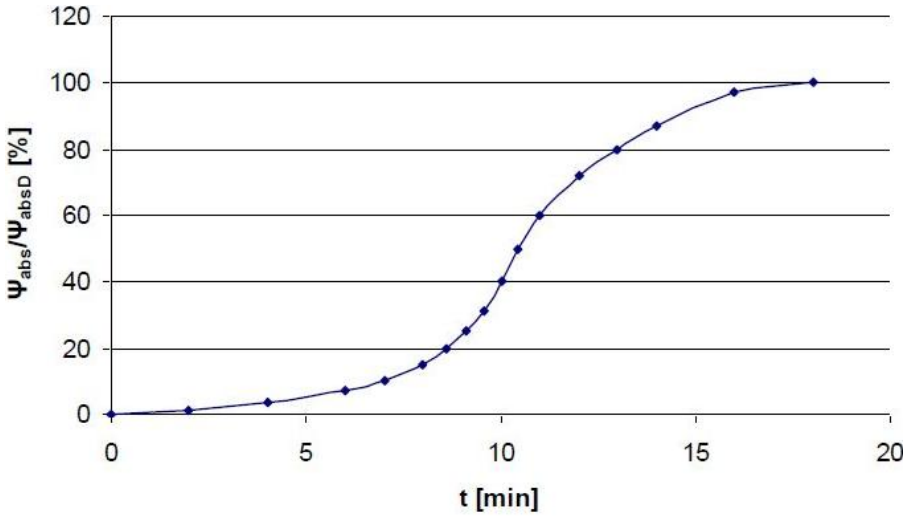

Figure 2.41. Gompertz function for load increase [Vallianou and Frangopoulos (2012)].

The heat flow rate required for the absorption chiller at nominal load is given as

$$\dot{Q}_{Dabs} = \frac{\dot{\Psi}_{Dabs}}{COP_{Dabs}} \tag{2.165}$$

where COP_{Dabs} is the coefficient of performance for the absorption chiller at its nominal load (design point). The heat flow rate at partial load is given by the equation

$$\dot{Q}_{abs} = \dot{Q}_{Dabs} \cdot \sum_{i=0}^{2} c_{Qabs,i} \cdot \left(\frac{\dot{\Psi}_{abs}}{\dot{\Psi}_{Dabs}} \right)^{i} \tag{2.166}$$

while the heat flow rate for operation during transients is given by the equation

$$\dot{Q}_{Dabs}(t) = \frac{\dot{\Psi}_{abs}(t)}{COP_{abs}(t)} \tag{2.167}$$

with

$$COP_{abs}(t)_{fcog} = COP_{Dabs} \cdot \sum_{i=0}^{6} c_{COP_{abs},i} \cdot \left(\frac{\dot{\Psi}_{abs}(t)}{\dot{\Psi}_{Dabs}} \right)^{i} \tag{2.168}$$

Next, the details of the dynamic optimization problem of the trigeneration system are discussed.

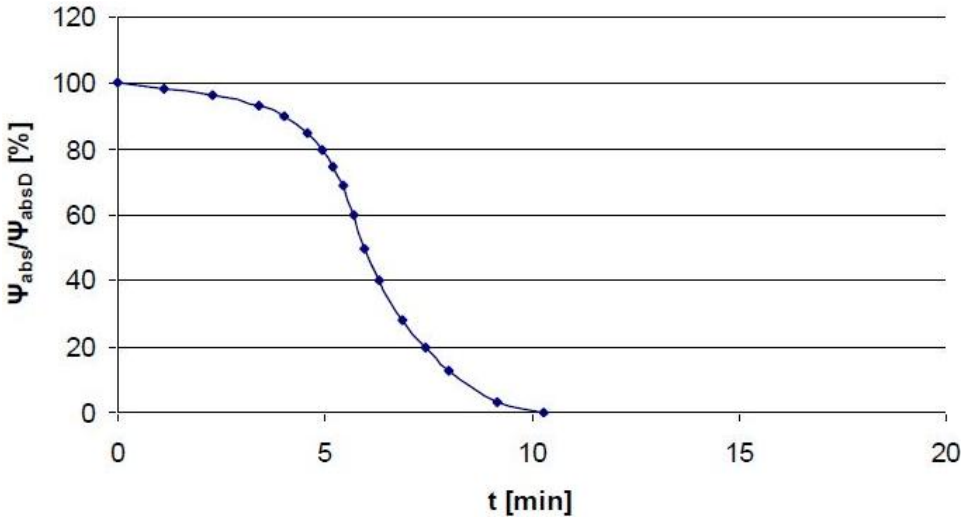

Figure 2.42. Gompertz function for load decrease [Vallianou and Frangopoulos (2012)].

2.7.3 Dynamic optimization of the Trigeneration system operation

The optimization problem of the trigeneration system can be characterized as a dynamic one due to two important factors: the presence of transient phenomena and the existence of storage tanks for hot and cold water.

The transient operation of the absorption chiller is a phenomenon that cannot be ignored due to the fact that its time constant is longer than the time constant of the cogeneration unit. So the assumption of steady state operation during time intervals would be inaccurate. The time needed for the absorption chiller to switch from zero load to full load (or any intermediate load) and the time needed to switch to zero load again are important parameters that should be taken into consideration during the optimization procedure.

Concerning the existence of storage tanks, the presence of energy storage during the period of operation of an energy system characterizes the corresponding optimization problem as a dynamic one. The key idea is that due to storage, the power output of each component in each time interval affects and is affected by the power output in other time intervals. Thus the problem can no longer be decomposed into time intervals of steady-state operation independent of each other and treated likewise, but dynamic optimization methods must be applied.

The objective of optimization is the minimization of the total annual cost for covering the energy needs of the building complex

$$\min C_{tot} = C_{ac} + C_p + C_m + C_f + C_e \tag{2.169}$$

where C_{ac}, C_p, C_m, C_f, C_e represent the annualized capital cost, personnel cost, maintenance cost, fuel and electricity cost, respectively. Details about the specific equations for each cost can be found in the original work [Vallianou (2009), Vallianou and Frangopoulos (2012)].

The change of the energy needs with time is represented with one typical day for each month and nine time intervals of constant needs in each interval during the typical day. Four independent variables are selected, namely the electric power output of the

cogeneration unit, $\dot{W}_{cog}$, the thermal power output of the boilers and the burner of the hot water tank, $\dot{Q}_B$, the cooling power of the absorption chiller, $\dot{\Psi}_{abs}$, and the cooling power of the compression chillers, $\dot{\Psi}_{chel}$. The building operates during five weekdays, while any stored energy is retained during the weekend, taking into consideration energy losses. Constraints that are not incorporated in the optimization problem by the model, but have to be declared separately in the NLP solver, are the following:

$$0.3 \cdot \dot{W}_{Dcog} \le \dot{W}_{cog} \le \dot{W}_{Dcog} \quad \text{and} \quad \dot{W}_{Dcog} = 0 \tag{2.170}$$

$$0.1 \cdot \dot{\Psi}_{Dabs} \le \dot{\Psi}_{Dabs} \le \dot{\Psi}_{abs} \quad \text{and} \quad \dot{\Psi}_{Dabs} = 0 \tag{2.171}$$

$$80^o C \le T_{hwt} \le 95^o C \tag{2.172}$$

$$7^o C \le T_{cwt} \le 12^o C \tag{2.173}$$

Equations (2.170) and (2.171) reveal the presence of a technical lower limit on the operating power of the cogeneration unit and the absorption chiller. Of course the value zero is included to cover the cases when the cogeneration unit or the absorption chiller is not operating. The optimization algorithm automatically sets the value of the power output equal to zero, if a value lower than the lower limit declared in the above equations is calculated during the optimization process.

In the original work, the dynamic optimization problem is solved by treating simultaneously 9×7=63 time intervals per week (9 time intervals per day), thus constructing a 4×63=252 variables NLP problem for the time horizon of a typical week. The CVP method is applied, and the Euler method for the solution of the differential equations, Eqs. (2.160) – 2.161), is used. For the solution of the NLP problem, an SQP algorithm is used via the SNOPT software supplemented with the necessary subroutines for calculating the state variables and the objective function values.

An issue that was left open for research in the original work was the fact that the increased number of variables, in the case where 1 hour intervals were used (which means 24 intervals per day instead of 9), made the problem impossible to solve because of the long computational time required. The contribution of the author in this problem was the modification/improvement of the original algorithm in order to solve the problem for 1 hour time intervals and for the whole 30-day month rather than simply one typical week per month. The model provided from the original work was not altered in any way. Also, the method of approach of the dynamic optimization problem was chosen to be Control Vector Parameterization with piecewise constant discretization for the control variables as in the original work, but the method of integration of the system of differential equations was upgraded from the 1st order Euler integration scheme that was originally used to 4th order Runge-Kutta.

The problem is solved for the typical week of every month using 24 intervals per day (24×7x4=672 variables) and for the whole month using both 9 intervals per day (9×30×4=1080 variables) and 24 intervals per day (24×30x4=2880 variables). Also the case of the whole year set as the time horizon is solved by optimizing successively every month while using the output of the previous month as the input the next, interconnecting in a way the 12 months. Of course, in the case of the whole year, the above procedure leads only to an approximation of the real optimal solution. In order to solve correctly and realistically the case of optimization of the whole year, all 30 days of all 12 months should be considered interconnected, thus forming a 24×365×4=35040 variable problem, which would be very hard to solve efficiently.

2.7.4 Results and Comments

For economy of space, optimization results for only two months (January and July) are presented in this section. The month January is selected as a representative of the cold period, while the month July is the representative of the hot period of operation. Optimization results for both months are presented in comparison with results of the original work. Furthermore, optimization results in terms of total cost using 24 time intervals per day for a whole month are compared to the results where 9 time intervals per day for a whole month were used.

The energy needs of the building that must be covered by the trigeneration system are given in Table 2.3 for a typical day of January and Table 2.6 for a typical day of July, while the optimization results (values of the independent variables as well as important dependent variables) of the original work and the current work for January are given in Tables 2.4 and 2.5, respectively. It can be observed that during January (cold period) the cogeneration unit operates at its nominal load from 06.00 to 20.00 and the thermal energy produced by the unit is used to cover the thermal loads. The use of thermal energy from the boilers in order to drive the absorption chiller is not recommended (Ψ_{ABS}=0), while the necessary cooling load is covered by the compression chillers.

Table 2.3. Building energy needs in a typical day in January [Vallianou and Frangopoulos (2012)].

Time period	W_{cons} (kW)	Q_{cons} (kW)	Ψ_{cons} (kW)
00.00-06.00	0	0	0
06.00-08.00	455	1380	700
08.00-10.00	580	1690	700
10.00-12.00	625	1530	700
12.00-14.00	650	1360	700
14.00-16.00	635	1320	700
16.00-18.00	605	1420	700
18.00-20.00	465	1210	700
20.00-00.00	0	0	0

Comparing the results of the current work with the results of the original work we can see a minor difference in the way the thermal power output of the boilers and the burner of the hot water tank, $\dot{Q}_B$, is exploited during the time interval 06.00-08.00. Indeed, as it is proven by the value of the objective function (total cost), a "more optimal" strategy for $\dot{Q}_B$ is determined in the case of 1-hour time intervals, which in turn leads to a more economical mode of operation for the trigeneration system. The optimal total cost in the case of the typical week is calculated at 8.265,16 € for 9 intervals per day and at 8.115,13 € for 24 intervals per day. Respectively, the optimal total costs in the case where the system is optimized for the whole month using 9 and 24 time intervals per day can be found in Table 2.9.

Table 2.4. Optimization results for a typical day in January [Vallianou and Frangopoulos (2012)].

Time period	W_{COG} (kW)	Q_{COG} (kW)	Q_B (kW)	Ψ_{ABS} (kW)	Q_{ABS} (kW)	Ψ_{CHEL} (kW)
00.00-06.00	0	0	0	0	0	0
06.00-08.00	540	759	625,7	0	0	701,0
08.00-10.00	540	759	932,2	0	0	700,2
10.00-12.00	540	759	772,2	0	0	700,2
12.00-14.00	540	759	602,2	0	0	700,2
14.00-16.00	540	759	562.2	0	0	700,2
16.00-18.00	540	759	662,2	0	0	700,2
18.00-20.00	540	759	452,2	0	0	700,2
20.00-24.00	0	0	0	0	0	0

Table 2.5. Optimization results for a typical day in January (current work).

Time period	W_{COG} (kW)	Q_{COG} (kW)	Q_B (kW)	Ψ_{ABS} (kW)	Q_{ABS} (kW)	Ψ_{CHEL} (kW)
00.00-06.00	0	0	0	0	0	0
06.00-07.00	540	759	629,2	0	0	701,7
07.00-08.00	540	759	622,2	0	0	700,2
08.00-09.00	540	759	932,2	0	0	700,2
09.00-10.00	540	759	932,2	0	0	700,2
10.00-11.00	540	759	772,2	0	0	700,2
11.00-12.00	540	759	772,2	0	0	700,2
12.00-13.00	540	759	602,2	0	0	700,2
13.00-14.00	540	759	602,2	0	0	700,2
14.00-15.00	540	759	562,2	0	0	700,2
15.00-16.00	540	759	562,2	0	0	700,2
16.00-17.00	540	759	662,2	0	0	700,2
17.00-18.00	540	759	662,2	0	0	700,2
18.00-19.00	540	759	452,2	0	0	700,2
19.00-20.00	540	759	452,2	0	0	700,2
20.00-00.00	0	0	0	0	0	0

The results for July (hot period) from the original work and the current work are presented in Tables 2.7 and 2.8. It can be observed that during July, the absorption chiller operates at its full capacity from 07.00 to 19.00, while the cogeneration unit operates at its nominal load from 06.00 to 20.00.

Table 2.6. Building energy needs in a typical day in July [Vallianou and Frangopoulos (2012)].

Time period	W_{cons} (kW)	Q_{cons} (kW)	Ψ_{cons} (kW)
00.00-06.00	0	0	0
06.00-08.00	455	465	1130
08.00-10.00	580	465	1650
10.00-12.00	625	465	2060
12.00-14.00	650	465	2430
14.00-16.00	635	465	2620
16.00-18.00	605	465	2490
18.00-20.00	465	465	2070
20.00-00.00	0	0	0

Table 2.7 Optimization results for a typical day in July [Vallianou and Frangopoulos (2012)].

Time period	W_{COG} (kW)	Q_{COG} (kW)	Q_B (kW)	Ψ_{ABS} (kW)	Q_{ABS} (kW)	Ψ_{CHEL} (kW)
00.00-06.00	0	0	0	0	0	0
06.00-08.00	540	759	0	189,1	283,6	973,4
08.00-10.00	540	759	0	206	293,9	1444,9
10.00-12.00	540	759	0	206	294,2	1854,6
12.00-14.00	540	759	0	206	294,2	2210,0
14.00-16.00	540	759	0	206	294,2	2414,4
16.00-18.00	540	759	0	206	294,2	2284,4
18.00-20.00	540	759	0	80.5	127,9	1985,3
20.00-24.00	540	759	0	0	6,8	0

Comparing the current results with the respective results from the original work, it can be once again verified that the use of 1-hour time intervals leads to a better optimal operation strategy for the absorption chiller (start-up and shut-down) combined with the compression chiller and cooling tank, thus to a better value for the total cost. The optimal total cost in the case of the typical week is calculated at 9.552,16 € for 9 intervals per day and at 9.389,16 € for 24 intervals per day. Same as above, the optimal total costs in the case where the system is optimized for the whole month using 9 and 24 time intervals per day can be found in Table 2.9.

Table 2.8. Optimization results for a typical day in July (current work).

Time period	W_{COG} (kW)	Q_{COG} (kW)	Q_B (kW)	Ψ_{ABS} (kW)	Q_{ABS} (kW)	Ψ_{CHEL} (kW)
00.00-06.00	0	0	0	0	0	0
06.00-07.00	540	759	0	166,1	268,4	1061,9
07.00-08.00	540	759	0	206	293,7	939,2
08.00-09.00	540	759	0	206	294,2	1445,1
09.00-10.00	540	759	0	206	294,2	1444,6
10.00-11.00	540	759	0	206	294,2	1854,5
11.00-12.00	540	759	0	206	294,2	1854,5
12.00-13.00	540	759	0	206	294,2	2195,5
13.00-14.00	540	759	0	206	294,2	2224,4
14.00-15.00	540	759	0	206	294,2	2414,4
15.00-16.00	540	759	0	206	294,2	2414,4
16.00-17.00	540	759	0	206	294,2	2284,4
17.00-18.00	540	759	0	206	294,2	2284,4
18.00-19.00	540	759	0	206	294,2	1864,4
19.00-20.00	540	759	0	33,2	100,0	2022,4
20.00-21.00	0	0	0	0	17,4	0
21.00-00.00	0	0	0	0	0	0

In the original work of Vallianou and Frangopoulos (2012) the effectiveness of the optimization procedure was verified by comparing the results with typical predetermined operation modes of the system in terms of overall cost. Here, since the results of optimization are improved in comparison with those of the original work, there is no need to repeat this comparison.

Finally, in Table 2.9 the total optimal costs for the cases of optimization of the trigeneration system for a whole 30-day period (month) using 9 time intervals per day and 24 time intervals per day are presented. It can be deduced that the case where 1-hour time intervals per day were used provides a superior optimal solution compared to the case of 9 time intervals per day. This result was expected due to two fairly logical reasons. Firstly, the use of 1-hour time intervals means that the differential equations that describe the transient operation of the storage tanks, Eq. (2.160), are solved more accurately than in the case where 2-hour and 6-hour intervals are used, as in essence a smaller time step is used. Secondly, the transient operation of the absorption chiller, as has already been mentioned before, lasts for 20 minutes. Thus, the use of time intervals with lengths longer than 20 minutes is expected to introduce an error in the simulation of the system, which decreases as the selected time interval becomes smaller and smaller. So, differences in the results are to be expected when using 1-hour intervals instead of 2-hour intervals and the closer the time interval used is to the recommended value of 20 minutes, the more "optimal" and more realistic solutions will be produced.

Table 2.9. Optimal Cost per Month (in Euros).

Month	Cost (Euros) 9 intervals	Cost (Euros) 24 intervals
January	38029,97	37339,94
February	31413,53	30813,30
March	33787,05	33126,92
April	32162,30	31532,28
May	34569,77	33847,61
June	37114,59	36437,70
July	42029,21	41313,16
August	22257,42	21567,69
September	31454,78	30823,24
October	30281,13	29590,56
November	34187,58	33527,55
December	35230,65	34600,44

Another important note that must be highlighted here and cannot be easily observed by studying the preceding tables is the fact that solving the problem for a typical week and for a typical month is in essence two very different optimization problems. Indeed, by taking for example the month January and optimizing (with 1-hour time intervals) for a time horizon of a week, the optimal total cost is found to be equal to 8.115 € while in the case of the whole month the optimal total cost is found to be equal to 37.339 €, which is not equal to the product of 8.115 € with the number of weeks per month. However, this result is to be expected, since in the case of the whole month each week is interconnected with its previous and next by the transient operation of the tanks during weekends, thus a more complex, more complete and closer to reality optimization problem is produced, which is different from the problem of optimizing the system for a single week and the two cases should not be compared to each other.

CHAPTER 3: THE GENERAL FRAMEWORK FOR DYNAMIC OPTIMIZATION OF MARINE ENERGY SYSTEMS

3.1 General

As described in the introductory chapter of this thesis, the aim of this work is to develop a comprehensive and efficient method for the dynamic optimization of synthesis, design and operation of marine energy systems. In this chapter the general formulation of the problem, accompanied with a suitable mathematical framework, based on a generic marine energy system is presented.

The term "generic" is used to highlight the fact that the energy system is modeled in a way that can encompass a multitude of synthesis, design and operation alternatives among which the dynamic optimization algorithm can search for the optimal, after a suitable objective function is determined, the necessary technical, operational or even economic constraints are imposed and the required parameters of the vessel mission are defined.

Since the generic marine energy system is composed of many individual components, whose existence in the final synthesis of the system, their design characteristics and their operation profile are under optimization, suitable component models have been developed and are thoroughly presented in the next chapter of this study, Chapter 4. Of course, all these components, both in terms of synthesis/design and in terms of operation are inherently interrelated to each other, to the mission characteristics and to the time (or time and space) varying operational requirements of the vessel. Thus, they cannot be treated separately but have to be optimized simultaneously as parts of the whole system. The formulation of the generic system serves as a basis for incorporating all the individual component models and their interrelations, under a single framework and also ensures that the problem is correctly stated in a suitable "dynamic optimization problem" formulation, so that dynamic optimization methods can be applied.

Special attention has been given to the construction of a superconfiguration that depicts all the available synthesis options and the possible interconnections among components. In the next section, the superconfiguration of the generic system that contains all the possible synthesis options is presented. However, for the case studies, presented in Chapter 5, simpler superconfigurations are used.

Furthermore, it is noted that the dynamic optimization problem of the generic marine energy system that will be described in the rest of this Chapter is set up as one-level dynamic optimization problem, and more specifically as a Mixed Integer Dynamic Optimization Problem (MIDO), since integer and binary variables are used to define the synthesis of the energy system. By the term "one-level", it is meant that the three levels of optimization (synthesis-design-operation) are stated in a single complex problem and treated by the optimizer simultaneously. A detailed discussion of this feature, as well as the method of treatment for the integer variables, is given in Section 3.3.2.

Finally, in Section 3.4, the appropriate dynamic optimization procedures that were developed for this study, along with the related software in which they were implemented, are presented.

3.2 Description of the generic energy system – The superconfiguration

In this study, the optimal configuration (synthesis), design specifications of components and operating conditions of an energy system that will cover all energy needs

of a ship on a fixed route under the scope of minimizing/maximizing a cost related objective function, are requested.

The requested propulsion power is not known in advance, but depends on the vessel speed and weather conditions along the route. The varying with time or space and time weather conditions encountered by the ship have an effect on the total resistance of the vessel, thus impact the required power from the propulsion plant in order to attain a certain speed. Furthermore, the ship speed at any instant of time is unknown and also under optimization, since only the route is predetermined in advance and the total travel time can be either predetermined or variable and under optimization, depending on the mission profile which is a parameter to the problem. This problem is an inherently dynamic one, since the speed in a certain instant of time affects and is affected by the speed in all other instants.

A superconfiguration of the generic energy system that will cover all energy needs is considered in Figure 3.1. A single propeller is driven by the propulsion plant which may comprise a number of two stroke diesel engines, four stroke diesel engines and a number of gas turbines. For the gas turbines, three different types are considered. Details considering the selection of the three possible gas turbine types are given in Chapter 4, Section 4.5, Figure 4.4. The type and number of engines that constitute the propulsion plant is under optimization. One or more (determined by optimization) single-pressure heat recovery steam generators (HRSGs) will serve part or all of the thermal demands by saturated steam extraction from the drum, while the superheated steam produced will drive one or more (determined by optimization) steam-turbines, if the optimization thus dictates. The power produced by the steam turbine(s) will be distributed between the propeller and a generator, which will supply electric power for the service of the electric loads. Diesel generator sets (the number is also determined by optimization) and an auxiliary boiler are included, which will cover the electric and thermal demands in port and will supply electric and thermal energy during voyages in case the STGs and HRSGs cannot fully cover the loads.

The type (e.g. four stroke diesel engines, two stroke diesel engines, gas turbines), number and design characteristics (e.g. nominal power output of the propulsion plant, the HRSGs, the gensets, etc.) of all the components described above are not predetermined but variable and under optimization. Also, the operational profile of each component at each instant/interval of time is also under optimization.

Regarding the weather conditions encountered by the ship during the trip, only the wind speed and direction and the wave height and direction are taken into consideration in this work, since other parameters such as pressure, temperature, fog, etc. are not crucial in the determination of ship speed and the required propulsion power. Once these four parameters are given as inputs, either as constants or as functions of space and time, the added resistances of wind and waves are calculated, thus the total resistance can also be calculated. All details considering the treatment of the weather as well as the calculation of ship resistance and propulsion are presented in Section 4.7 of Chapter 4, where the appropriate ship resistance and propulsion models are discussed.

The electric and thermal demands are parameters of the problem and are given as inputs. They can be defined in various ways; for example they can be considered constant or functions of variables such as time, distance travelled or brake power, depending on the profile of the mission.

Finally, it is noted that the problem can be set so that it optimizes the system for a single trip or for consecutive trips over a total period of time, which can span up to the full life cycle of the vessel taking into consideration the real conditions (if available) prevailing at each instant of time.

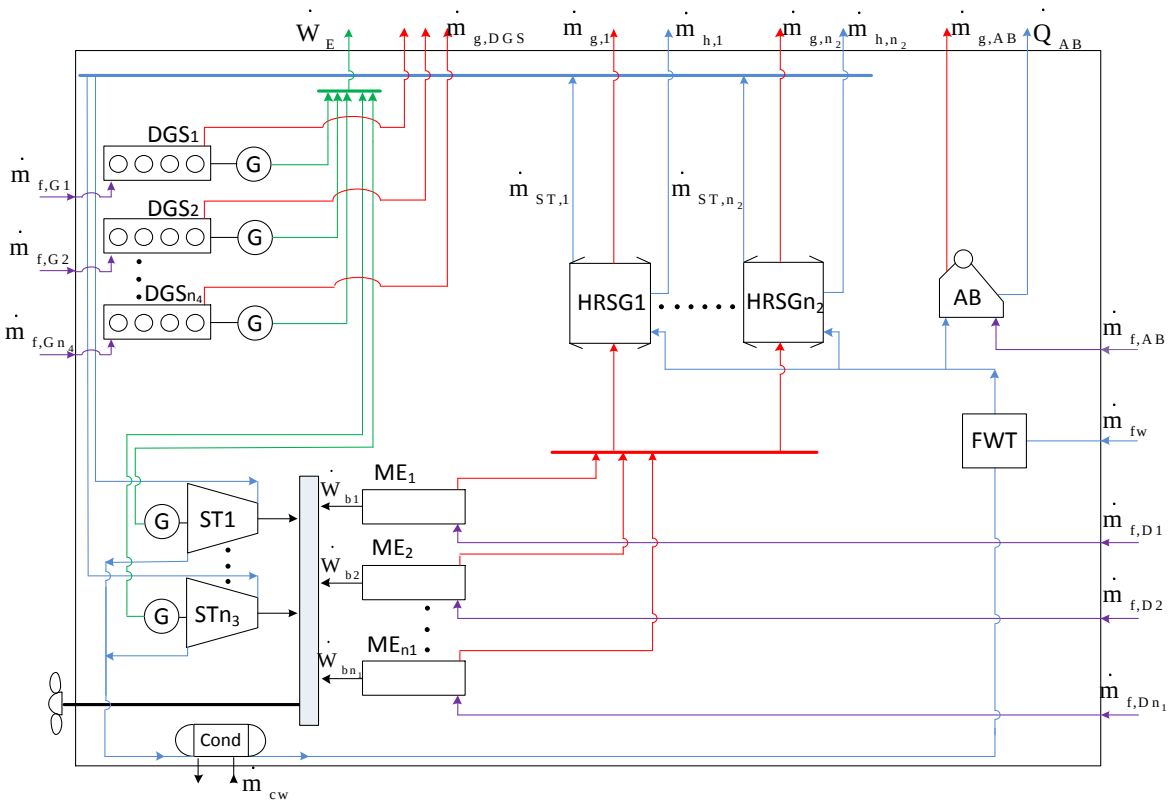

Figure 3.1. Superconfiguration of the generic energy system.
(AB: auxiliary boiler, Cond: condenser, DGS: diesel-generator set, FWT: feed water tank, G: generator, HRSG: heat recovery steam generator, ME: main engine, ST: steam turbine)

3.3 The General Dynamic Optimization Problem

3.3.1 Mathematical statement of the general problem

The dynamic optimization problem can be mathematically stated using a Differential – Algebraic Equation (DAE) formulation. The total time horizon of the optimization, t_f, can be either a predetermined parameter (fixed) or an optimization variable. Here, in the general case, it is stated as an optimization variable. The objective function is selected to be either the minimization of the present worth cost, PWC, which consists of capital, fuel and operation expenses, or the maximization of the Net Present Value (NPV). Analytic equations regarding the calculation of these economic criteria are given in Appendix B.

In the case of minimization of PWC, the objective function is mathematically stated as

$$\min_{\vec{x},t_f} PWC = PWC_c + PWC_f + PWC_{om} \tag{3.1a}$$

whereas in the case of maximization of NPV it is stated as

$$\max_{\vec{x},t_{fi}} NPV = PWR - PWC \tag{3.1b}$$

where

PWC_c capital present worth cost,
PWC_f fuel present worth cost,
PWC_{om} operation and maintenance present worth cost,
PWR present worth of revenue,
t_f final time (total time horizon of the optimization),

Vector $\vec{x}$, represents the vector of control (optimization) variables, consisting of the vectors of synthesis, design and operation optimization variables ($\vec{v}$, $\vec{w}$ and $\vec{z}$, respectively):

$$\vec{x} = (\vec{v}, \vec{w}, \vec{z}) \tag{3.2}$$

with

$$\vec{v} = \left(z_{D,2-X}, z_{D,4-X}, z_{GT1}, z_{GT2}, z_{GT3}, z_B, z_{ST}, z_{DG}, y_{AB} \right) \tag{3.3a}$$

$$\vec{w} = \left(\dot{W}_{bn,i,j}, \dot{m}_{g_n,k}, T_{g_n,k}, \dot{m}_{s_n,k}, \dot{m}_{ST_n,l}, \dot{W}_{DG_n,m}, \dot{Q}_{AB_n} \right) \tag{3.3b}$$

$$\vec{z} = \left(\dot{W}_{b,i,j}, \lambda_{h,k}, \lambda_{e,l}, \dot{W}_{DG,m} \right) \tag{3.3c}$$

where

$$j = \begin{cases} 0,...,z_{D,2-X} & \text{for} \quad i = D,2-X \\ 0,...,z_{D,4-X} & \text{for} \quad i = D,4-X \\ 0,...,z_{GT1} & \text{for} \quad i = GT1 \\ 0,...,z_{GT2} & \text{for} \quad i = GT2 \\ 0,...,z_{GT3} & \text{for} \quad i = GT3 \end{cases} \tag{3.4a}$$

$$k = 0,...,z_B \tag{3.4b}$$

$$l = 0,...,z_{ST} \tag{3.4c}$$

$$m = 0,...,z_{DG} \tag{3.4d}$$

and:

$z_{D,2-X}$ number of two stroke diesel engines (integer variable),
$z_{D,4-X}$ number of four stroke diesel engines (integer variable),
z_{GT1} number of type 1 gas turbines (integer variable),
z_{GT2} number of type 2 gas turbines (integer variable),
z_{GT3} number of type 3 gas turbines (integer variable),
z_B number of heat recovery steam generators (integer variable),
z_{ST} number of steam turbines (integer variable),
z_{DG} number of diesel generator sets (integer variable),
y_{AB} variable determining the existence of the auxiliary boiler (binary variable),

$\dot{W}_{bn,i,j}$ nominal brake power output of j th engine of type i (invariant[2]),

$\dot{m}_{g_n,k}$ nominal exhaust gas mass flow rate of k th HRSG (invariant),

$T_{g_n,k}$ nominal exhaust gas temperature of k th HRSG (invariant),

$\dot{m}_{s_n,k}$ nominal steam mass flow rate of k th HRSG (invariant),

$\dot{m}_{ST_n,l}$ nominal steam mass flow rate of l th ST (invariant),

$\dot{W}_{DG_n,m}$ nominal power output of m th generator set (invariant),

$\dot{Q}_{AB_n}$ nominal thermal power output of auxiliary boiler (invariant),

$\dot{W}_{b,i,j}$ brake power output of j th engine of type i,

$\lambda_{h,k}$ fraction of k th HRSG steam mass flow rate delivered to thermal loads:

$$\dot{m}_{s,h,k} = \lambda_{h,k} \cdot \dot{m}_{s,k} \tag{3.5a}$$

$\dot{m}_{s,h,k}$ steam mass flow rate drawn from k th HRSG drum for serving thermal loads,

$\dot{m}_{s,k}$ steam mass flow rate of k th HRSG unit,

$\lambda_{e,l}$ fraction of l th steam turbine power output delivered to generator:

$$\dot{W}_{STG,l} = \lambda_{e,l} \cdot \dot{W}_{ST,l} \tag{3.5b}$$

$\dot{W}_{STG,l}$ l th steam turbine generator power for serving electric loads,

$\dot{W}_{ST,l}$ l th steam turbine power output,

$\dot{W}_{DG,m}$ m th diesel generator set power output.

Indices j, k, l and m run through all the values from 0 up to an upper value. The upper values of indices j, k, l and m are not determined (fixed) at the beginning of the optimization, since they are in fact defined by the values of their respective –integer- synthesis variables. However, they are bound from above with the same upper bounds of these respective integer synthesis variables, which must be well determined and fixed at the start of the optimization. Specifically, as can be seen from Eq. (3.4a), the upper value of index j depends on the index i which determines the type of propulsion equipment and from the respective value of the, under optimization, integer variable that determines how many components of type i will be installed. Thus, the problem has as many design and operation variables for the components, as the integer values of the synthesis control variables dictate. Variable y_{AB} that determines the existence of the auxiliary boiler is binary. In both cases of integer and binary variables, value 0 denotes that the unit is not installed.

The main differential variables for this problem are the distance travelled by the ship, defined as:

$$\frac{d}{dt} d_{travel} = V \tag{3.6}$$

the fuel consumption of the propulsion engines and diesel generator sets, generally defined with the help of the Specific Fuel Oil Consumption (SFOC) of the component and the produced brake power as:

---

[2] Time-independent optimization variable.

$$\frac{d}{dt} m_f = b_f \dot{W}_b \tag{3.7}$$

and the fuel consumption of the auxiliary boiler, defined as:

$$\frac{d}{dt} m_{f,AB} = \frac{\dot{Q}_{AB}}{\eta_{AB} \cdot H_u} \tag{3.8}$$

where η_{AB} is considered a constant parameter.

Another family of differential variables is derived from the energy output of each component, which is generally given as:

$$\frac{d}{dt} E = \dot{Y}, \qquad \dot{Y} = \dot{W}, \dot{Q} \tag{3.9}$$

The fuel consumption and the energy output of each component are necessary in order to calculate the fuel, operation and maintenance costs for each component, which are main parts of the operational costs of the system and both the objective functions. The capital costs for each component are calculated using the values of the design variables (Eq. 3.3b). Detailed information considering the calculations of the capital cost for each component are given in Appendix C.

Since the propulsion plant characteristics, i.e. type and number of engines and their nominal power, are not known but they are the results of optimization, a unique Specific Fuel Oil Consumption (SFOC) curve as a function of load only is not sufficient. Thus, based on manufacturer data, SFOC surfaces are constructed, where the SFOC for each engine of type *i* as well as the exhaust gas mass flow rate and temperature are given as two-variable (nominal power and load factor) functions. The total exhaust gas mass flow rate and temperature from all engines is then calculated and supplied to the HRSGs. The same procedure (two variable functions) is also applied in the modeling of diesel generator sets SFOC and exhaust gas properties. The models used for the propulsion engines and the diesel generator sets are presented in Chapter 4.

The condition that the brake power of the main engines and the steam turbine, as well as the electric and thermal power produced by the integrated system must be equal to the required brake power, the electric and thermal demands at any instant of time, respectively, leads to the equality constraints:

$$\sum_{i,j} \dot{W}_{b,i,j} + \sum_{l} \dot{W}_{ST,p,l} = \sum_{i,j} \dot{W}_{b,i,j} + \sum_{l} \left(1 - \lambda_{e,l}\right) \cdot \dot{W}_{ST,l} = \dot{W}_b \tag{3.10}$$

$$\sum_{l} \dot{W}_{STG,l} + \sum_{m} \dot{W}_{DG,m} = \sum_{l} \lambda_{e,l} \cdot \dot{W}_{ST,l} + \sum_{m} \dot{W}_{DG,m} = \dot{W}_e \tag{3.11}$$

$$\sum_{k} \dot{Q}_{B,k} + \dot{Q}_{AB} = \dot{Q} \tag{3.12}$$

where

$\dot{W}_{ST,p,l}$ propulsion power from *l* th ST,

$\dot{W}_b$ required brake power from the engines,

$\dot{W}_e$ electric load,

$\dot{Q}_{B,k}$ heat drawn from *k* th HRSG drum for serving thermal loads,

$\dot{Q}$ thermal load.

The total required brake power of the engines is calculated as a function of the ship speed, ship resistance and propulsive efficiency as

$$\dot{W}_b = \frac{V \cdot R_{tot}(V, WS, \mathbf{p})}{\eta_{prop}(V, WS, \mathbf{p})} \tag{3.13}$$

where

WS weather state,

p constant parameters describing the vessel,

η_{prop} propulsive efficiency.

All terms of Eq. (3.13) are discussed in detail in Chapter 4 and in Appendixes D and E.

It is clarified that even though the ship speed is unknown and under optimization, it is not directly declared as a control variable. Instead, it is derived from the brake power outputs of the main engines, Eqs. (3.10), (3.13), which are declared as control variables. Thus, the ship speed is –indirectly– determined by optimization.

Finally, there are equalities developed by the simulation of the components as well as inequality constraints imposed on the variables, but their full presentation is beyond the limits of the present text. Noteworthy inequality constraints include the upper and lower bounds imposed on the speed of the ship

$$V_{\min} \le V \le V_{\max} \tag{3.14}$$

and the upper and lower bounds imposed on the load factor, f_L, of all components (main engines, diesel generator sets, steam turbines, etc.) that ensure their operation inside the limits specified by the manufacturer:

$$f_{L_{\min}} \le f_L \le f_{L_{\max}} \tag{3.15}$$

Of course all control variables, are accompanied by upper and lower limits. However, upper and lower limits may not be necessary for all state variables.

Additional constraints may be imposed by emission regulations if, for example, the ship travels within emission controlled areas (ECAs). Such a case is not examined in this work, but it is not difficult to include emission constraints wherever applicable.

3.3.2 Variables for the synthesis, design and operation levels

The general dynamic optimization problem stated in the previous section has been formulated so that the aspects of synthesis, design and operation, regarding a generic marine energy system are considered.

A common practice followed in the literature [Olsommer B. (1998), Munoz JR and von Spakovsky MR. (2003), Dimopoulos et al. (2008), Dimopoulos and Frangopoulos

(2008), Dimopoulos G. (2009)] denotes that a Synthesis–Design–Operation problem is usually stated as a two–level problem and the optimizer would firstly solve the Synthesis/Design problem (higher level) and then the Operation sub-problem (lower level) and reach to an optimal solution via iteration between the two levels.

In this study, as is evident from the mathematical statement presented in Section 3.3.1, the problem is stated and consequently treated by the optimization procedure in a single level as a Mixed Integer DO problem (MIDO). The distinction between the three levels of Synthesis, Design and Operation is only conceptual in terms of the solution procedure applied; however, it is reflected in the general mathematical formulation in terms of the *type of variables* used to describe each level.

Specifically, for the level of operation, "continuous" real variables are used that change at each instant of time. If present in the system, the power output of the main engines and diesel generators and the fractions of HRSGs steam mass flow rate and steam turbine power output, delivered to thermal and electric loads respectively, are all represented by time dependent (dynamic) control variables.

For the level of design, "static" or invariant real variables are used. The nominal power output of all, if present in the system, main engines, diesel generator sets, auxiliary boiler and the nominal values of the design parameters of the HRSGs and steam turbines are all denoted by variables that have a single static value throughout the time horizon of the optimization.

For the level of synthesis static, integer and binary, variables are used. Since several technology alternatives (two stroke DEs, four stroke DEs and three different types of GTs (discussed in Section 4.5) are available for the propulsion plant, five integer variables, each one representing the number of units of each alternative that may be installed, are used. For the HRSGs, since one technology alternative is considered, we are only interested in the number of units, thus one integer variable is used. The same applies for the steam turbines and the diesel generators. Finally, the existence of the auxiliary boiler is determined via the use of a binary variable.

From the discussion up until now and the mathematical formulation presented in the previous section it is evident that the values of the synthesis variables have a severe effect on the whole problem, since the specific value of each variable affects the underlying design and operation levels in terms of the number of (design and operation) variables that should be present in the problem as well as in terms of the underlying system of equations. Essentially, this means that each time one integer variable changes value, the optimization problem must be reformulated either by adding the necessary extra variables and their related equations or by subtracting them, depending on the increase or the decrease of the value of the integer variable.

Of course, this adversity could be treated by using a conventional "if…then…else" custom algorithmic formulation for each integer variable, where for each value of the variable the underlying system (variables and equations) would be reformulated. However, this would not be a true single–level treatment of the problem, and it would be impossible to apply any gradient based dynamic optimization method for the solution of the problem. Furthermore, the complexity of the required code would highly increase with the increase of the number of the integer variables and their possible values.

In order to tackle with this specific difficulty, a special technique based on the idea of the superconfiguration (Fig. 3.1), presented in Section 3.2, has been developed. The idea is to consider all possible technology alternatives initially present at the system, and also for each alternative to consider the maximum number of units, given by the upper bound of the respective integer variable. Then, each unit can be represented by a binary variable that determines the existence or not of the said unit. In this way, each integer variable that is

present in the formulation of Section 3.3.1 is translated into a series of binary variables and thus all integer variables are eliminated from the system, without in fact increasing the dimensionality of the problem. In other words, each value of each integer variable now corresponds to a binary variable.

Furthermore, since now only binary variables are used, it can be arranged so that the value 1 corresponds to the existence of the specific component while the value 0 will correspond to the exclusion of the specific component from the system. This feature can be used to our advantage, since, now instead of using an "if…then…else" strategy, a more compact formulation can be applied. The problem can be stated with the maximum possible number of design and operation variables with all their accompanying equations (model equations, constraints, costs, etc.) multiplied by the respective binary variable. The idea is that, if the optimizer dictates the installation of a component (thus it will set the relative binary variable equal to 1) the accompanying system of equations will not be affected. The cost calculations, pertinent to the component, will participate in the objective function calculations and the relative gradients will not be zero. However, if the relative binary variable is set to zero, all relative to the component variables and equations will still be present in the system but they will not affect the optimization. The costs pertinent to the component will not be added to the objective function while the necessary gradients will be calculated as zero. The same will stand for the constraints. From the point of view of the optimizer, the operation and design variables relative to the said component, cannot affect the objective function and constraints, thus their values are irrelevant to the optimization.

An example, based on Eq. (3.10) can be given. For simplicity, let's assume that only two stroke and four stroke diesel engines are possible propulsion alternatives and up to two units of each may be installed. Then Eq. (3.10) is re-stated using 4 binary variables as follows:

$$\sum_{i=1}^{2} y_{D,2-X,i}\dot{W}_{b,2-X,i} + \sum_{i=1}^{2} y_{D,4-X,i}\dot{W}_{b,4-X,i} = \dot{W}_b \tag{3.16}$$

where

$y_{D,2-X,1}$ variable determining the existence of first 2-X DE (binary),

$y_{D,2-X,2}$ variable determining the existence of second 2-X DE (binary),

$y_{D,4-X,1}$ variable determining the existence of first 4-X DE (binary),

$y_{D,4-X,2}$ variable determining the existence of second 4-X DE (binary),

$\dot{W}_{b,2-X,1}$ brake power of first 2-X DE (continuous variable),

$\dot{W}_{b,2-X,2}$ brake power of second 2-X DE (continuous variable),

$\dot{W}_{b,4-X,1}$ brake power of first 4-X DE (continuous variable),

$\dot{W}_{b,4-X,2}$ brake power of second 4-X DE (continuous variable).

Also, if the objective is the minimization of the PWC, then the corresponding PWC of the propulsion plant, which is part of the total PWC, must be stated as follows:

$$PWC_D = \sum_{i=1}^{2} y_{D,2-X,i} \cdot PWC_{D,2-X,i} + \sum_{i=1}^{2} y_{D,4-X,i} \cdot PWC_{D,4-X,i} \tag{3.17}$$

where

PWC_D total PWC for the propulsion plant,
$PWC_{D,2-X,i}$ total PWC of *i* th 2-X DE,
$PWC_{D,4-X,i}$ total PWC of *i* th 4-X DE.

Finally, it is noted that this transcription of integer to binary variables does not complicate the definition of several constraints that we may need to impose on the synthesis of the system. For example, in the case of optimizing a system where no more than three generator sets would be allowed, based on the integer formalism, the constraint would be stated as:

$$0 \le z_{DG} \le 3 \tag{3.18}$$

while the equivalent binary expression would simply be:

$$\sum_{i=0}^{3} y_{DG,i} \le 3 \tag{3.19}$$

with, $y_{DG,i}$,the binary variable determining the existence of the *i* th diesel generator set.

3.4 Dynamic Optimization Procedure and Related Software

Based on the analysis of all available solution methods for DOPs, that was presented in Chapter 2, two different approaches from the family of direct solution methods (Fig. 2.4) were formulated and implemented for the solution of the DOP that was stated in Section 3.3: a sequential method (based on the sequential approach) and a simultaneous method (based on the simultaneous approach).

From the comparative comments between sequential and simultaneous methods stated in Paragraph 2.6.6, it is evident that algorithms based on sequential methods are easier to develop and implement and can take advantage of very reliable existing DAE and NLP modern solvers (e.g. DASOLV, DASSL, NPSOL, SNOPT). Also, in terms of computational time, sequential methods have, in general, an advantage over the simultaneous methods in problems that contain few control variables and many state variables.

Considering the specific DO problem at hand, it can be either a closed loop dynamic optimization problem (trip duration known) or an open loop dynamic optimization problem (trip duration unknown) depending on the mission characteristics. However, in both cases, compared to the large number of state variables, we have few control variables (synthesis and design control variables are invariant) while at the same time the numerical integration of the underlying DAE model proves to be not too time consuming due to the high efficiency of modern solvers.

Based on these arguments, the main focus was given to the application of the sequential method, which proved able to tackle all the DO problems of all case studies and was used with success both in the case of closed loop (final time known) and open loop (final time under optimization) problems. The simultaneous method was applied only in the most complex cases (open loop problems with many synthesis alternatives) and while it also tackled those cases with success, in terms of accuracy, it proved less –or in very few cases equally – efficient than the sequential method in terms of computational time.

The sequential and simultaneous dynamic optimization methods and the dynamic models used to calculate ship resistance, propulsion, performance of main engines, HRSGs, steam turbines, diesel generator set units and their interconnections as well as the effects of the dynamically varying weather and loads were implemented in the commercial gPROMS® software.

The gPROMS® software is a unified modeling and solution platform that enables the user to program several models describing different components and combine them within a complete process flowsheet (the ship operation during a trip). This is a very important advantage in complex problems (such as those tackled in this study) since it allows the user to test and validate separately each specific model even while simulating the whole complex process. Another, helpful for the programmer, feature of the platform is that it allows the user to write the equations describing a process in any order, since they are all solved simultaneously, while steady-state and dynamic modeling can be carried out simultaneously within the same environment.

Furthermore, another reason that led to the selection of the gPROMS® platform lies in the fact that it provided two, convenient for this work, tools: the multiflash toolbox and the dynamic optimization toolbox. The multiflash toolbox uses tabulated data in order to calculate the physical properties of substances, which proved very useful in the case of calculating the steam/water properties for the HRSG and the steam turbine models. The dynamic optimization toolbox takes advantage of the gPROMS® platform capabilities and provides the opportunity to combine several robust solvers (NLP solver, MI solver, initialization solver) in order to coherently formulate and solve a dynamic optimization problem while avoiding several drawbacks encountered when writing custom code in any low level programming language.

The basic procedure/idea behind the sequential methods is presented in Figure 3.2 and has been described in detail in Chapter 2, Paragraph 2.4.3. For the sequential method implemented for the solution of all case study problems in this work, a Control Vector Parameterization (CVP) scheme is used for the discretization of the control variables. In this CVP scheme piecewise constant parameterization of the control variables, over equally spaced time intervals, is applied. In the gPROMS® environment, the overall sequential method is implemented via the solver CVP_SS of the gPROMS® optimization toolbox. The user imports the parameterization of the control variables and CVP_SS links everything to the NLPSQP solver for the solution of the NLP optimization problem. The DASOLV solver handles the numerical integration of the underlying DAE problem and the computation of sensitivities, while the BDNLSOL solver is used as the initialization and re-initialization solver when DASOLV is used for simulation activities. Finally, the mixed integer part of the problem (i.e. the binary variables) is handled via the OAERAP solver. Details on all solver codes can be found in gPROMS® user guides [gPROMS (2016)] which can be downloaded from the PSE website.

The application of the sequential method can be summarized in the following steps:

1. The user declares the duration of each control interval and the initial values of the control variables over the interval. (In case the duration is not fixed, it is also declared as a variable with an initial value.)
2. Starting from the initial point at time t=0 the dynamic system model is solved over the entire time horizon to determine the variation (with time) of all variables in the system.
3. The values of the objective function and constraints as well as the values of their partial derivatives (sensitivities) with respect to all quantities specified by the user are calculated.

4. The optimizer revises the choices made on step 1 and the procedure is repeated.

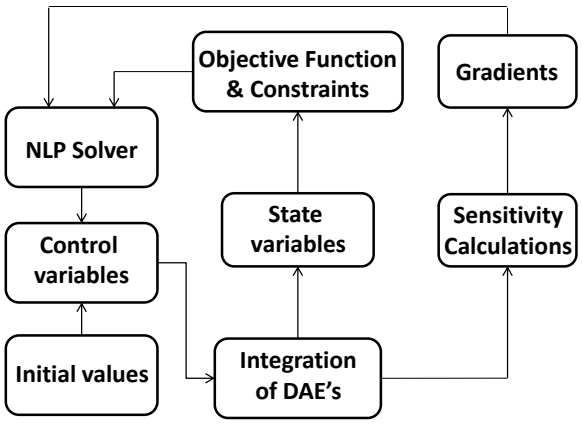

Figure 3.2. Sketch of the sequential approach used.

Often in the literature, as well as in the gPROMS® documentation, the sequential method presented above is referred to as a "single shooting" method. The term is derived from step 2 of the above algorithm, which involves a single integration of the dynamic model (DAE system of equations) over the entire horizon. Further details about the single shooting methods can be found in the literature [Bard (1974)].

The basic procedure/idea behind the simultaneous methods has been described in detail in Chapter 2, Paragraph 2.4.4. For the simultaneous method, the CVP_MS solver of the gPROMS® platform is used. Again, a piecewise constant parameterization of the control variables is performed, but in contrast to the CVP_SS solver, the control intervals are now optimized individually, while the control variables are manipulated to obtain a consistent solution at the interval boundaries. The same sub-solvers (NLPSQP, DASOLV, BDNLSOL, OAERAP) are used and linked together via CVP_MS.

This type of simultaneous method is often refered to as a "multiple-shooting" method in the literature. The term results from the fact that each control interval is treated independently and no integration of the DAE system of equations over the entire time horizon is performed. A more detailed description of the multiple shooting methods as well as further extensions of the direct multiple shooting methods to DAE systems can be found in the literature [Bock and Platt (1984), Schulz et al. (1998)].

CHAPTER 4: MODELING OF COMPONENTS

4.1 General

In this chapter the simulation models of the individual components that constitute the integrated marine energy system are presented. The general framework of dynamic optimization of marine energy systems, as was presented in the previous chapter, is essentially based on the accurate modeling of the individual components at both design and off-design operating point, which is essential in order to properly perform design and operation optimization. Thus, it is evident that the results of the dynamic optimization procedure on the overall system will be as accurate and efficient as these models are. Of course, it must also be noted that since economic criteria are used as objective functions for the optimizations performed in this work, apart from performance models, cost models are also developed for each component, which are presented in Appendix C.

The models used can be divided into two categories. Those that have been developed using a first principles approach combined with literature data, such as the models for the heat recovery steam generator, the steam turbine and the resistance – propulsion model, and those that are based on regression analysis of data, such as the models for the diesel engines (two and four stroke), the gas turbines, the auxiliary boiler and the diesel generator sets. Since, as it was presented in Chapter 3, all the models are incorporated into a general superconfiguration of the system and a dynamic optimization procedure is applied on the overall system, an effort was made to keep the model complexity and, thus, the computation/simulation times as low as possible during the modeling phase. It is noted that the optimizer may require the application of each model, as well as the calculation of the derivatives of the model output, several times and for many intervals during the optimization procedure. Thus, very detailed, complex and time consuming simulation models would have a dramatic effect on the required convergence time, or even accuracy, of the optimizer. However, caution was exercised in order not to diminish the validity and accuracy of the models.

Finally, it is noted that each model is separately inserted into the complete simulation structure in terms of coding. This essentially means that changes can be made in each specific model without affecting the overall simulation and optimization procedure. This feature is very convenient, since it enables the user/designer to easily replace each component model with another, more suitable for the requirements of the study, without having to make coding alterations to the overall algorithm. However, since the input and output specifications of each component model are pre-specified, the new model that will be used must obey to these specifications.

4.2 Heat Recovery Steam Generator (HRSG)

The models describing the heat recovery unit have been produced by the application of energy balances and heat transfer equations on the heat exchangers of the unit, in order to be able to simulate both nominal and off-design performance of the components. The nominal performance simulation model is used for the HRSG dimensioning, thus, it includes the design variables as inputs. Furthermore, the nominal performance model outputs are also used to evaluate the overall capital cost for the HRSG, which is assessed via semi-empirical cost functions adapted for marine applications (presented in Appendix C).

In this work, in order to avoid undue complications, only single pressure HRSG units have been considered. However, double or triple pressure HRSG units could be investigated.

4.2.1 Single pressure HRSG nominal performance

The schematic layout of a single pressure HRSG, with the heat exchangers and gas path configurations is depicted in Figure 4.1. The complete set of equations used for the simulation of this configuration is presented in the following.

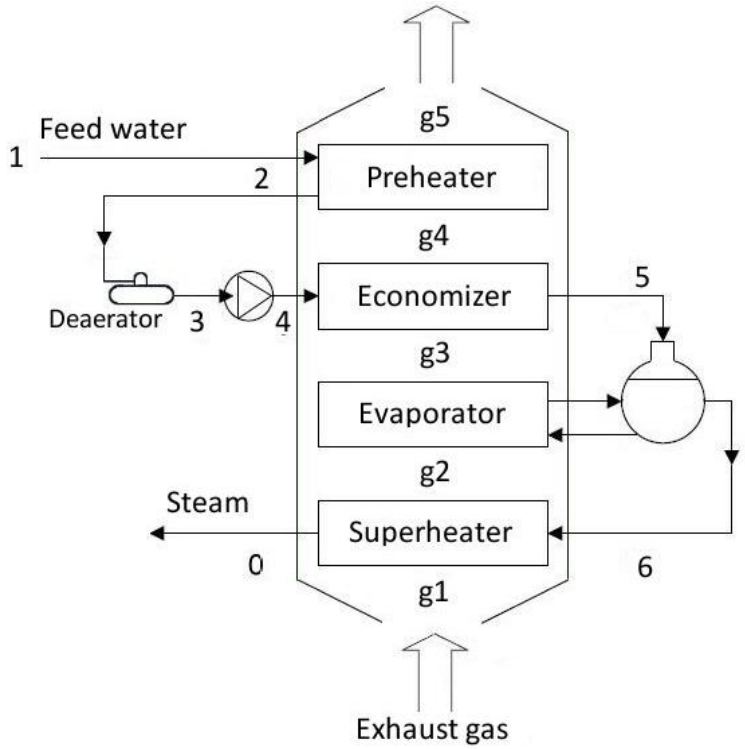

Figure 4.1. Single pressure HRSG configuration.

The main inputs to the nominal HRSG model are steam quality (pressure, temperature), steam mass flow rate and exhaust gas heat input (mass flow rate and temperature), while the main outputs are areas of heat exchangers and power of auxiliary equipment (pumps). Thus, the steam temperature, steam mass flow rate and the exhaust gas mass flow rate and temperature can be used as design variables (invariant over time) in the optimization set-up.

For each heat exchanger, two fundamental equations are used for nominal performance: a) the energy balance between exhaust gas heat input and useful heat production, and b) the heat transfer rate equation relating heat addition to temperature differences, material properties and the surface of the heat exchanger. In Figure 4.2 the exhaust gas and steam streams of a typical heat exchanger are depicted.

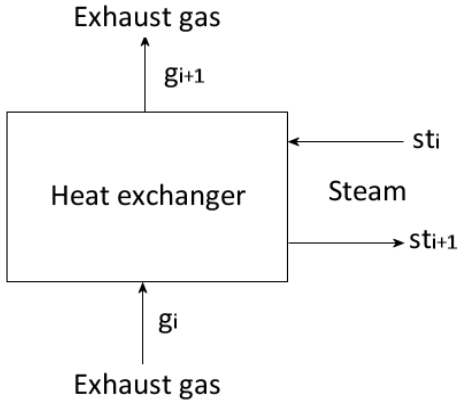

Figure 4.2. Typical heat exchanger inlet and outlet stream.

Based on the notation of Figure 4.2 the energy balance equations are written:

$$\dot{Q}_{HX} = \eta_{HX} \dot{m}_g c_{pg} (T_{g_i} - T_{g_{i+1}}) = \dot{m}_{st} (h_{st_{i+1}} - h_{st_i}) \tag{4.1}$$

$$\dot{Q}_{HX} = UA\Delta T_{lm} \tag{4.2}$$

The logarithmic mean temperature difference is defined as:

$$\Delta T_{lm} = \frac{(T_{g_{i+1}} - T_{st_i}) - (T_{g_i} - T_{st_{i+1}})}{\ln \dfrac{T_{g_{i+1}} - T_{st_i}}{T_{g_i} - T_{st_{i+1}}}} \tag{4.3}$$

where

$\dot{Q}_{HX}$	transferred heat rate
U	overall heat transfer coefficient
η_{HX}	efficiency of the heat exchanger (it accounts for thermal losses)
$\dot{m}_g$	gas mass flow rate
c_{pg}	gas specific heat capacity
T_{g_i}	gas inlet temperature
$T_{g_{i+1}}$	gas outlet temperature
T_{st_i}	water/steam inlet temperature
$T_{st_{i+1}}$	water/steam outlet temperature
$\dot{m}_{st}$	water/steam mass flow rate
h_{st_i}	water/steam inlet specific enthalpy
$h_{st_{i+1}}$	water/steam outlet specific enthalpy
A	heat transfer area of the heat exchanger.

The overall heat transfer coefficient, *U*, is a parameter dependent on the material and type of heat exchanger and is calculated according to Eq. (4.4) taken from Shah and Sekulic (2003).

$$\frac{1}{U} = \frac{1}{(\eta_0 \alpha)_{hot}} + R_{wall} A_{hot} + \frac{A_{hot}/A_{cold}}{(\eta_0 \alpha)_{cold}} \tag{4.4}$$

In this equation, η_0 is the (extended) surface overall heat transfer efficiency and R_w is the thermal resistance of the wall between the hot and cold streams. The heat transfer coefficients, α, for the exhaust gas (hot) and the water/steam (cold) are calculated based on Krupiczka et al. (2003), Annaratone (2008), respectively.

Equations (4.1)-(4.4) are applied in all four heat exchangers (superheater, evaporator, economizer, preheater), while water and steam properties are calculated via the Multiflash tool of the gPROMS simulation software.

Considering the water/steam cycle, we have the following equations:

Point 0: High Pressure steam outlet:

$$P_0 = P_{HP} \qquad T_0 = T_{HP} \qquad (h_0, s_0) = f(P_0, T_0) \tag{4.5}$$

with steam pressure P_{HP}, and temperature T_{HP} given as inputs.

Point 1: Water inlet:

$$P_1 = P_w \qquad T_1 = T_w \qquad (h_1, s_1) = f(P_1, T_1) \tag{4.6}$$

with water inlet pressure P_w, and temperature T_w given as inputs.

Point 2: Preheated water:

$$P_2 = P_1 \qquad T_2 = T_{w-pre} \qquad (h_2, s_2) = f(P_2, T_2) \tag{4.7}$$

with preheated water temperature T_{w-pre} given as input.

Point 3: Water after deaerator:

$$(P_3, T_3, h_3, s_3) = (P_2, T_2, h_2, s_2) \tag{4.8}$$

Point 4: Water after HP pump:

$$\begin{aligned} P_4 &= P_{HP} \\ (T_4, h_4, s_4) &= f_{pump}(P_4, P_3, T_3, h_3, \eta_P) \end{aligned} \tag{4.9}$$

where f_{pump}, the pump model, as described in Section 4.2.3.

Point 5: Saturated water at HP:

$$\begin{aligned} P_5 &= P_{HP} \\ (T_5, h_5, s_5) &= f_{sat,w}(P_5) \end{aligned} \tag{4.10}$$

Point 6: Saturated steam at HP:

$$\begin{aligned} P_6 &= P_{HP} \\ (T_6, h_6, s_6) &= f_{sat,s}(P_6) \end{aligned} \tag{4.11}$$

Furthermore, several inequality constraints are stated, during the simulation of the nominal performance, that ensure the functionality of the heat exchangers and of the overall system. Two very important constraints are the limit of the gas temperature at the exit of the HRSG

$$T_{g5} \geq T_{g5\min} \tag{4.12}$$

as well as the pinch point constraint

$$T_{g3} \geq T_5 + \Delta T_{pp\min} \tag{4.13}$$

where $\Delta T_{pp\min}$ is the minimum pinch point temperature difference.

Equations (4.1) – (4.13) constitute the complete model for nominal single pressure HRSG performance. In this study, the steam pressure, $P_{HP,nom}$, is set as a parameter (in both nominal and off-design operation), while the nominal steam temperature is stated as

$$T_{0,nom} = T_{g1,nom} - 20°\text{C} \tag{4.14}$$

thus, the remaining inputs, which are also used as design variables for the optimization, are the steam mass flow rate, $\dot{m}_{st,nom}$, and the exhaust gas mass flow rate, $\dot{m}_{g,nom}$, and temperature, $T_{g1,nom}$.

Once values are assigned to the three inputs, the nonlinear system of equations is solved by the gPROMS solver. This calculation procedure determines the thermodynamic properties at all points in the HRSG configuration depicted in Figure 4.1. After these properties are known, heat rates, logarithmic mean temperature differences and areas of heat exchangers, as well as the total capital cost of the unit can be evaluated.

4.2.2 Single pressure HRSG off-design performance

The goal of the off-design performance model is to evaluate the HRSG performance for exhaust gas flows and temperatures different from those at the nominal (design) point, as they are determined by the off-design operation of the diesel engine, once the heat exchanger areas have been determined.

Different exhaust gas flow and temperature conditions in a HRSG affect the performance of each heat exchanger in the configuration, and more specifically the heat transfer coefficient of each element. A semi-empirical correlation has been proposed by Kehlhofer (1997) to describe the deviation of the heat transfer coefficient of each heat exchanger from its nominal value with respect to the change in exhaust gas flow and temperature conditions. This correlation has been successfully applied to energy systems [Olsommer (1998), Pelster (1998); Dimopoulos (2009)]. The general form of this semi-empirical correlation, for each heat exchanger, is:

$$\frac{U}{U_n} = \left(\frac{\dot{m}_g}{\dot{m}_{g,n}} \right)^a \cdot \left[1 - b \cdot (T_g - T_{g,n}) \right] \tag{4.15}$$

where the exhaust gas mass flow rate and temperature appearing in this equation are those at the heat exchanger inlet. The regression constants have the values: a = 0.57 and b = 0.00025, which were found to be specific of exhaust gas to water/steam heat exchangers [Kehlhofer (1997), Olsommer (1998)].

In order to evaluate the HRSG performance at off-design / partial load conditions, Eqs. (4.1)-(4.3) are stated for each heat exchanger along with Eqs. (4.4)-(4.13) and (4.15), and with the necessary inequality constraints to ensure proper operation of each heat exchanger. However, Eq. (4.13) is stated with a lower value for the minimum pinch point difference, $\Delta T_{pp\min}$. A system of nonlinear equations is formed with the exhaust gas mass flow rate, $\dot{m}_g$, temperature, T_{g4}, steam pressure, P_{HP}, and temperature, T_{HP}, as inputs. However, in the optimization set up while the exhaust gas mass flow rate and temperature will be given by the propulsion engine (dependent variables), the steam temperature must be stated as a control/independent variable. Considering the steam pressure, it is considered to be a constant parameter, equal to the nominal steam pressure defined in the nominal performance model. The system of equations is solved by the gPROMS software, which also calculates the water/steam properties via the Multiflash tool.

The values of the various parameters appearing in the single pressure HRSG model are given in Table 4.1. It is noted that for certain parameters (exhaust gas minimum outlet temperature, minimum pinch point temperature difference) different values should be assigned depending on the type of the propulsion engine.

Table 4.1. Single pressure HRSG model parameters.

Parameter	Symbol	Value
Heat exchanger efficiency	η_{HX}	0.99
Exhaust gas minimum outlet temperature (K) – (diesel engines)	$T_{g5\min,DE}$	433
Exhaust gas minimum outlet temperature (K) – (gas turbines)	$T_{g5\min,GT}$	403
Gas specific heat capacity (kW/kgK)	c_{pg}	1.17
Minimum pinch point temperature difference (K) – (diesel engines)	$\Delta T_{pp\min,DE}$	15
Minimum pinch point temperature difference (K) – (gas turbines)	$\Delta T_{pp\min,GT}$	20
Preheater water outlet (K)	T_{w-pre}	368

4.2.3 Pumps

A very simple pump model with the input and output streams has been considered in this work. It consists of the following equations

$$h_i = h(P_i, T_i) \tag{4.16}$$

$$v = f\left(\frac{P_i + P_o}{2}, T_i\right) \tag{4.17}$$

$$h_o = h_i + \frac{v(P_o - P_i)}{\eta_{p,is}} \tag{4.18}$$

$$T_o = T(P_o, h_o) \tag{4.19}$$

$$\dot{W}_P = \frac{\dot{m}(h_o - h_i)}{\eta_{p,m}} \tag{4.20}$$

where

h_i specific enthalpy of input stream,
h_o specific enthalpy of output stream,
P_i pressure of input stream,
P_o pressure of output stream,
v specific volume,
T_i temperature of input stream,
T_o temperature of output stream,
$\dot{m}$ water mass flow rate,
$\dot{W}_P$ pump required power,
$\eta_{p,is}$ pump isentropic efficiency,
$\eta_{p,m}$ pump mechanical efficiency.

The inputs to the equations are the properties P_i, P_o and T_i, and the outputs are the properties T_o and $\dot{W}_P$. The function f denotes water/steam thermodynamic properties that are calculated by gPROMS Multiflash tool [gPROMS (2016)]. The various pump model parameters are presented in Table 4.2.

Table 4.2. Pump model parameters.

Parameter	Symbol	Value
Pump isentropic efficiency	$\eta_{p,is}$	0.80
Pump mechanical efficiency	$\eta_{p,m}$	0.98

4.3 Steam Turbine (ST)

Both nominal and off-design performance of steam turbines are simulated, using semi-empirical performance models [Kougioufas (2005), Dimopoulos (2009)]. In this Section, the equations describing nominal and part-load performance are presented.

4.3.1 Steam turbine nominal performance

A steam turbine semi-empirical nominal performance model has been developed using a standard methodology proposed in SNAME (1973). This methodology was further

adapted [Dimopoulos (2009)], to correctly assess steam turbines with intermediate steam extraction, using data from the work presented in Frangopoulos et al. (1996). A typical steam turbine unit is depicted in Figure 4.3. In this text no steam extraction is considered.

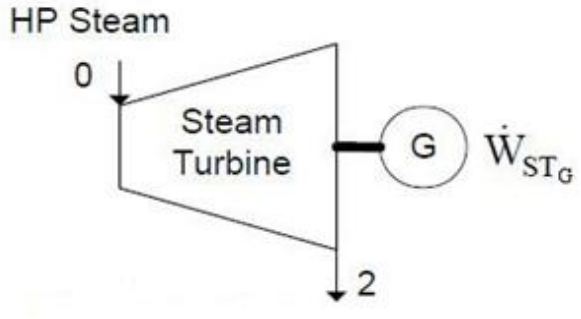

Figure 4.3. Steam turbine generator.

The ST nominal performance model is considered at the maximum output of the ST unit, which entails that no steam is extracted from the unit. Given the nominal steam mass flow rate and quality (as given by the HRSG unit), the steam turbine nominal power output and efficiency are evaluated, with the use of a number of parameters. The steam turbine nominal power output is calculated by the equation:

$$\dot{W}_{ST_n} = \dot{m}_{ST_n} \eta_{ST_n} (h_{0_n} - h_{2,is}) \tag{4.21}$$

where:

$$\begin{aligned} (h_{0_n}, s_{0_n}) &= f(P_{0_n}, T_{0_n}) \\ h_{2,is} &= f(P_2, s_{0_n}) \end{aligned} \tag{4.22}$$

The nominal efficiency, η_{ST_n}, is evaluated using the methodology of SNAME (1973) and Dimopoulos (2009), which relates nominal efficiency with a base value multiplied by a number of correction factors:

$$\eta_{ST_n} = \eta_{base} f_b f_P f_T \tag{4.23}$$

The base steam turbine efficiency is an empirical function of the nominal ST power output (in kW):

$$\eta_{base} = 0.047816 \ln \dot{W}_{ST_n} + 0.32132 \tag{4.24}$$

The term f_b is a correction factor for the condenser pressure (in Pascal):

$$f_b = -0.00008\left(750.062 P_2 / 10^5\right)^2 + 0.0081\left(750.062 P_2 / 10^5\right) + 0.796 \tag{4.25}$$

The term f_P is a correction factor for the inlet pressure (in Pascal) of the turbine:

$$f_P = \left(0.0003\ln\left(\dot{W}_{ST_n}\right) - 0.0035\right) P_2 / 10^5 - 0.0097\ln\left(\dot{W}_{ST_n}\right) + 1.1051 \tag{4.26}$$

The term f_T is a correction factor for the inlet temperature of the turbine:

$$f_T = a_{fLT} T_{0_n}{}^2 + b_{fLT} T_{0_n} + c_{fLT} \tag{4.27}$$

where:

$$a_{fLT} = 2.9516 \cdot 10^{-10} \left(P_{0_n} / 10^5\right)^2 - 2.30535 \cdot 10^{-8} \left(P_{0_n} / 10^5\right) - 7.38075 \cdot 10^{-7} \tag{4.28}$$

$$b_{fLT} = -2.58817 \cdot 10^{-7} \left(P_{0_n} / 10^5\right)^2 + 2.338015 \cdot 10^{-5} \left(P_{0_n} / 10^5\right) + 6.8779 \cdot 10^{-4} \tag{4.29}$$

$$c_{fLT} = 6.09528 \cdot 10^{-5} \left(P_{0_n} / 10^5\right)^2 - 6.56782 \cdot 10^{-3} \left(P_{0_n} / 10^5\right) + 8.76669 \cdot 10^{-1} \tag{4.30}$$

The equations for the correction factors have been derived from data given in SNAME (1973) in the form of diagrams. It is noted that Eqs. (4.21) - (4.30) are interrelated due to the fact that the nominal efficiency is used in the nominal power evaluation and vice versa. The steam turbine nominal inlet steam properties, P_{0_n}, T_{0_n} are given as inputs from the HRSG unit. The condenser pressure, P_2, is defined as a parameter (equal to 0.05 bar) in this model. Furthermore the nominal steam mass flow rate, m_{ST_n}, is also an input to the model, thus, declared as an invariant design optimization variable and determined by the optimization procedure.

4.3.2 Steam turbine off-design performance

Partial load performance of the ST has been considered for different steam mass flow rates, $\dot{m}_{ST}$, and different steam quality (pressure P_0, temperature T_0) to the unit. Given the inlet steam mass flow rate, steam quality and ST unit nominal characteristics, the steam turbine power output and efficiency are evaluated, with the use of a number of parameters.

The steam turbine power output is given as:

$$\dot{W}_{ST} = \eta_{ST_n} \left[\dot{m}_{ST} (h_0 - h_{2,is})\right] \tag{4.31a}$$

where:

$$\begin{aligned} (h_0, s_0) &= f(P_0, T_0) \\ h_{2,is} &= f(P_2, s_0) \end{aligned} \tag{4.31b}$$

Off-design efficiency is evaluated using the methodology in SNAME (1973), which relates efficiency with the nominal value multiplied by a load correction factor:

$$\eta_{ST} = \eta_{ST_n} f_L \tag{4.32}$$

where

$$f_L = 0.12441466 \ln f_{L,ST} + 1 \tag{4.33}$$

In Eq. (4.33), $f_{L,ST}$, is the steam turbine load factor, defined as:

$$f_{L,ST} = \frac{\dot{W}_{ST}}{\dot{W}_{ST_n}} \tag{4.34}$$

Equation (4.33) is based on a diagram given in SNAME (1973). The detailed form of all the conversions of SNAME graphs to analytic interpolation or regression functions is presented in Kougioufas (2005).

4.4 Diesel Engines (DE)

Two–stroke and four–stroke diesel engine models are utilized in order to calculate the fuel consumption, and the exhaust mass flow rates and temperatures at various operating points of a diesel engine. Since the optimization of the system is approached from the point of view of an integrated ship energy system viewed as a whole, we are interested only in the fuel consumption, which has a major contribution to the operational costs, and the exhaust gas properties, which have effect on the design of the steam bottoming cycle.

Very complex and detailed models would be computationally heavy and difficult to use with the dynamic optimization software in the present work. Instead, regression analysis of data provided by manufacturers of diesel engines has been performed here, which gives realistic estimates of performance accurate enough for the particular work.

Since the propulsion plant characteristics, i.e. how many engines and of what nominal power output (Maximum Continuous Rating - MCR), are not known in advance but they are under optimization, a unique Specific Fuel Oil Consumption (SFOC) curve as a function of load only is not sufficient. Therefore, a Specific Fuel Oil Consumption *surface* is created for each engine type (two–stroke or four–stroke), where the Specific Fuel Oil Consumption, for each engine j, is given as a two variable function:

$$b_{f_j} = b_{f_j}(\dot{W}_{bn_j}, f_{L_j}) \tag{4.35}$$

where

$\dot{W}_{bn_j}$ nominal brake power of the engine j

f_{L_j} engine load factor:

$$f_{L_j} = \frac{\dot{W}_{b_j}}{\dot{W}_{bn_j}} \tag{4.36}$$

In a similar way, the exhaust gas mass flow rate and temperature are calculated by functions of the form

$$\dot{m}_{g_j} = \dot{m}_{g_j}(\dot{W}_{bn_j}, f_{L_j}) \tag{4.37}$$

$$T_{g_j} = T_{g_j}(\dot{W}_{bn_j}, f_{L_j}) \tag{4.38}$$

4.4.1 Two-stroke diesel engines

A total of 23 two stroke diesel engines were used to build a data set covering the nominal power output range from 3,5 MW to 90 MW. The data were extracted from the on line Computerized Engine Application System (CEAS) application [MAN (2017)]. Several parameters had to be set, as the online application provides a wide variety of choices. In this work, official catalogue, standard heavy fuel oil, Tier II, super long stroke, same mark number diesel engines, of the latest electronically control technology were considered in order to ensure the continuity of the data.

The specific fuel oil consumption is given in gr/kWh, the exhaust gas mass flow rate in kg/s and the exhaust gas temperature in ^{o}C. As for the independent variables, the regressions presented consider the engine load factor in % and the nominal brake power in kW. For the SFOC we have the following function

$$b_{f,base} = \sum_{n=1}^{5} a_{1n} \ln^n(f_L) + \sum_{k=1}^{5} a_{2k} \dot{W}_{bn}{}^{-k} + a_3 \tag{4.39a}$$

with

$$H_u = 42700\ kJ/Kg,\ T_e = 25^oC,\ P_e = 1\ atm,\ T_{sea} = 20^oC, \tag{4.39b}$$

where

H_u LHV of the fuel actually used,
T_e atmospheric temperature in ^{o}C,
P_e atmospheric pressure in mbar,
T_{sea} sea water temperature in ^{o}C.

The maximum absolute error of regression (Eq. 4.39a) is $\varepsilon = 0.98\%$, with coefficient of determination $R^2 = 0.99$. The SFOC calculated by Eq. (4.39a) is denoted as a *base* SFOC, because it is assumed that it represents the fuel consumption when the engine operates at specified environmental conditions (Eq. 4.39b). To account for other possible environmental conditions, an additional correction must be made according to the following equation:

$$b_f = b_{f,base} \frac{42700}{H_u} \left[1 + 0.0002\left(25 - T_e\right) - 0.00002\left(1000 - P_e\right) + 0.006\left(25.0 - T_{sea}\right)\right] \tag{4.40}$$

For the exhaust gas mass flow rate we have:

$$\dot{m}_g = \exp(b_{11} + b_{12}/\dot{W}_{bn} + b_{13}\ln(\dot{W}_{bn}))M_{\text{mod}}$$
$$M_{\text{mod}} = \begin{cases} f_L/(b_{21} + b_{22} f_L + f_L\sqrt{f_L}), & f_L \le 30, \\ b_{31} f_L + b_{32}, & 30 \le f_L \le 35, \\ f_L/(b_{41} + b_{42} f_L + b_{43}\sqrt{f_L}), & f_L \ge 35 \end{cases} \tag{4.41}$$

with regression properties: $\varepsilon = 0.84\%$, $R^2 = 0.9983$. Finally, the exhaust gas temperature is given by the function

$$T_g = \begin{cases} c_{11} c_{12}{}^{f_L} f_L{}^{c_{13}}, & f_L \le 30 \\ c_{21} f_L + c_{22}, & 30 \le f_L \le 35 \\ \exp(c_{31} + c_{32} f_L + c_{33} f_L{}^2), & f_L \ge 35 \end{cases} \tag{4.42}$$

with regression properties: $\varepsilon = 0.90\%$, $R^2 = 0.989$. The values of all the parameters a_{ij}, b_{ij}, and c_{ij} are given in Table 4.3.

Table 4.3. Values of parameters appearing in Eqs. (4.39), (4.41) and (4.42).

a_{11}	2438.18952262	b_{11}	-5.67293497774	c_{11}	33.2515026494
a_{12}	-1556.11464220	b_{12}	-337.358555458	c_{12}	0.962399049025
a_{13}	483.951873881	b_{13}	0.956426808182	c_{13}	0.919161259303
a_{14}	-73.9862532113	b_{21}	-63.0637026295	c_{21}	8.4
a_{15}	4.46320111809	b_{22}	-4.31862595736	c_{22}	-11.9999999999
a_{21}	190821.995075	b_{23}	47.7672564816	c_{31}	6.08308573382
a_{22}	-2862722896.72	b_{31}	-2.45616599999E-03	c_{32}	-1.64281445770E-02
a_{23}	21777694084450.5	b_{32}	0.508764598999	c_{33}	1.12049849574E-04
a_{24}	-7.099613044E+16	b_{41}	99.2380932921		
a_{25}	8.210654599E+19	b_{43}	0.70666485205		
a_3	-1295.47263397	b_{43}	-6.97669704062		

4.4.2 Four-stroke diesel engines

A total of 11 four-stroke diesel engines were used to build a data set covering the nominal power output range from 3,5 MW to 21 MW. The data were extracted from manuals downloaded from MAN [MAN (2016)] and Wärtsila [Wärtsila (2014)].

Again, as in the previous section, the specific fuel oil consumption is given in gr/kWh, the exhaust gas mass flow rate in kg/s and the exhaust gas temperature in ^{o}C. As for the independent variables, the regressions presented consider the engine load factor in % and the nominal brake power in kW.

The SFOC is given by the following function:

$$b_{f,base} = \sum_{n=1}^{4} a_{1n} f_L{}^n + \sum_{k=1}^{5} a_{2k} \ln^k \dot{W}_{bn} + a_3 \tag{4.43}$$

Regression properties of Eq. (4.43): $\varepsilon = 0.95\%$, $R^2 = 0.988$. Again, the SFOC calculated by Eq. (4.43) is denoted as a *base* SFOC, because it is assumed that it represents the fuel consumption when the engine operates at the environmental conditions specified in equation (4.39b). For other environmental conditions, the correction of Eq. (4.40) must be applied.

For the exhaust gas mass flow rate we have:

$$\dot{m}_g = \left[\sum_{n=1}^{3} b_{1n} f_L{}^n + b_3 \right] \cdot \left[\sum_{k=1}^{3} b_{2k} \dot{W}_{bn}{}^k + b_4 \right] \tag{4.44}$$

Regression properties of Eq. (4.44): $\varepsilon = 0.83\%$, $R^2 = 0.983$. Finally, the exhaust gas temperature is given by the function:

$$T_g = \left[\sum_{n=1}^{3} c_{1n} \cdot f_L{}^n + c_2 \right] \cdot \left[c_3 \cdot \dot{W}_{bn} + c_4 / \dot{W}_{bn}{}^2 + c_5 \right] \tag{4.45}$$

with regression properties: $\varepsilon = 0.91\%$, $R^2 = 0.986$. The values of the parameters a_n, b_n, and c_n are given in Table 4.4.

Table 4.4. Values of parameters appearing in Eqs. (4.43)-(4.45).

a_{11}	-12.5130349	b_{11}	1.02464367E-03	c_{11}	0.012694694
a_{12}	0.308163035	b_{12}	9.36530362E-08	c_{12}	-3.3937952E-04
a_{13}	-3.3047702E-3	b_{13}	-2.15333815E-12	c_{13}	2.08274512E-06
a_{14}	1.27515182E-5	b_{21}	-1.30249958E-02	c_2	1.04404874
a_{21}	383687.174	b_{22}	3.69303720E-04	c_3	4.61515815E-04
a_{22}	-86467.7384	b_{23}	-1.9614900E-06	c_4	282274912.948
a_{23}	9719.36971	b_3	1.95718695	c_5	302.460757
a_{24}	-544.977166	b_4	0.561755635		
a_{25}	12.195741				
a_3	-678887.387				

4.5 Gas Turbines (GT)

For the simulation of the nominal and off-design performance of gas turbines as prime movers of ships, a software package that has been developed in collaboration with the Laboratory of Thermal Turbomachines of the School of Mechanical Engineering NTUA [Software MarineGTs (2015)] was used. The software is appropriate for simulations of

several types of gas turbines. In this study, three selected types of specific interest, presented in Fig. 4.4 are considered.

In order to use the software package, certain input data must be defined by the user. Then, the analysis of performance at the design point or at any off-design point is performed per user request. The user can also select one of four different fuels: two different types of diesel oils with equivalent chemical formulas $C_{12.9}H_{22.9}$ and $C_{12.8}H_{23.7}S_{0.05}$, methane CH_4 and natural gas. With the definition of the fuel and the design point inputs, a thermodynamic analysis is executed throughout the chosen GT type that determines the state of the working medium at all the points of interest inside the configuration. These quantities are required for creating performance maps for predicting the off−design operation of these components and, consequently, of the overall configuration.

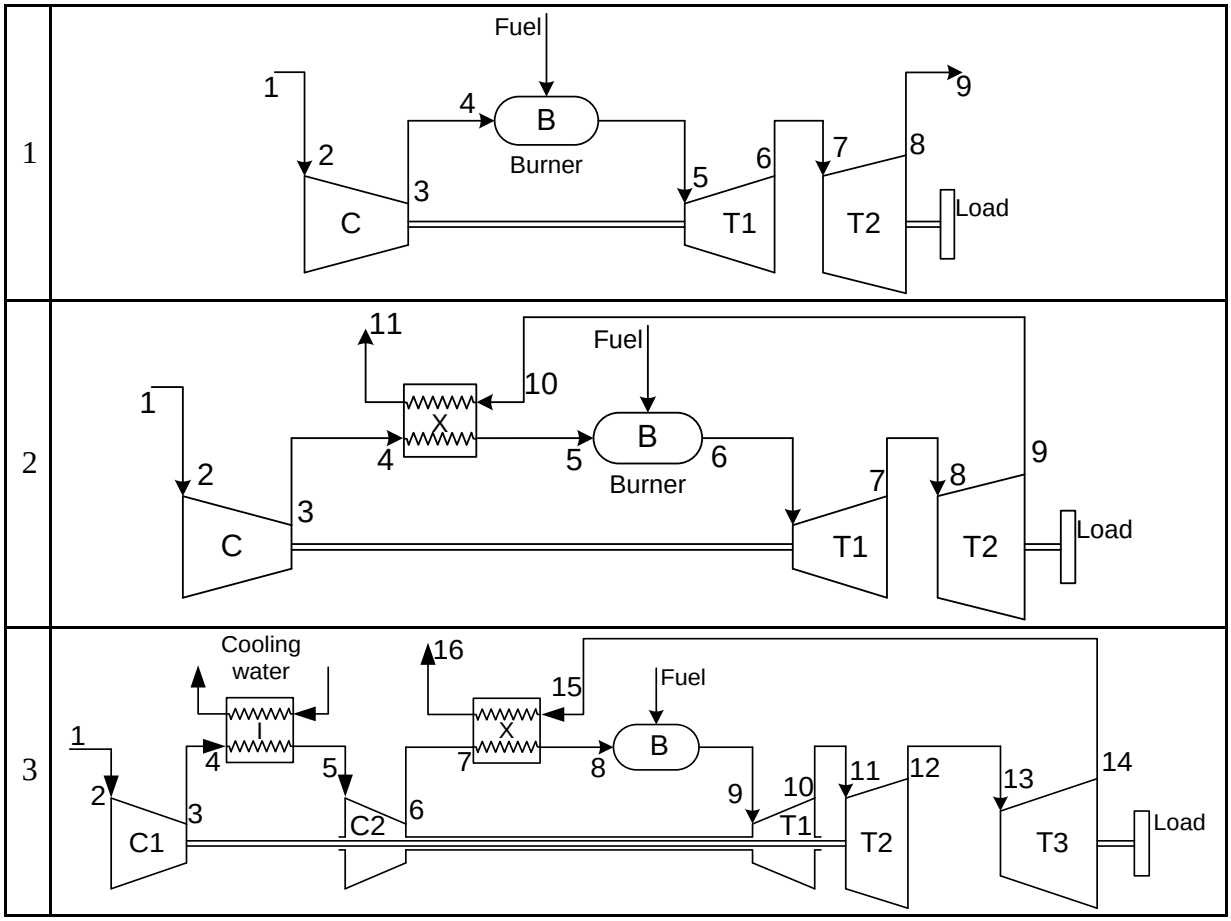

Figure 4.4: The three gas turbines types considered in the present work. (1: Simple cycle, 2: Recuperated cycle, 3: Intercooled recuperated cycle, all with separate power turbine.)

This specific software was not directly integrated in the simulation of the overall energy system. Instead, it was used for the collection of data in order to create performance curves via regression for the fuel consumption and the exhaust gas properties (as in the case of diesel engines) of the three gas turbine types (Fig. 4.4). This was due to the fact that the calculations performed by the software were rather complicated and time

consuming. Thus, directly integrating the software in the simulation model of the general energy system would inevitably increase the required simulation time which in turn would lead to a dramatic increase of computational time of the whole dynamic optimization procedure.

The diesel oil with chemical formula $C_{12.8}H_{23.7}S_{0.05}$ and LHV = 42500 kJ/kg was considered as fuel, and all GT types were simulated for variable rotational speed with 3000 RPM at full load and with variation according to the cubic propeller law at part load operation. The ambient temperature for design point operation for the simulations was considered constant at 15°C.

The nominal power rating had no effect on the calculation of the fuel oil consumption, as the results of the simulation program have indicated. However, the atmospheric temperature has an important impact on the fuel consumption, and the related equations are set up as functions of both the load factor and the atmospheric temperature. In these equations the load factor f_l has to be input in the range 0.2 to 1 and the environmental temperature T_e in the range of -25 to 45°C. The same holds for the exhaust gas temperature calculated from the simulation program.

It is noted that an effort was made for developing regression equations with similar mathematical form among the various GT types, thus, the equations derived for the fuel oil consumption from the regression analysis have the same form and only the coefficients are modified according to the gas turbine type. This general equation is of the following form

$$SFC_{GT} = \sum_{n=1}^{3} a_{1n} f_L^{-n} + \sum_{n=1}^{3} a_{2n} T_e^{\,n} + a_{31}\frac{T_e}{f_L} + a_{32}\frac{T_e^2}{f_L} + a_{33}\frac{T_e}{f_L^{\,2}} + a_{34} \qquad (4.46)$$

where

T_e environmental temperature in the range -25 to 45°C,

f_L load factor in the range 0.2 to 1,

SFC_{GT} specific fuel oil consumption in gr/kWh.

Regression properties of Eq. (4.46): $\varepsilon = 0.96\%$, $R^2 = 0.98$. The coefficients a_{ij} for each of the three gas turbine types are presented in Table 4.6.

Table 4.6. Coefficients for Specific Fuel Consumption (Eq. 4.46) for the three GT types.

Coefficient	GT1	GT2	GT3
a_{11}	4.47322148958418E-02	3.405351667679E-02	2.557248651794E-02
a_{12}	-1.400180543201E-03	-2.028288273915E-03	-2.196962614881E-03
a_{13}	3.867763952385E-05	8.714195263599E-05	8.781031932547E-05
a_{21}	1.1848757780596E-04	9.307213910424E-05	8.570210556930E-05
a_{22}	-4.947221948975E-07	-2.070508829023E-07	6.70232304529E-08
a_{23}	2.2864141416523E-08	2.971717172036E-09	4.361111111989E-09
a_{31}	6.5728891232741E-05	9.939587009403E-07	-7.04304395696E-06
a_{32}	7.3893657229541E-07	5.327267858972E-07	6.39671398453E-08
a_{33}	-7.114769815124E-06	-3.162810208413E-06	-3.023122907372E-07
a_{34}	0.1674760336643	0.1601942814552	0.1563163070215

For the exhaust gas mass flow rates, the regression is performed for a nominal power output of 20 MW for all the GT types. Thus, Eq. (4.47a) has been obtained, which gives the base value, $\dot{m}_{g,GT,base}$, in kg/s:

$$\dot{m}_{g,GT,base} = \sum_{n=1}^{3} a_{1n} \ln^n(f_L) + \sum_{n=1}^{3} a_{2n} T_e^{\,n} + a_{31} T_e \ln(f_L) + a_{32} T_e^2 \ln(f_L) + a_{33} T_e \ln^2(f_L) + a_{34} \tag{4.47a}$$

The coefficients are given in Table 4.7. The mass flow rate for other values of the nominal power rating is given by the equation

$$\dot{m}_{g,GT} = \dot{m}_{g,GT,base} \cdot \frac{\dot{W}_{GTn}}{20} \tag{4.47b}$$

where $\dot{W}_{GT,n}$ is the nominal power rating in MW. Regression properties of Eq. (4.47a): $\varepsilon = 0.98\%$, $R^2 = 0.99$.

Table 4.7. Coefficients for exhaust gas mass flow rate (Eq. 4.47a) for the three GT types.

Coefficient	GT1	GT2	GT3
a_{11}	23.47431928775	22.69808182124	19.93455959934
a_{12}	4.220403961559	4.233977115205	2.863072018236
a_{13}	0.2432678657330	0.3433450620947	1.250684978371E-04
a_{21}	-0.132431387748	-0.1548641305609	-7.426530923772E-02
a_{22}	2.91510452910E-04	3.430917714065E-04	-7.76228421058E-05
a_{23}	-3.067644444444E-06	-3.369186868789E-06	-1.970349494952E-06
a_{31}	-5.291689320007E-02	-5.433642333292E-02	-6.185227044037E-02
a_{32}	5.152894212379E-05	4.715371224612E-05	-1.122213017345E-05
a_{33}	-6.77988830307E-03	-7.807314222533E-03	-0.0155662006009
a_{34}	52.42219657425	64.28535211075	45.5527705728

Finally, for the exhaust gas temperature, three distinct equations are derived, one for each type. The corresponding coefficients are given in Table 4.8.

$$T_{g,GT1} = \sum_{n=1}^{3} a_{1n} f_L^{\,n} + \sum_{n=1}^{4} a_{2n} T_e^{\,n} + a_3 \tag{4.48a}$$

$$T_{g,GT2} = \sum_{n=1}^{3} b_{1n} \ln^n(f_L) + \sum_{n=1}^{3} b_{2n} T_e^{\,n} + b_{31} T_e \ln(f_L) + b_{32} T_e^2 \ln(f_L) + b_{33} T_e \ln^2(f_L) + b_{34} \tag{4.48b}$$

$$T_{g,GT3} = \sum_{n=1}^{3} c_{1n} f_L{}^n + \sum_{n=1}^{3} c_{2n} T_e{}^n + c_{31} T_e f_L + c_{32} T_e^2 f_L + c_{33} T_e f_L{}^2 + c_{34} \quad (4.48c)$$

Table 4.8. Coefficients for exhaust gas temperature (Eqs. 4.48a-4.48c) for the three GT types.

a_{11}	-109.3338625959	b_{11}	128.3101425101	c_{11}	195.7940716073
a_{12}	244.8577169885	b_{12}	35.95271343481	c_{12}	-140.344465376
a_{13}	-92.95504616657	b_{13}	5.240925095706	c_{13}	77.83859998768
a_{21}	2.756513727084	b_{21}	2.047513181407	c_{21}	0.4092610592856
a_{22}	-1.369993821229E-04	b_{22}	-1.53350577121E-03	c_{22}	1.05612756128E-03
a_{23}	-3.818296735099E-07	b_{23}	-2.92413199629E-05	c_{23}	-2.05798570711E-05
a_{24}	-1.982811549038E-08	b_{31}	0.2148387007573	c_{31}	0.177909971426
a_3	479.3289239962	b_{32}	-4.797576518103E-04	c_{32}	-9.878499638277E-04
		b_{33}	2.140043036109E-02	c_{33}	0.486252482879
		b_{34}	371.5830961622	c_{34}	231.4432373500

4.6 Diesel Generator Sets (DG)

In order to cover the electric needs of the ship, diesel generator sets may be used. In the same rationale of diesel engines, regression models have been developed for the specific fuel oil consumption, the exhaust gas mass flow rate and the exhaust gas temperature based on data collected from manufacturers.

A total of nine generator sets were used to build a data set covering the nominal power output range from 500 kW to 11 MW. The specific fuel oil consumption is given in gr/kWh, the exhaust gas mass flow rate in kg/s and the exhaust gas temperature in ^{o}C. As for the independent variables, the regressions presented consider the engine load factor in percentage points (%) and the nominal brake power in kW.

The specific fuel oil consumption is given as:

$$b_{f,base} = \sum_{n=1}^{3} a_{1n} \cdot \ln^n f_L + \sum_{n=1}^{3} a_{2k} \cdot \ln^k \dot{W}_{bn} + a_3 \cdot \ln f_L \cdot \ln \dot{W}_{bn} + a_4 \cdot \ln^2 f_L \cdot \ln \dot{W}_{bn} + a_5 \cdot \ln f_L \cdot \ln^2 \dot{W}_{bn} + a_6 \quad (4.49)$$

Regression properties of Eq. (4.49): $\varepsilon = 0.92\%$, $R^2 = 0.958$. As in the case of the diesel engines, this is the base SFOC and the same correction, given in Eq. (4.40) must be applied for the actual SFOC. For MCR>4800 kW, since the available data exhibit no differentiation, the value of MCR=4800 kW is used in all calculations. The exhaust gas mass flow rate is given by the equation

$$m_g = \left[\sum_{n=1}^{3} b_n \cdot f_L{}^n + b_4\right] \cdot \left[b_5 \cdot \dot{W}_{bn}{}^{b_6} \cdot \exp(b_7 \cdot \dot{W}_{bn})\right] \tag{4.50}$$

with regression properties: $\varepsilon = 0.95\%$, $R^2 = 0.966$. The exhaust gas temperature is given by the equation

$$T_g = \left[\sum_{n=1}^{3} c_n \cdot f_L{}^n + c_4\right] \cdot \left[c_5 \cdot \dot{W}_{bn}{}^{c_6/\dot{W}_{bn}}\right] \tag{4.51}$$

with regression properties: $\varepsilon = 0.97\%$, $R^2 = 0.987$. The values of the parameters a_{ij}, b_i, and c_i are given in Table 4.9.

As in the case of the fuel consumption regression equation, for the cases with MCR>4800 kW, the value of MCR=4800 kW is used for exhaust gas mass flow rate and temperature.

Table 4.9. Values of parameters appearing in Eqs. (4.49)-(4.51).

a_{11}	-112.3333723	b_1	-1.302499580E-2	c_1	0.0126946949
a_{12}	-77.25033231	b_2	6.693037204E-5	c_2	-3.39379522E-4
a_{13}	11.37912696	b_3	-1.96149009E-6	c_3	2.082745120E-6
a_{21}	-549.5713057	b_4	0.5617556354	c_4	1.044048741
a_{22}	53.00736007	b_5	3.644054500E-3	c_5	303.7136098
a_{23}	-2.024884015	b_6	0.91481054413	c_6	9.470141366
a_3	84.78846317	b_7	1.02097503E-5		
a_4	-5.416457726				
a_5	-2.682009390				
a_6	1863.361740				

4.7 Ship Resistance and Propulsion Models

The total resistance model, R_T, is made up of a number of different components which in this study, due to the interest of the dynamic behavior given to the problem by the weather considerations, is stated as the sum of two terms:

$$R_T = R_{calm} + R_{Added} \tag{4.52}$$

The total calm water resistance, R_{calm}, includes the terms [Holtrop and Mennen (1982), Holtrop (1984), Politis and Skamnelis (2007)]:

$$R_{calm} = R_F(1+k_1) + R_a + R_w + R_{APP} + R_{BB} + R_{TR} \tag{4.53}$$

where

R_F frictional resistance,

k_1 form factor of the hull (describes the viscous resistance from the hull, with relation to R_F),

R_a model ship correlation resistance,

R_w wave making and wave breaking resistance,

R_{APP} appendage resistance due to the presence of bilge keels, rudders, bossings, open shafts and struts,

R_{BB} additional resistance due to the bulbous bow near the water surface,

R_{TR} additional resistance of the immersed transom stern.

The added resistance, R_{Added}, includes the dynamic terms of added wind resistance, R_{Aw}, and added wave resistance, R_{As} [Politis and Skamnelis(2007)]:

$$R_{Added} = R_{Aw} + R_{As} \tag{4.54}$$

These two terms model the added effect of the weather (wind and waves) on the total ship resistance and are very important in this study. In contrast to the terms appearing in Eq. (4.53) that are generally dependent on the ship speed and characteristics (geometry, hull form), the added wind and wave resistances are dependent on the weather profile also, thus inserting time and space (e.g. distance from a port) dependency in the problem and making it inherently dynamic.

A method, based on regression upon multiple data from model tests in wind tunnels, proposed by Fujiwara et al. (2005) is used for the calculation of the added wind resistance component. The calculation of the added wave resistance term is based on the superposition principle for the components of the wave, motion and resistance spectra as well as on the assumption of linearity for the ship's response and utilizes Maruo's theory [Maruo (1957), Maruo (1960)] and the method given in Tsujimoto et al. (2008). If there is not enough information about the geometry of the ship's hull, the above formulas cannot be applied and a simplified empirical method [ITTC (1987), ITTC (2012)] is used, which requires only the basic ship dimensions and the ship speed as inputs.

Finally, as stated in Chapter 3, Section 3.3.1, Eq. (3.13), in order to correlate the required brake power from the propulsion plant (diesel engines, gas turbines) with the total ship resistance, the propulsive efficiency, η_{prop}, must first be calculated. This calculation is performed based on a model from the literature [Holtrop and Mennen (1982), Holtrop (1984)] which uses as inputs the ship speed and characteristics (geometry, hull form) as well as other details considering the gear, transmission shaft and propeller (i.e. gearing, bearings, stern tube, propeller and open water efficiencies).

The models, based on the literature, that are used for the calculation of total ship resistance, are described in depth in Appendix D. Furthermore, the models used for the required shaft power as well as the coupling of resistance and propulsion are given in Appendix E.

CHAPTER 5: CASE STUDIES

5.1 General

In this chapter, based on the general problem formulation and the generic energy system modeling presented in the previous two chapters, seven case studies of dynamic SDO optimization on specific vessels with determined mission characteristics are formulated and solved. Table 5.1 summarizes the characteristics of all seven case studies, for convenient reference.

For the first case study a LNG carrier is considered. The ship performs consecutive round trips between two ports so as to cover the time horizon of a whole year of operation. Then, based on this first year of operation, dynamic optimization is performed in order to minimize the PWC for 20 years of operation.

The next six case studies (Case Studies 2–7) are based on an existing containership. Real data are considered for the heat and electricity demands as well as for the weather conditions that the ship encounters. Four seasons (summer, winter, spring, fall) are considered and for each season the ship performs a characteristic round trip of predetermined distance between two ports so as to cover the time horizon of a whole year of operation.

Table 5.1. Characteristics of case studies.

Case study	Type of ship	Propulsion alternatives	Duration of single trip	Objective Function
1	LNG carrier	4-X diesel engines	Fixed	PWC
2	Containership	Gas turbines	Fixed	PWC
3	Containership	Gas turbines	Variable	PWC
4	Containership	Gas turbines	Variable	NPV
5	Containership	4-X diesel engines, 2-X diesel engines, Gas turbines	Fixed	PWC
6	Containership	4-X diesel engines, 2-X diesel engines, Gas turbines	Variable	PWC
7	Containership	4-X diesel engines, 2-X diesel engines, Gas turbines	Variable	NPV

In Case Study 2 the duration of each round trip for each season is predetermined and fixed. Considering the synthesis of the propulsion plant, only the three types of gas turbines (Chapter 4, Section 4.5) are allowed as alternatives. The economic criterion that serves as the objective function is the minimization of PWC.

For Case Study 3, the duration of each round trip for each season is variable and also under optimization. The objective function is again the minimization of PWC and again only gas turbines are allowed as propulsion alternatives.

In Case Study 4, the same problem as in Case Study 3 is posed again, but now an appropriate revenue for each trip is introduced and the maximization of NPV is selected as the objective function.

In the next three case studies, the three problems that were introduced in case studies 2–4 are posed once more, but now all possible technology alternatives (two stroke diesel

engines, four stroke diesel engines and three types of gas turbines) are allowed simultaneously for the synthesis of the propulsion plant.

In each of the Case Studies 2–7, the problem is solved once for the nominal case (nominal values of parameters) and then, based on this nominal case, a parametric study for different values of fuel cost is performed. Specifically in Case Studies 4 and 7, where the maximization of NPV is set as the objective function, the parametric study is performed for both the fuel price and the freight rate. In all cases, the horizon of optimization covers 20 years of operation.

5.2 Case Study 1: LNG Carrier with 4-X Diesel Engines, Trips of fixed Time, Minimization of PWC

5.2.1 Description of the system and the optimization problem

In this problem, the optimal synthesis, design specifications and operating conditions, as they change with time, of an energy system that will cover all energy needs (propulsion, thermal, electric) of a LNG carrier are requested.

The basic ship dimensions, areas and volumes along with the necessary coefficients for the resistance and propulsion calculations are presented in Table 5.2. The ship is assumed to perform consecutive round trips (Figure 5.1) between two ports, A and B, so as to complete the time horizon of a full year of operation. The time schedule of the ship for each round trip is given in Table 5.3. The distance between the two ports is fixed and known, d_{AB} = 460 km. The operation profile of the ship from the point of view of energy requirements is approximated with four modes of operation (loading, off-loading, loaded trip and ballast trip) with fixed and predetermined (known) time durations. The electric and thermal loads for each mode are given in Table 5.4. They are considered constant and known in port, but they are calculated as functions of the brake power of the engine(s) during the trip, based on regression performed on data from the literature [Dimopoulos (2009)].

Maneuvering periods are not considered in this work, because their duration is much smaller than the duration of the whole round trip and their effect on the objective function is negligible.

Table 5.2. Vessel dimensions, propulsion power and related coefficients.

Parameter	Symbol	Value
Basic Ship Dimensions		
Overall length (m)	L_{OA}	294
Length between perpendiculars (m)	L_{pp}	288
Length at the waterline (m)	L_{WL}	290
Breadth (m)	B	32.2
Draught (m)	T	8.8
Forward moulded draught (m)	T_F	9
Aft moulded draught (m)	T_A	8.6
Draught at midship (m)	T_M	8.5

Areas and Volumes		
Transverse area of the bulbous bow (m^2)	A_{BT}	0
Transverse immersed transom area at rest (m^2)	A_T	25
Wetted volume (m^3)	∇	57360
Ship Hull Coefficients		
Block coefficient	C_B	0.605
Prismatic coefficient	C_P	0.617
Waterplane area coefficient	C_{WP}	0.835
Midship section coefficient	C_M	0.98
Longitudinal position at the centre of buoyancy forward of $0.5L$ as a percentage of overall ship length	lcb	-4.5%
Equivalent appendage resistance factor	k_2	2
Half angle of entrance	i_E	25°
Stern shape coefficient	C_{stern}	0
Vertical position of the centre of transverse area of the bulbous bow (m)	h_B	7
Added Wind and Wave Related Coefficients		
Lateral projected area of superstructures on deck (m^2)	A_{OD}	750
Area of maximum transverse section exposed to the winds (m^2)	A_{XV}	450
Projected lateral area above the waterline (m^2)	A_{YV}	500
Horizontal distance from midship section to centre of lateral projected area (m)	C_{MC}	10
Height from waterline to centre of lateral projected area (m)	H_C	30
Height of the top of the superstructure (m)	H_{BR}	20
Propulsion Power Coefficients		
Bearing efficiency	η_b	0.98
Stern-tube efficiency	η_{st}	0.97
Gearing efficiency	η_g	0.99
Rotative efficiency	η_r	0.98
Open water efficiency	η_o	0.99
Service speed (kn)	V_S	21.5
Brake power at service speed (kW)		21000

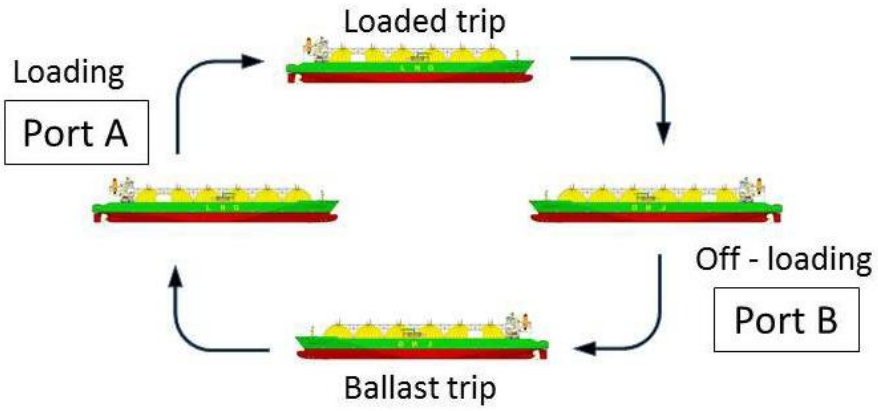

Figure 5.1. Modes of operation for characteristic round trip between Ports A and B.

Table 5.3. Time schedule of the ship.

Mode	Description	Duration
1	Loading at port A	9 h
2	Loaded trip from port A to port B	15 h
3	Off-loading at port B	9 h
4	Ballast trip from port B to port A	15 h
	Total round trip	48 h

Table 5.4. Electric and thermal load. $\dot{W}_b$: instantaneous total brake power of the main engines.

Mode	Electric load (kW)	Thermal load (kW)
1	1000	800
2	$-3451+540\ln(\dot{W}_b)$	$150+e^{5.39+3.73\cdot10^{-5}\cdot\dot{W}_b}$
3	3000	4000
4	$-3423+539\ln(\dot{W}_b)$	$150+e^{5.37+3.93\cdot10^{-5}\cdot\dot{W}_b}$

In this case study it is considered that a number (determined by the optimization) of four-stroke diesel engines will drive a single propeller. If determined by optimization, a single-pressure HRSG will serve part or all of the thermal loads by saturated steam extraction from the drum, while the superheated steam produced will, again if the optimization thus dictates, drive a steam-turbine generator (STG). It is noted that connecting exhaust pipes from more than one engine, if there is need, is allowed by the classification societies only if proper equipment (such as blowers and dampers) is installed. Diesel generator sets (the number is also determined by optimization) and an auxiliary boiler are included, which will cover the electric and thermal loads in ports and will supply electric and thermal energy during voyages, in case the STG or/and HRSG cannot fully cover the loads.

In Figure 5.2 a superconfiguration of the energy system that will cover all energy needs is presented.

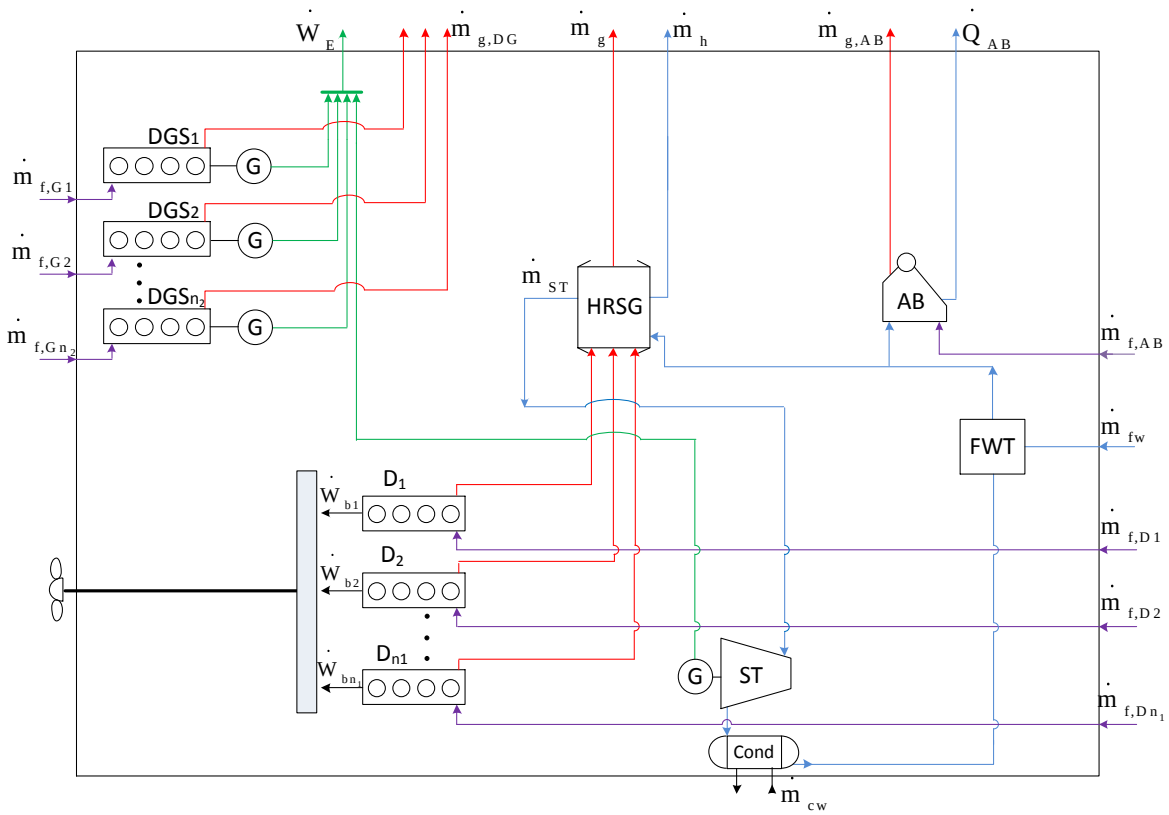

Figure 5.2. Superconfiguration of the energy system for Case Study 1.

The required propulsion power is not known in advance, but is under optimization, since various weather conditions that depend on space and time are encountered along the route. Furthermore, the ship speed at any instant of time is also under optimization.

Regarding the weather conditions encountered by the ship, as has been described in previous sections (Section 3.2.1), in this study only the wind speed and direction and wave height and direction are taken into consideration in order to estimate the total ship resistance and thus the required brake power at a certain speed. For the specific case study and without restricting the generality of the formulation, it is assumed for simplicity that the wind and waves are always in the heading direction:

$$\begin{aligned} \psi_{wind} &= 0.0 \\ \theta_{waves} &= 0.0 \end{aligned} \tag{5.1}$$

thus decreasing the number of required inputs and calculations (since wind and wave direction angle have zero value). This scenario, although not realistic, is chosen for simplicity and is mathematically equivalent with every other possible scenario. Furthermore, by utilizing the Beaufort scale, the wave height generated by the wind above the sea level is associated with its corresponding wind speed. Therefore, the weather conditions are adequately described solely by the wind speed, which, in this case study is considered as function of space (distance from port) and time. A 3-D plot (contour) is used (Figure 5.3) to describe the wind speed as a function of space and time during the loaded and ballast trips. More details considering the Beaufort scale and the correlation of wave height and wind speed can be found in Appendix G.

Even though in this application a typical weather profile has been considered, the problem could be solved for various weather states.

Finally, regarding the objective function, the present worth cost (PWC) is selected as an appropriate economic criterion and the problem is set up as a PWC minimization problem. In the following section, the mathematical statement of the optimization problem is presented.

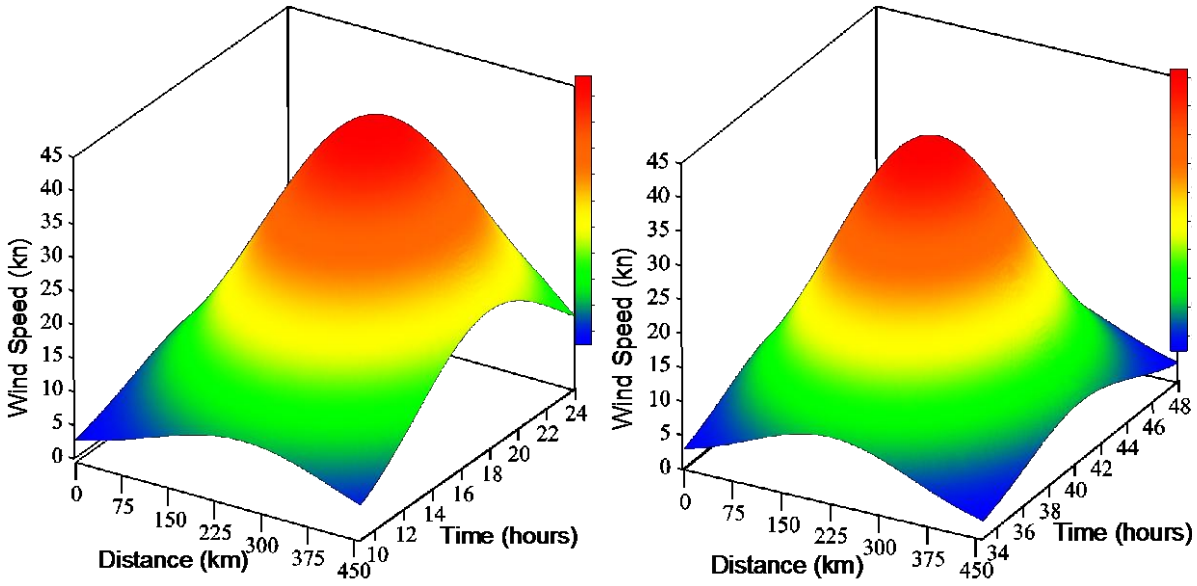

(a) (b)

Figure 5.3. Wind speed for the base case as a function of space and time: (a) Loaded trip, distance from port A. (b) Ballast trip, distance from port B.

5.2.2 Mathematical statement of the optimization problem

The dynamic optimization problem can be mathematically stated as a minimization problem using a Differential − Algebraic Equation (DAE) formulation. Of course, this formulation is based on the mathematical formulation of the general problem presented in Section 3.3.1 combined with the technique for handling integer variables presented in Section 3.3.2. The objective is selected to be the minimization of the present worth cost, which consists of capital, fuel and operation expenses. All symbols as well as all calculations necessary for the estimation of the total PWC are presented in detail in Chapter 3 and Appendices B, C. The objective function is stated as

$$\min_{\vec{x}} PWC = PWC_c + PWC_f + PWC_{om} \tag{5.2}$$

with vector $\vec{x}$, representing the vector of control (optimization) variables, consisting of the vectors of synthesis, design and operation optimization variables ($\vec{v}$, $\vec{w}$ and $\vec{z}$, respectively)

$$\vec{x} = (\vec{v}, \vec{w}, \vec{z}) \tag{5.3}$$

with:

$$\vec{v} = \left(y_{D,4-X,J}, y_B, y_{STG}, y_{DG,M}, y_{AB}\right) \tag{5.4a}$$

$$\vec{w} = \left(\dot{W}_{bn,J}, \dot{m}_{g_n}, T_{g_n}, \dot{m}_{s_n}, \dot{m}_{STG_n}, \dot{W}_{DG_n,M}, \dot{Q}_{AB_n} \right) \tag{5.4b}$$

$$\vec{z} = \left(\dot{W}_{b,J}, \dot{W}_{DG,M}, \lambda_h \right) \tag{5.4c}$$

where

$y_{D,4-X,J}$ set of variables j determining the existence of the j th 4–X diesel engine (binary): $y_{D,4-X,J} = \left\{ y_{D,4-X,1}, y_{D,4-X,2}, ..., y_{D,4-X,j}, .., y_{D,4-X,j\max} \right\}$ (5.5a)

y_B variable determining the existence of the HRSG (binary),

y_{STG} variable determining the existence of the STG (binary),

$y_{DG,M}$ set of variables m determining the existence of the m th generator set (binary):

$$y_{DG,M} = \left\{ y_{DG,1}, y_{DG,2}, ..., y_{DG,m}, ..., y_{DG,m\max} \right\} \tag{5.5b}$$

y_{AB} variable determining the existence of the auxiliary boiler (binary),

$\dot{W}_{bn,J}$ set of variables j determining the nominal brake power output of j th 4–X diesel engine (invariant): $\dot{W}_{bn,J} = \left\{ \dot{W}_{bn,1}, \dot{W}_{bn,2}, ..., \dot{W}_{bn,j}, .., \dot{W}_{bn,j\max} \right\}$ (5.6a)

$\dot{m}_{g_n}$ nominal exhaust gas mass flow rate of HRSG (invariant),

T_{g_n} nominal exhaust gas temperature of HRSG (invariant),

$\dot{m}_{s_n}$ nominal steam mass flow rate of HRSG (invariant),

$\dot{m}_{STG_n}$ nominal steam mass flow rate of STG (invariant),

$\dot{W}_{DG_n,M}$ set of variables m determining the nominal power output of m th generator set (invariant): $\dot{W}_{DG_n,M} = \left\{ \dot{W}_{DG_n,1}, \dot{W}_{DG_n,2}, ..., \dot{W}_{DG_n,m}, .., \dot{W}_{DG_n,m\max} \right\}$ (5.6b)

$\dot{Q}_{AB_n}$ nominal thermal power output of auxiliary boiler (invariant),

$\dot{W}_{b,J}$ set of variables j determining the j th 4–X diesel engine brake power output:

$$\dot{W}_{b,J} = \left\{ \dot{W}_{b,1}, \dot{W}_{b,2}, ..., \dot{W}_{b,j}, ..., \dot{W}_{b,j\max} \right\} \tag{5.7a}$$

$\dot{W}_{DG,M}$ set of variables m determining the m th diesel generator set power output:

$$\dot{W}_{DG,M} = \left\{ \dot{W}_{DG,1}, \dot{W}_{DG,2}, ..., \dot{W}_{DG,m}, ..., \dot{W}_{DG,m\max} \right\} \tag{5.7b}$$

λ_h fraction of HRSG steam mass flow rate delivered to thermal loads:

$$\dot{m}_{s,h} = \lambda_h \cdot \dot{m}_s \tag{5.8}$$

$\dot{m}_{s,h}$ steam mass flow rate drawn from HRSG drum for serving thermal loads,

$\dot{m}_s$ steam mass flow rate of HRSG unit.

Indices j and m run through all the values from 1 up to an upper bound. It is noted that the upper values of indices j and m, quantify the maximum number of diesel engines and diesel generator sets, respectively, that are allowed to be installed in the system and are pre-determined parameters, given at the beginning of the optimization. Once these upper values for j and m are defined, the problem is set with as many binary variables for the diesel engines and the diesel generator sets as necessary. Binary variables y_{HRSG}, y_{STG},

and y_{AB} determine the existence of the HRSG, STG and auxiliary boiler in the energy system. For all binary variables, value 0 denotes that the unit is not installed.

Details for the calculation of PWC are presented in Appendix B. In this specific case study, since the assumption that the same round trip is repeated over the first year is made, the first year fuel cost of component n can be calculated by the equations:

$$C_{fa,n} = C_{f,n} N_{trips} \tag{5.9}$$

$$N_{trips} = \frac{\tau}{t_{trip,AB} + t_{trip,BA} + t_{port,A} + t_{port,B}} \tag{5.10}$$

$$C_{f,n} = c_{f,n} m_{f,n} \tag{5.11}$$

where

$C_{fa,n}$ first year annual fuel cost of component n,
N_{trips} number of total round trips of the ship in a year,
$C_{f,n}$ fuel cost of component n per round trip.
τ maximum permissible annual hours of operation,
t_{trip} duration of travel for a round trip,
$t_{trip,AB}$ duration of travel from port A to B (in a round trip),
$t_{trip,BA}$ duration of travel from port B to A (in a round trip),
$t_{port,A}$ time spend in port A (in a round trip),
$t_{port,B}$ time spend in port B (in a round trip),
$c_{f,n}$ fuel price for component n,
$m_{f,n}$ fuel consumption for component n in a round trip.

The same methodology is used for the first year operation and maintenance costs of each component:

$$C_{oma,n} = C_{om,n} N_{trips} \tag{5.12}$$

$$C_{om,n} = c_{om,n} E_n \tag{5.13}$$

where

$C_{om,n}$ operation and maintenance cost per trip for each component n,
$c_{om,n}$ operation and maintenance unit cost for component n,
E_n useful energy output of the component n for a round trip.

The main differential variables for this problem are the distance travelled by the ship, the fuel consumption of the propulsion engines, diesel generator sets and auxiliary boiler. Another family of differential variables is derived from the energy output of each component, which is generally given as the integral of output power of the component over the time horizon. All the respective equations for each component have been presented in detail in Chapter 3, Section 3.3.1, Eqs. (3.6)–(3.9) and in Appendix C.

Since the number of diesel engines and the nominal power of each engine are not known but they are the result of optimization, the SFOC for each engine as well as the exhaust gas mass flow rate and temperature are given as two-variable (nominal power and

load factor) functions. The total exhaust gas mass flow rate and temperature from all engines is then calculated and supplied to the HRSG, if a HRSG is installed. The same procedure (two variable functions) is also applied in the modeling of diesel generator sets SFOC and exhaust gas characteristics. The models used for the propulsion engines and the diesel generator sets are presented in extent in Chapter 4.

The brake power of the propulsion engines, as well as the electric and thermal power produced by the integrated system must be equal to the required brake power, the electric and thermal loads at any instant of time:

$$\sum_{j} y_{D,4-X,j} \cdot \dot{W}_{b,4-X,j} = \dot{W}_b \tag{5.14}$$

$$y_{STG} \cdot \dot{W}_{STG} + \sum_{m} y_{DG,m} \cdot \dot{W}_{DG,m} = \dot{W}_e \tag{5.15}$$

$$y_B \cdot \dot{Q}_B + \dot{Q}_{AB} = \dot{Q} \tag{5.16}$$

where:

$\dot{W}_b$ required brake power from the engines,
$\dot{W}_e$ electric load,
$\dot{Q}_B$ heat from HRSG serving thermal loads,
$\dot{Q}$ thermal load.

The total required brake power of the engines is calculated as a function of the ship speed, weather state, ship resistance and propulsive efficiency. The respective equation is given in Chapter 3 (Eq. 3.13). All details considering the underlying mathematical calculations are presented in Chapter 4 and in Appendixes D and E.

Finally, there are multiple equalities correlated with the simulation of the components as well as inequality constraints imposed on certain variables, but their full presentation is beyond the limits of the present text. Noteworthy inequality constraints are the upper and lower bounds imposed on the speed of the ship and the upper and lower bounds imposed on the load factor of all components (main engines, diesel generator sets, steam turbines, etc.) that ensure their operation inside the limits specified by the manufacturer:

$$V_{\min} \le V \le V_{\max} \tag{5.17a}$$

$$f_{L_{\min}} \le f_L \le f_{L_{\max}} \tag{5.17b}$$

Other important technical constraints are related with the nominal (design) characteristics of the components. A good example is the allowed upper and lower values for the nominal power output of the 4–X diesel engines and diesel generator sets:

$$\dot{W}_{bn,j_{\min}} \le \dot{W}_{bn,j} \le \dot{W}_{bn,j_{\max}} \tag{5.18a}$$

$$\dot{W}_{DGn,m_{\min}} \le \dot{W}_{DGn,m} \le \dot{W}_{DGn,m_{\max}} \tag{5.18b}$$

Of course all control variables, are accompanied by upper and lower limits. However, upper and lower limits may not be necessary for all state variables.

In the next section all the necessary values of input parameters and data assumptions in order to set up and solve the optimization problem stated in the current section are presented.

5.2.3 Additional data and assumptions

The values of economic parameters used in the calculation of the objective function are given in Table 5.5. The operation and maintenance unit costs for each component are given in Appendix C and are repeated here for reference. For the diesel engines, the diesel generator sets and the auxiliary boiler, the same type of fuel is considered (Heavy Fuel Oil) which has a Lower Heating Value (LHV) of 39550 kJ/kg.

Table 5.5. Economic parameters.

Parameter	Value
Fuel price (all components)	300 € / ton
Technical life of the system	20 years
Market interest rate	10%
Maximum permissible annual number of operation hours	6000 hours
Diesel engines O&M unit cost	6.000 € / MWh
HRSG O&M unit cost	4.558 € / MWh
STG O&M unit cost	3.646 € / MWh
Genset O&M unit cost	6.381 € / MWh
Auxiliary boiler O&M unit cost	4.558 € / MWh

In Table 5.6 a list of lower and upper bounds of several important synthesis, design and operation variables is presented. Details regarding the time discretization that is used in order to model the operation of the energy system for the total time horizon are presented in Table 5.7. It is clarified that, in essence, each control variable is decomposed to as many static variables as the number of intervals considered for the operation, thus increasing significantly the scale of the problem and the computing time.

Table 5.6. Bounds on synthesis, design and operation variables.

Variable	Lower value	Upper value
Number of diesel engines	1	4
Number of DG sets	0	4
Diesel engine nominal power output (kW)	3500	21000
DG set nominal power output (kW)	300	5000
Load factors (all equipment)	0.1	1
Ship speed (kn)	6	22

Table 5.7. Numerical solution parameters.

Parameter	Value
Length of time intervals on trips	1 h
Length of time intervals in ports	9 h
Number of time intervals used	32
Optimization convergence tolerance	10^{-4}

5.2.4 Solution procedure

The problem is set up and solved once with the nominal set of parameter values and weather conditions, and then a sensitivity analysis with respect to the fuel price and the capital cost of equipment is performed. In addition, in order to investigate the effect of the weather on the optimal solution, an alternative weather profile is introduced while all other parameters are kept constant, and the optimization problem is solved once again.

For the solution of all the dynamic optimization problems pertaining to this case study, a sequential method is applied. All the relevant solution procedure specifics, such as the algorithms and the related software, are described in detail in Section 3.4. All optimizations are performed on an Intel® Core™2 Quad Processor Q9650 CPU at 3GHz with 8Gb of RAM.

5.2.5 Numerical results for the nominal case

The optimal values of the synthesis variables are presented in Table 5.8. Optimal values for the design variables are presented in Table 5.9, along with the optimal values of HRSG nominal thermal power and STG nominal power output, which are dependent variables but are given for completeness. The optimal values of the objective function and its constituents are given in Table 5.10. In Figure 5.4a, the optimal ship speed profiles for both trips (fully loaded and ballast) are presented for the 15 hour duration of each trip. Operation optimization results for the diesel engines, HRSG, steam turbine, auxiliary boiler and generator sets are presented in Figures 5.4b-5.7 for the whole round trip of 48 hours.

Table 5.8. Optimal synthesis of the system.

Number of diesel engines (prime movers)	2
Number of HRSGs	1
Number of STGs	1
Number of DG sets	2
Number of auxiliary boilers	1

Table 5.9. Optimal design specifications of the system components.

Variable	Engine 1	Engine 2
Main engine nominal brake power (kW)	14790	6210
DG sets nominal electric power (kW)	1020	2040
Heat recovery steam generator		
Thermal power (kW)	4441	
Exhaust gas mass flow rate (kg/s)	29	
Nominal inlet exhaust gas temperature (°C)	292	
Auxiliary boiler nominal thermal power (kW)	4000	
Steam-turbine generator		
Nominal electric power (kW)	1419	
Nominal steam mass flow rate (kg/s)	2.09	

Table 5.10. Cost items (present worth costs).

Component	Costs (€)		
	Capital	Operation & maintenance	Fuel
Diesel Engines	9,250,000	3,371,267	33,013,477
STG	603,875	133,629	0
HRSG	742,977	817,605	0
Auxiliary boiler	390,000	212,517	1,215,745
DG sets	1,877,678	385,534	3,880,468
Subtotal	12,864,530	4,920,552	38,109,690
Total PWC	55,894,772		

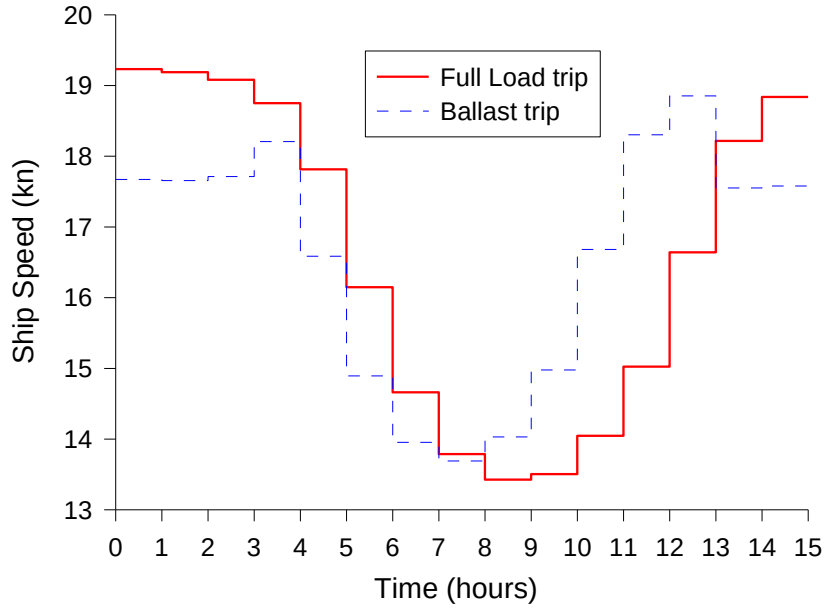

Figure 5.4a. Optimal ship speed versus time.

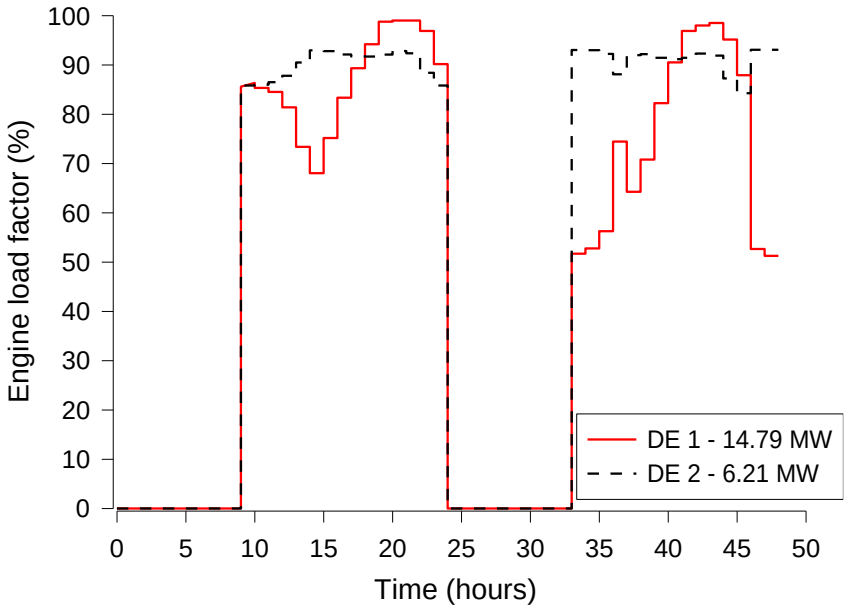

Figure 5.4b. Optimal load factors versus time.

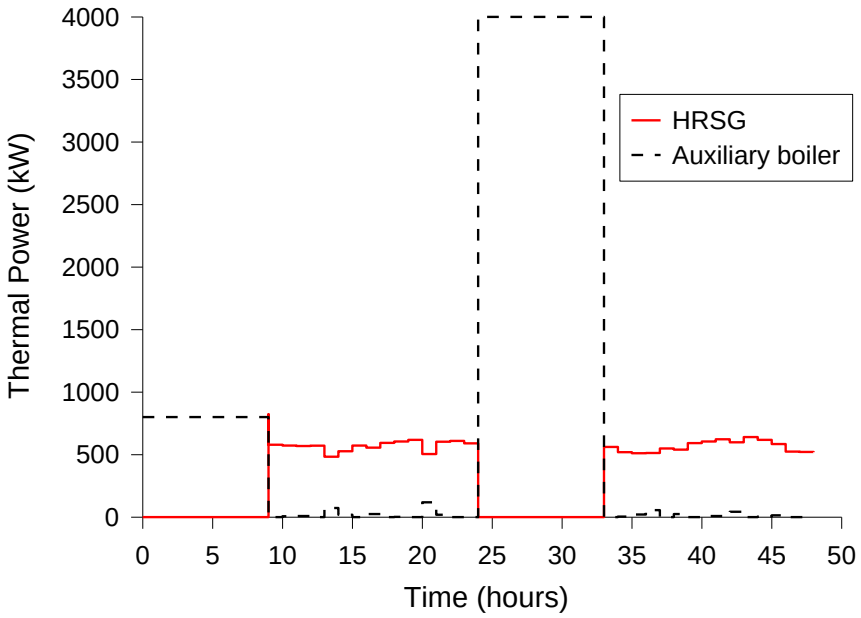

Figure 5.5. Contribution of the HRSG and auxiliary boiler to thermal loads versus time.

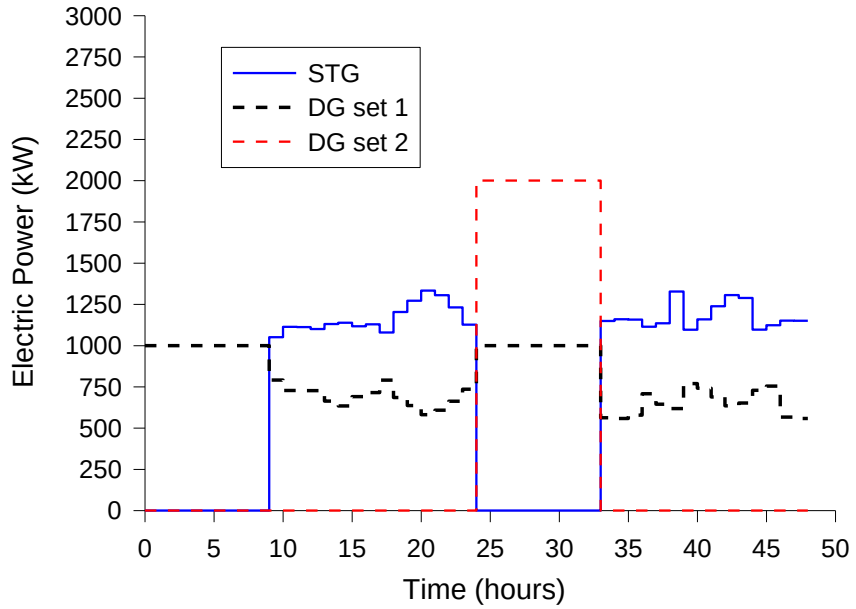

Figure 5.6. Electric power of the DG sets and the STG versus time.

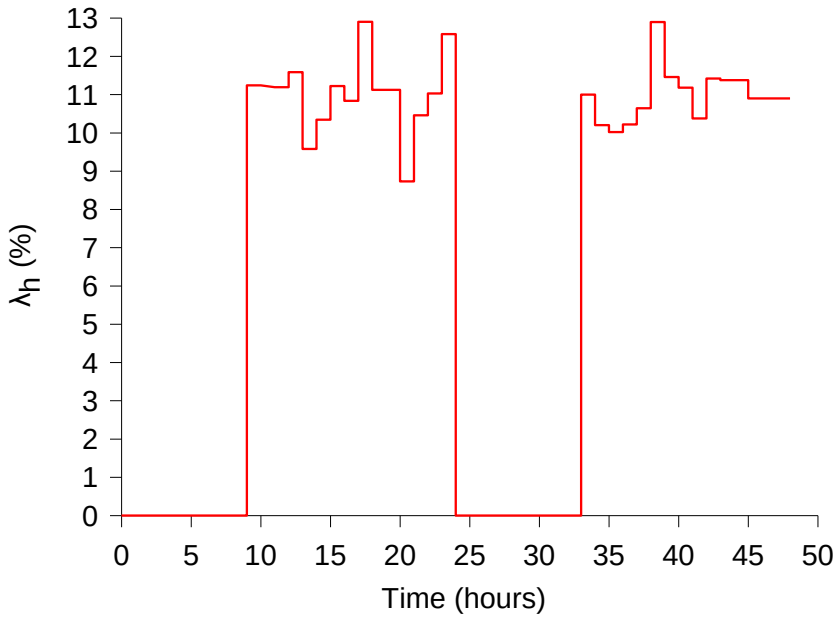

Figure 5.7. Optimal percentage of steam mass from HRSG to thermal loads versus time.

The optimal present worth cost after 20 years of operation (125 trips per year) is 55,894,772 €. The optimization was concluded in 24100 seconds, performing 57 Major NLP iterations. For the optimal solution two four-stroke diesel engines of 14.79 and 6.21 MW and two diesel generator sets of 1020 and 2040 kW were selected. Also the installation of a HRSG unit along with a STG (1419 kW) is determined. Slow steaming through the "storms" (15 – 20 hours for port A to B and 38 – 43 hours for port B to A) is the result of optimization, in order to minimize the diesel engine fuel costs. The load factors vary from 50% to 98% for the larger engine and from 86% to 99% for the smaller engine (area of minimum consumption in 4-X diesel engines).

The thermal demands are almost fully covered by the HRSG during the trips, while the auxiliary boiler supplies a small part of the heat required during the trips and fully covers the heat demand in ports. The STG covers approximately 2/3 of the electric demand during the trips, while the remaining 1/3 is covered by DG set 1. Furthermore, the electric demand in port A is fully covered by the DG set 1, while DG set 2 operates only in port B in parallel with DG set 1, in order to cover the increased electric demand.

5.2.6 Parametric study

For the parametric study, two parameters are considered: the fuel price and the capital cost of equipment. For the fuel price four values, apart from the nominal value of 300 €/ton, were considered (20, 150, 450 and 600 €/ton), while capital costs were varied from 50% to 200% of the nominal value. This has been performed by using a scale factor on the total capital cost value in the objective function. Selected results regarding the optimal synthesis and design characteristics of the system for various values of fuel price and capital cost are presented in Tables 5.11 and 5.12. More detailed results regarding the optimal PWC, HRSG power output and STG power output are presented in Figures 5.8, 5.9 and 5.10, respectively.

Table 5.11. Effect of fuel price and capital cost on the optimal synthesis of the system.

	Capital Cost	50%	50%	100%	100%	200%	200%
	Fuel Price (€/ton)	20	300	150	600	150	450
Synthesis	DEs	1	2	2	2	2	2
	HRSGs	–	1	–	1	–	1
	STGs	–	1	–	1	–	1
	DG sets	1	2	2	2	2	2
	AB	1	1	1	1	1	1

In all cases, with the exception of 20 €/ton fuel price, two diesel engines, one auxiliary boiler and two generator sets are installed. As can be observed in Figure 5.7, for the fuel price of 20 €/ton and for all capital cost cases the optimal PWC values are very close. This indicates that for very low fuel prices all the possible system configurations tend to degenerate into a single solution with one diesel engine, one generator set, one auxiliary boiler and no bottoming cycle.

Table 5.12. Effect of fuel price and capital cost on the optimal design specifications of the system.

	Capital Cost	50%	50%	100%	100%	200%	200%
	Fuel Price (€/ton)	20	300	150	600	150	450
Nominal power (kW)	DE 1	21000	14790	14850	14830	14850	14850
	DE 2	–	6210	6150	6170	6150	6150
	HRSG	–	4525	–	4597	–	4488
	STG	–	1427	–	1434	–	1415
	DG set 1	3000	1025	1080	1000	1010	1000
	DG set 2	–	2035	1980	2040	2050	2050
	AB	4000	4000	4000	4000	4000	4000

For fuel prices 300, 450 and 600 €/ton and for all capital costs a bottoming cycle is always installed, while for fuel prices 150 and 20 €/ton the bottoming cycle is economically non feasible. The only exception is found at fuel price of 150 €/ton and capital costs at 50%. This behavior reveals the existence of a fuel marginal price in each capital cost case. Indeed, additional executions of the program – only for the nominal case – reveal the exact marginal price of the fuel at 214.4 €/ton (marked in Figure 5.8); below this price the optimal system does not include a bottoming cycle. It is noted that for fixed capital costs, the fuel price increase leads to higher optimal HRSG and STG nominal power output values. Also, for every fixed fuel price, the decrease of capital costs leads to higher optimal HRSG and STG nominal power output values.

The optimal nominal power output of the diesel engines, does not vary significantly (variation lower than 1%) for different fuel prices and capital costs.

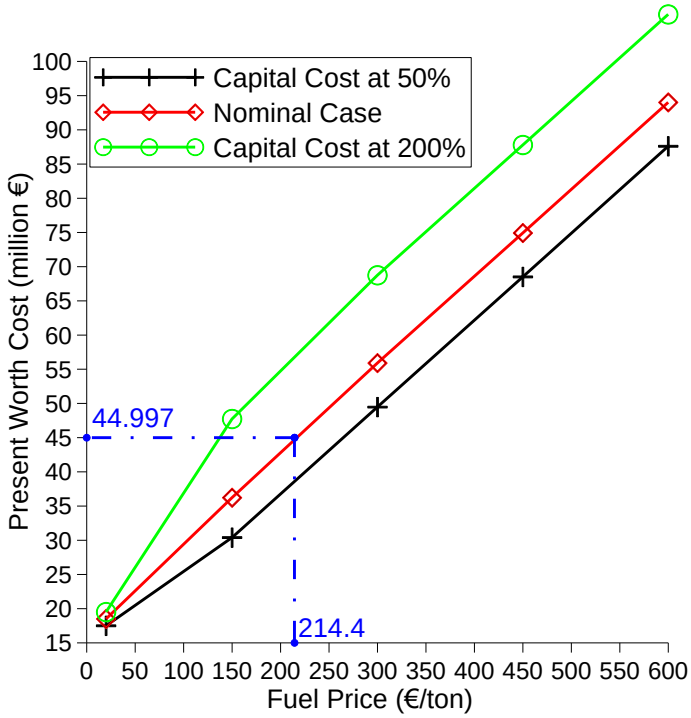

Figure 5.8. Effect of fuel price and capital cost on the optimal PWC.

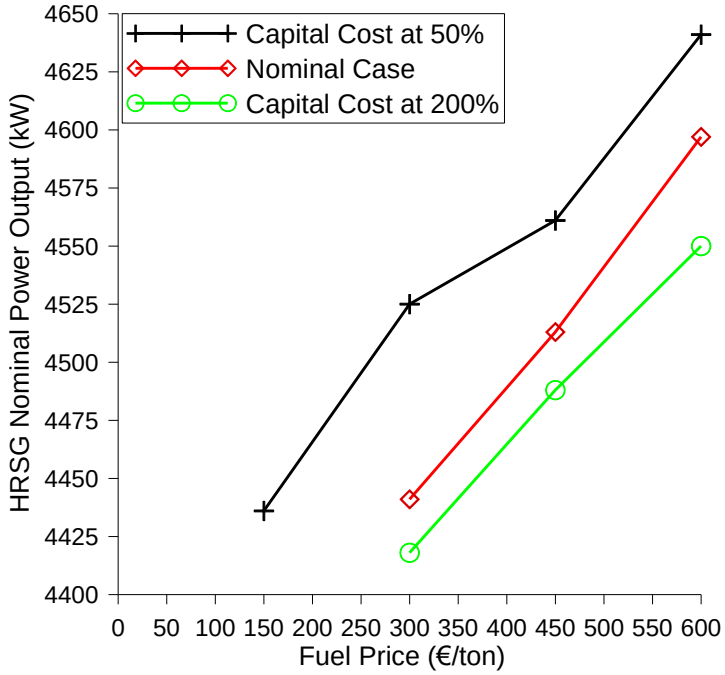

Figure 5.9. Effect of fuel price and capital cost on the optimal HRSG nominal power.

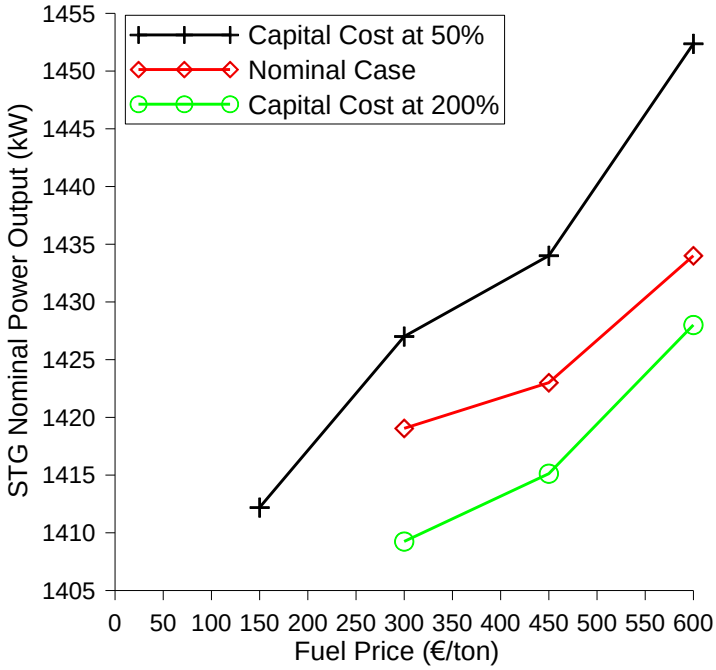

Figure 5.10. Effect of fuel price and capital cost on the optimal STG nominal power.

5.2.7 Effect of weather on the optimal solution

In order to study the effect of weather on the optimal solution, a different weather profile is considered, while all other parameters are kept the same as in the nominal case. Again a 3-D plot (contour) is used (Fig. 5.11) to describe the wind speed as a function of space and time during the loaded and ballast trips. Here, comparing with the nominal case (Fig. 5.2), a weather profile with two peaks ("storms") is introduced for the fully loaded trip, while a milder and "flat" weather profile is introduced for the ballast trip.

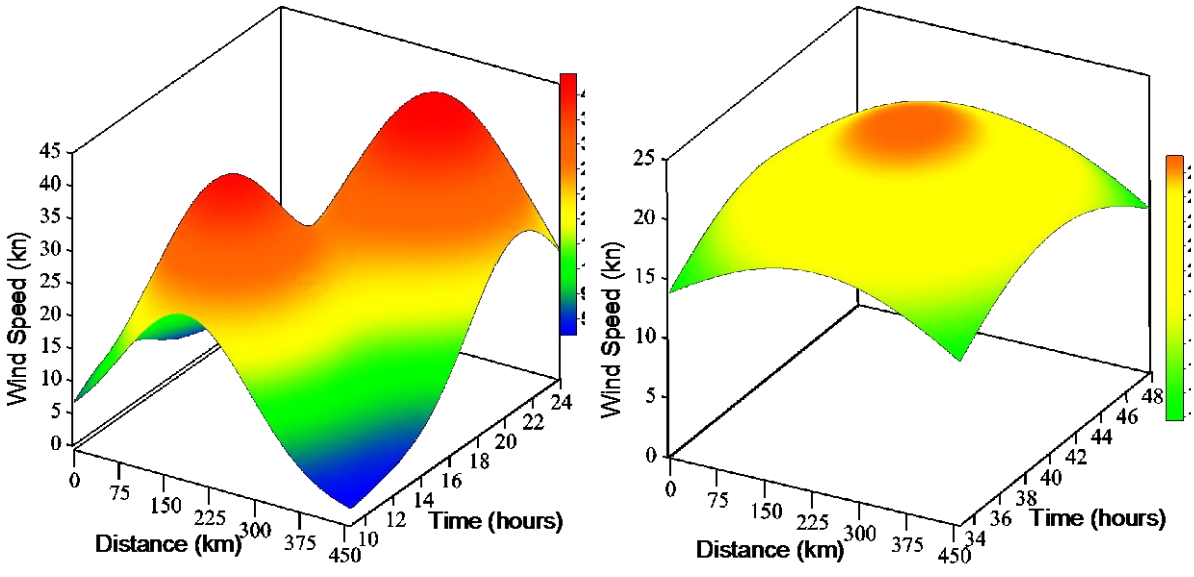

(a) (b)

Figure 5.11. Wind speed as a function of space and time: (a) Loaded trip, distance from port A. (b) Ballast trip, distance from port B.

Following the same format as in the presentation of the nominal case, the optimization results are presented in Tables 5.13, 5.14 and 5.15, and in Figures 5.12-5.16.

Table 5.13. Optimal synthesis of the system.

Number of diesel engines (prime movers)	2
Number of HRSGs	1
Number of STGss	1
Number of DG sets	2
Number of auxiliary boilers	1

Table 5.14. Optimal design specifications of the system components.

Variable	Engine 1	Engine 2
Main engine nominal brake power (kW)	15580	6060
DG sets nominal electric power (kW)	810	2200
Heat recovery steam generator		
Thermal power (kW)	4590	
Exhaust gas mass flow rate (kg/s)	30.5	
Nominal inlet exhaust gas temperature (°C)	294	
Auxiliary boiler nominal thermal power (kW)	4000	
Steam-turbine generator		
Nominal electric power (kW)	1560	
Nominal steam mass flow rate (kg/s)	2.29	

Table 5.15. Cost items (present worth costs).

Component	Costs (€)		
	Capital	Operation & maintenance	Fuel
DEs	9,659,265	3,342,232	32,514,962
ST	627,487	130,309	
HRSG	752,636	809,299	
Auxiliary boiler	390,000	210,660	1,205,123
DG sets	1,828,315	388,831	3,929,107
Subtotal	13,257,703	4,881,331	37,649,192
Total PWC	55,788,226		

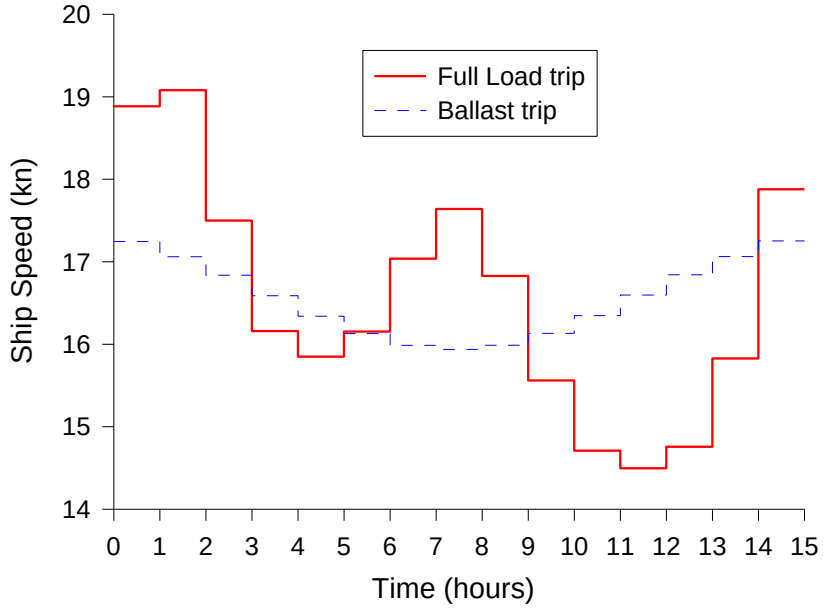

Figure 5.12. Optimal ship speed versus time.

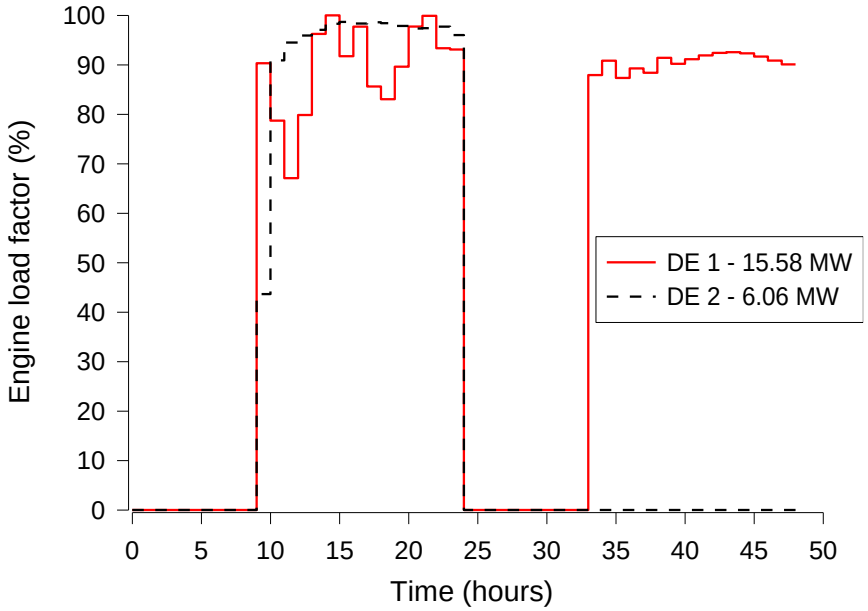

Figure 5.13. Optimal load factors versus time.

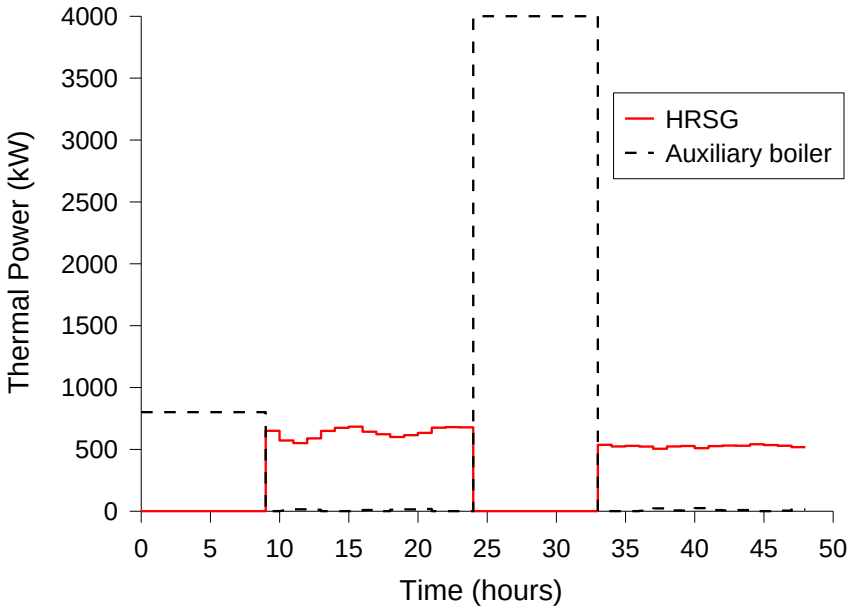

Figure 5.14. Contribution of the HRSG and auxiliary boiler to thermal loads versus time.

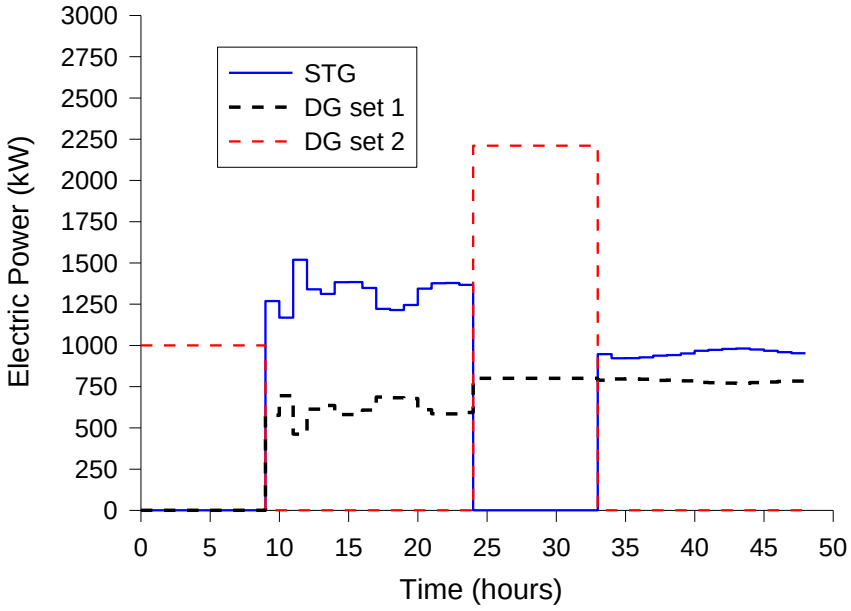

Figure 5.15. Electric power from the DG sets and the STG versus time.

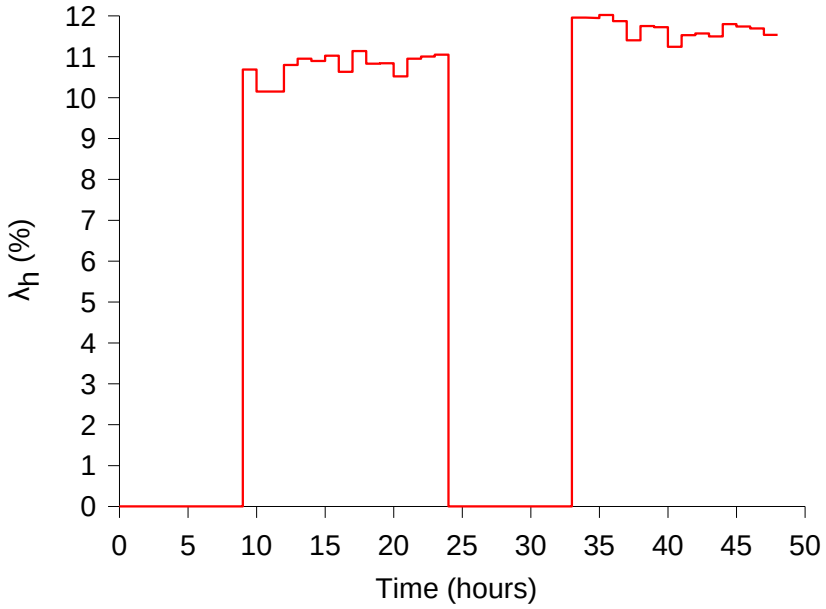

Figure 5.16. Optimal percentage of steam mass from HRSG to thermal loads versus time.

The optimization was concluded in 23500 seconds, performing 48 Major NLP iterations. Similarly to the solution of the nominal case, two four-stroke diesel engines and two diesel generator sets are selected. However in this case, diesel engine 1 is designed with a 5% higher MCR and diesel engine 2 with a 2% lower MCR. Also, the installation of a HRSG unit along with a STG is again dictated, but the STG is now designed with approximately a 10% higher nominal power output. This leads to significant differences in both the optimal nominal power output and the optimal operational strategy for each diesel generator set. Specifically, when compared to the nominal case, DG set 1 is designed with nominal power output significantly below 1 MW (800 kW), while DG set 2 is designed with nominal power output higher than 2 MW (2200 kW). Furthermore, during the fully loaded trip, now the STG covers slightly more than 2/3 of the electric demand, while the remaining load is covered by the DG set 1. During the ballast trip the STG performance drops (lower exhaust gas mass flow rates) and the DG set 1 operates constantly near full load. In contrast to the nominal case, the electric demand in port A is now covered by DG set 2, since DG set 1 has now been designed with output power lower than 1MW in order to more efficiently accommodate the ballast trip. Both DG sets operate in parallel in port B.

As in the nominal case, the thermal demands are almost fully covered by the HRSG during the trips.

Finally, the ship slow steams through both “storms” in the fully loaded trip utilizing both engines. However on the ballast trip a large difference is observed compared with the nominal case, since the small engine is not operating at all.

5.3 Case Study 2: Containership with Gas Turbines, Trips of fixed Time, Minimization of PWC

5.3.1 Description of the system and the optimization problem

In this case study, the optimal configuration (synthesis), design specifications of components and operating conditions of an energy system that will cover all energy needs of a containership under the scope of minimizing the PWC, are requested.

A containership with carrying capacity 9572 TEU and DWT of 111529 MT is considered. All vessel characteristics, such as ship dimensions and coefficients that are used in order to provide an accurate calculation of ship resistance and required propulsion power are given in Table 5.16.

Figure 5.17. Containership during voyage.

Table 5.16. Vessel dimensions propulsion power and related coefficients for containership.

Parameter	Symbol	Value
Ship Dimensions		
Overall length (m)	L_{OA}	336
Length between perpendiculars (m)	L_{pp}	321
Length at the waterline (m)	L_{WL}	317
Breadth (m)	B	45
Draught (m)	T	15
Forward moulded draught (m)	T_F	14.7
Aft moulded draught (m)	T_A	15.2
Draught at midship (m)	T_M	15
Wetted volume (m^3)	∇	146491
Wetted Surface	S	19029

Ship Hull Coefficients		
Block coefficient	C_B	0.6506
Prismatic coefficient	C_P	0.6605
Waterplane area coefficient	C_{WP}	0.8560
Midship section coefficient	C_M	0.9850
Longitudinal position at the centre of buoyancy (m)	lcb	152.7
Height at the centre of transverse area (m)	h_B	22
Propulsion Power Coefficients		
Bearing efficiency	η_b	0.98
Stern-tube efficiency	η_{st}	0.97
Gearing efficiency	η_g	0.99
Rotative efficiency	η_r	0.98
Open water efficiency	η_o	0.99
Service speed (kn)	V_S	24
Brake power at service speed (kW)		69439

The problem is formulated in such a way that, simultaneously, the time horizon of a whole year of operation is considered. Specifically, for each of the four seasons, the ship will perform a characteristic round trip (Figure 5.18) of 6000 nm between ports A and B, with $d_{AB} = 3000\ nm$, which will include the necessary amount of time (and service of energy needs) that is required during the stay at both ports. In this case study the duration of this round trip for each season is predetermined and fixed. The time schedule of the ship for each round trip and all seasons is given in Table 5.17.

Table 5.17. Time schedule of the ship.

Mode	Description	Duration
1	Loading at port A (all seasons)	2 days
2	Loaded trip from port A to port B (all seasons)	6 days
3	Off-loading and loading at port B (all seasons)	2 days
4	Loaded trip from port B to port A (all seasons)	6 days
	Total round trip	16 days

The electric and thermal loads are given as inputs in Tables 5.18 and 5.19. They are defined as functions of time for an 8-day time horizon, differing for each season. Also they are considered constant at ports.

Figure 5.18. Characteristic round trip between Ports A and B.

Table 5.18. Thermal energy demands for each season.

Time (Days)	Thermal Power (kW)			
	Summer	Fall	Winter	Spring
From port A to port B				
1	850	860	1000	990
2	880	900	1050	980
3	860	950	1080	1010
4	900	970	1100	1020
5	840	930	1060	950
6	850	960	1100	970
7	845	959	1100	980
8	851	963	1090	970
From port B to port A				
1	860	930	1100	1040
2	870	950	1080	970
3	870	980	1060	960
4	890	970	990	950
5	860	890	1040	980
6	870	910	1070	960
7	880	920	1080	970
8	870	910	1050	960
	Ports			
A	950	950	950	950
B	950	950	950	950

Table 5.19. Electric energy demands for each season.

Time (Days)	Electric Power (kW)			
	Summer	Fall	Winter	Spring
From port A to port B				
1	1495	1508	1482	1625
2	1599	1573	1586	1599
3	1560	1547	1482	1547
4	1514	1560	1508	1495
5	1508	1495	1586	1534
6	1495	1495	1495	1521
7	1490	1495	1485	1525
8	1495	1495	1490	1520
From port B to port A				
1	1625	1547	1534	1521
2	1560	1625	1521	1625
3	1534	1664	1625	1573
4	1521	1508	1651	1625
5	1560	1501	1495	1599
6	1521	1547	1521	1586
7	1520	1539	1520	1580
8	1525	1550	1521	1580
	Ports			
A	1500	1500	1500	1500
B	1500	1500	1500	1500

A superconfiguration of the energy system that will serve all energy needs is considered in Figure 5.19. Three types of gas turbines, as presented in Section 4.5, are available as technology alternatives for the synthesis of the propulsion plant. The number and type of gas turbines that will be installed is determined by the optimization and they will drive a single propeller. Also, single-pressure HRSGs may be installed that will serve part or all of the thermal loads by saturated steam extraction from the drum, while the superheated steam produced will be led to steam turbine(s), if the optimization thus dictates. The number of HRSGs and STs that will be installed is again determined by the optimization. The power produced by the steam turbine(s) will be distributed between the propeller and a generator, which will supply electric power for the service of the electric loads. Diesel generator sets, whose number is determined by the optimization, and an auxiliary boiler are included, which will serve the electric and thermal loads in port and will supply electric and thermal energy during voyages, in case the STGs and HRSGs cannot fully cover the demands.

The requested propulsion power is not known in advance, but it is calculated as a function of speed and weather conditions, since the varying with space and time weather conditions encountered by the ship along the route are taken into consideration. Thus, the ship speed at any instant of time is unknown and also under optimization. Regarding the weather conditions encountered by the ship during each trip, for each season, the wind speed and direction are given as inputs. The wave height and direction are then calculated, since they are correlated with the wind speed with the help of the Beaufort scale

(Appendix G). Once these parameters are determined, the resistance and propulsion power calculations are performed.

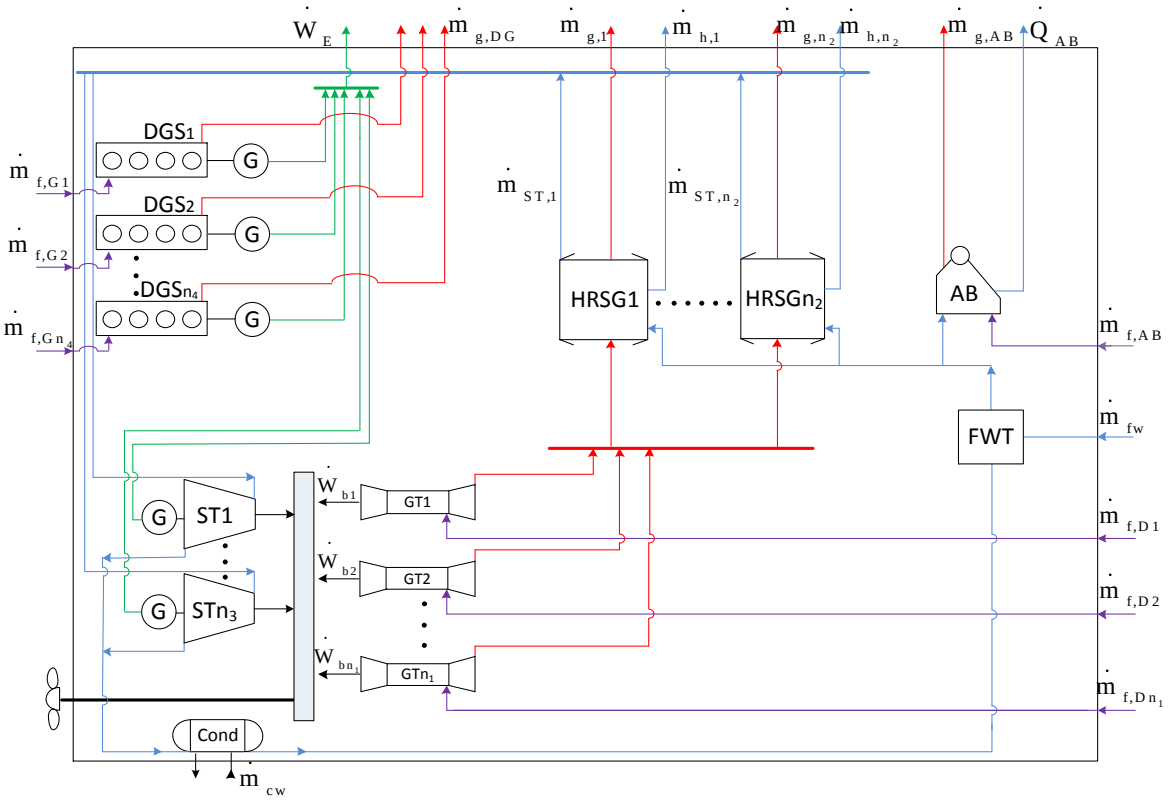

Figure 5.19. Superconfiguration of the energy system for Case Studies 2,3 and 4.

The wind speed is given as a function of time and space for each season in Tables 5.20a – 5.20d. The wind direction is given in Table 5.20e, also as a function of time and space, but is assumed to remain constant over all seasons. All data have been gathered from a list of internet sites[3] –accessible to anyone– which are specialized in accurate real–time as well as historical weather data for any region (sea or land).

In Figure 5.20 the simulated power – speed curves for weather conditions of BF0, BF4 and BF5 are given, for reference. For drawing this figure, the wind direction was assumed to be heading in all cases.

Finally, for the objective function, the present worth cost (PWC) is selected as an appropriate economic criterion and the problem is set up as a PWC minimization problem.

[3] https://earth.nullschool.net, http://www.meteoearth.com, http://www.accuweather.com, http://enterprisesolutions.accuweather.com,

Table 5.20a. Wind speed (in kn) as a function of time and space in Summer.

Time (Days)	Distance from Port A (nm)					
	513	1026	1539	2052	2565	3078
1	4.43	4.91	4.32	5.45	4.91	6.05
2	13.61	15.87	16.41	13.71	13.12	16.36
3	17.87	16.25	17.44	18.03	16.79	15.71
4	9.18	11.39	9.40	9.94	10.48	17.87
5	24.95	19.22	16.79	24.19	26.30	24.35
6	21.65	23.00	24.62	26.84	26.35	22.89
7	22.73	21.06	27.21	24.62	26.89	23.98
8	23.65	23.97	22.08	22.30	22.89	25.11

Table 5.20b. Wind speed (in kn) as a function of time and space in Fall.

Time (Days)	Distance from Port A (nm)					
	513	1026	1539	2052	2565	3078
1	4.75	5.35	4.75	5.94	5.35	6.53
2	14.85	17.22	17.82	14.85	14.25	17.82
3	19.60	17.82	19.01	19.60	18.41	17.22
4	10.10	12.47	10.10	10.69	11.28	19.60
5	27.32	20.79	18.41	26.13	28.51	27.73
6	23.76	24.95	26.73	29.10	28.51	26.95
7	24.95	23.16	29.70	26.73	29.10	23.76
8	25.54	26.13	23.76	24.35	24.95	24.95

Table 5.20c. Wind speed (in kn) as a function of time and space in Winter.

Time (Days)	Distance from Port A (nm)					
	513	1026	1539	2052	2565	3078
1	5.23	5.88	5.23	6.53	5.88	7.19
2	16.33	18.95	19.60	16.33	15.68	19.60
3	21.56	19.60	20.91	21.56	20.25	18.95
4	11.11	13.72	11.11	11.76	12.41	21.56
5	30.05	22.87	20.25	28.75	31.36	29.40
6	26.13	27.44	29.40	32.01	31.36	28.44
7	27.44	25.48	32.67	29.40	32.01	28.13
8	28.09	28.75	26.13	26.79	28.44	29.44

Table 5.20d. Wind speed (in kn) as a function of time and space in Spring.

Time (Days)	Distance from Port A (nm)					
	513	1026	1539	2052	2565	3078
1	3.89	4.37	3.89	4.86	4.37	5.35
2	12.15	14.09	14.58	12.15	11.66	14.58
3	16.04	14.58	15.55	16.04	15.06	14.09
4	8.26	10.21	8.26	8.75	9.23	16.04
5	22.35	17.01	15.06	21.38	23.33	21.87
6	19.44	20.41	21.87	23.81	23.33	20.41
7	20.41	18.95	24.30	21.87	23.81	19.94
8	20.90	21.38	19.44	19.92	22.41	21.41

Table 5.20e. Wind direction in degrees (^{O}) with respect to north, counting counterclockwise, as a function of time and space for all seasons.

Time (Days)	Distance from Port A (nm)					
	513	1026	1539	2052	2565	3078
1	318	320	310	345	300	260
2	315	330	330	330	300	250
3	315	325	334	300	285	260
4	320	325	330	250	265	255
5	321	328	345	260	244	230
6	317	320	305	255	230	225
7	323	333	300	245	250	228
8	320	330	328	260	242	230

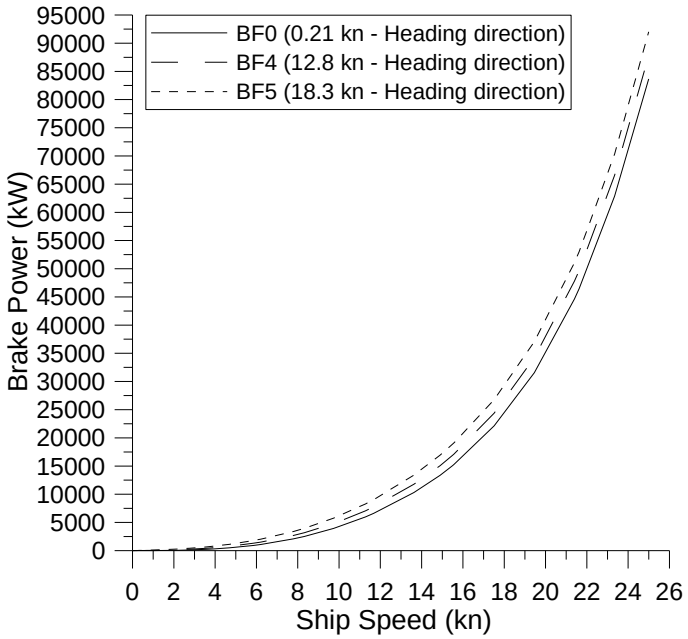

Figure 5.20. Power – speed curve for different Beaufort numbers.

5.3.2 Mathematical statement of the optimization problem

The dynamic optimization problem of this case study can be mathematically stated as a minimization problem using a Differential − Algebraic Equation (DAE) formulation. Again, this mathematical formulation is based on the mathematical formulation of the general problem presented in Section 3.3.1 combined with the technique for handling the synthesis variables presented in Section 3.3.2. The objective for this case study is selected to be the minimization of PWC. All symbols as well as all calculations necessary for the estimation of the total PWC are presented in detail in Chapter 3 and Appendices B, C. The objective function is stated as

$$\min_{\vec{x}} PWC = PWC_c + PWC_f + PWC_{om} \tag{5.19}$$

with vector $\vec{x}$, representing the vector of control (optimization) variables, consisting of the vectors of synthesis, design and operation optimization variables ($\vec{v}$, $\vec{w}$ and $\vec{z}$, respectively):

$$\vec{x} = (\vec{v}, \vec{w}, \vec{z}) \tag{5.20}$$

with:

$$\vec{v} = \left(y_{GT1,J1}, y_{GT2,J2}, y_{GT3,J3}, y_{B,K}, y_{ST,L}, y_{DG,M}, y_{AB} \right) \tag{5.21a}$$

$$\vec{w} = \left(\dot{W}_{bn,GT1,J1}, \dot{W}_{bn,GT2,J2}, \dot{W}_{bn,GT3,J3}, \dot{m}_{g_n,K}, T_{g_n,K}, \dot{m}_{s_n,K}, \dot{m}_{ST_n,L}, \dot{W}_{DG_n,M}, \dot{Q}_{AB_n} \right) \tag{5.21b}$$

$$\vec{z} = \left(\dot{W}_{b,GT1,J1}, \dot{W}_{b,GT2,J2}, \dot{W}_{b,GT3,J3}, \lambda_{h,K}, \lambda_{e,L}, \dot{W}_{DG,M} \right) \tag{5.21c}$$

where

$y_{GT1,J1}$ set of variables *j1* determining the existence of the *j1* th gas turbine of type 1 (binary): $y_{GT1,J1} = \left\{ y_{GT1,1}, y_{GT1,2}, ..., y_{GT1,j1}, .., y_{GT1,j1\max} \right\}$ (5.22a)

$y_{GT2,J2}$ set of variables *j2* determining the existence of the *j2* th gas turbine of type 2 (binary): $y_{GT2,J2} = \left\{ y_{GT2,1}, y_{GT2,2}, ..., y_{GT2,j2}, .., y_{GT2,j2\max} \right\}$ (5.22b)

$y_{GT3,J3}$ set of variables *j3* determining the existence of the *j3* th gas turbine of type 3 (binary): $y_{GT3,J3} = \left\{ y_{GT3,1}, y_{GT3,2}, ..., y_{GT3,j3}, .., y_{GT3,j3\max} \right\}$ (5.22c)

$y_{B,K}$ set of variables *k* determining the existence of the *k* th HRSG (binary): $y_{B,K} = \left\{ y_{B,1}, y_{B,2}, ..., y_{B,k}, .., y_{B,k\max} \right\}$ (5.22d)

$y_{ST,L}$ set of variables *l* determining the existence of the *l* th ST (binary): $y_{ST,L} = \left\{ y_{ST,1}, y_{ST,2}, ..., y_{ST,l}, .., y_{ST,l\max} \right\}$ (5.22e)

$y_{DG,M}$ set of variables *m* determining the existence of the *m* th generator set (binary): $y_{DG,M} = \left\{ y_{DG,1}, y_{DG,2}, ..., y_{DG,m}, ..., y_{DG,m\max} \right\}$ (5.22f)

y_{AB} variable determining the existence of the auxiliary boiler (binary),

$\dot{W}_{bn,GT1,J1}$ set of variables *j1* determining the nominal brake power output of *j1* th gas turbine of type 1 (invariant):

$$\dot{W}_{bn,GT1,J1} = \left\{\dot{W}_{bn,GT1,1}, \dot{W}_{bn,GT1,2}, ..., \dot{W}_{bn,GT1,j1}, ..., \dot{W}_{bn,GT1,j1\max}\right\} \quad (5.23a)$$

$\dot{W}_{bn,GT2,J2}$ set of variables *j2* determining the nominal brake power output of *j2* th gas turbine of type 2 (invariant):

$$\dot{W}_{bn,GT2,J2} = \left\{\dot{W}_{bn,GT2,1}, \dot{W}_{bn,GT2,2}, ..., \dot{W}_{bn,GT2,j2}, ..., \dot{W}_{bn,GT2,j1\max}\right\} \quad (5.23b)$$

$\dot{W}_{bn,GT3,J3}$ set of variables *j3* determining the nominal brake power output of *j3* th gas turbine of type 3 (invariant):

$$\dot{W}_{bn,GT3,J3} = \left\{\dot{W}_{bn,GT3,1}, \dot{W}_{bn,GT3,2}, ..., \dot{W}_{bn,GT3,j3}, ..., \dot{W}_{bn,GT3,j3\max}\right\} \quad (5.23c)$$

$\dot{m}_{g_n,K}$ set of variables *k* determining nominal exhaust gas mass flow rate of *k* th HRSG (invariant): $\dot{m}_{g_n,K} = \left\{\dot{m}_{g_n,1}, \dot{m}_{g_n,2}, ..., \dot{m}_{g_n,k}, ..., \dot{m}_{g_n,k\max}\right\}$ (5.23d)

$T_{g_n,K}$ set of variables *k* determining nominal exhaust gas temperature of *k* th HRSG (invariant): $T_{g_n,K} = \left\{T_{g_n,1}, T_{g_n,2}, ..., T_{g_n,k}, ..., T_{g_n,k\max}\right\}$ (5.23e)

$\dot{m}_{s_n,K}$ set of variables *k* determining nominal steam mass flow rate of *k* th HRSG (invariant): $\dot{m}_{s_n,K} = \left\{\dot{m}_{s_n,1}, \dot{m}_{s_n,2}, ..., \dot{m}_{s_n,k}, ..., \dot{m}_{s_n,k\max}\right\}$ (5.23f)

$\dot{m}_{ST_n,L}$ set of variables *l* determining the nominal steam mass flow rate of *l* th ST (invariant): $\dot{m}_{ST_n,L} = \left\{\dot{m}_{ST_n,1}, \dot{m}_{ST_n,2}, ..., \dot{m}_{ST_n,l}, ..., \dot{m}_{ST_n,l\max}\right\}$ (5.23g)

$\dot{W}_{DG_n,M}$ set of variables *m* determining the nominal power output of *m* th generator set (invariant): $\dot{W}_{DG_n,M} = \left\{\dot{W}_{DG_n,1}, \dot{W}_{DG_n,2}, ..., \dot{W}_{DG_n,m}, .., \dot{W}_{DG_n,m\max}\right\}$ (5.23h)

$\dot{Q}_{AB_n}$ nominal thermal power output of auxiliary boiler (invariant),

$\dot{W}_{b,GT1,J1}$ set of variables *j1* determining the brake power output of *j1* th gas turbine of type 1: $\dot{W}_{b,GT1,J1} = \left\{\dot{W}_{b,GT1,1}, \dot{W}_{b,GT1,2}, ..., \dot{W}_{b,GT1,j1}, ..., \dot{W}_{b,GT1,j1\max}\right\}$ (5.24a)

$\dot{W}_{b,GT2,J2}$ set of variables *j2* determining the brake power output of *j2* th gas turbine of type 2: $\dot{W}_{b,GT2,J2} = \left\{\dot{W}_{b,GT2,1}, \dot{W}_{b,GT2,2}, ..., \dot{W}_{b,GT2,j2}, ..., \dot{W}_{b,GT2,j2\max}\right\}$ (5.24b)

$\dot{W}_{b,GT3,J3}$ set of variables *j3* determining the brake power output of *j3* th gas turbine of type 3: $\dot{W}_{b,GT3,J3} = \left\{\dot{W}_{b,GT3,1}, \dot{W}_{b,GT3,2}, ..., \dot{W}_{b,GT3,j3}, ..., \dot{W}_{b,GT3,j3\max}\right\}$ (5.24c)

$\lambda_{h,K}$ set of variables *k* determining the fraction of *k* th HRSG steam mass flow delivered to thermal loads: $\lambda_{h,K} = \left\{\lambda_{h,1}, \lambda_{h,2}, ..., \lambda_{h,k}, ..., \lambda_{h,k\max}\right\}$ (5.24d)

$$\dot{m}_{s,h,k} = \lambda_{h,k} \cdot \dot{m}_{s,k} \quad (5.24e)$$

$\dot{m}_{s,h,k}$ steam mass flow rate drawn from *k* th HRSG drum for serving thermal loads,

$\dot{m}_{s,k}$ steam mass flow rate of *k* th HRSG unit,

$\lambda_{e,L}$ set of variables *l* determining the fraction of the *l* th steam turbine power output delivered to generator: $\lambda_{e,L} = \left\{\lambda_{e,1}, \lambda_{e,2}, ..., \lambda_{e,l}, ..., \lambda_{e,l\max}\right\}$ (5.24f)

$$\dot{W}_{STG,l} = \lambda_{e,l} \cdot \dot{W}_{ST,l} \quad (5.24g)$$

$\dot{W}_{STG,l}$ l th steam turbine generator power for serving electric loads,

$\dot{W}_{ST,l}$ l th steam turbine power output,

$\dot{W}_{DG,M}$ set of variables m determining the m th diesel generator set power output:

$$\dot{W}_{DG,M} = \left\{\dot{W}_{DG,1}, \dot{W}_{DG,2}, ..., \dot{W}_{DG,m}, ..., \dot{W}_{DG,m\max}\right\} \tag{5.24h}$$

Indices *j1*, *j2* and *j3* run through all the values from 1 up to an upper bound. It is noted that these upper bounds quantify the upper value of gas turbines of type 1, 2 and 3, respectively, that are allowed to be installed in the system and are pre-determined parameters, given at the start of the optimization. Once these upper values for all *j*'s are defined, the problem is set with as many binary variables for the gas turbines as necessary. The same idea stands also for the HRSGs, STs and diesel generator sets, which are modeled by indices *k*, *l* and *m* respectively. For all binary variables, value 0 denotes that the unit is not installed.

Since, in this case study, the assumption that for each of the four seasons of the year the same round trip is repeated over the season, the first year annual fuel cost of component n can be calculated by the equations:

$$C_{fa,n} = \sum_{s=1}^{4} C_{f,n,s} N_{trips,s} \tag{5.25}$$

$$C_{f,n,s} = c_{f,n} m_{f,n,s} \tag{5.26}$$

$$N_{trips,s} = \frac{\tau_s}{t_{trip,AB,s} + t_{trip,BA,s} + t_{port,A,s} + t_{port,B,s}} \tag{5.27}$$

where

$C_{fa,n}$ first year annual fuel cost of component n,

$C_{f,n,s}$ fuel cost of component n per round trip in season s.

$c_{f,n}$ fuel cost for component n,

$m_{f,n,s}$ fuel consumption for component n in a round trip for season s,

$N_{trips,s}$ number of total round trips of the ship for season s,

τ_s maximum permissible annual hours of operation for season s,

$t_{trip,AB,s}$ duration of travel from port A to B for season s,

$t_{trip,BA,s}$ duration of travel from port B to A for season s,

$t_{port,A,s}$ time spend in port A for season s (in a round trip),

$t_{port,B,s}$ time spend in port B for season s (in a round trip).

The same methodology is used for the first year operation and maintenance costs of each component,

$$C_{oma,n} = C_{om,n,s} N_{trips,s} \tag{5.28}$$

$$C_{om,n,s} = c_{om,n} E_{n,s} \tag{5.29}$$

where

$C_{om,n,s}$ operation and maintenance cost for component n per trip for each season s,

$c_{om,n}$ operation and maintenance unit cost for component n,

$E_{n,s}$ energy output of the component n for the duration of the round trip in season s.

The main differential variables for this problem are the distance travelled by the ship, the fuel consumption of the propulsion engines, diesel generator sets and auxiliary boiler. Another family of differential variables is derived from the energy output of each component which is generally given as the integral of output power of the component over the time horizon. All the respective equations for each component have been presented in detail in Chapter 3, Section 3.3.1, Eqs. (3.6)–(3.9) and in Appendix C.

Since the type and number of gas turbines and the nominal power of each one are not known but they are the result of optimization, the SFOC for each gas turbine as well as the exhaust gas mass flow rate and temperature are given as two-variable (nominal power and load factor) functions. The total exhaust gas mass flow rate and temperature from all engines is then calculated and supplied to the HRSGs, if HRSGs are installed. The same modeling procedure (two variable functions) is also applied in the case of diesel generator sets' SFOC and exhaust gas characteristics. The models used for the gas turbines and the diesel generator sets are presented in extent in Chapter 4.

The brake power of the propulsion engines and power from the steam turbines, as well as the electric and thermal power produced by the integrated system must be equal to the required brake power, the electric and thermal demands at any instant of time:

$$\sum_{j1} y_{GT1,j1}\dot{W}_{b,GT1,j1} + \sum_{j2} y_{GT2,j2}\dot{W}_{b,GT2,j2} + \sum_{j3} y_{GT3,j3}\dot{W}_{b,GT3,j3} + \sum_{l} \dot{W}_{ST,p,l} = \dot{W}_b \tag{5.30a}$$

$$\dot{W}_{ST,p,l} = (1-\lambda_{e,l})\cdot\dot{W}_{ST,l} \tag{5.30b}$$

$$\sum_{l} y_{ST,l}\cdot\dot{W}_{STG,l} + \sum_{m} y_{DG,m}\cdot\dot{W}_{DG,m} = \dot{W}_e \tag{5.31}$$

$$\sum_{k} y_{B,k}\cdot\dot{Q}_{B,k} + \dot{Q}_{AB} = \dot{Q} \tag{5.32}$$

where

$\dot{W}_b$ required brake power from the engines,

$\dot{W}_{ST,p,l}$ output power from l th ST given to the propeller,

$\dot{W}_e$ electric load,

$\dot{Q}_B$ heat drawn from HRSG drum for serving thermal loads,

$\dot{Q}$ thermal load.

The total required brake power of the engines is calculated as a function of the ship speed, weather state, ship resistance and propulsive efficiency. The respective equation is given in Chapter 3 (Eq. 3.13). All details considering the underlying mathematical calculations are presented in Chapter 4 and in Appendixes D and E of this thesis.

As it was stated in Case Study 1, there are multiple equalities correlated with the simulation of the components as well as inequality constraints (Eqs. 5.17a,b) imposed on certain variables, but their full presentation is beyond the limits of the present text.

Other important technical constraints are related with the nominal (design) characteristics of the components. Good example are the allowed upper and lower values for the nominal power output of the gas turbines and diesel generator sets:

$$\dot{W}_{bn,GT1,\min} \le \dot{W}_{bn,GT1,j1} \le \dot{W}_{bn,GT1,\max} \quad (5.33a)$$

$$\dot{W}_{bn,GT2,\min} \le \dot{W}_{bn,GT2,j2} \le \dot{W}_{bn,GT2,\max} \quad (5.33b)$$

$$\dot{W}_{bn,GT3,\min} \le \dot{W}_{bn,GT3,j3} \le \dot{W}_{bn,GT3,\max} \quad (5.33c)$$

$$\dot{W}_{DGn,\min} \le \dot{W}_{DGn,m} \le \dot{W}_{DGn,\max} \quad (5.34)$$

Of course all control variables, are accompanied by upper and lower limits. However, upper and lower limits may not be necessary for all state variables.

In the next section all the necessary values of input parameters and data assumptions in order to set up and solve the optimization problem stated in the current section are presented.

5.3.3 Additional data and assumptions

Values of certain cost parameters that are used for the PWC calculations are given in Table 5.21. For the gas turbines and diesel generator sets, the same type of fuel is considered (Marine Diesel Oil – MDO) which a Lower Heating Value (LHV) of 42700 kJ/kg. For the auxiliary boiler, Heavy Fuel Oil (HFO) with a Lower Heating Value (LHV) of 39550 kJ/kg is considered.

Table 5.21. Values of cost parameters for Case Study 2.

Parameter	Symbol	Value
MDO fuel cost nominal value (GTs, DG sets)	$c_{f,MDO}$	0.450 € / kg
HFO fuel cost nominal value (auxiliary boiler)	$c_{f,HFO}$	0.300 € / kg
Technical life of the system	N_t	20 years
Maximum permissible hours of operation – Summer	τ_1	2136
Maximum permissible hours of operation – Fall	τ_2	2136
Maximum permissible hours of operation – Winter	τ_3	1450
Maximum permissible hours of operation – Spring	τ_4	2136
Market interest rate	i	10 %

In Table 5.22 a list of lower and upper bounds of several important synthesis, design and operation variables is presented. Details regarding the time discretization that is used in order to model the operation of the energy system for the total time horizon are presented in Table 5.23. It is clarified that in essence, each control variable is decomposed to as many static variables as the number of intervals considered for the operation, thus increasing significantly the scale of the problem and the computing time.

Table 5.22. Bounds on synthesis, design and operation variables for Case Study 2.

Variable	Lower value	Upper value
Number of gas turbines of type 1	0	2
Number of gas turbines of type 2	0	2
Number of gas turbines of type 3	0	2
Number of total gas turbine units	1	4
Number of DG sets	0	4
Number of HRSGs	0	2
Number of STs	0	2
Gas turbine nominal power output (kW) (any type)	2500	90000
DG set nominal power output (kW)	300	5000
Load factors (all equipment)	0.1	1
Ship speed (kn)	14	25.4

Table 5.23. Numerical solution parameters for Case Study 2.

Parameter	Value
Distance from port A to B	3000 nm
Round trip distance	6000 nm
Single trip duration (from port A to B, all seasons)	6 days
Single trip duration (from port B to A, all seasons)	6 days
Total round trip duration	16 days
Length of time intervals on trips	1 day
Length of time intervals in ports	2 days
Number of time intervals used	50
Optimization convergence tolerance	10^{-4}

5.3.4 Solution procedure

For the solution of all the dynamic optimization problems pertaining to this case study, a sequential method is applied. All the relevant solution procedure specifics, such as the algorithms and the related software, are described in detail in Section 3.4 of Chapter 3. All optimizations are performed on an Intel® Core™2 Quad Processor Q9650 CPU at 3GHz with 8Gb of RAM.

It is noted that in the period Case Studies 2–7 were solved, updated and more robust solvers for the gPROMS software were available. Thus, they were much more efficient in terms of computational time.

5.3.5 Numerical results for the nominal case

In this section detailed results of the optimal solution for the nominal fuel price are presented.

The algorithm is able to successfully determine the optimal choice, among the three types of gas turbines (or any possible combinations of them), automatically. For reasons of completeness and to test its proper functionality, the problem is solved once again, for each

type separately, at the nominal fuel price. Optimal cost elements of the optimal solution of each type are presented in Table 5.24. The optimal solution given by the algorithm for the complete problem is verified by these results.

Table 5.24. Optimal costs (in €) of the system for each GT type.

GT type	Capital Cost	Fuel PWC	O&M PWC	Total PWC
1	21,783,196	165,549,466	18,700,482	206,033,144
2	22,486,258	165,343,458	16,989,449	204,819,165
3	22,949,592	166,256,995	14,207,511	203,414,098

Since the best choice is the 3rd type, and thus the optimal solution to the problem, a more thorough presentation of the optimal values of synthesis, design and operation variables is given below. The results of optimization, in terms of optimal synthesis and design are presented in Tables 5.25 and 5.26. Table 5.27 summarizes the hours of operation, trips per season and total trips per year. Optimal cost values for the system are given in Table 5.28. Optimal values of certain control variables per time interval and for all seasons are presented in Tables 5.29 – 5.32.

Table 5.25. Optimal synthesis of the system.

Type of GT	3
Number of GTs (prime movers)	1
Number of HRSGs	1
Number of STs	1
Number of DG sets	1
Number of auxiliary boilers	1

Table 5.26. Optimal design specifications of the system components.

Variable	Optimal Value
Main engine nominal brake power (kW)	44929
DG set nominal electric power (kW)	1652
Heat recovery steam generator	
Thermal power (kW)	24107
Exhaust gas mass flow rate (kg/s)	94.5
Nominal inlet exhaust gas temperature (°C)	385.7
Auxiliary boiler nominal thermal power (kW)	950
Steam-turbine	
Nominal power (kW)	6355
Nominal steam mass flow rate (kg/s)	7.98

Table 5.27. Hours of operation and round trips per season.

Season	Summer	Fall	Winter	Spring
Hours of operation	2074	2074	1421	2112
Number of round trips	5.4	5.4	3.7	5.5
Total round trips per year	20			

Table 5.28. Cost items (in €).

Season	Summer	Fall	Winter	Spring
Present worth cost of fuel	44,329,039	44,750,310	32,362,378	44,815,268
Present worth cost of O&M	3,795,651	3,825,489	2,733,964	3,852,407
Capital cost	22,949,592			
Total PWC (objective function)	203,414,098			

Table 5.29. Optimal ship speed versus time (in kn).

Day	Summer	Fall	Winter	Spring
	From port A to B			
1	20.89	20.88	20.91	20.90
2	20.84	20.84	20.86	20.84
3	20.87	20.87	20.88	20.89
4	20.88	20.88	20.91	20.90
5	20.72	20.72	20.69	20.68
6	20.79	20.79	20.72	20.78
	From port B to A			
1	20.79	20.84	20.74	20.81
2	20.28	19.94	19.13	20.47
3	21.09	21.18	21.74	20.99
4	21.02	21.08	21.46	20.95
5	20.89	20.95	20.98	20.89
6	20.91	20.99	20.93	20.87

Table 5.30. Propulsion power from diesel engine(s) and ST versus time (in kW).

Day	Summer		Fall		Winter		Spring	
	$\dot{W}_b$	$\dot{W}_{STP}$	$\dot{W}_b$	$\dot{W}_{STP}$	$\dot{W}_b$	$\dot{W}_{STP}$	$\dot{W}_b$	$\dot{W}_{STP}$
	From port A to port B							
1	37079.0	4330.2	37221.2	4323.7	37501.8	4362.6	37219.6	4206.6
2	37549.8	4247.8	37586.8	4275.5	37949.8	4278.9	37198.2	4231.6
3	37292.9	4275	37358.6	4291	37722.8	4372.7	37259.1	4286.5
4	37151.4	4314.5	37270.8	4273.9	37526.6	4337.7	37279.5	4339.4
5	38451.3	4379.6	38476.9	4393.8	39322.6	4340.5	37137.7	4293.9
6	37867.7	4366.3	37937.7	4369.4	38967.9	4415.8	37178.6	4308.8

	From port B to port A							
1	42256.4	4428.4	43351.3	4552.4	44929.6	6164.5	41284.3	4491.0
2	44929.3	4604.5	44928.9	4539.5	44929.5	6164.5	44476.6	4520.9
3	39532.7	4401.8	40356.0	4307.9	44930.2	6164.5	39758.3	4372.7
4	40153.5	4442.1	41107.8	4496.4	44929.5	6164.5	40220.9	4341.0
5	41276.9	4451.8	42285.1	4553.7	44929.2	6164.5	40654.2	4385.9
6	41049.7	4480.91	41980.8	4494.7	44929.8	6164.5	40816.6	4405.9

Table 5.31. Contribution of the HRSG and auxiliary boiler to thermal loads versus time for all seasons (in kW).

	Summer		Fall		Winter		Spring	
Day	$\dot{Q}_h$	$\dot{Q}_{AB}$	$\dot{Q}_h$	$\dot{Q}_{AB}$	$\dot{Q}_h$	$\dot{Q}_{AB}$	$\dot{Q}_h$	$\dot{Q}_{AB}$
	From port A to port B							
1	850	0	860	0	1000	0	990	0
2	880	0	900	0	1050	0	980	0
3	860	0	950	0	1080	0	1010	0
4	900	0	970	0	1100	0	1020	0
5	840	0	930	0	1060	0	950	0
6	850	0	960	0	1100	0	970	0
	From port B to port A							
1	860	0	930	0	1100	0	1040	0
2	870	0	950	0	1080	0	970	0
3	870	0	980	0	1060	0	960	0
4	890	0	970	0	990	0	950	0
5	860	0	890	0	1040	0	980	0
6	870	0	910	0	1070	0	960	0
	Ports							
A	0	950	0	950	0	950	0	950
B	0	950	0	950	0	950	0	950

Table 5.32. Electricity from STG and DG sets versus time for all seasons (in kW).

Day	Summer		Fall		Winter		Spring	
	$\dot{W}_{STG}$	$\dot{W}_{DG1}$	$\dot{W}_{STG}$	$\dot{W}_{DG1}$	$\dot{W}_{STG}$	$\dot{W}_{DG1}$	$\dot{W}_{STG}$	$\dot{W}_{DG1}$
	From port A to Port B							
1	1495	0	1508	0	1482	0	1625	0
2	1599	0	1573	0	1586	0	1599	0
3	1560	0	1547	0	1482	0	1547	0
4	1514	0	1560	0	1508	0	1495	0
5	1508	0	1495	0	1586	0	1534	0
6	1495	0	1495	0	1495	0	1521	0
	From port B to port A							
1	1625	0	1547	0	0	1534	1521	0
2	1560	0	1625	0	0	1521	1625	0
3	1534	0	1664	0	0	1625	1573	0

4	1521	0	1508	0	0	1651	1625	0
5	1560	0	1501	0	0	1495	1599	0
6	1521	0	1547	0	0	1521	1586	0
	Ports							
A	0	1500	0	1500	0	1500	0	1500
B	0	1500	0	1500	0	1500	0	1500

The optimal present worth cost after 20 years of operation is 203,414,098 €. The optimization was concluded in 5680 seconds, performing 39 Major NLP iterations at an Intel® Core™2 Quad Processor Q9650 cpu at 3GHz with 8Gb of RAM. Indeed, although this problem is dimensionally more complicated when compared with the problem of Case Study 1, we conclude that the computational efficiency of the gPROMS solvers has improved due to the upgrade.

In the solution of this nominal case, one gas turbine of type #3 is selected by the optimizer as the optimal propulsion plant synthesis solution, although it is noted that the optimal PWC values for all three GT types are relatively close. A bottoming cycle is installed with one HRSG and one ST. Thermal loads during the trips are always served by the HRSG, while at ports they are covered by the auxiliary boiler. Also, with the exception of the trip from port B to A during winter, in all other trips the bottoming cycle fully serves the electric demands and provides the remaining power to the propeller. However, during this winter return trip (from port B to A), where the propulsion demand is augmented, the optimizer selects to provide all the available ST power to the propeller (while letting the DG set to fully serve the electric loads) in order to decrease the needed nominal power output (and thus capital cost) of the gas turbine. Finally, a single diesel generator unit is installed.

5.3.6 Parametric study

For the sensitivity analysis the fuel price is considered to vary. Apart from the nominal value of 450 €/ton, three more values were considered: 300, 600, and 750 €/ton. Selected sensitivity analysis results regarding the optimal synthesis and design characteristics of the system are presented in Tables 5.33 and 5.34. The variation of the optimal PWC is given in Table 5.35. It is noted that for the specific hours of operation (not variable) in this problem the optimal solution always chooses to install gas turbine type #3.

Table 5.33. Effect of fuel price on the optimal synthesis of the system.

	Fuel Price (€/ton)	300	450	600	750
Synthesis	GT type	3	3	3	3
	Number of GTs	1	1	1	1
	Number of HRSG	1	1	1	1
	Number of ST	1	1	1	1
	Number of DG sets	1	1	1	1
	Number of AB	1	1	1	1

Table 5.34. Effect of fuel price on the optimal design specifications of the system.

	Fuel Price (€/ton)	300	450	600	750
Nominal power (kW)	GT	44921	44929	44937	44945
	HRSG	23883	24107	24255	24375
	ST	6350	6358	6363	6370
	DG set	1652	1652	1652	1652
	AB	950	950	950	950

Table 5.35. Effect of fuel price on the optimal PWC.

Costs (€)	Fuel Price (€/ton)			
	300	450	600	750
Capital Cost	22,925,374	22,949,592	22,965,668	22,981,674
Fuel PWC (total)	110,837,520	166,256,995	221,677,226	277,098,251
O&M PWC (total)	14,207,538	14,207,511	14,207,545	14,207,548
Total PWC (objective)	147,970,432	203,414,098	258,850,439	314,287,473

For the parametric study, many comments that were stated for the nominal case solution, can be repeated. One type #3 gas turbine unit and a bottoming cycle, comprising a single HRSG and a single ST, are always installed for all fuel prices. Also a single diesel generator set is installed. It is interesting that the nominal (design) values of components seem to increase slightly as the fuel price rises. An explanation is given in Paragraph 5.10.2.

5.4 Case Study 3: Containership with Gas Turbines, Trips of Variable Time, Minimization of PWC

5.4.1 Description of the system and the optimization problem

In Case Study 3, the optimal configuration (synthesis), design specifications of components and operating conditions of an energy system that will cover all energy needs of a containership under the scope of minimizing the PWC with variable trip durations, are requested.

The same system as in Case Study 2 is used, with the main difference that now the duration of each trip for each season is variable and under optimization. Thus, the number of round trips per season and consequently the total number of round trips per year is no longer fixed but it is the result of optimization. It is noted that the number or round trips for each season can be a decimal number so as to model the (possible) passage from one season to the next in the same round trip. However, the problem is set in an appropriate manner so as the total number of round trips per year is integer.

All other details regarding the energy system, the mission characteristics and the dynamic optimization problem can be found in Section 5.3.1, as they are the same with Case Study 2. The superconfiguration of the energy system can be found in Figure 5.19. Data regarding the vessel characteristics can be found in Table 5.16. The weather and the thermal and electric loads per trip and per season can be found in Tables 5.18-5.20e. The time schedule of the ship is given in Table 5.36.

Table 5.36. Time schedule of the ship.

Mode	Description	Duration
1	Loading at port A (all seasons)	2 days
2	Loaded trip from port A to port B (all seasons)	Variable
3	Off-loading and loading at port B (all seasons)	2 days
4	Loaded trip from port B to port A (all seasons)	Variable
	Total round trip	variable

5.4.2 Mathematical statement of the optimization problem

The dynamic optimization problem of this case study is mathematically stated as a minimization problem using the same Differential − Algebraic Equation (DAE) formulation (Eq. 5.19-5.34) as in Case Study 2.

The main difference is that in this case study, the round trip durations are also optimization variables, thus the objective function (Eq. 5.19) must be correctly restated as:

$$\min_{\vec{t}_f,\vec{x}} PWC = PWC_c + PWC_f + PWC_{om} \tag{5.35}$$

with vector $\vec{x}$, again representing the vector of control (optimization) variables, consisting of the vectors of synthesis, design and operation optimization variables as stated in Eqs. (5.20)-(5.24h) and vector $\vec{t}_f$ representing the vector of control (optimization) variables consisting of the single trip durations for each season:

$$\vec{t}_f = (t_{trip,AB,s}, t_{trip,BA,s}) \quad for \quad s = 1,2,3,4 \tag{5.36}$$

where

$t_{trip,AB,s}$ duration of trip from port A to B for season *s*,

$t_{trip,BA,s}$ duration of trip from port B to A for season *s*.

that appear in the definition of the number of round trips per season, Eq. (5.27). Of course, since now these durations are control variables, appropriate upper and lower bounds are defined:

$$t_{trip,AB,s,\min} \le t_{trip,AB,s} \le t_{trip,AB,s,\max} \quad , \quad s = 1,2,3,4 \tag{5.37a}$$

$$t_{trip,BA,s,\min} \le t_{trip,BA,s} \le t_{trip,BA,s,\max} \quad , \quad s = 1,2,3,4 \tag{5.37b}$$

In the next section the necessary values of input parameters and data assumptions for the dynamic optimization problem of Case Study 3 are presented.

5.4.3 Additional data and assumptions

Values of certain cost parameters that are used for the PWC calculations are given in Table 5.21. Considering the fuel, for the gas turbines and diesel generator sets, Marine Diesel Oil (MDO) with a Lower Heating Value (LHV) of 42700 kJ/kg is considered, while

for the auxiliary boiler, Heavy Fuel Oil (HFO) with a Lower Heating Value (LHV) of 39550 kJ/kg, is considered. In Table 5.37 a list of lower and upper bounds of several important synthesis, design and operation variables is presented. Details regarding the time discretization that is used in order to model the operation of the energy system for the total time horizon and other numerical solution parameters are presented in Table 5.38.

Table 5.37. Bounds on synthesis, design and operation variables for Case Study 3.

Variable	Lower value	Upper value
Number of gas turbines of type 1	0	2
Number of gas turbines of type 2	0	2
Number of gas turbines of type 3	0	2
Number of total gas turbine units	1	4
Number of DG sets	0	4
Number of HRSGs	0	2
Number of STs	0	2
Gas turbine nominal power output (kW) (any type)	2500	90000
DG set nominal power output (kW)	300	5000
Load factors (all equipment)	0.1	1
Ship speed (kn)	14	25.4
Single trip duration, all seasons (days)	5	8

Table 5.38. Numerical solution parameters for Case Study 3.

Parameter	Value
Single trip distance	3000 nm
Round trip distance	6000 nm
Single trip duration from port A to B (all seasons)	variable
Single trip duration from port B to A, (all seasons)	variable
Total round trip duration	variable
Length of time intervals on trips	1 day
Length of time intervals in port	2 days
Number of time intervals used	66
Optimization convergence tolerance	10^{-4}

5.4.4 Solution procedure

For the solution of all the dynamic optimization problems pertaining to this case study, both a sequential method and a simultaneous method were applied. The sequential method was found to be as efficient as the simultaneous method in terms of accuracy but better in terms of computational time, since the simultaneous method required more Major Iterations of the optimization algorithm in order to converge to a solution.

All the relevant solution procedure specifics, such as the algorithms and the related software, are described in detail in Section 3.4 of Chapter 3. All optimizations are performed on an Intel® Core™2 Quad Processor Q9650 CPU at 3GHz with 8Gb of RAM.

The updated solvers of the gPROMS software were used.

5.4.5 Numerical results for the nominal case

The algorithm is able to determine the optimal, between the three, type of gas turbine automatically. As in the previous case study, for reasons of completeness and to determine its proper functionality, along with the general case, three distinct optimizations (one for each GT type) are also performed. The optimal cost elements of the optimal solution for each GT type are presented in Table 5.39 and verify that the general problem is indeed solved correctly.

Table 5.39. Optimal cost (in €) of the system for each GT type.

GT type	Capital Cost	Fuel PWC	O&M PWC	Total PWC
1	14,017,586	77,106,458	9,100,805	100,224,849
2	14,836,182	76,777,255	8,334,553	99,947,990
3	15,428,136	77,095,837	7,114,045	99,638,018

Since the best choice is the 3rd type, and thus the optimal solution to the problem, a more thorough presentation of the optimal values of synthesis, design and operation variables is given below. The results of optimization, in terms of optimal synthesis and design are presented in Tables 5.40 and 5.41. Table 5.42 summarizes the hours of operation, trips per season and total trips per year. Optimal cost values for the system are given in Table 5.43. Optimal values of certain control variables per time interval and for all seasons are presented in Tables 5.45 – 5.47

Table 5.40. Optimal synthesis of the system.

Type of GT	3
Number of GTs (prime movers)	1
Number of HRSGs	1
Number of STs	1
Number of DG sets	1
Number of auxiliary boilers	1

Table 5.41. Optimal design specifications of the system components.

Variable	Optimal Value
Main engine nominal brake power (kW)	19558
DG set nominal electric power (kW)	1652
Heat recovery steam generator	
Thermal power (kW)	9090
Exhaust gas mass flow rate (kg/s)	38
Nominal inlet exhaust gas temperature (°C)	376
Auxiliary boiler nominal thermal power (kW)	950
Steam-turbine	
Nominal power (kW)	2527
Nominal steam mass flow rate (kg/s)	3.34

Table 5.42. Hours of operation and round trips per season.

Season	Summer	Fall	Winter	Spring
Hours of operation	2064	2064	1440	2112
Trip from port A to B duration (days)	8	8	8	8
Trip from port B to A duration (days)	8	8	8	8
Round trip duration (days)	20	20	20	20
Number of round trips	4.3	4.3	3	4.4
Total round trips per year	16			

Table 5.43. Cost items (in €).

Season	Summer	Fall	Winter	Spring
Present worth cost of fuel	20,308,659	20,552,807	15,653,183	20,581,188
Present worth cost of O&M	1,878,182	1,899,753	1,421,041	1,915,069
Capital cost	15,428,136			
Total PWC (objective function)	99,638,018			

Table 5.44. Optimal ship speed versus time (in kn).

Summer		Fall		Winter		Spring	
Day	*V*	Day	*V*	Day	*V*	Day	*V*
From port A to port B							
1	15.77	1	15.76	1	15.84	1	15.73
2	15.67	2	15.67	2	15.75	2	15.65
3	15.73	3	15.73	3	15.78	3	15.74
4	15.76	4	15.76	4	15.84	4	15.76
5	15.41	5	15.42	5	15.39	5	15.41
6	15.56	6	15.56	6	15.46	6	15.57
7	15.52	7	15.60	7	15.45	7	15.60
8	15.58	8	15.52	8	15.47	8	15.55
	From port B to port A						
1	15.46	1	15.49	1	15.42	1	15.56
2	14.63	2	14.17	2	13.43	2	14.89
3	16.10	3	16.21	3	16.87	3	15.94
4	15.94	4	16.00	4	16.45	4	15.84
5	15.68	5	15.72	5	15.77	5	15.73
6	15.73	6	15.80	6	15.69	6	15.68
7	15.81	7	15.71	7	15.68	7	15.70
8	15.73	8	15.85	8	15.70	8	15.66

Table 5.45. Propulsion power from gas turbine and ST versus time (in kW).

Summer			Fall			Winter			Spring		
Day	$\dot{W}_b$	$\dot{W}_{STP}$	Day	$\dot{W}_b$	$\dot{W}_{STP}$	Day	$\dot{W}_b$	$\dot{W}_{STP}$	Day	$\dot{W}_b$	$\dot{W}_{STP}$
	From port A to port B										
1	15475	816	1	15550	806	1	15862	847	1	15463	682
2	15712	720	2	15726	747	2	16098	750	2	15442	708
3	15592	755	3	15625	770	3	15947	851	3	15504	764
4	15512	799	4	15601	755	4	15888	821	4	15525	819
5	16001	826	5	16020	841	5	16631	773	5	15380	772
6	15771	830	6	15814	832	6	16441	859	6	15421	787
7	15765	835	7	15800	841	7	16441	859	7	15401	798
8	15780	825	8	15825	825	8	16440	861	8	15431	780
	From port B to port A										
1	18294	802	1	18796	903	1	19558	2527	1	17826	890
2	19558	919	2	19558	852	2	19558	2527	2	19321	843
3	17141	849	3	17646	736	3	19558	2527	3	17240	812
4	17394	873	4	17878	906	4	19558	2527	4	17462	768
5	17875	852	5	18358	933	5	19558	2527	5	17623	802
6	17762	888	6	18262	881	6	19558	2527	6	17681	817
7	17750	896	7	18250	892	7	19558	2527	7	17731	805
8	17765	890	8	18265	879	8	19558	2527	8	17720	831

Table 5.46. Contribution of the HRSG and auxiliary boiler to thermal loads versus time for all seasons (in kW).

Summer			Fall			Winter			Spring		
Day	$\dot{Q}_h$	$\dot{Q}_{AB}$	Day	$\dot{Q}_h$	$\dot{Q}_{AB}$	Day	$\dot{Q}_h$	$\dot{Q}_{AB}$	Day	$\dot{Q}_h$	$\dot{Q}_{AB}$
	From port A to port B										
1	850	0	1	860	0	1	1000	0	1	990	0
2	880	0	2	900	0	2	1050	0	2	980	0
3	860	0	3	950	0	3	1080	0	3	1010	0
4	900	0	4	970	0	4	1100	0	4	1020	0
5	840	0	5	930	0	5	1060	0	5	950	0
6	850	0	6	960	0	6	1100	0	6	970	0
7	845	0	7	959	0	7	1100	0	7	980	0
8	851	0	8	963	0	8	1090	0	8	970	0
	From port B to port A										
1	860	0	1	930	0	1	1100	0	1	1040	0
2	870	0	2	950	0	2	1080	0	2	970	0
3	870	0	3	980	0	3	1060	0	3	960	0
4	890	0	4	970	0	4	990	0	4	950	0
5	860	0	5	890	0	5	1040	0	5	980	0
6	870	0	6	910	0	6	1070	0	6	960	0
7	880	0	7	920	0	7	1080	0	7	970	0
8	870	0	8	910	0	8	1050	0	8	960	0

	Ports										
A	0	950	A	0	950	A	0	950	A	0	950
B	0	950	B	0	950	B	0	950	B	0	950

Table 5.47. Electric power of STG and DG sets versus time for all seasons (in kW).

Summer			Fall			Winter			Spring		
Day	$\dot{W}_{STG}$	$\dot{W}_{DG1}$	Day	$\dot{W}_{STG}$	$\dot{W}_{DG1}$	Day	$\dot{W}_{STG}$	$\dot{W}_{DG1}$	Day	$\dot{W}_{STG}$	$\dot{W}_{DG1}$
	From port A to port B										
1	1495	0	1	1508	0	1	1482	0	1	1625	0
2	1599	0	2	1573	0	2	1586	0	2	1599	0
3	1560	0	3	1547	0	3	1482	0	3	1547	0
4	1514	0	4	1560	0	4	1508	0	4	1495	0
5	1508	0	5	1495	0	5	1586	0	5	1534	0
6	1495	0	6	1495	0	6	1495	0	6	1521	0
7	1490	0	7	1495	0	7	1485	0	7	1525	0
8	1495	0	8	1495	0	8	1490	0	8	1520	0
	From port B to port A										
1	1625	0	1	1547	0	1	0	1534	1	1521	0
2	1560	0	2	1625	0	2	0	1521	2	1625	0
3	1534	0	3	1664	0	3	0	1625	3	1573	0
4	1521	0	4	1508	0	4	0	1651	4	1625	0
5	1560	0	5	1501	0	5	0	1495	5	1599	0
6	1521	0	6	1547	0	6	0	1521	6	1586	0
7	1520	0	7	1539	0	7	0	1520	7	1580	0
8	1525	0	8	1550	0	8	0	1521	8	1580	0
	Ports										
A	0	1500	A	0	1500	A	0	1500	A	0	1500
B	0	1500	B	0	1500	B	0	1500	B	0	1500

The optimal present worth cost after 20 years of operation is 99,638,018 €. The optimization was concluded in 6050 seconds, performing 41 Major NLP iterations at an Intel® Core™2 Quad Processor Q9650 cpu at 3GHz with 8Gb of RAM.

A single type #3 gas turbine unit along with one HRSG, one ST and one diesel generator set are selected for the optimal synthesis of the system.

In order to make the system cost effective, the optimizer selects as optimal duration for all trips in all seasons the upper limit of 8 days. This leads to a significant decrease in the nominal power design characteristics of the gas turbine, the HRSG and the ST when compared to Case Study 2. Especially, for the propulsion plant, the optimal nominal power output (19558 kW) drops by 56% when compared with the nominal power output (44929 kW) result of Case Study 2 and by 72% when compared with the required nominal power output (70817 kW) for the design speed of 25.4 knots (Table 5.16). This is expected, since by taking all trip durations to the upper limit of 8 days, the average speed (for all trips) decreases and a smaller number of trips are performed in each season. Indeed, by comparing Tables 5.29 and 5.44 we observe that all speeds in all trips have decreased by 25% on average.

Considering the distribution of ST power to the propeller and electric loads, the same behavior as in case study 2 is observed. With the exception of the trip from port B to A during winter, in all other trips the bottoming cycle fully serves the electric demands. However, during this winter return trip (from port B to A), where the propulsion demand happens to be augmented, the optimizer selects to provide all the available ST power to the propeller (while letting the DG to fully serve the electric loads). All thermal loads during the trips are fully covered by the HRSG.

5.4.6 Parametric study

For the sensitivity analysis the fuel price is considered to vary. Apart from the nominal value of 450 €/ton, three more values were considered: 300, 600, and 750 €/ton. Selected sensitivity analysis results regarding the optimal synthesis and design characteristics of the system are presented in Tables 5.48 and 5.49. The variation of the optimal PWC is given in Table 5.50. The optimal results for trip durations and number of round trips are summarized in Tables 5.51 and 5.52.

Table 5.48. Effect of fuel price on the optimal synthesis of the system.

	Fuel Price (€/ton)	300	450	600	750
Synthesis	GT type	3	3	3	3
	GT 3	1	1	1	1
	HRSG	1	1	1	1
	ST	1	1	1	1
	DG sets	1	1	1	1
	AB	1	1	1	1

Table 5.49. Effect of fuel price on the optimal design specifications of the system.

	Fuel Price (€/ton)	300	450	600	750
Nominal power (kW)	GT 3	19143	19558	19812	20203
	HRSG	9050	9090	9180	9273
	ST	2518	2527	2544	2561
	DG set 1	1652	1652	1652	1652
	AB	950	950	950	950

Table 5.50a. Effect of fuel price on the optimal PWC.

Costs (€)	Fuel Price (€/ton)			
	300	450	600	750
Capital Cost	15,406,136	15,428,136	15,444,136	15,459,704
Fuel PWC (total)	51,505,222	77,095,837	102,503,460	128,277,117
O&M PWC (total)	7,114,047	7,114,045	7,114,156	7,114,045
Total PWC (objective)	74,025,405	99,638,018	125,061,752	150,850,866

Table 5.51. Effect of fuel price on the optimal trip durations (numbers in days).

Trip	Fuel Price (€/ton)			
	300	450	600	750
Summer 1	8	8	8	8
Summer 2	8	8	8	8
Fall 1	8	8	8	8
Fall 2	8	8	8	8
Winter 1	8	8	8	8
Winter 2	8	8	8	8
Spring 1	8	8	8	8
Spring 2	8	8	8	8

Table 5.52. Effect of fuel price on the optimal number of round trips.

Season	Fuel Price (€/ton)			
	300	450	600	750
Summer	4.3	4.3	4.3	4.3
Fall	4.3	4.3	4.3	4.3
Winter	3	3	3	3
Spring	4.4	4.4	4.4	4.4
Total per year	16	16	16	16

A noteworthy comment on the results of this parametric analysis is that for all fuel prices examined here, the optimizer always selects the upper limit as the optimal choice for all the trip durations. In all cases, one type #3 gas turbine unit and a bottoming cycle, comprising a single HRSG and a single ST, are always installed for all fuel prices. Also a single diesel generator set is always installed. Again, it is observed that the nominal (design) values of components seem to increase slightly (<2%) as the fuel price rises.

5.5 Case Study 4: Containership with Gas Turbines, Trips of Variable Time, Maximization of NPV

5.5.1 Description of the system and the optimization problem

In Case Study 4 the optimal configuration (synthesis), design specifications of components and operating conditions of an energy system that will cover all energy needs of a containership under the scope of maximizing the NPV, are requested.

The same formulation as in Case Study 3 is used. Again, the duration of each trip for each season is variable and under optimization. However, in this case study, a different objective function is used. For each trip, a suitable freight rate is defined, thus, a corresponding revenue can be calculated. The economic criterion that serves as the objective function is the NPV and the goal is its maximization.

All other details regarding the energy system,the mission characteristics and the dynamic optimization problem can be found in Sections 5.3.1 and 5.4.1, as they are the same with Case Study 3. The superconfiguration of the system is depicted in Figure 5.19.

5.5.2 Mathematical statement of the optimization problem

The DAE formulation that is presented in Eqs. (5.19)-(5.34) of Section 5.3.2 with the addition of Eqs. (5.36)-(5.37b) of Section 5.4.2 serves as a suitable mathematical statement or this case study. However, a different objective function in the place of Eq. (5.19) is defined

$$\max_{\vec{t}_f,\vec{x}} NPV = PWR - PWC \tag{5.38}$$

with vector $\vec{x}$, representing the vector of control (optimization) variables, consisting of the vectors of synthesis, design and operation optimization variables as stated in Eqs. (5.20)-(5.24h) and vector $\vec{t}_f$ representing the vector of control (optimization) variables consisting of the single trip durations (Eq. 5.36) for each season. The PWC term is calculated in the same way as in Eq. (5.35). The present worth of revenue is given by the equation

$$PWR = f_r \cdot C_{load} \cdot \left(2d_{AB}\right) \cdot TEU \cdot N_{trips,a} \cdot PWF(N_n, i) \tag{5.39}$$

where

f_r	freight rate (in €/nm/TEU),
C_{load}	safety loading factor of containership,
TEU	containership cargo capacity,
$N_{trips,a}$	total (annual) number of round trips,
PWF	Present Worth Factor (Appendix B).

The total annual number of round trips is given as the sum of the round trips of each season:

$$N_{trips,a} = \sum_{s=1}^{4} N_{trips,s} \tag{5.40}$$

In the next section the necessary values of input parameters and data assumptions for the dynamic optimization problem of Case Study 4 are presented.

5.5.3 Additional data and assumptions

The same containership, as in Case Study 2, with carrying capacity 9572 TEU and DWT of 111529 MT is considered with the same round trip distance of 6000 nm. Values of certain cost parameters that are used for the NPV calculations are given in Table 5.53. Considering the fuel, for the gas turbines and diesel generator sets, Marine Diesel Oil (MDO) with a Lower Heating Value (LHV) of 42700 kJ/kg is considered, while for the auxiliary boiler, Heavy Fuel Oil (HFO) with a Lower Heating Value (LHV) of 39550 kJ/kg, is considered. A list of lower and upper bounds of several important synthesis, design and operation variables is given in Table 5.37. Details regarding the time discretization that is used in order to model the operation of the energy system for the total time horizon, the mission characteristics and other numerical solution parameters are presented in Table 5.38.

Table 5.53. Values of cost parameters for Case Study 4.

Parameter	Symbol	Value
MDO fuel cost nominal value (all components)	$c_{f,MDO}$	0.450 € / kg
HFO fuel cost nominal value (all components)	$c_{f,HFO}$	0.300 € / kg
Technical life of the system	N_t	20 years
Maximum permissible hours of operation – Summer	τ_1	2136
Maximum permissible hours of operation – Fall	τ_2	2136
Maximum permissible hours of operation – Winter	τ_3	1450
Maximum permissible hours of operation – Spring	τ_4	2136
Market interest rate	i	10 %
Freight rate (nominal value)	f_r	0.0326 € / TEU.nm
Loading factor of containership	C_{load}	0.85

5.5.4 Solution procedure

The same comments as in Section 5.4.4 apply here.

5.5.5 Numerical results for nominal case

The algorithm is first set to perform the optimization for each type of GT fixed as the prime mover for the nominal fuel price and freight rate. Then the generalized case is solved where the optimal type of gas turbine (or combinations of types) must be determined. The optimal cost elements of the optimal solution of each type are presented in Table 5.54. The optimal solution of the general problem, in which the optimal type of GT type must also be determined, agrees with the results of Table 5.54.

Table 5.54. Optimal NPV (in €) of the system for each GT type.

GT type	Capital Cost	Fuel PWC	O&M PWC	Total PWC	PWR	NPV (objective)
1	14,017,586	77,106,458	9,100,805	100,224,849	215,363,516	115,138,667
2	14,836,182	76,777,255	8,334,553	99,947,990	215,363,516	115,415,526
3	15,428,136	77,095,837	7,114,045	99,638,018	215,363,516	115,725,498

The analysis of the optimal solution (for the best GT type #3), in terms of optimal synthesis and design is presented in Tables 5.55 and 5.56. Optimal round trip duration and hours of operation for each season are given in Table 5.57. Optimal cost values for each component of the system and revenues are given in Table 5.58. Optimal values of certain control variables per time interval and season are presented in Tables 5.59 – 5.62.

Table 5.55. Optimal synthesis of the system.

Type of GT	3
Number of GT (prime mover)	1
Number of HRSGs	1
Number of steam turbines	1
Number of DG sets	1
Number of auxiliary boilers	1

Table 5.56. Optimal design specifications of the system components.

Variable	Optimal Value
Main engine nominal brake power (kW)	19558
DG set nominal electric power (kW)	1652
Heat recovery steam generator	
Thermal power (kW)	9090
Exhaust gas mass flow rate (kg/s)	38
Nominal inlet exhaust gas temperature (^{o}C)	377
Auxiliary boiler nominal thermal power (kW)	950
Steam-turbine	
Nominal power (kW)	2527
Nominal steam mass flow rate (kg/s)	3.34

Table 5.57 Hours of operation and round trips per season.

Season	Summer	Fall	Winter	Spring
Hours of operation	2064	2064	1440	2112
Trip from port A to B (days)	8	8	8	8
Trip from port B to A (days)	8	8	8	8
Round trip duration (days)	20	20	20	20
Number of round trips	4.3	4.3	3	4.4
Total round trips per year	16			

Table 5.58. Cost items (in €).

Season	Summer	Fall	Winter	Spring
Present worth of revenue	57,878,945	57,878,945	40,380,659	59,224,967
Present worth cost of fuel	20,308,659	20,552,807	15,653,183	20,581,188
Present worth cost of O&M	1,878,182	1,899,753	1,421,041	1,915,069
Capital cost	15,428,136			
Total PWC	99,638,018			
Total present worth of revenue	215,363,516			
Net Present Value (objective function)	115,725,498			

Table 5.59. Optimal ship speed versus time (in kn).

Summer		Fall		Winter		Spring	
Day	V	Day	V	Day	V	Day	V
From port A to port B							
1	15.77	1	15.76	1	15.84	1	15.73
2	15.67	2	15.67	2	15.75	2	15.65
3	15.73	3	15.73	3	15.78	3	15.74
4	15.76	4	15.76	4	15.84	4	15.76
5	15.41	5	15.42	5	15.39	5	15.41
6	15.56	6	15.56	6	15.46	6	15.57
7	15.52	7	15.60	7	15.45	7	15.60
8	15.58	8	15.52	8	15.47	8	15.55
From port B to port A							
1	15.46	1	15.49	1	15.42	1	15.56
2	14.63	2	14.17	2	13.43	2	14.89
3	16.10	3	16.21	3	16.87	3	15.94
4	15.94	4	16.00	4	16.45	4	15.84
5	15.68	5	15.72	5	15.77	5	15.73
6	15.73	6	15.80	6	15.69	6	15.68
7	15.81	7	15.71	7	15.68	7	15.70
8	15.73	8	15.85	8	15.70	8	15.66

Table 5.60. Propulsion power from gas turbine and ST versus time (in kW).

Summer			Fall			Winter			Spring		
Day	$\dot{W}_b$	$\dot{W}_{STP}$	Day	$\dot{W}_b$	$\dot{W}_{STP}$	Day	$\dot{W}_b$	$\dot{W}_{STP}$	Day	$\dot{W}_b$	$\dot{W}_{STP}$
	From port A to port B										
1	15475	816	1	15550	806	1	15862	847	1	15463	682
2	15712	720	2	15726	747	2	16098	750	2	15442	708
3	15592	755	3	15625	770	3	15947	851	3	15504	764
4	15512	799	4	15601	755	4	15888	821	4	15525	819
5	16001	826	5	16020	841	5	16631	773	5	15380	772
6	15771	830	6	15814	832	6	16441	859	6	15421	787
7	15765	835	7	15800	841	7	16441	859	7	15401	798
8	15780	825	8	15825	825	8	16440	861	8	15431	780
	From port B to port A										
1	18294	802	1	18796	903	1	19558	2527	1	17826	890
2	19558	919	2	19558	852	2	19558	2527	2	19321	843
3	17141	849	3	17646	736	3	19558	2527	3	17240	812
4	17394	873	4	17878	906	4	19558	2527	4	17462	768
5	17875	852	5	18358	933	5	19558	2527	5	17623	802
6	17762	888	6	18262	881	6	19558	2527	6	17681	817
7	17750	896	7	18250	892	7	19558	2527	7	17731	805
8	17765	890	8	18265	879	8	19558	2527	8	17720	831

Table 5.61. Contribution of the HRSG and auxiliary boiler to thermal loads versus time for all seasons (in kW).

Summer			Fall			Winter			Spring		
Day	$\dot{Q}_h$	$\dot{Q}_{AB}$	Day	$\dot{Q}_h$	$\dot{Q}_{AB}$	Day	$\dot{Q}_h$	$\dot{Q}_{AB}$	Day	$\dot{Q}_h$	$\dot{Q}_{AB}$
	From port A to port B										
1	850	0	1	860	0	1	1000	0	1	990	0
2	880	0	2	900	0	2	1050	0	2	980	0
3	860	0	3	950	0	3	1080	0	3	1010	0
4	900	0	4	970	0	4	1100	0	4	1020	0
5	840	0	5	930	0	5	1060	0	5	950	0
6	850	0	6	960	0	6	1100	0	6	970	0
7	845	0	7	959	0	7	1100	0	7	980	0
8	851	0	8	963	0	8	1090	0	8	970	0
	From port B to port A										
1	860	0	1	930	0	1	1100	0	1	1040	0
2	870	0	2	950	0	2	1080	0	2	970	0
3	870	0	3	980	0	3	1060	0	3	960	0
4	890	0	4	970	0	4	990	0	4	950	0
5	860	0	5	890	0	5	1040	0	5	980	0
6	870	0	6	910	0	6	1070	0	6	960	0
7	880	0	7	920	0	7	1080	0	7	970	0
8	870	0	8	910	0	8	1050	0	8	960	0
	Ports										
A	0	950	A	0	950	A	0	950	A	0	950
B	0	950	B	0	950	B	0	950	B	0	950

Table 5.62. Electric power of STG and DG set versus time for all seasons (in kW).

Summer			Fall			Winter			Spring		
Day	$\dot{W}_{STG}$	$\dot{W}_{DG1}$	Day	$\dot{W}_{STG}$	$\dot{W}_{DG1}$	Day	$\dot{W}_{STG}$	$\dot{W}_{DG1}$	Day	$\dot{W}_{STG}$	$\dot{W}_{DG1}$
	From port A to port B										
1	1495	0	1	1508	0	1	1482	0	1	1625	0
2	1599	0	2	1573	0	2	1586	0	2	1599	0
3	1560	0	3	1547	0	3	1482	0	3	1547	0
4	1514	0	4	1560	0	4	1508	0	4	1495	0
5	1508	0	5	1495	0	5	1586	0	5	1534	0
6	1495	0	6	1495	0	6	1495	0	6	1521	0
7	1490	0	7	1495	0	7	1485	0	7	1525	0
8	1495	0	8	1495	0	8	1490	0	8	1520	0
	From port B to port A										
1	1625	0	1	1547	0	1	0	1534	1	1521	0
2	1560	0	2	1625	0	2	0	1521	2	1625	0
3	1534	0	3	1664	0	3	0	1625	3	1573	0
4	1521	0	4	1508	0	4	0	1651	4	1625	0
5	1560	0	5	1501	0	5	0	1495	5	1599	0

6	1521	0	6	1547	0	6	0	1521	6	1586	0
7	1520	0	7	1539	0	7	0	1520	7	1580	0
8	1525	0	8	1550	0	8	0	1521	8	1580	0
	Ports										
A	0	1500	A	0	1500	A	0	1500	A	0	1500
B	0	1500	B	0	1500	B	0	1500	B	0	1500

The optimal NPV after 20 years of operation is 115,725,498 €. The optimal number of total round trips per year is 16. The optimization was concluded in 10650 seconds, performing 53 Major NLP iterations at an Intel® Core™2 Quad Processor Q9650 cpu at 3GHz with 8Gb of RAM.

For the nominal values of fuel price and freight rate, one type #3 gas turbine, with a single HRSG, a single ST and one diesel generator set are installed. All trip durations go to the upper limit and in fact this solution coincides with the solution of the nominal case of Case Study 3, where the minimization of PWC was the objective. This shows that in this system and for these mission parameters, the system has no room to increase the revenues by increasing the speeds in every trip and thus the total trips per season (and per year), so the optimizer chooses a cost effective system. Consequently, the same comments that were stated in Section 5.4.5 apply.

5.5.6 Parametric study

For the sensitivity analysis, variation of the fuel price and freight rate is considered. For the fuel price, in consistency with the PWC study, apart from the nominal value of 450 €/ton, four more values were considered: 300, 600, and 750 €/ton. For the freight rate, apart from the nominal, the double price is also considered. Sensitivity analysis results regarding the optimal synthesis and design characteristics of the system are presented in Tables 5.63a,b and 5.64a,b. The variation of the optimal NPV is given in Tables 5.65a,b. Tables 5.66a,b and 5.67ab summarize the optimal trip durations and number of round trips per season for the whole year respectively.

Table 5.63a. Effect of fuel price on the optimal synthesis of the system for nominal freight rate.

	Fuel Price (€/ton)	300	450	600	750
Synthesis	Type	3	3	3	3
	DE	1	1	1	1
	HRSG	1	1	1	1
	ST	1	1	1	1
	DG	1	1	1	1
	AB	1	1	1	1

Table 5.63b. Effect of fuel price on the optimal synthesis of the system for double freight rate.

	Fuel Price (€/ton)	300	450	600	750
Synthesis	Type	3	3	2	2
	DE	1	1	1	1
	HRSG	1	1	1	1
	ST	1	1	1	1
	DG	1	1	1	1
	AB	1	1	1	1

Table 5.64a. Effect of fuel price on the optimal design specifications of the system for nominal freight rate price.

	Fuel Price (€/ton)	300	450	600	750
Nominal power (kW)	Type	3	3	3	3
	GT	20455	19558	19812	20203
	HRSG	12371	9090	9180	9273
	ST	3242	2527	2544	2561
	DG 1	1500	1652	1652	1652
	AB	950	950	950	950

Table 5.64b. Effect of fuel price on the optimal design specifications of the system for double freight rate.

	Fuel Price (€/ton)	300	450	600	750
Nominal power (kW)	Type	3	3	2	2
	GT	39574	28420	20439	17684
	HRSG	24913	17597	19747	16886
	ST	6521	4610	5229	4488
	DG 1	1500	1500	1500	1652
	AB	950	950	950	950

Table 5.65a. Effect of fuel price on the optimal NPV for nominal freight rate.

Costs\Revenue (€)	Fuel Price (€/ton)			
	300	450	600	750
Capital Cost	16,160,569	15,428,136	15,444,136	15,459,704
Fuel PWC (total)	59,550,135	77,095,837	102,503,460	128,277,117
O&M PWC (total)	8,626,161	7,114,045	7,114,156	7,114,045
Total PWC	84,336,865	99,638,018	125,061,752	150,850,866
Total PWR	228,823,736	215,363,516	215,363,516	215,363,516
NPV (objective)	144,486,871	115,725,498	90,301,764	64,512,650

Table 5.65b. Effect of fuel price on the optimal NPV for double freight rate.

Costs\Revenue (€)	Fuel Price (€/ton)			
	300	450	600	750
Capital Cost	22,093,996	18,876,508	16,161,690	15,086,063
Fuel PWC (total)	108,008,269	122,932,876	130,782,014	141,425,993
O&M PWC (total)	14,646,478	11,505,197	11,073,655	9,679,542
Total PWC	144,748,744	153,314,581	158,017,360	166,191,599
Total PWR	538,408,790	511,488,350	484,567,911	457,647,471
NPV (objective)	393,660,045	358,173,769	326,550,550	291,455,872

Table 5.66a. Effect of fuel price on the optimal trip durations for nominal freight rate (numbers in days).

Trip	Fuel Price (€/ton)			
	300	450	600	750
Summer 1	7.27	8	8	8
Summer 2	7.57	8	8	8
Fall 1	7.27	8	8	8
Fall 2	7.63	8	8	8
Winter 1	7.33	8	8	8
Winter 2	7.99	8	8	8
Spring 1	7.23	8	8	8
Spring 2	7.55	8	8	8

Table 5.66b. Effect of fuel price on the optimal trip durations for double freight rate (numbers in days).

Season	Fuel Price (€/ton)			
	300	450	600	750
Summer 1	5.91	6.52	7.08	7.48
Summer 2	6.07	6.74	7.36	7.78
Fall 1	5.91	6.52	7.08	7.47
Fall 2	6.1	6.78	7.41	7.83
Winter 1	5.92	6.56	7.13	7.51
Winter 2	6.27	7.04	7.75	8
Spring 1	5.89	6.5	7.05	7.42
Spring 2	6.05	6.72	7.34	7.75

Table 5.67a. Effect of fuel price on the optimal number of round trips for nominal freight rate.

Season	Fuel Price (€/ton)			
	300	450	600	750
Summer	4.6	4.3	4.3	4.3
Fall	4.6	4.3	4.3	4.3
Winter	3.1	3	3	3
Spring	4.7	4.4	4.4	4.4
Total per year	17	16	16	16

Table 5.67b. Effect of fuel price on the optimal number of round trips for double freight rate.

Season	Fuel Price (€/ton)			
	300	450	600	750
Summer	5.4	5.2	4.9	4.6
Fall	5.4	5.1	4.9	4.6
Winter	3.7	3.5	3.3	3.1
Spring	5.5	5.2	4.9	4.7
Total per year	20	19	18	17

For all fuel price and freight rate values a single gas turbine is installed. However, the type of the gas turbine depends on the fuel price and freight rate. For fuel prices 600 and 700 €/ton and for double freight rate, a type #2 gas turbine is selected as the optimal choice, whereas in all other cases a type #3 gas turbine is selected. In all cases, a bottoming cycle is installed with a single HRSG and ST. Also, one diesel generator set is always installed.

Trip durations generally seem to increase as fuel price rises (need for cost effective system). This is observed clearly in the results for double freight rate (Table 5.66b). For nominal freight rate and fuel prices 450 €/ton and above, trip durations are on the upper limit, all solutions are the same as the solutions for minimization of PWC (for variable time) of Case Study 3, since the optimal trip durations coincide at the upper limit (8 days). For these solutions, the same comment, as in PWC case, stands: the design values of the system components slightly increase as the fuel price increases.

For double freight rate, the gas turbine nominal power output decreases as the fuel price increases, since the trip durations increase and the average speed drops. However, in comparison with the nominal freight rate case, the gas turbine nominal power output is generally augmented (17 – 40 MW), thus the bottoming cycle system is also of higher nominal power output.

Considering the total round trips per year, it is noted that the maximum number of round trips per year is observed in the smallest fuel price for both freight rates. For nominal freight rate, the number of round trips per year remains the same (at its lower limit) for fuel price 450 €/ton and above, while for double freight rate, the number of round trips per year decreases as the fuel price increases. It is evident that, as freight rate increases, the need for more trips (and more revenue) becomes more important than reducing travel costs.

5.6 Case Study 5: Containership with 4-X Diesel Engines, 2-X Diesel Engines and Gas Turbines, Trips of fixed Time, Minimization of PWC

5.6.1 Description of the system and the optimization problem

The description of the energy system and the optimization problem for Case Study 5 is similar as in Case Study 2. The main difference lies in the fact that more technology alternatives are now allowed for the synthesis of the propulsion plant: apart from the three possible gas turbine types, two stroke and four stroke diesel engines are also available for installation. This increases significantly the complexity of the problem, since the optimizer searches for the optimal solution by taking also into account every possible combination between all alternatives.

All the remaining details about the problem, the energy system and the mission characteristics can be found in Section 5.3.1 of Case Study 2. However, a new superconfiguration of the energy system, Fig. 5.21, is defined.

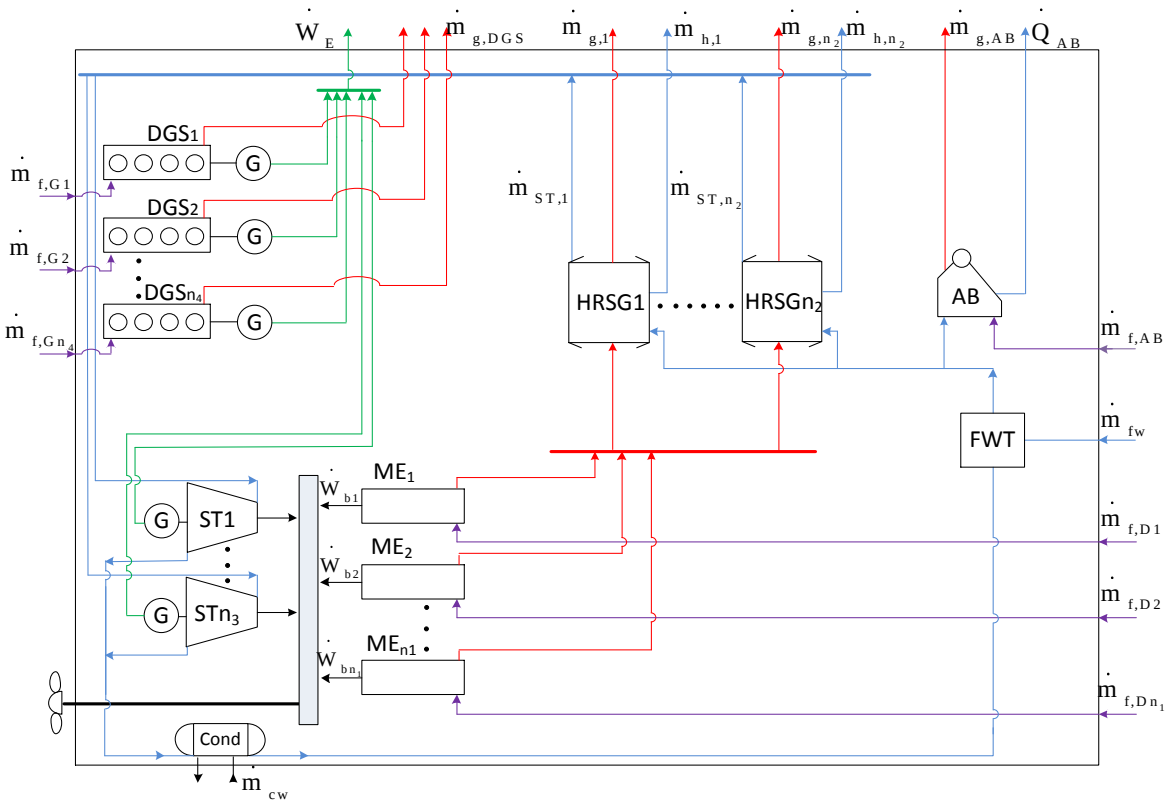

Figure 5.21. Superconfiguration of the energy system for Case Studies 5,6 and 7.

5.6.2 Mathematical statement of the optimization problem

The dynamic optimization problem of this case study is mathematically stated as a minimization problem using a Differential − Algebraic Equation (DAE) formulation. The objective function can be found in Eq. (5.19) with vector $\vec{x}$, representing the vector of control (optimization) variables, consisting of the vectors of synthesis, design and operation, Eq. (5.20). However, since more technology alternatives are added as choices

for the propulsion plant, the vectors of synthesis, design and operation control variables are re-stated:

$$\vec{v} = \left(y_{GT1,J1}, y_{GT2,J2}, y_{GT3,J3}, y_{4X,J4}, y_{2X,J5}, y_{B,K}, y_{ST,L}, y_{DG,M}, y_{AB} \right) \quad (5.41a)$$

$$\vec{w} = \left(\dot{W}_{bn,GT1,J1}, \dot{W}_{bn,GT2,J2}, \dot{W}_{bn,GT3,J3}, \dot{W}_{bn,4X,J4}, \dot{W}_{bn,2X,J5}, \dot{m}_{g_n,K}, T_{g_n,K}, \dot{m}_{s_n,K}, \dot{m}_{ST_n,L}, \dot{W}_{DG_n,M}, \dot{Q}_{AB_n} \right) \quad (5.41b)$$

$$\vec{z} = \left(\dot{W}_{b,GT1,J1}, \dot{W}_{b,GT2,J2}, \dot{W}_{b,GT3,J3}, \dot{W}_{b,4X,J4}, \dot{W}_{b,2X,J5}, \lambda_{h,K}, \lambda_{e,L}, \dot{W}_{DG,M} \right) \quad (5.41c)$$

where:

$y_{GT1,J1}$ set of variables *j1* determining the existence of the *j1* th gas turbine of type 1 (binary): $y_{GT1,J1} = \left\{ y_{GT1,1}, y_{GT1,2}, ..., y_{GT1,j1}, .., y_{GT1,j1\max} \right\}$ (5.42a)

$y_{GT2,J2}$ set of variables *j2* determining the existence of the *j2* th gas turbine of type 2 (binary): $y_{GT2,J2} = \left\{ y_{GT2,1}, y_{GT2,2}, ..., y_{GT2,j2}, .., y_{GT2,j2\max} \right\}$ (5.42b)

$y_{GT3,J3}$ set of variables *j3* determining the existence of the *j3* th gas turbine of type 3 (binary): $y_{GT3,J3} = \left\{ y_{GT3,1}, y_{GT3,2}, ..., y_{GT3,j3}, .., y_{GT3,j3\max} \right\}$ (5.42c)

$y_{4X,J4}$ set of variables *j4* determining the existence of the *j4* th 4X diesel engine (binary): $y_{4X,J4} = \left\{ y_{4X,1}, y_{4X,2}, ..., y_{4X,j4}, .., y_{4X,j4\max} \right\}$ (5.42d)

$y_{2X,J5}$ set of variables *j4* determining the existence of the *j4* th 4X diesel engine (binary): $y_{2X,J5} = \left\{ y_{2X,1}, y_{2X,2}, ..., y_{2X,j5}, .., y_{2X,j5\max} \right\}$ (5.42e)

$y_{B,K}$ set of variables *k* determining the existence of the *k* th HRSG (binary): $y_{B,K} = \left\{ y_{B,1}, y_{B,2}, ..., y_{B,k}, .., y_{B,k\max} \right\}$ (5.42f)

$y_{ST,L}$ set of variables *l* determining the existence of the *l* th ST (binary): $y_{ST,L} = \left\{ y_{ST,1}, y_{ST,2}, ..., y_{ST,l}, .., y_{ST,l\max} \right\}$ (5.42e)

$y_{DG,M}$ set of variables *m* determining the existence of the *m* th generator set (binary): $y_{DG,M} = \left\{ y_{DG,1}, y_{DG,2}, ..., y_{DG,m}, ..., y_{DG,m\max} \right\}$ (5.42g)

y_{AB} variable determining the existence of the auxiliary boiler (binary),

$\dot{W}_{bn,GT1,J1}$ set of variables *j1* determining the nominal brake power output of *j1* th gas turbine of type 1 (invariant): $\dot{W}_{bn,GT1,J1} = \left\{ \dot{W}_{bn,GT1,1}, \dot{W}_{bn,GT1,2}, ..., \dot{W}_{bn,GT1,j1}, ..., \dot{W}_{bn,GT1,j1\max} \right\}$ (5.43a)

$\dot{W}_{bn,GT2,J2}$ set of variables *j2* determining the nominal brake power output of *j2* th gas turbine of type 2 (invariant): $\dot{W}_{bn,GT2,J2} = \left\{ \dot{W}_{bn,GT2,1}, \dot{W}_{bn,GT2,2}, ..., \dot{W}_{bn,GT2,j2}, ..., \dot{W}_{bn,GT2,j1\max} \right\}$ (5.43b)

$\dot{W}_{bn,GT3,J3}$ set of variables *j3* determining the nominal brake power output of *j3* th gas turbine of type 3 (invariant): $\dot{W}_{bn,GT3,J3} = \left\{ \dot{W}_{bn,GT3,1}, \dot{W}_{bn,GT3,2}, ..., \dot{W}_{bn,GT3,j3}, ..., \dot{W}_{bn,GT3,j3\max} \right\}$ (5.43c)

$\dot{W}_{bn,4X,J4}$ set of variables *j4* determining the nominal brake power output of *j4* th 4X diesel engine (invariant):

$$\dot{W}_{bn,4X,J4} = \left\{\dot{W}_{bn,4X,1}, \dot{W}_{bn,4X,2}, ..., \dot{W}_{bn,4X,j4}, ..., \dot{W}_{bn,4X,j4\max}\right\} \quad (5.43d)$$

$\dot{W}_{bn,2X,J5}$ set of variables *j5* determining the nominal brake power output of *j5* th 2X diesel engine (invariant):

$$\dot{W}_{bn,2X,J5} = \left\{\dot{W}_{bn,2X,1}, \dot{W}_{bn,2X,2}, ..., \dot{W}_{bn,2X,j5}, ..., \dot{W}_{bn,2X,j5\max}\right\} \quad (5.43e)$$

$\dot{m}_{g_n,K}$ set of variables *k* determining nominal exhaust gas mass flow rate of *k* th HRSG (invariant): $\dot{m}_{g_n,K} = \left\{\dot{m}_{g_n,1}, \dot{m}_{g_n,2}, ..., \dot{m}_{g_n,k}, ..., \dot{m}_{g_n,k\max}\right\}$ (5.43f)

$T_{g_n,K}$ set of variables *k* determining nominal exhaust gas temperature of *k* th HRSG (invariant): $T_{g_n,K} = \left\{T_{g_n,1}, T_{g_n,2}, ..., T_{g_n,k}, ..., T_{g_n,k\max}\right\}$ (5.43g)

$\dot{m}_{s_n,K}$ set of variables *k* determining nominal steam mass flow rate of *k* th HRSG (invariant): $\dot{m}_{s_n,K} = \left\{\dot{m}_{s_n,1}, \dot{m}_{s_n,2}, ..., \dot{m}_{s_n,k}, ..., \dot{m}_{s_n,k\max}\right\}$ (5.43h)

$\dot{m}_{ST_n,L}$ set of variables *l* determining the nominal steam mass flow rate of *l* th ST (invariant): $\dot{m}_{ST_n,L} = \left\{\dot{m}_{ST_n,1}, \dot{m}_{ST_n,2}, ..., \dot{m}_{ST_n,l}, ..., \dot{m}_{ST_n,l\max}\right\}$ (5.43j)

$\dot{W}_{DG_n,M}$ set of variables *m* determining the nominal power output of *m* th generator set (invariant): $\dot{W}_{DG_n,M} = \left\{\dot{W}_{DG_n,1}, \dot{W}_{DG_n,2}, ..., \dot{W}_{DG_n,m}, .., \dot{W}_{DG_n,m\max}\right\}$ (5.43k)

$\dot{Q}_{AB_n}$ nominal thermal power output of auxiliary boiler (invariant),

$\dot{W}_{b,GT1,J1}$ set of variables *j1* determining the brake power output of *j1* th gas turbine of type 1: $\dot{W}_{b,GT1,J1} = \left\{\dot{W}_{b,4X,1}, \dot{W}_{b,4X,2}, ..., \dot{W}_{b,4X,j1}, ..., \dot{W}_{b,4X,j1\max}\right\}$ (5.44a)

$\dot{W}_{b,GT2,J2}$ set of variables *j2* determining the brake power output of *j2* th gas turbine of type 2: $\dot{W}_{b,GT2,J2} = \left\{\dot{W}_{b,GT2,1}, \dot{W}_{b,GT2,2}, ..., \dot{W}_{b,GT2,j2}, ..., \dot{W}_{b,GT2,j2\max}\right\}$ (5.44b)

$\dot{W}_{b,GT3,J3}$ set of variables *j3* determining the brake power output of *j3* th gas turbine of type 3: $\dot{W}_{b,GT3,J3} = \left\{\dot{W}_{b,GT3,1}, \dot{W}_{b,GT3,2}, ..., \dot{W}_{b,GT3,j3}, ..., \dot{W}_{b,GT3,j3\max}\right\}$ (5.44c)

$\dot{W}_{b,4X,J4}$ set of variables *j4* determining the brake power output of *j4* th 4–X diesel engine: $\dot{W}_{b,4X,J4} = \left\{\dot{W}_{b,4X,1}, \dot{W}_{b,4X,2}, ..., \dot{W}_{b,4X,j4}, ..., \dot{W}_{b,4X,j4\max}\right\}$ (5.44d)

$\dot{W}_{b,2X,J5}$ set of variables *j5* determining the brake power output of *j5* th 2–X diesel engine: $\dot{W}_{b,2X,J5} = \left\{\dot{W}_{b,2X,1}, \dot{W}_{b,2X,2}, ..., \dot{W}_{b,2X,j5}, ..., \dot{W}_{b,2X,j5\max}\right\}$ (5.44e)

$\lambda_{h,K}$ set of variables *k* determining the fraction of *k* th HRSG steam mass flow delivered to thermal loads: $\lambda_{h,K} = \left\{\lambda_{h,1}, \lambda_{h,2}, ..., \lambda_{h,k}, ..., \lambda_{h,k\max}\right\}$ (5.44f)

$$\dot{m}_{s,h,k} = \lambda_{h,k} \cdot \dot{m}_{s,k} \quad (5.44g)$$

$\dot{m}_{s,h,k}$ steam mass flow rate drawn from *k* th HRSG drum for serving thermal loads,

$\dot{m}_{s,k}$ steam mass flow rate of *k* th HRSG unit,

$\lambda_{e,L}$ set of variables l determining the fraction of the l th steam turbine power output delivered to generator: $\lambda_{e,L} = \{\lambda_{e,1}, \lambda_{e,2}, ..., \lambda_{e,l}, ..., \lambda_{e,l\max}\}$ (5.44h)

$$\dot{W}_{STG,l} = \lambda_{e,l} \cdot \dot{W}_{ST,l} \quad (5.44i)$$

$\dot{W}_{STG,l}$ l th steam turbine generator power for serving electric loads,

$\dot{W}_{ST,l}$ l th steam turbine power output,

$\dot{W}_{DG,M}$ set of variables m determining the m th diesel generator set power output:

$$\dot{W}_{DG,M} = \{\dot{W}_{DG,1}, \dot{W}_{DG,2}, ..., \dot{W}_{DG,m}, ..., \dot{W}_{DG,m\max}\} \quad (5.44j)$$

Indices *j1*, *j2*, *j3*, *j4* and *j5* run through all the values from 1 up to an upper bound. It is noted that these upper bounds quantify the upper value of gas turbines of type 1, 2, 3, four stroke diesel engines and two stroke diesel engines, respectively, that are allowed to be installed in the system and are pre-determined parameters, given at the beginning of the optimization. Once these upper values for all *j*'s are defined, the problem is set with as many binary variables for the gas turbines and diesel engines as necessary. The same idea stands also for the HRSGs, STs and diesel generator sets, which are modeled by indices *k*, *l* and *m*, respectively. For all binary variables, value 0 denotes that the unit is not installed.

The optimization problem is stated with Eqs. (5.19) and (5.25)–(5.29) of Section 5.3.2.

The main differential variables for this problem are the distance travelled by the ship, the fuel consumption of the propulsion engines, diesel generator sets and auxiliary boiler. Another family of differential variables is derived from the energy output of each component, which is generally given as the integral of output power of the component over the time horizon. All the respective equations for each component have been presented in detail in Chapter 3, Section 3.3.1, Eqs. (3.6)–(3.9) and in Appendix C.

Two-variable (nominal power and load factor) functions are used to describe the SFOC and exhaust gas characteristics for all propulsion engine alternatives. The total exhaust gas mass flow rate and temperature from all engines is then calculated and supplied to the HRSGs, if HRSGs are installed. The same modeling procedure (two variable functions) is also applied in the case of diesel generator sets' SFOC and exhaust gas properties. The models used for the gas turbines, diesel engines and the diesel generator sets are presented in extent in Chapter 4.

The brake power of the propulsion engines, must be equal to the required brake power at any instant of time:

$$\sum_{j1} y_{GT1,j1}\dot{W}_{b,GT1,j1} + \sum_{j2} y_{GT2,j2}\dot{W}_{b,GT2,j2} + \sum_{j3} y_{GT3,j3}\dot{W}_{b,GT3,j3} + \sum_{j4} y_{4X,j4}\dot{W}_{b,4X,j4} + \sum_{j5} y_{2X,j5}\dot{W}_{b,2X,j5} + \sum_{l} \dot{W}_{ST,p,l} = \dot{W}_b \quad (5.45)$$

Also the electric and thermal power produced by the integrated system must be equal to the electric and thermal demands at any instant of time, as stated in Eqs. (5.31), (5.32). The total required brake power of the all engines is calculated as a function of the ship speed, weather state, ship resistance and propulsive efficiency. The respective equation is given in Chapter 3 (Eq. 3.13). All details considering the underlying mathematical calculations are presented in Chapter 4 and in Appendixes D and E.

Multiple equalities correlated with the simulation of the components as well as inequality constraints imposed on certain variables, exist but their complete presentation is

beyond the limits of the present text. Noteworthy inequality constraints for the upper and lower bounds imposed on important variables can be found in Eqs. (5.33a,b).

Equations (5.34a)–(5.34d) summarize other important technical constraints related with the nominal (design) characteristics of the components. For reasons of completeness the respective expression for the two stroke and four stroke diesel engines are given:

$$\dot{W}_{bn,4X,\min} \le \dot{W}_{bn,4X,j4} \le \dot{W}_{bn,4X,\max} \tag{5.46a}$$

$$\dot{W}_{bn,2X,\min} \le \dot{W}_{bn,2X,j5} \le \dot{W}_{bn,2X,\max} \tag{5.46b}$$

Of course all control variables, are accompanied by upper and lower limits. However, upper and lower limits may not be necessary for all state variables.

In the next section all the necessary values of input parameters and data assumptions in order to set up and solve the optimization problem stated in the current section are presented.

5.6.3 Additonal data and assumptions

The same containership with carrying capacity 9572 TEU and DWT of 111529 MT is considered performing for each season the same round trip of 6000 nm between two ports, A and B. Values of certain cost parameters that are used for the PWC calculations are given in Table 5.21. For the gas turbines, MDO is considered as fuel with a Lower Heating Value (LHV) of 42700 kJ/kg, while for the 2-X diesel engines, the 4-X diesel engines, the diesel-generator sets and the auxiliary boiler, HFO is considered as fuel with a Lower Heating Value (LHV) of 39550 kJ/kg. All fuel costs are given in Table 5.21. In Table 5.68 a list of lower and upper bounds of several important synthesis, design and operation variables is presented. Details regarding the time discretization that is used in order to model the operation of the energy system for the total time horizon and other numerical solution parameters are given in Table 5.23.

Table 5.68. Bounds on synthesis, design and operation variables for Case Study 5.

Variable	Lower value	Upper value
Number of gas turbines of type 1	0	2
Number of gas turbines of type 2	0	2
Number of gas turbines of type 3	0	2
Number of 2−X diesel engines	0	3
Number of 4−X diesel engines	0	3
Number of total propulsion engines	1	6
Number of DG sets	0	4
Number of HRSGs	0	2
Number of STs	0	2
Gas turbine nominal power output (kW) (any type)	3000	90000
2−X diesel engines nominal power output (kW)	3500	90000
4−X diesel engines nominal power output (kW)	3500	21000
Generator set nominal power output (kW)	300	5000
Load factors (all equipment)	0.1	1
Ship speed (kn)	14	25.4

5.6.4 Solution procedure

The same comments as in Section 5.4.4 can be repeated here. Due to the augmented number of control variables, both methods (sequential and simultaneous) are applied. The sequential method proved to be as accurate as the simultaneous, but faster.

5.6.5 Numerical results for nominal case

The results of optimization, in terms of optimal synthesis and design are presented in Tables 5.69 and 5.70. Hours of operation and round trips per season and for the whole year are given in Table 5.71. Optimal cost values for the system are given in Table 5.72. Optimal values of certain control variables per time interval and for all seasons are presented in Tables 5.73 – 5.76.

Table 5.69. Optimal synthesis of the system.

Type of propulsion engines	2 – X Diesel
Number of diesel engines (prime movers)	1
Number of HRSGs	1
Number of steam turbines	1
Number of DG sets	2
Number of auxiliary boilers	1

Table 5.70. Optimal design specifications of the system components.

Variable	Optimal Value
Main engine nominal brake power (kW)	52320
DG set 1 nominal electric power (kW)	485
DG set 2 nominal electric power (kW)	1041
Heat recovery steam generator	
Thermal power (kW)	8874
Exhaust gas mass flow rate (kg/s)	95.6
Nominal inlet exhaust gas temperature (^{o}C)	249
Auxiliary boiler nominal thermal power (kW)	950
Steam-turbine	
Nominal power (kW)	2060
Nominal steam mass flow rate (kg/s)	2.98

Table 5.71. Hours of operation and round trips per season.

Season	Summer	Fall	Winter	Spring
Hours of operation	2074	2074	1421	2112
Number of round trips	5.4	5.4	3.7	5.5
Total round trips per year	20			

Table 5.72. Cost items (in €).

Season	Summer	Fall	Winter	Spring
Present worth cost of fuel	31,228,418	31,585,101	22,909,230	31,539,831
Present worth cost of O&M	3,640,600	3,677,583	2,641,898	3,687,850
Capital cost	17,984,660			
Total PWC (objective function)	148,895,171			

Table 5.73. Optimal ship speed versus time (in kn).

Day	Summer	Fall	Winter	Spring
	From port A to B			
1	20.92	20.91	20.94	20.88
2	20.85	20.85	20.88	20.85
3	20.89	20.89	20.90	20.87
4	20.91	20.91	20.94	20.87
5	20.68	20.68	20.65	20.74
6	20.78	20.78	20.69	20.80
	From port B to A			
1	20.75	20.75	20.82	20.81
2	20.16	20.00	19.43	20.30
3	21.19	21.26	21.51	21.07
4	21.08	21.11	21.31	21.00
5	20.90	20.92	20.99	20.93
6	20.93	20.97	20.95	20.90

Table 5.74. Propulsion power from diesel engine(s) and ST versus time (in kW).

Day	Summer		Fall		Winter		Spring	
	$\dot{W}_b$	$\dot{W}_{STP}$	$\dot{W}_b$	$\dot{W}_{STP}$	$\dot{W}_b$	$\dot{W}_{STP}$	$\dot{W}_b$	$\dot{W}_{STP}$
	From port A to port B							
1	41078	479	41333	343	41650	425	41105	185
2	41575	252	41559	337	42092	232	41226	217
3	41298	369	41393	356	41802	433	41085	258
4	41091	506	41364	311	41712	363	41051	307
5	42444	92	41766	824	43041	251	41481	396
6	41768	360	42138	65	41650	425	41233	395
	From port B to port A							
1	45922	447	46717	486	50414	1298	45366	372
2	47767	805	48807	1060	51202	2004	46985	718
3	44248	381	44916	279	48161	935	44369	320
4	44658	397	45387	405	48804	1049	44684	282
5	45387	387	46109	448	49908	1186	44962	311
6	45240	411	45936	399	50012	1228	45059	332

Table 5.75. Contribution of the HRSG and auxiliary boiler to thermal loads versus time for all seasons (in kW).

	Summer		Fall		Winter		Spring	
Day	$\dot{Q}_h$	$\dot{Q}_{AB}$	$\dot{Q}_h$	$\dot{Q}_{AB}$	$\dot{Q}_h$	$\dot{Q}_{AB}$	$\dot{Q}_h$	$\dot{Q}_{AB}$
	From port A to port B							
1	850	0	860	0	1000	0	990	0
2	880	0	900	0	1050	0	980	0
3	860	0	950	0	1080	0	1010	0
4	900	0	970	0	1100	0	1020	0
5	840	0	930	0	1060	0	950	0
6	850	0	960	0	1100	0	970	0
	From port B to port A							
1	860	0	930	0	1100	0	1040	0
2	870	0	950	0	1080	0	970	0
3	870	0	980	0	1060	0	960	0
4	890	0	970	0	990	0	950	0
5	860	0	890	0	1040	0	980	0
6	870	0	910	0	1070	0	960	0
	Ports							
A	0	950	0	950	0	950	0	950
B	0	950	0	950	0	950	0	950

Table 5.76. Electric power of STG and DG sets versus time for all seasons (in kW).

Day	Summer			Fall			Winter			Spring		
	$\dot{W}_{STG}$	$\dot{W}_{G1}$	$\dot{W}_{G2}$	$\dot{W}_{STG}$	$\dot{W}_{G1}$	$\dot{W}_{G2}$	$\dot{W}_{STG}$	$\dot{W}_{G1}$	$\dot{W}_{G2}$	$\dot{W}_{STG}$	$\dot{W}_{G1}$	$\dot{W}_{G2}$
	From port A to Port B											
1	1368	127	0	1508	0	0	1396	86	0	1625	0	0
2	1599	0	0	1508	65	0	1586	0	0	1599	0	0
3	1481	79	0	1472	75	0	1371	111	0	1547	0	0
4	1328	186	0	1511	49	0	1433	75	0	1495	0	0
5	1510	0	0	1020	475	0	1586	0	0	1434	100	0
6	1503	0	0	1498	0	0	1326	169	0	1424	97	0
	From port B to port A											
1	1507	118	0	1465	82	0	684	0	850	1521	0	0
2	1184	376	0	930	0	695	0	480	1036	1229	396	0
3	1534	0	0	1620	44	0	1012	0	613	1573	0	0
4	1521	0	0	1508	0	0	930	0	721	1620	5	0
5	1555	5	0	1501	0	0	802	0	693	1589	10	0
6	1525	0	0	1542	5	0	754	0	767	1576	10	0
	Ports											
A	0	480	1020	0	480	1020	0	480	1020	0	480	1020
B	0	480	1020	0	480	1020	0	480	1020	0	480	1020

The optimal present worth cost after 20 years of operation is 148,895,171 €. The optimization was concluded in 6900 seconds, performing 29 Major NLP iterations at an Intel® Core™2 Quad Processor Q9650 cpu at 3GHz with 8Gb of RAM.

One, two stroke, diesel engine is determined as the optimal choice for the propulsion plant. A bottoming cycle with a single HRSG and a single ST and two diesel generator sets are installed. The excess of ST power is given to electric loads with the remaining power directed to the propeller, with the exception of certain intervals where the brake power requirements are augmented. Two diesel generator sets are installed: one of low nominal power output (485 kW) in order to cover the remaining electric loads that are not fully served by the STG during trips, and a second one (1041 kW) that operates at ports, in parallel with the first, and in the winter return trip where the ST power is mostly given in the propeller. Thermal loads during the trips are always covered by the HRSG, while at ports they are covered by the auxiliary boiler.

Since, essentially, this case study is based on Case Study 2 with the significant alteration that more technology alternatives are allowed for the propulsion plant, it is worth mentioning that the optimal PWC achieved with the selection of a two stroke diesel engine is 25% lower than the respective optimal PWC for the gas turbine case.

5.6.6 Parametric study

For the sensitivity analysis the fuel price is considered to vary. Apart from the nominal value of 300 €/ton, four more values were considered: 200, 400, 500 and 600 €/ton. Selected sensitivity analysis results regarding the optimal synthesis and design characteristics of the system are presented in Tables 5.77 and 5.78. The variation of the optimal PWC is given in Table 5.79.

Table 5.77. Effect of fuel price on the optimal synthesis of the system.

	Fuel Price (€/ton)	200	300	400	500	600
Synthesis	DEs	1	1	1	1	1
	HRSGs	–	1	1	1	1
	STs	–	1	1	1	1
	DG sets	1	2	2	2	2
	AB	1	1	1	1	1

Table 5.78. Effect of fuel price on the optimal design specifications of the system.

	Fuel Price (€/ton)	200	300	400	500	600
Nominal power (kW)	DE	51094	52320	54068	56857	57214
	HRSG	–	8874	8898	8933	8984
	ST	–	2060	2080	2139	2171
	DG set 1	1664	485	360	343	340
	DG set 2	–	1041	1161	1170	1175
	AB	1100	950	950	950	950

Table 5.79. Effect of fuel price on the optimal PWC.

Costs (€)	Fuel Price (€/ton)				
	200	300	400	500	600
Capital Cost	14,505,140	17,984,660	18,243,420	18,646,960	18,709,660
Fuel PWC (total)	82,938,516	117,262,580	156,057,884	194,372,376	233,181,997
O&M PWC (total)	11,833,736	13,647,931	13,644,719	13,660,131	13,664,666
Total PWC (objective)	109,277,392	148,895,171	187,946,022	226,679,468	265,556,323

For all fuel price values, one two–stroke diesel engine is selected. A bottoming cycle, with a single HRSG and a single ST, is always installed, except for the fuel price of 200 €/ton. When a bottoming cycle is installed, the HRSG serves all thermal demands during trips and two diesel generator sets are installed: one of relatively low power output (<500 kW), that covers the remainder electric loads that the STG cannot cover during trips and one of higher power output (1000–1200 kW) that operates at ports, in parallel with the first one. Also, the second DG set operates during winter (trip from port A to port B) since then the ST power is mainly diverted to the propeller in order to accommodate the high brake power demands. The installation of two DG sets with this specific operational strategy can be attributed to the fact that in all those cases the required ship speeds are high and the propulsion system is designed with a high nominal power output. This leads to the installation of a bottoming cycle with high nominal output characteristics that can serve a large percentage of the electric demands during the trips, leaving only a small part (of electric demands) that can be accommodated by a DG set of low power output. If a single DG set was to be installed, it would have to be of adequate power output in order to serve the electric demand at ports (1500 kW) and thus it would operate in very low load factors in order to cover the low remaining electric demands during trips. This would be very inefficient in terms of SFOC and thus not optimal.

For the fuel price of 200 €/ton, where no BC is present, the auxiliary boiler is of higher nominal power output than for all other fuel prices, since now it has to cover the thermal demands during trips. Also, in that case a single DG set is installed that covers all electric load during trips and at port. Since the electric demands generally range from 1450–1670 kW (at trips and ports) the selection of a single DG set is explained.

Considering Table 5.78, the same observation that was made in Case Study 2 nominal case, stands: the nominal power output design values of the propulsion engine, HRSG and ST seem to increase as fuel price rises but, unlike in Case Study 2, this increase seems to be higher (2.5-3.5%) in this case.

5.7 Case Study 6: Containership with 4-X Diesel Engines, 2-X Diesel Engines and Gas Turbines, Trips of Variable Time, Minimization of PWC

5.7.1 Description of the system and the optimization problem

The description of the energy system and the optimization problem for Case Study 6 is similar as in Case Study 3. The main difference lies in the fact that more technology alternatives are now allowed for the synthesis of the propulsion plant. Specifically, apart from the three possible gas turbine types, two-stroke and four-stroke diesel engines are also available for installation.

All the details about the problem and the energy system can be found in Section 5.4.1 of Case Study 3. The superconfiguration of the energy system is depicted in Figure 5.21.

5.7.2 Mathematical statement of the optimization problem

The dynamic optimization problem of this case study is mathematically stated as a minimization problem using the same Differential − Algebraic Equation (DAE) formulation that was presented in Section 5.4.2 of Case Study 3. Minimization of the PWC, Eq. (5.35), is used as the objective function with vector $\vec{x}$, representing the vector of control (optimization) variables, consisting of the vectors of synthesis, design and operation optimization variables as stated in Eqs. (5.41a)-(5.44j) and vector $\vec{t}_f$ representing the vector of control (optimization) variables consisting of the the single trip durations as stated in Eqs. (5.36).

5.7.3 Additional data and assumptions

The same containership with carrying capacity 9572 TEU and DWT of 111529 MT is considered performing for each season the same round trip of 6000 nm between two ports, A and B. Values of certain cost parameters that are used for the PWC calculations are given in Table 5.21. For the gas turbines, MDO is considered as fuel with a Lower Heating Value (LHV) of 42700 kJ/kg, while for the 2-X diesel engines, the 4-X diesel engines, the diesel-generator sets and the auxiliary boiler, HFO is considered as fuel with a Lower Heating Value (LHV) of 39550 kJ/kg. In Table 5.80 a list of lower and upper bounds of certain synthesis, design and operation variables is presented. Details regarding the time discretization that is used in order to model the operation of the energy system for the total time horizon and other numerical solution parameters are given in Table 5.38.

Table 5.80. Bounds on synthesis, design and operation variables for case Study 6.

Variable	Lower value	Upper value
Number of gas turbines of type 1	0	2
Number of gas turbines of type 2	0	2
Number of gas turbines of type 3	0	2
Number of 2−X diesel engines	0	3
Number of 4−X diesel engines	0	3
Number of total propulsion engines	1	6
Number of DG sets	0	4
Number of HRSGs	0	2
Number of STs	0	2
Gas turbine nominal power output (kW) (any type)	3000	90000
2−X diesel engines nominal power output (kW)	3500	90000
4−X diesel engines nominal power output (kW)	3500	21000
Generator set nominal power output (kW)	300	5000
Load factors (all equipment)	0.1	1
Ship speed (kn)	14	25.4
Single trip duration (days)	5	8

5.7.4 Solution procedure

In this case study, also, both available methods (sequential and simultaneous) were applied. For all previous case studies up until now the sequential method had proved to be superior in terms of computational times, since it converged in fewer iterations. However, in the problems solved in this case study, probably due to the increased number of control variables (several propulsion alternatives combined with variable trip durations), it is observed that the simultaneous method manages to solve the optimization problems in fewer Major Iterations of the optimization algorithm than the sequential one. Of course, it has to be noted that, in general, each simultaneous method iteration is not equal to each sequential method iteration in terms of computational time. Nevertheless, it was observed that the simultaneous method achieved equal or slightly better computational times (<3%) when compared with those of the sequential.

5.7.5 Numerical results for nominal case

For the nominal fuel price, the results of optimization, in terms of optimal synthesis and design are presented in Tables 5.81 and 5.82. Optimal values for hours of operation, round trips per season and total trips per year are given in Table 5.83. Optimal cost values for the system are given in Table 5.84. Optimal values of certain control variables per time interval and for all seasons are presented in Tables 5.85 – 5.88.

Table 5.81. Optimal synthesis of the system.

Type of Propulsion engines	2 – X Diesel
Number of diesel engines (prime movers)	1
Number of HRSGs	1
Number of steam turbines	1
Number of DG sets	1
Number of auxiliary boilers	1

Table 5.82. Optimal design specifications of the system components.

Variable	Optimal Value
Main engine nominal brake power (kW)	21459
DG set 1 nominal electric power (kW)	1500
DG set 2 nominal electric power (kW)	–
Heat recovery steam generator	
Thermal power (kW)	3566
Exhaust gas mass flow rate (kg/s)	39.2
Nominal inlet exhaust gas temperature (°C)	250
Auxiliary boiler nominal thermal power (kW)	950
Steam-turbine	
Nominal power (kW)	724
Nominal steam mass flow rate (kg/s)	1.11

Table 5.83. Hours of operation and round trips per season.

Season	Summer	Fall	Winter	Spring
Hours of operation				
Trip from port A to B (days)	8	8	8	8
Trip from port B to A (days)	8	8	8	8
Round trip duration (days)	20	20	20	20
Number of round trips	4.3	4.3	3	4.4
Total round trips per year	16			

Table 5.84. Cost items (in €).

Season	Summer	Fall	Winter	Spring
Present worth cost of fuel	14,540,709	14,755,292	11,268,793	14,749,692
Present worth cost of O&M	1,694,455	1,718,192	1,292,969	1,727,540
Capital cost	10,310,417			
Total PWC (objective function)	72,058,059			

Table 5.85. Optimal ship speed versus time (in kn).

Day	Summer	Fall	Winter	Spring
	From port A to B			
1	15.79	15.77	15.88	15.73
2	15.68	15.68	15.77	15.66
3	15.74	15.74	15.81	15.70
4	15.77	15.77	15.88	15.70
5	15.37	15.39	15.36	15.47
6	15.55	15.55	15.44	15.58
7	15.49	15.48	15.40	15.50
8	15.59	15.56	15.44	15.55
	From port B to A			
1	15.43	15.42	15.42	15.55
2	14.41	14.10	13.43	14.69
3	16.19	16.30	16.87	16.01
4	16.01	16.04	16.45	15.89
5	15.70	15.71	15.77	15.75
6	15.75	15.81	15.69	15.70
7	15.70	15.75	15.73	15.75
8	15.63	15.80	15.71	15.70

Table 5.86. Propulsion power from diesel engine(s) and ST versus time (in kW).

Day	Summer		Fall		Winter		Spring	
	$\dot{W}_b$	$\dot{W}_{STP}$	$\dot{W}_b$	$\dot{W}_{STP}$	$\dot{W}_b$	$\dot{W}_{STP}$	$\dot{W}_b$	$\dot{W}_{STP}$
	From port A to port B							
1	16331	0	16391	0	16796	0	16102	0
2	16431	0	16474	0	16892	0	16157	0
3	16371	0	16418	0	16856	0	16120	0
4	16345	0	16391	0	16796	0	16125	0
5	16703	0	16740	0	17262	0	16322	0
6	16548	0	16593	0	17193	0	16226	0
7	16555	0	16599	0	17250	0	16220	0
8	16561	0	16611	0	17234	0	16231	0
	From port B to port A							
1	18965	0	19441	0	21459	551	18671	0
2	19730	0	20171	0	21459	551	19468	0
3	18297	0	18674	0	21459	551	18267	0
4	18470	0	18916	0	21459	551	18377	0
5	18749	0	19211	0	21459	551	18496	0
6	18702	0	19127	0	21459	551	18541	0
7	18798	0	19220	0	21459	551	18550	0
8	18755	0	19221	0	21459	551	18545	0

Table 5.87 Contribution of the HRSG and auxiliary boiler to thermal loads versus time for all seasons (in kW).

Day	Summer		Fall		Winter		Spring	
	$\dot{Q}_h$	$\dot{Q}_{AB}$	$\dot{Q}_h$	$\dot{Q}_{AB}$	$\dot{Q}_h$	$\dot{Q}_{AB}$	$\dot{Q}_h$	$\dot{Q}_{AB}$
	From port A to port B							
1	850	0	860	0	1000	0	990	0
2	880	0	900	0	1050	0	980	0
3	860	0	950	0	1080	0	1010	0
4	900	0	970	0	1100	0	1020	0
5	840	0	930	0	1060	0	950	0
6	850	0	960	0	1100	0	970	0
7	845	0	959	0	1100	0	980	0
8	851	0	963	0	1090	0	970	0
	From port B to port A							
1	860	0	930	0	1100	0	1040	0
2	870	0	950	0	1080	0	970	0
3	870	0	980	0	1060	0	960	0
4	890	0	970	0	990	0	950	0
5	860	0	890	0	1040	0	980	0
6	870	0	910	0	1070	0	960	0
7	880	0	920	0	1080	0	970	0
8	870	0	910	0	1050	0	960	0

	Ports							
A	0	950	0	950	0	950	0	950
B	0	950	0	950	0	950	0	950

Table 5.88. Electric power of STG and DG set versus time for all seasons (in kW).

Day	Summer		Fall		Winter		Spring	
	$\dot{W}_{STG}$	$\dot{W}_{DG1}$	$\dot{W}_{STG}$	$\dot{W}_{DG1}$	$\dot{W}_{STG}$	$\dot{W}_{DG1}$	$\dot{W}_{STG}$	$\dot{W}_{DG1}$
	From port A to Port B							
1	632	863	631	877	604	878	589	1036
2	626	973	622	951	593	993	593	1006
3	630	930	608	939	584	898	585	962
4	619	895	602	958	577	931	582	913
5	643	865	621	874	599	987	605	929
6	637	858	609	886	587	908	598	923
7	634	856	609	886	597	988	600	926
8	637	858	609	886	634	856	594	926
	From port B to port A							
1	689	936	680	867	122	1412	635	886
2	702	858	682	943	127	1394	670	955
3	672	862	651	1013	132	1493	647	926
4	670	851	659	849	151	1500	652	973
5	684	876	686	815	138	1357	647	952
6	681	840	679	868	130	1391	653	933
7	594	926	675	864	594	926	650	930
8	600	926	679	871	596	925	650	930
	Ports							
A	0	1500	0	1500	0	1500	0	1500
B	0	1500	0	1500	0	1500	0	1500

The optimal present worth cost after 20 years of operation is 72,058,059 €. The optimization was concluded in 7100 seconds, performing 32 Major NLP iterations at an Intel® Core™2 Quad Processor Q9650 cpu at 3GHz with 8Gb of RAM.

A two-stroke diesel engine along with one HRSG, one ST and one diesel generator set are selected for the optimal synthesis of the system. As in Case Study 3, in order to make the system cost effective, the optimizer selects as optimal duration for all trips in all seasons the upper limit of 8 days. This leads to a significant decrease in the nominal power design characteristics of the diesel engine, the HRSG and the ST when compared to those of Case Study 5. This is expected, since the increase of the trip durations leads to lower average speeds (for all trips) which translates to lower propulsion power.

The HRSG serves all thermal demands during trips. Also, it is noteworthy that all ST power is directed to the electric loads except of the case of trip from port B to port A in winter, where the propulsion demands are augmented due to the weather, and approximately 75% of the total ST power output is provided to the propeller.

When comparing with the equivalent Case Study 3, the choice of a two stroke diesel engine instead of a gas turbine leads to a 27% decrease in the value of the optimal PWC

and to a 10% increase in nominal power output of the propulsion plant. This has been discussed in Section 5.6.5 and the same comments apply here.

5.7.6 Parametric study

For the sensitivity analysis the fuel price is considered to vary. Apart from the nominal value of 300 €/ton, four more values were considered: 200, 400, 500 and 600 €/ton. Selected sensitivity analysis results regarding the optimal synthesis and design characteristics of the system are presented in Tables 5.89 and 5.90. The variation of the optimal PWC is given in Table 5.91. The optimal trip durations, round trips per season and total round trips per year are given in Tables 5.92 and 5.93.

Table 5.89. Effect of fuel price on the optimal synthesis of the system.

	Fuel Price (€/ton)	200	300	400	500	600
Synthesis	DEs	1	1	1	1	1
	HRSGs	–	1	1	1	1
	STs	–	1	1	1	1
	DG sets	1	1	1	1	1
	AB	1	1	1	1	1

Table 5.90. Effect of fuel price on the optimal design specifications of the system.

	Fuel Price (€/ton)	200	300	400	500	600
Nominal power (kW)	DE	22010	21459	21797	22665	23414
	HRSG	–	3566	3588	3611	3629
	ST	–	724	744	750	762
	DG set 1	1664	1500	1500	1500	1500
	DG set 2	–	–	–	–	–
	AB	1100	950	950	950	950

Table 5.91. Effect of fuel price on the optimal PWC.

Costs (€)	Fuel Price (€/ton)				
	200	300	400	500	600
Capital Cost	9,076,406	10,310,417	10,404,230	10,603,600	10,769,740
Fuel PWC (total)	39,066,143	55,314,486	73,607,171	91,767,488	109,912,009
OPM PWC (total)	5.628.583	6,433,156	6,432,542	6,440,651	6,450,140
Total PWC (objective)	53,771,132	72,058,059	90,443,943	108,811,739	127,131,889
Total PWR	215,363,516	215,363,516	215,363,516	215,363,516	215,363,516
NPV	161,592,384	143,305,457	124,919,573	106,551,776	88,231,627

Table 5.92. Effect of fuel price on the optimal trip durations (numbers in days).

Trip	Fuel Price (€/ton)				
	200	300	400	500	600
Summer 1	8	8	8	8	8
Summer 2	8	8	8	8	8
Fall 1	8	8	8	8	8
Fall 2	8	8	8	8	8
Winter 1	8	8	8	8	8
Winter 2	8	8	8	8	8
Spring 1	8	8	8	8	8
Spring 2	8	8	8	8	8

Table 5.93. Effect of fuel price on the optimal number of round.

Season	Fuel Price (€/ton)				
	200	300	400	500	600
Summer	4.3	4.3	4.3	4.3	4.3
Fall	4.3	4.3	4.3	4.3	4.3
Winter	3	3	3	3	3
Spring	4.4	4.4	4.4	4.4	4.4
Total per year	16	16	16	16	16

Considering the sensitivity analysis results, it is observed that all optimal trip durations for all seasons go to the upper limit of 8 days. In all fuel prices, a single two-stroke diesel engine is selected for the propulsion plant. A bottoming cycle with a single HRSG and a single ST is always installed, with the exception of fuel price 200 €/ton. Also, one diesel generator set is always installed for all fuel prices. In the case of fuel price 200 €/ton the selection of a single DG set can be explained by the same logic that was presented in the comments of Section 5.6.6. For the rest fuel prices, it is noted that in comparison with the previous case study, the ship speed at all trips is severely diminished and this leads to a significant decrease in the power output of the propulsion plant. Thus, in all cases, a bottoming cycle of lower power output (than in Case Study 5) is installed that serves a smaller percentage of electric loads during trips when compared to Case Study 5. Now, the remaining electric demand (that cannot be covered by the STG) is higher (820–1050 kW) and the installation of a single DG set (instead of two) is cost effective, in terms of capital and fuel consumption costs.

Lastly, for fuel price 300 €/ton and above, it is observed that the nominal (design) values of the diesel engine and the bottoming cycle components seem to increase slightly as the fuel price rises.

5.8 Case Study 7: Containership with 4-X Diesel engines, 2-X Diesel Engines and Gas Turbines, Trips of Variable Time, Maximization of NPV

5.8.1 Description of the system and the optimization problems

The description of the energy system and the optimization problem for Case Study 7 is similar as in Case Study 4 with the main difference that more technology alternatives are now allowed for the synthesis of the propulsion plant. Specifically, apart from the three possible gas turbine types, two-stroke and four-stroke diesel engines are also available for installation.

All the details about the problem and the energy system can be found in Section 5.5.1 of Case Study 4. The superconfiguration of the energy system can is depicted in Figure 5.21.

5.8.2 Mathematical statement of the optimization problem

The dynamic optimization problem can be mathematically stated by using the DAE formulation that was presented in Section 5.4.2 of Case Study 3. Maximization of the NPV, Eqs. (5.38), (5.39), is used as the objective function with vector $\vec{x}$, representing the vector of control (optimization) variables, consisting of the vectors of synthesis, design and operation optimization variables as stated in Eqs. (5.41)-(5.44j) and vector $\vec{t}_f$ representing the vector of control (optimization) variables consisting of the the single trip durations as stated in Eqs. (5.36).

5.8.3 Additional data and assumptions

The same containership, as in Case Studies 2–6, with carrying capacity 9572 TEU and DWT of 111529 MT is considered with the same round trip distance of 6000 nm.

Values of certain cost parameters that are used for the PWC calculations are given in Table 5.53. Considering the type of fuel for each component and the corresponding LHV's, the same considerations as in Cases Studies 5 and 6 are made. In Table 5.80 a list of lower and upper bounds of certain synthesis, design and operation variables is presented. Details regarding the time discretization that is used in order to model the operation of the energy system for the total time horizon and other numerical solution parameters are given in Table 5.38.

5.8.4 Solution procedure

The same comments as in Section 5.7.4 can be repeated here.

5.8.5 Numerical results for nominal case

The results of optimization, in terms of optimal synthesis and design are presented in Tables 5.94 and 5.95. Optimal round trip duration and hours of operation for each season are given in Table 5.96. Optimal cost values for each component of the system and

revenues are given in Table 5.97. Optimal values of certain control variables per time interval and season are presented in Tables 5.98 – 5.101.

Table 5.94. Optimal synthesis of the system.

Type of propulsion engines	2 – X Diesel
Number of diesel engines (prime movers)	1
Number of HRSGs	1
Number of steam turbines	1
Number of DG sets	1
Number of auxiliary boilers	1

Table 5.95. Optimal design specifications of the system components.

Variable	Optimal Value
Main engine nominal brake power (kW)	22411
DG set 1 nominal electric power (kW)	1500
DG set 2 nominal electric power (kW)	–
Heat recovery steam generator	
Thermal power (kW)	4115
Exhaust gas mass flow rate (kg/s)	41.8
Nominal inlet exhaust gas temperature (^oC)	252.5
Auxiliary boiler nominal thermal power (kW)	950
Steam-turbine	
Nominal power (kW)	836
Nominal steam mass flow rate (kg/s)	1.24

Table 5.96. Hours of operation and round trips per season.

Season	Summer	Fall	Winter	Spring
Hours of operation	2143	2151	1464	2186
Trip from port A to B duration (days)	7.61	7.62	7.68	7.59
Trip from port B to A duration (days)	7.81	7.87	8	7.79
Round trip duration (days)	19.42	19.49	19.68	19.38
Number of round trips	4.6	4.6	3.1	4.7
Total round trips per year	17			

Table 5.97. Cost items (in €).

Season	Summer	Fall	Winter	Spring
Present worth of revenue	61,917,011	61,917,011	41,726,681	63,263,033
Present worth cost of fuel	16,481,054	16,587,940	11,901,074	16,789,753
Present worth cost of O&M	1,927,287	1,942,087	1,383,655	1,969,489
Capital cost	10,665,380			
Total PWC	79,647,719			
Total present worth of revenue	228,823,736			
Net Present Value (obj)	149,176,017			

Table 5.98. Optimal ship speed versus time (in kn).

Summer		Fall		Winter		Spring	
Day	V	Day	V	Day	V	Day	V
From port A to port B							
1	16.59	1	16.55	1	16.51	1	16.58
2	16.47	2	16.46	2	16.40	2	16.51
3	16.54	3	16.52	3	16.44	3	16.55
4	16.57	4	16.55	4	16.51	4	16.55
5	16.18	5	16.17	5	16.00	5	16.33
6	16.35	6	16.33	6	16.08	6	16.44
7	16.33	7	16.34	7	16.01	7	16.35
7.61	16.36	7.62	16.32	7.68	16.18	7.59	16.50
	From port B to port A						
1	15.80	1	15.68	1	15.49	1	15.98
2	14.82	2	14.40	2	13.58	2	15.09
3	16.55	3	16.55	3	16.68	3	16.43
4	16.37	4	16.30	4	16.34	4	16.31
5	16.06	5	15.97	5	15.78	5	16.18
6	16.11	6	16.06	6	15.71	6	16.13
7	16.05	7	15.95	7	15.69	7	16.10
7.81	16.17	7.87	16.11	8	15.73	7.79	16.18

Table 5.99. Propulsion power from diesel engine(s) and ST versus time (in kW).

Summer			Fall			Winter			Spring		
Day	$\dot{W}_b$	$\dot{W}_{STP}$	Day	$\dot{W}_b$	$\dot{W}_{STP}$	Day	$\dot{W}_b$	$\dot{W}_{STP}$	Day	$\dot{W}_b$	$\dot{W}_{STP}$
	From port A to port B										
1	19000	0	1	18991	0	1	18924	0	1	18935	0
2	19108	0	2	19080	0	2	19026	0	2	18995	0
3	19043	0	3	19020	0	3	18989	0	3	18955	0
4	19015	0	4	18991	0	4	18924	0	4	18960	0
5	19398	0	5	19362	0	5	19418	0	5	19171	0
6	19232	0	6	19206	0	6	19345	0	6	19069	0
7	19240	0	7	19225	0	7	19314	0	7	19100	0
7.61	19290	0	7.62	19208	0	7.68	19423	0	7.59	19050	0
	From port B to port A										
1	20188	53	1	20356	0	1	21889	358	1	20158	0
2	20310	776	2	21047	128	2	22131	422	2	20762	45
3	19536	0	3	19549	0	3	21145	122	3	19731	0
4	19717	0	4	19802	0	4	21415	174	4	19847	0
5	20011	0	5	20113	0	5	21683	373	5	19973	0
6	19962	0	6	20024	0	6	21752	352	6	20020	0
7	19980	0	7	20100	0	7	21761	345	7	20010	0
7.81	19960	0	7.87	20050	0	8	21751	353	7.79	20030	0

Table 5.100. Contribution of the HRSG and auxiliary boiler to thermal loads versus time for all seasons (in kW).

Summer			Fall			Winter			Spring		
Day	$\dot{Q}_h$	$\dot{Q}_{AB}$	Day	$\dot{Q}_h$	$\dot{Q}_{AB}$	Day	$\dot{Q}_h$	$\dot{Q}_{AB}$	Day	$\dot{Q}_h$	$\dot{Q}_{AB}$
	From port A to port B										
1	850	0	1	860	0	1	1000	0	1	990	0
2	880	0	2	900	0	2	1050	0	2	980	0
3	860	0	3	950	0	3	1080	0	3	1010	0
4	900	0	4	970	0	4	1100	0	4	1020	0
5	840	0	5	930	0	5	1060	0	5	950	0
6	850	0	6	960	0	6	1100	0	6	970	0
7	845	0	7	959	0	7	1100	0	7	980	0
7.61	851	0	7.62	963	0	7.68	1090	0	7.59	970	0
	From port B to port A										
1	860	0	1	930	0	1	1100	0	1	1040	0
2	870	0	2	950	0	2	1080	0	2	970	0
3	870	0	3	980	0	3	1060	0	3	960	0
4	890	0	4	970	0	4	990	0	4	950	0
5	860	0	5	890	0	5	1040	0	5	980	0
6	870	0	6	910	0	6	1070	0	6	960	0
7	880	0	7	920	0	7	1080	0	7	970	0
7.81	870	0	7.87	910	0	8	1050	0	7.79	960	0
	Ports										
A	0	950	A	0	950	A	0	950	A	0	950
B	0	950	B	0	950	B	0	950	B	0	950

Table 5.101. Electric power of STG and DG versus time for all seasons (in kW).

Summer			Fall			Winter			Spring		
Day	$\dot{W}_{STG}$	$\dot{W}_{G1}$	Day	$\dot{W}_{STG}$	$\dot{W}_{G1}$	Day	$\dot{W}_{STG}$	$\dot{W}_{G1}$	Day	$\dot{W}_{STG}$	$\dot{W}_{G1}$
	From port A to port B										
1	786	709	1	784	724	1	745	737	1	748	877
2	781	818	2	775	798	2	734	852	2	752	847
3	785	775	3	760	787	3	725	757	3	743	804
4	774	740	4	755	805	4	719	789	4	741	754
5	798	710	5	774	721	5	741	845	5	764	770
6	792	703	6	762	733	6	728	767	6	756	765
7	789	701	7	762	733	7	721	763	7	757	769
7.61	792	703	7.62	762	733	7.68	725	765	7.59	755	765
	From port B to port A										
1	758	867	1	796	751	1	425	1109	1	763	758
2	35	1525	2	678	947	2	371	1150	2	749	876
3	794	740	3	765	899	3	656	969	3	774	799
4	792	729	4	773	735	4	628	1023	4	779	846
5	807	753	5	801	700	5	422	1073	5	774	825

6	803	718	6	794	753	6	436	1085	6	781	805
7	801	719	7	790	749	7	434	1086	7	780	804
7.81	803	722	7.87	793	757	8	436	1085	7.79	780	802
	Ports										
A	0	1500	A	0	1500	A	0	1500	A	0	1500
B	0	1500	B	0	1500	B	0	1500	B	0	1500

The optimal NPV after 20 years of operation is 149,176,017 €. The optimal number of total round trips per year is 17. The optimization was concluded in 11060 seconds, performing 41 Major NLP iterations at an Intel® Core™2 Quad Processor Q9650 cpu at 3GHz with 8Gb of RAM.

For the nominal values of fuel price and freight rate, one two-stroke diesel engine with a single HRSG, a single ST and one diesel generator set are installed. Unlike the equivalent nominal case in Case Study 4, trip durations in each season do not go to the upper limit, and compared to Case Studies 4 and 6, average speeds per season are slightly augmented as one extra trip is performed per year.

Thermal loads are always fully covered by the bottoming cycle and the ST power output is given to serve the electric loads with the exception of the return trip in winter, when brake power demand is the highest and 35% –on average– of the ST power output is directed to the propeller.

5.8.6 Parametric study

For the sensitivity analysis, variation of the fuel price and the freight rate is considered. For the fuel price, in consistency with the PWC study, apart from the nominal value of 300 €/ton, four more values were considered: 200, 400, 500 and 600 €/ton. For the freight rate, apart from the nominal, the double price is also considered. Sensitivity analysis results regarding the optimal synthesis and design characteristics of the system are presented in Tables 5.102a,b and 5.103a,b. The variation of the optimal NPV is given in Tables 5.104a,b. Tables 5.105a,b and 5.106a,b summarize the effect of fuel price and freight rate on the optimal trip durations and number of round trips per season for the whole year.

Table 5.102a. Effect of fuel price on the optimal synthesis of the system for nominal freight rate.

	Fuel Price (€/ton)	200	300	400	500	600
Synthesis	DEs	1	1	1	1	1
	HRSGs	–	1	1	1	1
	STs	–	1	1	1	1
	DG sets	1	1	1	1	1
	AB	1	1	1	1	1

Table 5.102b. Effect of fuel price on the optimal synthesis of the system for double freight rate.

	Fuel Price (€/ton)	200	300	400	500	600
Synthesis	DE	1	1	1	1	1
	HRSG	–	1	1	1	1
	ST	–	1	1	1	1
	DG	1	2	2	2	2
	AB	1	1	1	1	1

Table 5.103a. Effect of fuel price on the optimal design specifications of the system for nominal freight rate price.

	Fuel Price (€/ton)	200	300	400	500	600
Nominal power (kW)	DE	31051	22411	21797	22665	23414
	HRSG	–	4115	3588	3611	3629
	ST	–	836	744	750	762
	DG 1	1664	1500	1500	1500	1500
	DG 2	–	–	–	–	–
	AB	1100	950	950	950	950

Table 103b. Effect of fuel price on the optimal design specifications of the system for double freight rate.

	Fuel Price (€/ton)	200	300	400	500	600
Nominal power (kW)	DE	64117	48114	38359	32019	27224
	HRSG	–	8456	6713	5364	4562
	ST	–	1882	1477	1150	934
	DG 1	1664	490	326	610	697
	DG 2	–	1020	1180	900	812
	AB	1100	950	950	950	950

Table 5.104a. Effect of fuel price on the optimal NPV for nominal freight rate.

Costs\Revenue (€)	Fuel Price (€/ton)				
	200	300	400	500	600
Capital Cost	10,954,420	10,665,380	10,404,230	10,603,600	10,769,740
Fuel PWC (total)	56,663,379	61,759,821	73,607,171	91,767,488	109,912,009
OPM PWC (total)	8,073,774	7,222,518	6,432,542	6,440,651	6,450,140
Total PWC	75,691,573	79,647,719	90,443,943	108,811,739	127,131,889
Total PWR	242,283,956	228,823,736	215,363,516	215,363,516	215,363,516
NPV (objective)	166,592,383	149,176,017	124,919,573	106,551,776	88,231,627

Table 5.104b. Effect of fuel price on the optimal NPV for double freight rate.

Costs\Revenue (€)	Fuel Price (€/ton)				
	200	300	400	500	600
Capital Cost	16,525,690	17,161,440	14,994,690	13,501,900	12,315,590
Fuel PWC (total)	102,168,004	110,804,019	119,978,572	125,697,852	128,678,938
OPM PWC (total)	14,573,599	12,949,546	10,548,733	8,856,380	7,566,637
Total PWC	133,267,293	140,915,005	145,521,995	148,056,132	148,561,165
Total PWR	565,329,230	538,408,790	511,488,351	484,567,911	457,647,472
NPV (objective)	432,061,936	397,493,785	365,966,355	336,511,779	309,086,306

Table 5.105a. Effect of fuel price on the optimal trip durations for nominal freight rate (numbers in days).

Trip	Fuel Price (€/ton)				
	200	300	400	500	600
Summer 1	6.78	7.61	8	8	8
Summer 2	6.93	7.81	8	8	8
Fall 1	6.79	7.62	8	8	8
Fall 2	6.97	7.87	8	8	8
Winter 1	6.82	7.68	8	8	8
Winter 2	7.14	8	8	8	8
Spring 1	6.77	7.59	8	8	8
Spring 2	6.99	7.79	8	8	8

Table 5.105b. Effect of fuel price on the optimal trip durations for double freight rate (numbers in days).

Trip	Fuel Price (€/ton)				
	200	300	400	500	600
Summer 1	5.57	6.08	6.54	6.97	7.38
Summer 2	5.64	6.18	6.66	7.12	7.56
Fall 1	5.57	6.09	6.56	6.97	7.39
Fall 2	5.65	6.20	6.69	7.15	7.61
Winter 1	5.58	6.11	6.57	7.01	7.44
Winter 2	5.72	6.30	6.83	7.34	7.83
Spring 1	5.56	6.08	6.53	6.95	7.36
Spring 2	5.63	6.16	6.65	7.10	7.54

Table 5.106a. Effect of fuel price on the optimal number of round trips for nominal freight rate.

Season	Fuel Price (€/ton)				
	200	300	400	500	600
Summer	4.9	4.6	4.3	4.3	4.3
Fall	4.8	4.6	4.3	4.3	4.3

Winter	3.4	3.1	3	3	3
Spring	4.9	4.7	4.4	4.4	4.4
Total per year	18	17	16	16	16

Table 5.106b. Effect of fuel price on the optimal number of round trips for double freight rate.

Season	Fuel Price (€/ton)				
	200	300	400	500	600
Summer	5.7	5.3	5.1	4.8	4.7
Fall	5.6	5.5	5.2	4.9	4.5
Winter	4	3.7	3.5	3.3	3.1
Spring	5.7	5.5	5.2	5.0	4.7
Total per year	21	20	19	18	17

For all fuel price and freight rate values a single two-stroke diesel engine is installed. For both freight rates and fuel prices 300 €/ton and above, a bottoming cycle is installed with a single HRSG and ST, while for fuel price 200 €/ton and all freight rates no bottoming cycle is installed. For double freight rate and fuel price 300 €/ton and above two diesel generator sets are installed, while in all other cases a single diesel generator set is selected. Thermal loads are always fully covered by the bottoming cycle, when installed; alternatively an auxiliary boiler of higher nominal power output is installed.

Trip durations generally seem to increase as fuel price rises (need for cost effective system) and for nominal freight rate and fuel price 400 €/ton and above they reach their upper limit. In those cases, all solutions are the same as the solutions for minimization of PWC (for variable time) of Case Study 6, since the optimal trip durations coincide with the upper limit (8 days).

It is interesting the fact that for double freight rate and fuel price at 200 €/ton, all trip durations fall under the 6 day duration, that is considered as the nominal trip duration for all trips and was examined in Case Study 5.

For nominal freight rate and fuel price values 300 €/ton and above, the diesel engine nominal power is low (21 – 24 MW) since speeds are decreased, thus reducing the available thermal energy of the exhaust gas. As a result a ST in the area of 750 – 850 kW is designed in all cases. This was also the case in Case Study 6 and the same argument that was stated in Section 5.7.6 applies here: Due to the small power output of the ST, the installation of two generator sets is no longer optimal since at most 50% of electric loads can be covered during trips by the STG. Thus, the installation of a single diesel generator set is prefered. However, for double freight rate, ship speeds are higher and thus the nominal power output is higher (28 – 64 MW). This, as was also the case in Case Study 5, means that the bottoming cycle system is of higher nominal power output too and can serve a large percentage of electric loads during trips leaving only a small remainder that is covered by a DG set of low power output. Thus, for the same reasons explained in Section 5.6.6, two diesel generator sets are installed.

Considering the total round trips per year, it is noted that the maximum number of round trips per year is observed in the lowest fuel price for both freight rates. For nominal freight rate, the number of round trips per year remains the same (at its lower limit) for fuel price 400 €/ton and above while for double freight rate, the number of round trips per year decreases as the fuel price increases. Once more, as it was observed in Case Study 4, it is

evident that, as freight rates increase, the need for more trips (and more revenue) becomes more important than cost effectiveness.

5.9 Comparison with a Conventional Energy System

The containership considered in Case Studies 2–7 is based on an existing containership whose energy system synthesis as well as the design characteristics of its components are known. This provides us with the opportunity to consider several possible operational profiles (for the remaining operational variables since now synthesis and design variables are defined) and simulate the performance of the original–existing energy system for the characteristic "6000 nm round trip per season" scenario that is used in all problems throughout Case Studies 2–7. The synthesis and design characteristics of the energy system are given in Tables 5.107 and 5.108 respectively. The system consists of one large 2 – X Diesel engine, two DG sets, and two boilers: an exhaust gas and an auxiliary. Also, no bottoming cycle is installed.

Considering the mission profile, the same time schedule as in Case Studies 2 and 5 is assumed. For each season, the trip durations, from port A to B and conversely, are fixed and are given in Table 5.109. For the ship speed, three different cases, A, B and C, are considered (Tables 5.110a,b,c). Case A is constructed based on the idea of slow steaming. Thus, in each trip, the ship is set to travel through the "bad weather" regions, with very low speeds. For the rest of the trip the speeds are set as near as possible to the nominal speed of 24 kns, adapted accordingly so as to ensure that the ship will cover the required distance of 3000 nm over exactly 6 days. The same strategy is followed in Cases B and C, however now all these low speeds throughout the bad weather regions are increased by 2 kns (and the rest adapted accordingly) for Case B and 3 kns for Case C.

Table 5.107. Synthesis of the system.

Type of propulsion engines	2 – X Diesel
Number of diesel engines	1
Number of HRSGs	–
Number of steam turbines	–
Number of DG sets	2
Number of exhaust gas boilers	1
Number of auxiliary boilers	1

Table 5.108. Design specifications of the system components.

Component	Value
Main engine nominal brake power (kW)	69439
DG set 1 nominal electric power (kW)	2880
DG set 2 nominal electric power (kW)	2880
Exhaust gas boiler nominal thermal power (kW)	3400
Auxiliary boiler nominal thermal power (kW)	3800

Table 5.109. Time schedule of the ship.

Season	Summer	Fall	Winter	Spring
Trip from port A to B (days)	6	6	6	6
Trip from port B to A (days)	6	6	6	6
Round trip duration (days)	16	16	16	16
Number of round trips	5.4	5.4	3.7	5.5
Total round trips per year	20			

Table 5.110a. Ship speed versus time for case A (in kn).

Day	Summer	Fall	Winter	Spring
	From port A to B			
1	23	23	23.5	22.5
2	21	21	22	22
3	22	22	22.5	22.5
4	23	23	23.5	22
5	17	17	17	18
6	19	19	16.5	18
	From port B to A			
1	17.5	17	19	21
2	16.5	15.5	14.5	17
3	23.5	23.5	23.5	22.5
4	23	23.5	23	22.5
5	22.5	22.5	22.5	21
6	22	23	22.5	21

Table 5.110b. Ship speed versus time for case B (in kn).

Day	Summer	Fall	Winter	Spring
	From port A to B			
1	22	22	22.5	21.5
2	20	20	21	21
3	21	21	21.5	21.5
4	22	22	22.5	21
5	19	19	19	20
6	21	21	18.5	20
	From port B to A			
1	19.5	19	21	20.5
2	18.5	17.5	16.5	19
3	22.5	22.5	22.5	21.5
4	22	22.5	22	21.5
5	21.5	21.5	21.5	20.5
6	21	22	21.5	20.5

Table 5.110c. Ship speed versus time for case C (in kn).

Day	Summer	Fall	Winter	Spring
	From port A to B			
1	21	21	21.5	21
2	20	20	21	20
3	21	21	21.5	21
4	22	22	21.5	21
5	20	20	20	21
6	21	21	19.5	21
	From port B to A			
1	20.5	20	21	20.5
2	19.5	18.5	17.5	20
3	21.5	21.5	22.5	21.5
4	21	21.5	22	21
5	21.5	21.5	21	21
6	21	22	21	21

In Table 5.111 economic data from the simulation of Cases A, B and C are presented in comparison with the optimal solution of the nominal case of Case Study 5 (minimization of PWC). It is observed that Cases A, B and C all give a higher PWC than the minimum PWC value calculated in Case Study 5. The fact that Case C has the lower PWC among the three simulated cases is not surprising once we observe closely the optimal ship speed profile (Table 5.74) of Case Study 5; in Case C the proposed ship speed profile happens to be closer to the optimal ship speed profile. For the specific time schedule and weather characteristics of the problem the strategy of decreasing too much the ship speed in regions of bad weather leads to severe increase of the speeds in the remaining intervals, thus resulting in augmented and far from optimal fuel consumptions. This is partly alleviated in Cases B and C, where a smaller decrease of speed in bad weather regions is enforced. Of course, this is not a general result that applies in all problems of this kind; in fact it is dependent on the specific weather conditions and mission profile considered.

Next, the calculations of the PWC and NPV for Cases A, B and C and for all fuel prices and freight rates are performed. The results are presented in Tables 5.112a,b,c. It is observed that for each fuel price the optimum (minimum) PWC values from Case Studies 5 and 6 are lower than the respective PWC values from Cases A, B and C. Also, for each fuel price and freight rate, the optimum (maximum) NPV value from Case Study 7 is higher than the calculated NPV values from Cases A, B and C. These results are expected and serve as an indication\validation of the good functionality of the optimization procedure.

Table 5.111. Comparison of economic data between Cases A, B, C and the optimal solution of Case Study 5 at nominal fuel price (300 €/ton).

Costs\Revenue (€)	Case			
	A	B	C	Case Study 5 (Optimal PWC)
Capital Cost	19,333,390	19,333,390	19,333,390	17,984,660
Fuel PWC	131,668,600	124,626,200	123,111,700	117,262,580
OPM PWC	12,622,180	12,033,030	11,901,370	13,647,931
Total PWC	163,624,100	155,992,620	154,346,460	148,895,171
PWR (nominal freight rate)	269,204,395	269,204,395	269,204,395	269,204,395
NPV (nominal freight rate)	105,580,295	113,211,775	114,857,935	120,309,225
PWR (double freight rate)	538,408,790	538,408,790	538,408,790	538,408,790
NPV (double freight rate)	374,784,690	382,416,170	384,062,330	389,513,620

Table 5.112a. PWC for Cases A, B, C and Case Studies 5, 6 for all fuel prices (in €).

Case	Fuel Price (€/ton)				
	200	300	400	500	600
Case A	119,734,637	163,624,100	207,513,703	251,403,237	295,292,770
Case B	114,450,553	155,992,620	197,534,687	239,076,753	280,618,820
Case C	113,309,227	154,346,460	195,383,693	236,420,927	277,458,160
Case Study 5	109,277,392	148,895,171	187,946,022	226,679,468	265,556,323
Case Study 6	53,771,132	72,058,059	90,443,943	108,811,739	127,131,889

Table 5.112b. NPV for Cases A, B, C and Case Study 7 for all fuel prices and nominal freight rate (in €).

Case	Fuel Price (€/ton)				
	200	300	400	500	600
Case A	149,469,658	105,580,195	61,690,592	17,801,058	-26,088,475
Case B	154,753,742	113,211,675	71,669,608	30,127,542	-11,414,525
Case C	155,895,168	114,857,935	73,820,702	32,783,468	-8,253,765
Case Study 7	166,592,383	149,176,017	124,919,573	106,551,776	88,231,627

Table 5.112c. NPV for Cases A, B, C and Case Study 7 for all fuel prices and double freight rate (in €).

Case	Fuel Price (€/ton)				
	200	300	400	500	600
Case A	418,674,153	374,784,620	330,895,087	287,005,553	243,116,020
Case B	423,958,237	382,416,170	340,874,103	299,332,037	257,789,970
Case C	425,099,563	384,062,330	343,025,097	301,987,863	260,950,630
Case Study 7	432,061,936	397,493,785	365,966,355	336,511,779	309,086,306

5.10 General Comments

5.10.1 Comments on convergence, computational times and global optimization

For the solution of all the DO problems in Case Studies 1–7 two main convergence criteria are used to denote a successful optimization The primary convergence criterion consists of four tolerances that must be simultaneously satisfied for a solution to be reached:

1. Feasibility tolerance calculates the magnitude of the sum over all constraint and bound violations.
2. Complementarity tolerance represents the sum over all violation of constraints and bounds weighted by their influence on the gradient of the objective function.
3. Taylor tolerance represents the rate of change in the objective function between two iterations.
4. Optimization tolerance serves as a measure of proximity to a local optimum. Convergence is deemed to occur when a linear combination of the gradients of the Lagrangian function on one hand, and the violation of the constraints on the other, drops below this tolerance.

Otherwise, a secondary criterion is applied that checks if there is no progress in the values of the objective function and the decision variables, as well as no constraint violations and if so, it terminates the optimization. If the two main criteria are not satisfied, then several other fail safe criteria exist that check if the numerical procedure of the solution of the system of the algebraic equations is stuck to a loop and if the maximum number of iterations or function evaluations has been exceeded; if so, they terminate the optimization and the problem fails to converge. For the problems solved in this chapter, all optimizations were concluded successfully by satisfying the primary convergence criterion. The relative tolerances for the first and second convergence criteria were set to 10^{-4} and 10^{-12} respectively.

Computational times for all the optimizations that were performed are presented in Table 5.113. Since, for each case study, many DO problems are solved in order to perform sensitivity analysis on several parameters, a range of values is given rather than a single value.

Table 5.113. Computational times for all Case Studies.

Case Study	Time (hrs)	
	Sequential method	Simultaneous method[4]
1	6.4–6.8	–
2	1.5–1.7	–
3	1.7–2	2–2.3
4	3–3.3	3.2–3.6
5	1.9–2.2	2.2–2.5
6	2–2.3	2.2–2.4
7	3.1–3.3	3.2–3.5

[4] The simultaneous method was only applied to some–randomly selected–cases.

It is noted that, while the problems associated with Case Study 1 are simpler and not extremely (computationally) demanding compared to the respective problems of all other cases, the corresponding computational times were higher. This is attributed to the fact that shortly after the solution of Case Study 1, new versions of gPROMS solvers were released that were considerably faster and more robust than their previous counterparts. The upgrated solvers were used for Case Studies 2–7. The sequential method was used for the solution of all problems, while the simultaneous method was applied in only a few cases. From Table 5.113 it is evident that in all cases, with the exception of Case Study 7, the sequential method always proved faster. Also, it is observed that, as was expected, the required computational time grows along with the complexity of the problem, however it still remains within reasonable limits.

Since both the solution approaches are based on a gradient based method (SQP) for the solution of the MINLP problem, a global optimal solution cannot be guaranteed with certainty. However, several techniques can be applied. One of the most popular and frequently used is the multistart method which addresses the global optimization problem by starting a local optimization routine (such as a gradient based algorithm) from many different starting points. If the best of the resulting solutions is retained, then we might be willing to accept this as a global solution. Of course there is no guarantee that a global minimum has been found, but increased confidence might be gained by running the program again many times with different initial points.

For the problems tackled in the Case Studies 2–7 such a multistart procedure was employed.

Three different scenarios were considered for the operational/continuous variables that involved initialization of each variable in each time interval: close to the middle of its upper and lower bounds, at 10-30% higher than its lower bound and at 10-30% lower than its upper bound. In general, it was observed that, when initialized near the upper bound, or close to the middle of the domain defined by the bounds, the operational variables tended to converge to their best values in reasonable times. When initialized near the lower bound, convergence was slower and in several occasions, depending on the values of the design variables, the optimization failed or led to suboptimal solutions.

Considering the design/invariant variables, again, the three same scenarios as for the operation variables were considered. It was observed that values close to the lower bound should be chosen with care since they may lead to initialization of the optimization with very large values (beyond bounds) for the load factors of equipment and cause quadratic subproblem failures in the SQP method. Also, it was observed that, when initializing many units of the same type of equipment, it is best not to use the same value for the initial point of the nominal power output in all equipment, since it may lead to suboptimal solutions.

It must be noted that since this motif of selection of initial points for the operation and design variables is based on the values of their upper and lower bounds, special care should be taken when defining those bounds. Setting them to be very close to each other means that significant solutions may be omitted; additionaly the motif of selection of initial values described above cannot be applied properly. On the other hand, defining them very far apart augments the search space, thus the application of the motif leaves big regions of initial point values untested.

Another important observation concerning the selection of initial points is the following: it is best to collectively choose points that initialize the system in a feasible or near–feasible state. For example, if the propulsion engines are initialized with small nominal power output while high initial values are used for the speeds, the values for the load factors may blow up causing optimization failures. For the problems solved in this chapter this was achieved by trial and error: After some initial unsuccessful attempts, the

relative data (from these attempts) provided good insight concerning the selections of the appropriate bounds –and thus initial points– for the variables.

For the synthesis/binary variables two scenarios were used: initialization of all variables at value 1 and initialization of 50% of the variables that refered to the same type of component at value 1. For example, if the number of 2–X diesel engines is under optimization and up to 4 engines are allowed, then 4 binary variables are defined, while half of them are initialized at value 1 and the rest to 0. If the number of allowed engines is odd, then the remaining variable is also initialized at 1. Initialization of all variables to the value 0 would be meaningless and was avoided. Thankfully, in any synthesis problem certain initial configurations exist that can be excluded a priori due to the nature of the problem. For example in a problem which involves stay in a port (and perhaps loading and unloading operations) it is meaningless to initialize the problem with zero DG sets and no auxiliary boiler.

For the synthesis variables it was observed that the strategy of initializing all variables in their upper values worked best. The success of the strategy of initializing half of them to 0 and half to 1 was dependent upon the convergence of the design and operation variables.

In Tables 5.114a,b convergence results for several initial point configurations for the solution of the nominal case problem of Case Studies 1 and 4 are given.

Table 5.114a. Initialization schemes for the solution of nominal case problem of Case Study 1.

Variable	Bounds	Initial points			
		1	2	3	4
$y_{D,4X,\{2-4\}}$	0 or 1	all 1	all 1	1,1,0,0	1,0,1,0
y_B	0 or 1	0	1	1	1
y_{STG}	0 or 1	0	1	1	1
$y_{DG,\{2-4\}}$	0 or 1	all 1	all 1	1,0,1	1,0,1
y_{AB}	0 or 1	1	1	1	1
$\dot{W}_{bn,\{1-4\}}$ (MW)	3.5-21	13, 11 5, 6	4, 5 5.5, 7	15, 10 6, 5	9
$\dot{W}_{DGn,\{1-4\}}$ (MW)	0.3-5	4, 4.5 3.5, 3.8	2.5, 2 1.5, 1.8	3.5	4.5
T_{gn} (°C)	220-360	340	280	330	345
$\dot{m}_{gn}$ (kg/s)	20-600	55	25	50	35
$\dot{m}_{sn}$ (kg/s)	0.5-3.5	5.5	1.8	5	2.5
$\dot{m}_{STGn}$ (kg/s)	1.5-3	3	1.2	2.5	1.9
$\dot{Q}_{AB,n}$ (MW)	0.5-8	6.5	5	5	6
$\dot{V}$ (kg/s)	0-22	18	21	14	12
$\dot{W}_{b,\{2-4\}}$ (MW)	0.5-21	10, 8 4, 4	3.5, 4.5 5.5, 6.5	14, 14 8, 11	8
$\dot{W}_{DG,\{2-4\}}$ (MW)	0.5-5	3.5	2	3	4
λ_h (-)	0-0.2	0.12	0.8	0.10	0.05
Solution		Best	Failure	Best	Suboptimal

Table 5.114b. Initialization schemes for the solution of nominal case problem of Case Study 4.

Variable	Bounds	Initial points			
		1	2	3	4
$y_{GT1,\{0-2\}}$	0 or 1	all 1	all 1	1,0	1,0
$y_{GT2,\{0-2\}}$	0 or 1	all 1	all 1	1,0	1,0
$y_{GT3,\{0-2\}}$	0 or 1	all 1	all 1	1,0	1,0
$y_{B,\{0-2\}}$	0 or 1	all 1	all 1	1,0	1,0
$y_{ST,\{0-2\}}$	0 or 1	all 1	all 1	1,0	1,0
$y_{DG,\{2-4\}}$	0 or 1	all 1	all 1	1,0,1	1,0,1
y_{AB}	0 or 1	1	1	1	1
$\dot{W}_{GT1n,\{1-2\}}$ (MW)	2.5-50	30, 35	30, 20	30	10
$\dot{W}_{GT2n,\{1-2\}}$ (MW)	2.5-50	30, 35	30, 20	30	10
$\dot{W}_{GT3n,\{1-2\}}$ (MW)	2.5-50	30, 35	30, 20	30	10
$\dot{W}_{DGn,\{1-4\}}$ (MW)	0.3-4	4, 3 2.5, 3.5	4, 3 3.5, 2.5	2.5	1
$T_{gn,\{1-2\}}$ (°C)	250-750	600, 500	550, 500	600	400
$\dot{m}_{gn,\{1-2\}}$ (kg/s)	25-90	40, 55	50, 40	85	29
$\dot{m}_{sn,\{1-2\}}$ (kg/s)	0.5-16	6, 7	7, 5.5	12	6.5
$\dot{m}_{STGn,\{1-2\}}$ (kg/s)	0.5-12	5, 5.5	6, 4	11	3
$\dot{Q}_{AB,n}$ (MW)	0.5-3	3	3	3	2
V (kg/s)	14-24.5	21	18	15.5	24
$\dot{W}_{GT1n,\{1-2\}}$ (MW)	0.5-40	15, 17	15, 10	20	8
$\dot{W}_{GT2n,\{1-2\}}$ (MW)	0.5-40	15, 17	15, 10	20	8
$\dot{W}_{GT3n,\{1-2\}}$ (MW)	0.5-40	15, 17	15, 10	20	8
$\dot{W}_{DG,\{2-4\}}$ (MW)	0.5-5	3.5, 2.5 2, 3	3.5, 2.8 3, 2	2	0.8
λ_h (-)	0-0.2	0.12	0.1	0.05	0.08
λ_e (-)	0-1	0.5	0.4	0.2	0.3
$t_{trip,AB,\{1-4\}}$ (days)	5-8	6	7	6	5.5
$t_{trip,BA,\{1-4\}}$ (days)	5-8	6	7	6	5.5
Solution		Best	Best	Suboptimal	Failure

In Table 5.114a the solution denoted as best refers to the solution given in Paragraph 5.2.5 with PWC*=55.894.772 €. For the suboptimal solution, the objective function value is PWC*=57.032.402 €. The energy system consists of: two 4-X diesel engines of nominal

power 13.912 kW and 7.771 kW, one DG set of 3.000 kW and a bottoming cycle with a HRSG and a STG of nominal power 4.650 kW and 1.480 kW, respectively.

In Table 5.114b the solution denoted as best refers to the solution given in Section 5.5.5 with NPV*=115,725,498 €. For the suboptimal solution, the objective function value is NPV*=115,415,526 €. The energy system consists of one GT of type 2 of nominal power 18.889 kW, one DG set of 1.652 kW and a bottoming cycle with one HRSG and one ST of nominal power 18.110 kW and 4.813 kW, respectively.

5.10.2 Comparative comments on the results

In general it would be wrong to draw conclusions from the comparison of the solution of Case Study 1 with the solutions of the rest case studies (2–7), since it tackles with a different vessel, a different energy system (ST can provide power only on electric loads and not on the propeller) and a completely different mission profile and time schedule for the ship. Also, a single repeated round trip is used to model a whole year of operation in contrast to all other cases, where four characteristic round trips (each one repeated in every season) are used.

However, a noteworthy general comment that can be made is that in all case studies, with the exception of Case Study 1, a single engine is determined as the optimal solution. A possible explanation of this may lie in the observation that in Case Study 1 only 4–X diesel engines are allowed as propulsion alternatives, which in fact have a low upper limit (20 MW) for the nominal power output. So, increased demands in propulsion power (due to bad weather and high ship speeds) cannot be covered by the power output of a single 4–X diesel engine. In contrast, it can be observed that in Case Studies 2–7, where the optimal choice for the propulsion engine is either a gas turbine or a 2-X diesel engine, which both have a very high upper limit for the nominal power output (90 MW), a single unit is always installed.

Focusing on Case Studies 2–7, that are relatively more comparable, several general observations can be made.

In Case Studies 2, 3 and 4 only gas turbines are allowed as propulsion alternatives. For all three objective functions (min PWC with fixed trip durations, min PWC with variable trip durations, max NPV with variable trip durations) a single GT with a bottoming cycle (with a single HRSG and ST) are always installed for all fuel prices and freight rates. The type #3 gas turbine is always selected, with the exception of Case Study 4 (maximization of NPV), in which for double freight rate and fuel prices 600 and 700 €/ton the type #2 GT unit is selected. In order to gain some insight into why this happens, the problem is solved again for fuel prices 600 and 700 €/ton while only the type #3 GT is allowed for the main engine. Economic data from the solutions are presented in Table 5.115. The results verify that the GT type #2 system is indeed the optimal solution. For 600 €/ton both systems perform 18 round trips per year and for 750 €/ton they perform 17 round trips per year, thus the total PWR is the same between the two systems for each fuel price. However, for both fuel prices the type #2 GT energy system, when compared with the type #3, has lower capital costs (3.4-3.6%), lower fuel costs (1-1.5%) and higher O&M costs (14-16%). The same behavior can be observed in Table 5.54 where the results for all GT types and nominal values of fuel price and freight rate are presented: the type #2 GT system has lower capital and fuel costs and higher O&M costs than the type #3 GT system. It is, thus, expected that as fuel price rises, there will be some point that the difference in fuel costs will overcome the difference in O&M costs and will lead to a total PWC for the type #2 system lower than the total PWC for the type #3 system. Indeed, this is what happens here:

a lower PWC for the type #2 GT system is achieved for both fuel prices and specifically for the fuel price of 750 €/ton where the difference is more than 1.3 million €, mainly due to the difference in fuel consumption. This can be justified, since the type #2 GT has higher exhaust gases energy content (when compared with GT #3), which leads to the design of a bottoming cycle of higher power output. Thus, a larger ST is installed that can serve a higher percentage of the electric and propulsion demands and consequently save fuel from the main engine and DG sets.

Table 5.115. Results of NPV maximization for GT types 2 and 3 with double freight rate and fuel prices 600 and 750 €/ton for Case Study 4.

Fuel price:	600 €/ton		750 €/ton	
GT type:	GT 2 (optimal)	GT 3	GT 2 (optimal)	GT 3
Costs\Revenue (€)				
Capital Cost	16,161,690	16,770,789	15,086,063	15,620,972
Fuel PWC (total)	130,782,014	132,088,765	141,425,993	143,669,718
O&M PWC (total)	11,073,655	9,517,971	9,679,542	8,290,478
Total PWC	158,017,360	158,377,525	166,191,599	167,581,168
Total PWR	484,567,911	484,567,911	457,647,471	457,647,471
NPV (objective)	326,550,550	326,190,386	291,455,872	290,066,303
Total round trips per year	18	18	17	17

Furthermore, in all cases the thermal loads during trips are covered by the HRSG and also a single DG set is installed, which is mainly used at ports. This may be explained by the fact that the exhaust gases from the GTs are of high energy content (compared to any system with diesel engines) and thus the installation of a bottoming cycle of high nominal power output that can cover the thermal and electric demands during trips is possible.

Other interesting observations that verify the functionality of the methods proposed in this study can be made, if the corresponding values of NPV are calculated in the cases of PWC minimization (Case Studies 2 and 3). Next, in Tables 5.116a,b and 5.117a,b, the effect of fuel price on the optimal PWC and the corresponding – calculated value of NPV for nominal and double freight rates for Case Studies 2 and 3, is presented. Also, Tables 5.65a,b, where the effect of fuel price on the optimal NPV for nominal and double freight rates for Case Study 4 is demonstrated, are repeated here for convenience.

Table 5.116a. Effect of fuel price on the optimal PWC and corresponding value of NPV for nominal freight rate for Case Study 2.

Costs (€)	Fuel Price (€/ton)			
	300	450	600	750
Capital Cost	22,925,374	22,949,592	22,965,668	22,981,674
Fuel PWC (total)	110,837,520	166,256,995	221,677,226	277,098,251
O&M PWC (total)	14,207,538	14,207,511	14,207,545	14,207,548
Total PWC (objective)	147,970,432	203,414,098	258,850,439	314,287,473
Total PWR	269,204,395	269,204,395	269,204,395	269,204,395
NPV	121,233,963	65,790,297	10,353,956	-45,083,078

Table 5.116b. Effect of fuel price on the optimal PWC, and corresponding value of NPV for double freight rate for Case Study 2.

Costs (€)	Fuel Price (€/ton)			
	300	450	600	750
Capital Cost	22,925,374	22,949,592	22,965,668	22,981,674
Fuel PWC (total)	110,837,520	166,256,995	221,677,226	277,098,251
O&M PWC (total)	14,207,538	14,207,511	14,207,545	14,207,548
Total PWC (objective)	147,970,432	203,414,098	258,850,439	314,287,473
Total PWR	538,408,790	538,408,790	538,408,790	538,408,790
NPV	390,438,358	334,994,692	279,558,351	224,121,317

Table 5.117a. Effect of fuel price on the optimal PWC and corresponding value of NPV for nominal freight rate in Case Study 3.

Costs (€)	Fuel Price (€/ton)			
	300	450	600	750
Capital Cost	15,406,136	15,428,136	15,444,136	15,459,704
Fuel PWC (total)	51,505,222	77,095,837	102,503,460	128,277,117
O&M PWC (total)	7,114,047	7,114,045	7,114,156	7,114,045
Total PWC (objective)	74,025,405	99,638,018	125,061,752	150,850,866
Total PWR	215,363,516	215,363,516	215,363,516	215,363,516
NPV	141,338,110	115,725,498	90,301,764	64,512,650

Table 5.117b. Effect of fuel price on the optimal PWC and corresponding value of NPV for double freight rate in Case Study 3.

Costs (€)	Fuel Price (€/ton)			
	300	450	600	750
Capital Cost	15,406,136	15,428,136	15,444,136	15,459,704
Fuel PWC (total)	51,505,222	77,095,837	102,503,460	128,277,117
O&M PWC (total)	7,114,047	7,114,045	7,114,156	7,114,045
Total PWC (objective)	74,025,405	99,638,018	125,061,752	150,850,866
Total PWR	430,727,032	430,727,032	430,727,032	430,727,032
NPV	356,701,626	331,089,014	305,665,280	279,876,166

Comparing Tables 5.116a,b and 5.117a,b it can be observed that in Case Study 3, all optimal values of PWC are lower that in Case Study 2. This is a natural result of the fact that in Case Study 3 the duration of trips is variable and under optimization and the maximum duration of 8 days is determined as optimal for every trip. This leads to lower ship speeds and thus a smaller (in terms of power output) energy system with decreased capital, O&M and fuel costs. When calculating the corresponding NPV, it is observed that for nominal freight rate the Case Study 3 NPV values are higher than those of Case Study 2 (need for cost effectiveness). However, for double freight rate something very interesting happens; for fuel prices 300 and 450 €/ton the corresponding NPV values (where more round trips are performed) are higher in Case Study 2 than in Case Study 3. This reveals

that there is a critical point in the fuel price – freight rate space, where the need for more trips (and thus more profit) becomes more important than the cost effectiveness of the system.

Table 5.65a. Effect of fuel price on the optimal NPV and corresponding value of PWC for nominal freight rate for Case Study 4.

Costs\Revenue (€)	Fuel Price (€/ton)			
	300	450	600	750
Capital Cost	16,160,569	15,428,136	15,444,136	15,459,704
Fuel PWC (total)	59,550,135	77,095,837	102,503,460	128,277,117
O&M PWC (total)	8,626,161	7,114,045	7,114,156	7,114,045
Total PWC	84,336,865	99,638,018	125,061,752	150,850,866
Total PWR	228,823,736	215,363,516	215,363,516	215,363,516
NPV (objective)	144,486,871	115,725,498	90,301,764	64,512,650

Table 5.65b. Effect of fuel price on the optimal NPV and corresponding value of PWC for double freight rate for Case Study 4.

Costs\Revenue (€)	Fuel Price (€/ton)			
	300	450	600	750
Capital Cost	22,093,996	18,876,508	16,161,690	15,086,063
Fuel PWC (total)	108,008,269	122,932,876	130,782,014	141,425,993
O&M PWC (total)	14,646,478	11,505,197	11,073,655	9,679,542
Total PWC	144,748,744	153,314,581	158,017,360	166,191,599
Total PWR	538,408,790	511,488,350	484,567,911	457,647,471
NPV (objective)	393,660,045	358,173,769	326,550,550	291,455,872

Comparing Tables 5.116a,b and 5.117a,b with 5.65a,b it can be observed that the results of Case Study 4 (maximization of NPV) always yield NPV equal or higher than the NPV obtaibed with the minimization of PWC in Case Studies 2 and 3 for all fuel prices and freight rates, as expected. It is noteworthy that for nominal freight rate, and fuel prices 450 €/ton and higher, all solutions of Case Study 4 coincide with those of Case Study 3. The low value of freight rate does not allow the system to gain more revenue by increasing the number of round trips, so cost effectiveness is pursued and all trip durations go to the upper limit. However, for double freight rate, more expensive (in terms of PWC) systems are selected that can perform more round trips per year and the NPV is maximized.

In Case Studies 5, 6 and 7, gas turbines and diesel engines (2–X and 4–X) are simultaneously allowed as propulsion alternatives. For all three objective functions (min PWC with fixed trip durations, min PWC with variable trip durations, max NPV with variable trip durations) a single 2–X diesel engine is installed. Also, a bottoming cycle, with a single HRSG and ST, is always installed, except for the fuel price of 200 €/ton. This was also observed in Case Study 1 and reveals that for low fuel prices the capital and O&M costs of installing and operating a bottoming cycle is higher than serving the energy demands with the auxiliary boiler and the DG set(s); especially since in the case of diesel

engines the energy content of the exhaust gases is generally low (compared to gas turbines) and leads to bottoming cycles with low nominal power outputs.

Another interesting general observation regarding Case Studies 5, 6 and 7 is the following: In Case Study 6, for all fuel prices, and Case Study 7, for all fuel prices and nominal freight rate, one DG set is always installed. However, in Case Study 5, for all fuel prices, and Case Study 7 for all fuel prices and double freight rate, 2 DG sets, one of nominal power lower than 700 MW and one of nominal power slightly higher than 1 MW are installed. Also, in those cases, where two DG sets are present, a certain operational strategy is observed: a large percentage of the electric loads is served by the STG with the remainder complemented by the first DG set. Then, in ports, the second DG set, which is of higher nominal power output, operates in parallel to the first one, in order to completely serve the demand. The question of why, in those cases, two DG sets are installed instead of one is answered in the reasoning of the closing comment of the previous paragraph. In Case Study 5 and Case Study 7, for double freight rate, the ship speeds are high (when compared with Case Studies 6 and 7 – for nominal freight rate) and the propulsion system is of higher nominal power output, thus leading to bottoming cycles with higher nominal output characteristics. This means that during trips a higher percentage of electric demands can be served and the remaining demand can be accommodated by a DG set with relatively low power output (<0.7 MW). Then, a second (> 1 MW) DG set is also installed to accommodate electric demands at ports in parallel with the first one. Finally, it should be clarified that in all cases where no bottoming cycle is installed, a single DG set is always chosen. This is easily explained by observing the electric demands (trips and ports) for all seasons in Table 5.19. All demands lie in the range of 1450–1670 kW and thus can be optimally covered by a single DG set.

Other interesting observations that verify the functionality of the methods proposed in this study can be made by calculating the corresponding values of NPV for the cases of PWC minimization (Case Studies 4 and 5). Next, in Tables 5.118a,b and 5.119a,b, the effect of fuel price on the optimal PWC and the corresponding value of NPV for nominal and double freight rates for Case Studies 4 and 5, is presented. Also, Tables 5.104a,b where the effect of fuel price on the optimal NPV for nominal and double freight rates for Case Study 7 is demonstrated, are repeated here for convenience.

Table 5.118a. Effect of fuel price on the optimal PWC and corresponding value of NPV for nominal freight rate for Case Study 5.

Costs (€)	Fuel Price (€/ton)				
	200	300	400	500	600
Capital Cost	14,505,140	17,984,660	18,243,420	18,646,960	18,709,660
Fuel PWC (total)	82,938,516	117,262,580	156,057,884	194,372,376	233,181,997
O&M PWC (total)	11,833,736	13,647,931	13,644,719	13,660,131	13,664,666
Total PWC (objective)	109,277,392	148,895,171	187,946,022	226,679,468	265,556,323
Total PWR	269,204,395	269,204,395	269,204,395	269,204,395	269,204,395
NPV	159,927,003	120,309,225	81,258,373	42,524,927	3,648,072

Table 5.118b. Effect of fuel price on the optimal PWC and corresponding value of NPV for double freight rate for Case Study 5.

Costs (€)	Fuel Price (€/ton)				
	200	300	400	500	600
Capital Cost	14,505,140	17,984,660	18,243,420	18,646,960	18,709,660
Fuel PWC (total)	82,938,516	117,262,580	156,057,884	194,372,376	233,181,997
OPM PWC (total)	11,833,736	13,647,931	13,644,719	13,660,131	13,664,666
Total PWC (objective)	109,277,392	148,895,171	187,946,022	226,679,468	265,556,323
Total PWR	538,408,790	538,408,790	538,408,790	538,408,790	538,408,790
NPV	429,131,398	389,513,620	350,462,768	311,729,322	272,852,467

Table 5.119a. Effect of fuel price on the optimal PWC and corresponding value of NPV for nominal freight rate for Case Study 6.

Costs (€)	Fuel Price (€/ton)				
	200	300	400	500	600
Capital Cost	9,076,406	10,310,417	10,404,230	10,603,600	10,769,740
Fuel PWC (total)	39,066,143	55,314,486	73,607,171	91,767,488	109,912,009
OPM PWC (total)	5.628.583	6,433,156	6,432,542	6,440,651	6,450,140
Total PWC (objective)	53,771,132	72,058,059	90,443,943	108,811,739	127,131,889
Total PWR	215,363,516	215,363,516	215,363,516	215,363,516	215,363,516
NPV	161,592,384	143,305,457	124,919,573	106,551,776	88,231,627

Table 5.119b. Effect of fuel price on the optimal PWC and corresponding value of NPV for double freight rate for Case Study 6.

Costs (€)	Fuel Price (€/ton)				
	200	300	400	500	600
Capital Cost	9,076,406	10,310,417	10,404,230	10,603,600	10,769,740
Fuel PWC (total)	39,066,143	55,314,486	73,607,171	91,767,488	109,912,009
O&M PWC (total)	5.628.583	6,433,156	6,432,542	6,440,651	6,450,140
Total PWC (objective)	53,771,132	72,058,059	90,443,943	108,811,739	127,131,889
Total PWR	430,727,032	430,727,032	430,727,032	430,727,032	430,727,032
NPV	376,955,900	358,668,973	340,283,039	321,915,293	303,595,143

Comparing Tables 5.118a,b with 5.119a,b the same observations that were made for the gas turbine cases are also verified for the diesel engines. All optimal values of PWC in Case Study 6 are lower than those in Case Study 5, since the maximum duration of 8 days is determined as optimal for every trip. For the corresponding NPV, for nominal freight rate the Case Study 6, NPV values are higher than those of Case Study 5 (need for cost effectiveness). However, for double freight rate, once again, something very interesting

happens; for fuel prices 200, 300 and 400 €/ton the calculated NPV is higher in Case Study 5 (where more round trips are performed) than in Case Study 6.

Table 5.104a. Effect of fuel price on the optimal NPV and corresponding value of PWC for nominal freight rate for Case Study 7.

Costs\Revenue (€)	Fuel Price (€/ton)				
	200	300	400	500	600
Capital Cost	10,954,420	10,665,380	10,404,230	10,603,600	10,769,740
Fuel PWC (total)	56,663,379	61,759,821	73,607,171	91,767,488	109,912,009
OPM PWC (total)	8,073,774	7,222,518	6,432,542	6,440,651	6,450,140
Total PWC	75,691,573	79,647,719	90,443,943	108,811,739	127,131,889
Total PWR	242,283,956	228,823,736	215,363,516	215,363,516	215,363,516
NPV (objective)	166,592,383	149,176,017	124,919,573	106,551,776	88,231,627

Table 5.104b. Effect of fuel price on the optimal NPV and corresponding value of PWC for double freight rate for Case Study 7.

Costs\Revenue (€)	Fuel Price (€/ton)				
	200	300	400	500	600
Capital Cost	16,525,690	17,161,440	14,994,690	13,501,900	12,315,590
Fuel PWC (total)	102,168,004	110,804,019	119,978,572	125,697,852	128,678,938
OPM PWC (total)	14,573,599	12,949,546	10,548,733	8,856,380	7,566,637
Total PWC	133,267,293	140,915,005	145,521,995	148,056,132	148,561,165
Total PWR	565,329,230	538,408,790	511,488,351	484,567,911	457,647,472
NPV (objective)	432,061,936	397,493,785	365,966,355	336,511,779	309,086,306

From Tables 5.104a,b (reapeated here for the convenience of the reader) it is comfirmed that the results of Case Study 7 (maximization of NPV) always yield NPV equal to or higher than the NPV obtained with the minimization of PWC in Case Studies 5 and 6 for all fuel prices and freight rates. Also, for nominal freight rate and fuel prices 400 €/ton and above, all solutions of Case Study 6 coincide with those of Case Study 7. The low value of freight rate does not allow the system to gain revenue by increasing the number of round trips and drives the system to cost effectiveness (all trip durations go to the upper limit). For double freight rate, more expensive (in terms of PWC) systems are selected that can perform more round trips per year leading to better NPV values.

A comment that can be made when comparing the GT cases (Case Studies 2–4) with the equivalent diesel engine cases (Case Studies 5–7) is the following: Generally an increase is observed for the optimal nominal power output of the propulsion plant in the two-stroke diesel engine cases. This can be explained by the fact that for the gas turbine the optimal SFOC is achieved near 100% load factor, while for the two-stroke diesel engine it is achieved near 80-85% load factor. In other words, in the two-stroke diesel engine cases, the optimizer designs the engine with a nominal power output higher than the actual maximum brake power demand, thus sacrificing capital costs to gain better fuel consumption.

Another general comment comes from the observation that the nominal power characteristics of the propulsion engine and the bottoming cycle (when installed) seem to slightly increase as fuel price rises. This has been observed in the parametric study results of all seven case studies. An argument that can explain this is the following: As fuel price increases, a trade–off between the fuel cost (fuel consumption) and the capital cost of equipment takes place. The more expensive the fuel is, the more the optimizer sacrifices capital costs by installing larger equipment in an attempt to operate the main engine in a load factor range that is closer to the range of minimum SFOC. Furthermore, by installing propulsion engines of higher power output, exhaust gases of higher energy content are produced and the design of a bottoming cycle with increased nominal power characteristics is facilitated. This leads to more efficient bottoming cycle systems that can serve a bigger portion of the thermal and electric demands during trips, thus leading to decreased fuel consumption in the auxiliary boiler and DG sets.

CHAPTER 6: CLOSURE

6.1 Concluding Remarks

A method for the dynamic synthesis, design and operation optimization of integrated energy systems of ships has been developed in a general form and applied successfully in certain case studies. For the synthesis optimization, the superconfiguration approach is followed and models of all the components that may exist in the system have been developed. The features that render the optimization problem dynamic, such as weather state and operating conditions changing with time, are highlighted.

A complete mathematical formulation of the dynamic SDO optimization problem has been presented and a solution procedure has been proposed in which the synthesis, design and operation levels of optimization are tackled simultaneously. In this way, nested optimization is avoided and the risk of overlooking optimal solutions is minimized.

A mixed integer modeling procedure that views the system as a whole has been applied. Integer, invariant and continuous variables have been used for modeling the levels of synthesis, design and operation, respectively. Then, a specific technique has been used that transposes all integer variables to binary without affecting the dimensionality of the problem. This leads to the formulation of a methodology which can be characterized as a single–level approach in contrast with the majority of methods appearing in the literature that tackle the SDO problem in two, three or even multiple levels. Usually, in order to correctly apply these two–, three– or multi–level approaches certain strict conditions must be met otherwise the search space of the optimization problem is not fully considered leading to non–global optimal solutions. The single–level approach proposed in this study requires no applicability conditions and thus can be considered universal in the context that it can be applied to any dynamic SDO optimization problem.

Also, suitable dynamic optimization approaches (both sequential and simultaneous) that can tackle the dynamic SDO optimization problem in satisfactory computational times and computational accuracy have been formulated and presented. The general methods have been applied successfully to several case studies.

Among other results, it is interesting to note that in several cases the optimal system, under the specific objective and constraints, consists of more than one prime movers of not equal power output and/or of more than one diesel generator sets also of not equal electric power output. Of course, predicting the optimal power output of each engine or generator is not possible by experience alone.

For each case study, sensitivity analysis with respect to the fuel price and in certain cases also with respect to the freight rate, the capital costs and even a different weather profile has been performed and interesting results of their impact on the optimal solution are recorded. In most cases, the economic benefit from installing a steam bottoming cycle has been demonstrated. Also, the result of the mathematical procedure for sailing through severe weather regions not only agrees with the usual practice of slow steaming, but also reveals the optimal speed profile for minimum fuel consumption, which could hardly be identified by experience alone.

A general comment regarding the application of the method to the case studies is that the power output of the equipment (main engines, generator sets, steam turbines etc.) has been treated as a continuous variable. If, for example, a diesel engine of the optimal power output is not available in the market, the one with the closest power will be selected. With so many sizes available, the deviation most probably will be small. If, however, the deviation is significant, the following actions can be taken: The system simulation software

is used to evaluate the effect of the change of power on the value of the objective function. If this is significant, the optimization software is used again with the power output fixed at the closest available size, so that the new optimal values of the remaining variables are determined.

Considering the applicability and practicality of the method, the following comment can be made: The design of a ship is traditionally performed in three stages [Papanikolaou (2010)]: (i) concept or preliminary design, (ii) contractual design and (iii) detailed design. In each stage, the ship can be considered as a complex system integrating a variety of subsystems: hull, energy system (as defined in the preceding), cargo handling, navigation equipment, etc. In each stage, design optimization can be performed for each subsystem. Thus, the procedure presented in the preceding chapters can be applied in each stage, with increasing complexity and accuracy of the system modeling from the first to the third stage. With the concrete results obtained, the designer will be more confident in search for rational decisions regarding the design and operation of the system.

It has to be mentioned that the configuration of the system on board ships has to comply with rules and regulations of classification societies and national agencies. For example, the number and nominal power of the generator sets have to be determined so that sufficient redundancy exists and, under extreme conditions, at least the critical loads are covered. Therefore, results of optimization have to be considered in connection with pertinent rules and regulations in order to reach the final selection of equipment.

As a final comment, it is noted that the general method is not restricted only to applications such as those presented in this work, but with proper modifications can be applied to even more complex systems not only on vessels but also on land.

6.2 Future Work Recommendations

The current study is a first attempt in tackling the complex problem of dynamic SDO optimization of marine energy systems. The method can be further developed, in order to address aspects such as the following.

The method has been developed for single-objective optimization. However, optimization problems of real life may involve several –often contradicting– goals, such as safety, reliability, emissions or risk considerations, that cannot be represented by or combined in a single objective function. Thus, multi–criteria or multi–objective optimization schemes may be required. Multi–objective optimization has been successfully applied to a wide range of engineering problems in the past.

There is need for even more efficient and robust optimization algorithms. Although in this study the gradient based algorithms (in order to solve the transcribed MINLP problem) have been proven to be fairly efficient in terms of convergence and computational time and able to handle the mixed integer part of the problem with success, this may not be always the case, if even more complex problems with numerous synthesis alternatives are posed. Alternatively, hybrid algorithms may be employed that combine the speed of gradient based optimization schemes and the diversity of evolutionary based optimization schemes. Specifically, of great particular interest would be algorithms that in a single step can apply an evolutionary method for the treatment of the mixed integer part of the problem (synthesis) and a gradient based method for the treatment of the invariant and continuous part (design, operation).

One more aspect is the transient behavior of the components and of the overall energy system. Characteristic examples may include the start-up time, the period of adjustment of

the system from one ship speed to another, the behavior of the HRSG and ST when adjusting to different loads, etc. In this work for simplicity, transients have not been considered, because the time scales of the transient operation of all components are very small compared to the whole operating time of the system, for which optimization is performed. Ideally, if possible, transient operation of at least the most important components should be modeled and included in the optimization process. However, this would require more detailed and computationally heavy models for each component, thus having a detrimental effect on the required computational time and computer memory in order to solve the optimization problem of the overall energy system.

Of course, complex simulation models for each component may also be required in other cases apart from the modeling of transient operation. For example, the components included in the superconfigurations investigated in the present work have predetermined and invariant internal structures and are in a sense tackled as boxes with inputs and outputs. However, in many cases, this internal structure (of each component) plays a crucial role in the efficiency and operating capability of the component and one could argue that ideally it should also be optimized along with the overall energy system. In order to achieve this, again more detailed and accurate and thus computationally heavy models for the components would be used.

One –crude but effective– approach that could possibly tackle the issue of computationally heavy models would be to use the complex and detailed model of each component in order to produce detailed look–up tables by executing all the time consuming calculations in advance, and then use them for representation of each component to the overall energy system. However, since this would require the use of a lot of memory in each optimization step, a more elegant approach would involve the application of machine learning algorithms (e.g. neural networks), in order to derive fast and simple but nonetheless accurate models for each component by utilizing all the data from the abovementioned look–up tables. This would preserve the satisfactory computational times of the proposed dynamic optimization methods, while at the same time improving the accuracy in component simulation.

Another area for improvement lies in the models used for the calculation of ship resistance and propulsion, which play a critical role in the accurate calculation of the optimal ship speed during the trip. The models used in this study have been taken from the literature and have been constructed based on theoretical considerations as well as experimental results. Newer versions of appropriate analytical models for the calculation of total ship resistance and propulsion can be found in Politis (2008) (available for download[5]). Also, along with the book, the GRID software (in Fortran code) for calculating propeller efficiency in free flow is provided[6].

For the two vessels assumed in the case studies, the predictions of the resistance and propulsion models were in good agreement with the few experimental data that were available. However, since these models are fairly general they are not expected to be accurate for every vessel, especially in the case of calculation of the added wave resistance which, as shortly discussed in Appendix D, is still an open problem in the literature. Thus, in case of application of the proposed method in existing vessels, for which many experimental data for the ship resistance and propulsion could be available, the real data rather than the theoretical models should be used (perhaps, again, via a neural network). Of course, the same comment also stands in the case of each component; if enough experimental data are available they are far more preferable than any theoretical model,

[5] https://1drv.ms/b/s!AuhmkWH18AWoiDXr-F9dA0_CO2v8
[6] https://1drv.ms/u/s!AuhmkWH18AWoiDpU7Ftg1Q6ujMCx

since the accuracy of the optimal solution is directly related with the accuracy in which the component performance is modeled.

One more aspect is related to the weather state. The methodology that has been proposed in this study assumes that the weather that the ship will encounter throughout its route, although time and space dependent, is deterministically known in advance. There may be cases when this assumption may be accurate up to a certain degree but, in general, the weather conditions are stochastic and should be treated likewise. Based on this remark, stochastic optimization methods (e.g. optimization under uncertainties, stochastic programming with recourse) should be combined/integrated with the dynamic optimization method proposed in this study.

Finally, in order to focus on the main objective, which was the development and demonstration of the applicability of the method and avoid undue complication in the present work, it was necessary to make certain simplifying assumptions. For example, hull and propeller fouling as well as component degradation of machinery during the operation of the ship have been ignored. These simplifications can be relaxed by modifying accordingly the existing models (or by adding supplementary models if necessary) for more accurate results.

APPENDIX A. AN STABILITY

Before a proper definition of AN-stability is given, the definition of A-stability must be clarified. The simplest concept of stability for ODE methods is related to the linear scalar autonomous test equation

$$\begin{aligned} y'(t) &= \lambda y(t), \quad t \geq t_0 \\ y(t_0) &= y_0 \end{aligned} \tag{A.1}$$

where $\lambda \in C$.

It is well known that the solution is $y(t) = e^{\lambda(t-t_0)} y_0$ and, hence,

$$|y(t)| = e^{\Re(\lambda)(t-t_0)} |y_0| \tag{A.2}$$

Therefore, whenever $y_0 \neq 0$ the condition

$$\Re(\lambda) \leq \lambda_0 \tag{A.3}$$

is equivalent to

$$|y(t)| = e^{\lambda_0(t-t_0)} |y_0| \tag{A.4}$$

In particular, the condition $\Re(\lambda) < 0$ is equivalent to the asymptotic stability property

$$\lim_{t \to +\infty} y(t) = 0 \tag{A.5}$$

whereas the slightly weaker condition $\Re(\lambda) \leq 0$ is equivalent to the contractivity, or dissipativity, property

$$|y(t)| \leq |y_0|, \quad t \geq t_0 \tag{A.6}$$

Thus, we have:

Definition of A-Stability:

The A-stability region of a numerical method for ODEs is the set S_A of complex numbers $\alpha=h\lambda$ such that the numerical solution $\{y_n\}_{n\geq 0}$ of Eq. (A.1) obtained with the constant stepsize h satisfies $\lim_{n\to+\infty} y_n = 0$.

Thus, a numerical method for ODEs is considered A-stable if

$$S_A \supseteq \{a \in C \,|\, \Re(a) < 0\} \tag{A.7}$$

In other words, a numerical method for ODEs is A-stable if, when implemented with constant stepsize h, it preserves the asymptotic stability properties of the solution y(t) of Eq. (A.1).

The second stability concept of importance for ODE methods is called AN-stability. AN-stability is related to the linear scalar non-autonomous test equation

$$\begin{aligned} y'(t) &= \lambda(t)y(t), \quad t \geq t_0 \\ y(t_0) &= y_0 \end{aligned} \tag{A.8}$$

where λ(t) is a continuous complex valued function.

It is known that the solution is $y(t) = \exp\left(\int_{t_0}^{t} \lambda(x)dx\right) y_0$, therefore, if

$$\Re(\lambda(t)) \leq \Lambda_0, \quad t \geq t_0 \tag{A.9}$$

then

$$|y(t)| \leq e^{\Lambda_0 (t-t_0)} |y_0|, \quad t \geq t_0 \tag{A.10}$$

In particular, if

$$\Re(\lambda(t)) \leq 0, \quad t \geq t_0 \tag{A.11}$$

then Eq. (A6) holds. Moreover, if

$$\Lambda_0 < 0 \tag{A.12}$$

then the solution y(t) asymptotically vanishes, that is Eq. (A.5) holds.

Thus, we have:

Definition of AN-Stability:

A numerical method for ODEs is said to be AN-stable if the numerical solution $\{y_n\}_{n\geq 0}$ *of Eq. (A8) satisfying Eq. (A.11) is such that* $|y_{n+1}| \leq |y_n|$ *for any mesh* Δ.

It is clear that the concept of AN-stability is stronger than the concept of A-stability.

APPENDIX B. PRESENT WORTH COST

As stated in Chapter 3, the total PWC of the system is given by the equation:

$$PWC = PWC_c + PWC_f + PWC_{om} \tag{B.1}$$

Following the notation of Chapter 3, Section 3.3.1, Eqs. (3.3a)-(3.4d), for the total capital present worth cost we have:

$$PWC_c = \sum_{i,j} C_{c,i,j} + \sum_{k} C_{c,B,k} + \sum_{l} C_{c,ST,l} + \sum_{m} C_{c,G,m} + C_{c,AB} \tag{B.2}$$

where

$C_{c,i,j}$ capital cost of j th propulsion engine of type i,
$C_{c,B}$ capital cost of k th HRSG,
$C_{c,ST}$ capital cost of l th steam turbine,
$C_{c,G}$ capital cost of m th diesel generator set,
$C_{c,AB}$ capital cost of auxiliary boiler.

Indices i, j, k, l and m are defined in detail in Chapter 3, Eqs. (3.4a)–(3.4d). All capital cost calculation models are presented in Appendix C.

For the total fuel present worth cost we have:

$$PWC_f = \sum_{i,j} PWC_{f,i,j} + \sum_{m} PWC_{f,G,m} + PWC_{f,AB} \tag{B.3}$$

where

$PWC_{f,i,j}$ fuel present worth cost of j th propulsion engine of type i,
$PWC_{f,G,m}$ fuel present worth cost of m th Diesel generator set,
$PWC_{f,AB}$ fuel present worth cost of auxiliary boiler.

In order to calculate each of the aforementioned costs, the annual (first year) fuel cost for each component is calculated, since the present worth cost (for each component) can generally be defined as:

$$PWC_{f,n} = C_{fa,n} \cdot PWF(N_n, i) \tag{B.4}$$

where

N_n engine life of component n in years,
i market interest rate,
$C_{fa,n}$ first year fuel cost of component n,
PWF present worth factor.

For a constant value analysis, which ignores the inflation rate, it is

$$PWF(N_n, i) = \frac{(1+i)^{N_n} - 1}{i \cdot (1+i)^{N_n}} \tag{B.5}$$

Based on the definition of the engine life of each component, N_n, several considerations can be followed. In this study, the engine life for all components is considered equal to a constant value, defined as the nominal technical life of the system

$$N_n = N_t \tag{B.6}$$

The calculation of each components' first year annual fuel cost, $C_{fa,n}$, is dependent on the specific mission assumptions and parameters (time horizon of optimization) for each case study, thus it is discussed separately for each case study (Chapter 5). The general mathematical formulas for calculating fuel costs of each component are given in Appendix C.

For the operation and maintenance (O&M) present worth cost we have:

$$PWC_{om} = \sum_{i,j} PWC_{om,i,j} + \sum_{k} PWC_{om,B,k} + \sum_{l} PWC_{om,ST,l} + \sum_{m} PWC_{om,G,m} + PWC_{om,AB} \tag{B.7}$$

where:

$PWC_{om,i,j}$ O&M present worth cost of j th engine of type i,
$PWC_{om,B,k}$ O&M present worth cost of k th HRSG,
$PWC_{om,ST,l}$ O&M present worth cost of l th steam turbine,
$PWC_{om,G}$ O&M present worth cost of m th diesel generator set,
$PWC_{om,AB}$ O&M present worth cost of auxiliary boiler.

The annual (first year) O&M cost formalism is used, thus for each component n, the present worth cost of O&M is given as:

$$PWC_{om,n} = C_{oma,n} \cdot PWF(N_n, i) \tag{B.8}$$

where, $C_{oma,n}$, is the first year O&M cost of component n, which is dependent on the specific mission assumptions and parameters for each case study. The general mathematical formulas for calculating O&M costs of each component are given in Appendix C.

APPENDIX C. COMPONENT COST MODELS

Appropriate mathematical models for the evaluation of the costs for each component are needed, which are essential for the calculation of the economic function that will serve as the objective function in our dynamic optimization problem. The costs for each component are divided into the capital cost of installation and the operation costs. The operation costs for each component comprise the operation and maintenance (O&M) cost and the fuel cost, if applicable. In the following sections, the mathematical models for the capital cost, O&M cost and fuel cost for each component, which was described in Chapter 4, are presented.

C.1 Single Pressure Heat Recovery Steam Generator Costs

Capital cost

The cost function appearing in Frangopoulos (1994) and Pelster (1998) has been used for the capital cost of the HRSG, with its coefficients adapted according to data found in GTW (2010). The form of the function is:

$$C_{c,B} = C_{HX} + C_{piping} + C_{gaspath} + C_{pump} \tag{C.1}$$

where

C_{HX} total heat exchangers capital cost,
C_{piping} piping capital cost,
$C_{gaspath}$ gas path system capital cost,
C_{pump} pump capital cost.

The cost components are further analyzed as follows:

$$C_{HX} = c_1 \cdot \sum_{i=1}^{N_{HX}} \left[f_{P_{st}} \cdot f_{T_{st}} \cdot f_{T_g} \cdot (UA)^{0.8} \right]_i \tag{C.2}$$

$$C_{piping} = c_2 \cdot f_P \cdot \dot{m}_{st} \tag{C.3}$$

$$C_{gaspath} = c_3 \cdot \dot{m}_g^{1.2} \tag{C.4}$$

$$C_{pump} = c_4 \cdot \dot{W}_P^{0.71} \cdot \left(1 + \frac{1-0.8}{1-\eta_{p,is}} \right) \tag{C.5}$$

where

$f_{P_{st}}$ correction factor for operating steam pressure,
$f_{T_{st}}$ correction factor for operating steam temperature,
f_{T_g} correction factor for operating exhaust gas temperature,
f_P correction factor for piping,
$\dot{W}_P$ power input to the pump.

The correction factors appearing in Eqs. (C.2) – (C.3) are given as

$$f_{P_{st,j}} = 0.0971 \cdot \left(\frac{P_{st,j}}{30} \right) + 0.9029 \tag{C.6}$$

$$f_{T_{st,j}} = 1 + \exp\left(\frac{T_{st,j} - 830}{500} \right) \tag{C.7}$$

$$f_{T_{g,i}} = 1 + \exp\left(\frac{T_{g,i} - 990}{500} \right) \tag{C.8}$$

where P is given in bar and T in Kelvin.

Constants c_1, c_2, c_3 and c_4 were determined using data found in GTW (2010) and have the following values:

$$\begin{aligned} c_1 &= \ 8797 \ \ Euros/(kW/K)^{0.8} \\ c_2 &= 10775 \ \ Euros/(kg/s) \\ c_3 &= \ 600 \ \ Euros/(kg/s)^{1.2} \\ c_4 &= \ 568 \ \ Euros/(kW)^{0.71} \end{aligned} \tag{C.9}$$

Operation and maintenance cost

For the O&M costs of the HRSG, a constant unit cost value is considered,

$$c_{om,B} = 0.004558 \ \text{Euros/kWh} \tag{C.10}$$

derived from market data surveys [Kougioufas (2005), Andrianos (2006), Dimopoulos (2009)]. The operation and maintenance cost is then calculated as:

$$C_{om,B} = c_{om,B} \cdot \int_0^{t_f} \dot{Q}_{rec} \cdot dt \tag{C.11}$$

where $\dot{Q}_{rec}$ is the thermal power recovered from exhaust gas by HRSG.

C.2 Steam Turbine Costs

Capital cost

The unit capital cost of a marine steam turbine unit is expressed as a function of the mechanical nominal power output, $\dot{W}_{ST_n}$, and is derived by regression analysis of market data [GTW (2010), EPA (2014)] and a cost function expression appearing in Pelster (1998):

$$c_{c,ST} = a \cdot \left(\frac{\dot{W}_{ST_n}}{\dot{W}_{ref}} \right)^b \tag{C.12}$$

with parameter values:

$$\begin{aligned} a &= 375.7 \ \text{Euros} \\ b &= -0.38 \\ W_{ref} &= 7500 \ \text{kW} \end{aligned} \tag{C.13}$$

The capital cost is then given as:

$$C_{c,ST} = c_{c,ST} \cdot \dot{W}_{ST_n} \tag{C.14}$$

It is noted that the electric generator and condenser unit capital costs are incorporated in the capital cost equation.

Operation and maintenance cost

For the specific O&M unit cost of the ST, a constant value derived from market data surveys performed in Kougioufas (2005) and Andrianos (2006) and data found in EPA (2014), is used,

$$c_{om,ST} = 0.3646 \ \text{Euros/kWh} \tag{C.15}$$

Thus, the operation and maintenance cost is calculated as:

$$C_{om,ST} = c_{om,ST} \cdot \int_0^{t_f} \dot{W}_{ST} \cdot dt \tag{C.16}$$

where $\dot{W}_{ST}$ is the mechanical power produced by the steam turbine for the total horizon of optimization t_f .

C.3 Diesel Engines Cost Models

Capital cost

The installed investment cost of a diesel engine (purchase and installation cost) is derived from literature data as an equation of the nominal brake power of the engine in both cases of 2-X and 4-X engines. For 2-X diesel engines we have

$$C_{c,DE,2X} = a \cdot \left(\dot{W}_{bn} \right)^b, \qquad 6 \le \dot{W}_{bn} \le 90 \ \text{MW} \tag{C.17}$$

with

$$a = 16100 \text{ Euros/(kW)}^{b}$$
$$b = 0.62 \tag{C.18}$$

while for 4-X diesel engines we have

$$C_{c,DE,4X} = a_1 + a_2 \cdot \dot{W}_{bn}, \qquad 5 \le \dot{W}_{bn} \le 20 \text{ MW} \tag{C.19}$$

where $a_1 = 2 \cdot 10^6$ € and $a_2 = 250$ €/kW.

Operation and maintenance cost

For both types of diesel engines, the O&M cost per engine j is given as:

$$C_{om,DE_j} = c_{om,DE_j} \cdot E_{b_j} \tag{C.20}$$

where

c_{om,D_j} unit cost of O&M of engine j

E_{b_j} brake energy produced by engine j for the total horizon of optimization:

$$E_{b_j} = \int_0^{t_f} \dot{W}_{b_j} \cdot dt \tag{C.21}$$

For the unit cost of O&M, a constant value derived from data found in EPA (2014) is used for both types of engines

$$c_{om,DE} = 0.006 \text{ Euros/kWh} \tag{C.22}$$

Fuel cost

Considering the fuel cost, if a constant unit cost of fuel, $c_{f,DE}$, is assumed, then the fuel cost per diesel engine, C_{f,DE_j}, is calculated by the fuel consumption, m_{f,DE_j}, of each diesel engine j as

$$C_{f,DE_j} = c_{f,DE} \cdot m_{f,DE_j} = c_{f,DE} \cdot \int_0^{t_f} b_{f,DE_j} \cdot \dot{W}_{b,DE_j} \cdot dt \tag{C.23}$$

where

b_{f,DE_j} specific fuel oil consumption of engine j

$\dot{W}_{b,DE_j}$ brake power of engine j.

C.4 Gas Turbine Costs

Capital cost

The capital cost of each of the three types of gas turbines is expressed as a function of the nominal power output, $\dot{W}_{GT_n}$. As in Section 4.4 of Chapter 4, an effort was made for developing regression equations with similar mathematical form among the various GT types. The equation was derived based on cost calculation considerations found in Frangopoulos (1991) and Frangopoulos (1994) combined with data taken from manufacturers [GTW (2010), NTC (2018)]:

$$C_{c,GT} = a \cdot \dot{W}_{G_n}{}^{b} \cdot \exp(c - d \cdot \dot{W}_{G_n}) \tag{C.24}$$

The parameter values for each type are given in Table C.1.

Table C.1. Coefficients for capital cost (Eq. C.24) for all GT types.

Coefficient	GT1	GT2	GT3
a (E/kW^b)	0.9116	1.0628	1.1844
b (-)	0.451124718	0.451124718	0.451124718
c (-)	11.660166099	11.660166099	11.660166099
d $(1/\text{kW})$	8.1530518977E-07	8.1530518977E-07	8.1530518977E-07

Operation and maintenance cost

For the gas turbines the unit cost of O&M is modeled as a function of the GT nominal power output with data found in EPA (2014),

$$c_{c,GT} = a \cdot \left(\dot{W}_{GT_n}\right)^{b} \tag{C.25}$$

with parameter values:

$$\begin{aligned} a &= 0.3549 \\ b &= -0.2104 \end{aligned} \tag{C.26}$$

Thus the O&M cost is calculated as

$$C_{om,GT} = c_{om,GT} \cdot \int_0^{t_f} \dot{W}_{GT} \cdot dt \tag{C.27}$$

with $\dot{W}_{GT}$ the power output of the GT. The same formula is used for all three gas turbine types.

Fuel cost

Considering the fuel cost, if a constant unit cost of fuel, $c_{f,GT}$, is assumed, then the fuel cost per GT, C_{f,GT_j}, is calculated as a function of the fuel consumption, m_{f,GT_j}, as

$$C_{f,GT_j} = c_{f,GT} \cdot m_{f,GT_j} = c_{f,GT} \cdot \int_0^{t_f} b_{f,GT_j} \cdot \dot{W}_{b,GT_j} \cdot dt \tag{C.28}$$

where

b_{f,GT_j} specific fuel oil consumption of GT j

$\dot{W}_{b,GT_j}$ brake power of GT j.

C.5 Diesel Generator Set Costs

Capital cost

The unit capital cost of a diesel generator set is expressed as a function of the nominal power output, $\dot{W}_{G_n}$, derived by data taken from manufacturers:

$$c_{c,G} = a \cdot \left(\frac{\dot{W}_{G_n}}{\dot{W}_{ref}} \right)^b \tag{C.29}$$

with parameter values:

$$\begin{aligned} a &= 730 \text{ Euros} \\ b &= -0.6 \\ \dot{W}_{ref} &= 1000 \text{ kW} \end{aligned} \tag{C.30}$$

Thus, the capital cost is given as:

$$C_{c,G} = c_{c,G} \cdot \dot{W}_{G_n} \tag{C.31}$$

Operation and maintenance cost

For the diesel generator set, the same approach as for the diesel engines is used:

$$C_{om,G} = c_{om,G} \cdot \int_0^{t_f} \dot{W}_G \cdot dt \tag{C.32}$$

with the unit cost of O&M considered as a constant value [EPA (2014)]:

$$c_{om,G} = 0.006381 \text{ Euros/kWh} \tag{C.33}$$

Fuel cost

Considering the fuel cost, a constant unit cost of fuel, $c_{f,G}$, is assumed. The fuel cost per trip, $C_{f,G}$, is calculated via the fuel consumption, $m_{f,G}$, as:

$$C_{f,G} = c_{f,G} \cdot m_{f,G} = c_{f,G} \cdot \int_0^{t_f} b_{f,G} \cdot \dot{W}_G \cdot dt \tag{C.34}$$

where

$b_{f,G}$ specific fuel oil consumption of diesel generator set (Appendix D)

$\dot{W}_G$ electric power demand covered by the diesel generator set.

C.6 Auxiliary Boiler Costs

Capital cost

The capital cost (in €) of the auxiliary boiler is estimated by the equation:

$$C_{c,AB} = 70000 + 80 \cdot \dot{Q}_{AB_n} \tag{C.35}$$

where $\dot{Q}_{AB_n}$ is the nominal thermal power output of the auxiliary boiler in kW.

Operation and maintenance cost

For the O&M costs of the auxiliary boiler, $c_{om,AB}$, a constant unit O&M value used.

$$c_{om,AB} = 0.00458 \text{ Euros/kWh} \tag{C.36}$$

so the O&M cost is given as

$$C_{om,AB} = c_{om,AB} \cdot \int_0^{t_f} \dot{Q}_{AB} \cdot dt \tag{C.37}$$

Fuel cost

For the fuel cost, a constant unit cost of fuel, $c_{f,AB}$, is assumed. The fuel cost, $C_{f,AB}$, is then calculated by the fuel consumption, $m_{f,AB}$, as:

$$C_{f,AB} = c_{f,AB} \cdot m_{f,AB} \tag{C.38}$$

where the fuel consumption of the auxiliary boiler is calculated as follows:

$$m_{f,AB} = \int_0^{t_f} \frac{\dot{Q}_{AB}}{\eta_{AB} \cdot H_u} \cdot dt \tag{C.39}$$

where

H_u	lower heating value of the auxiliary boiler fuel,
η_{AB}	efficiency of the auxiliary boiler,
$\dot{Q}_{AB}$	thermal power covered by the auxiliary boiler.

APPENDIX D. TOTAL SHIP RESISTANCE

A ship differs from land based large engineering structures in that, in addition to all its other functions, it must be designed to move efficiently through the water. In this appendix the specific mathematical models used in this work for the calculation of the total resistance of a ship are presented.

The resistance of a ship at a given speed is the force required to tow the ship at that speed, assuming no interference from the towing ship. Thus, the total resistance of a ship, R_T, is not exactly the same as the *propulsion* resistance due to hull/propeller interactions. In order to calculate R_T, the propulsive efficiency, η_{prop}, needs to be calculated also (discussed in Appendix E). This total resistance is made up of a number of different components, which are caused by a variety of factors and which interact with each other in a rather complex way. In order to deal with the question more efficiently, it is customary to decompose the total resistance as a sum of different terms [Politis and Skamnelis (2007)]:

$$R_T = R_{calm} + R_{Aw} + R_{As} \tag{D.1}$$

where

R_{calm} calm water resistance

R_{Aw} additional resistance due to the effects of wind (added wind resistance)

R_{As} additional resistance due to the effects of waves (added wave resistance)

The first term of Eq. (D.1) is usually referred to in the literature as calm water resistance and is a static term that is generally dependent on the ship speed and characteristics (geometry, hull form). The last two terms model the effect of the weather, wind and waves, on the total ship resistance and are very important in this study, since they are dependent on the weather profile also, thus "inserting" time and space dependency in the problem and making it inherently dynamic.

It must be stated that also other terms of added resistance can be included, with a very good example being the added resistance due to *turning* (for surface ships) or *diving* (for submarines), but since they are just static terms with, in most cases, very small contribution in the total resistance, they are not taken into account in this work.

In the next sections a brief presentation of the physical characteristics as well as the mathematical models used in this work to calculate the total calm water, the added wind and the added wave resistance is given.

D.1 Calm Water Resistance

From a physical as well as a computational point of view, the calm water resistance includes several components:

$$R_{calm} = R_F(1+k_1) + R_a + R_w + R_{APP} + R_{BB} + R_{TR} \tag{D.2}$$

where

R_F frictional resistance, due to the motion of the hull through a viscous fluid,

$1+k_1$ form factor of the hull, describing the viscous resistance from the hull in relation to R_F, (*form drag*)

R_a model-ship correlation resistance necessary to reconcile or "correlate" the predictions of calm water resistance results from smaller scaled models to the real ship. It also includes the -still- air resistance the ship encounters while sailing,

R_w wave-making and wave-breaking resistance, due to the energy that must be supplied continuously by the ship to the wave system created on the free surface,

R_{APP} appendage resistance due to the presence of bilge keels, rudders, bossings or open shafts and struts,

R_{BB} additional pressure resistance of bulbous bow near the water surface,

R_{TR} additional pressure resistance of immersed transom stern.

A streamlined body moving on a straight horizontal line at constant forward speed, deeply immersed in an unlimited ocean, presents the “simplest” (still far from trivial) case of resistance, frictional resistance. Since there is no free surface, there is no wave formation and therefore no wave making resistance. In a real fluid, the boundary layer alters the virtual shape and length of the body, the pressure distribution at the stern is changed and there is a net force on the body acting against the motion, giving rise to a resistance, which is known as form drag or viscous pressure drag. Also, the fluid immediately in contact with the surface of the body is carried along with the surface and a boundary layer which becomes gradually thicker from the bow to the stern, is formed. The momentum supplied to the water in the boundary layer by the hull is a measure of the frictional resistance. If the body is rather blunt at the after end, the flow may detach at some point, called the *separation point*, thus reducing the total pressure on the afterbody and adding to the resistance. This separation resistance is evidenced by a pattern of eddies which is a drain of energy.

A ship moving on the surface of the sea experiences all of the aforementioned forms of resistance in much the same way as does a submerged body. However, the presence of the free surface adds a further component. The resulting pressure distribution on the hull results in the creation of a wave system which spreads out astern of the ship and has to be continuously recreated. This corresponds to a drain of energy supplied by the ship and is termed the wave making resistance.

Several examples of the plot of calm water resistance (effective horsepower, EHP, per ton of displacement) versus the speed–length ratio $V/\sqrt{L_{OA}}$ (V in knots, L_{OA} in feet) for different types of ships are presented in Fig. D.1.

Next, we proceed to examine all the components of total calm water resistance one by one and provide an appropriate mathematical model for their estimation.

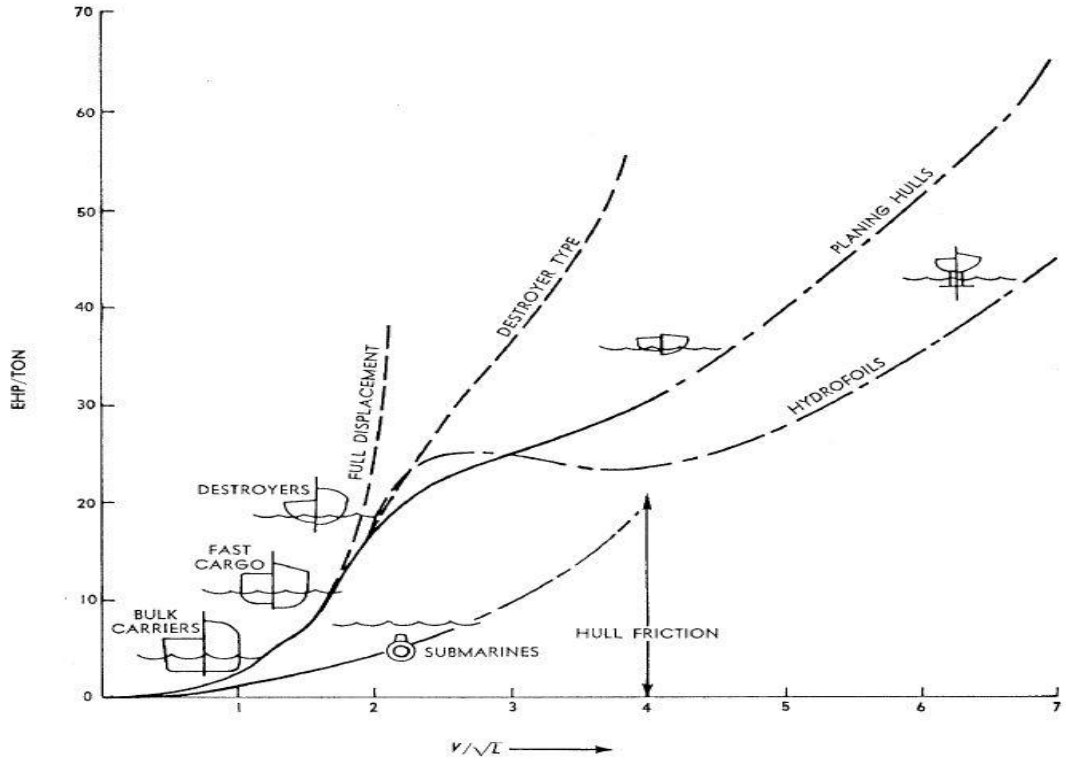

Figure D.1. Speed-power trends for different ship types [Politis and Skamnelis (2007)].

D.1.1 Frictional resistance

The frictional resistance is usually the most significant component of the total ship resistance. For relatively slow ships with high block coefficients it contributes to about 85% of the total resistance, whereas for high speed streamlined displacement hulls it may drop to about 50%. These values may become higher in time due to the increased roughness of the ship surface. The first theoretical considerations regarding the calculation of frictional resistance were made by Froude [Froude (1872), (1874)]. However, until Osborne Reynolds [Reynolds (1883)] the dependence of frictional resistance on the Reynolds number

$$\mathrm{Re} = \frac{VL_{OA}}{\nu} \tag{D.3}$$

with L_{OA} the ship's length, V its velocity, and ν the kinematic viscosity of the water, was unknown to the scientific community. Later theoretical considerations due to Prandtl and von Karman [Politis and Skamnelis (2007)] led to the development of a theoretical formula:

$$\frac{A}{\sqrt{C_F}} = \log_{10}\left(\mathrm{Re}\, C_F\right) + B \tag{D.4}$$

with A, B constants and C_F the frictional resistance coefficient defined as:

$$C_F = \frac{R_F}{\frac{1}{2}\rho V^2 S} \tag{D.5}$$

where ρ denotes the water density and S the ship's wetted surface.

Extensive sets of experimental data were analyzed by Schoenherr in the light of Eq. (D.4), and he found that he could obtain a good fit to the experimental data by making *B* zero and *A* equal to 0.242, arriving at the Schoenherr formula [Schoenherr (1932)] which was adopted in 1947 by the ATTC (American Towing Tank Conference) for use with standard ship resistance computations [ATTC (1947)]. However, with the introduction of larger ships, and comparatively smaller models, it was observed that the Schoenherr line had a slope which was not considered to be sufficiently steep at the low Reynolds numbers appropriate to small models, so that it did not give good correlation between the results of small and large models. To alleviate this problem, the International Towing Tank Conference (ITTC) adopted in 1957 a new formula:

$$C_F = \frac{0.075}{(\log_{10} \mathrm{Re} - 2)^2} \tag{D.6}$$

which is known as the ITTC line and is the current standard.

The formula stated in Eq. (D.6) will be also used in this study for the calculation of the frictional resistance coefficient, C_F, and thus the frictional resistance, R_F.

D.1.2 Form resistance

Form resistance originates from the change of pressure distribution upon a body as it travels through a real fluid due to the formation of a boundary layer. The virtual shape and length of the body is altered, thus the pressure distribution at the stern is changed and its forward component is reduced, leading to the formation of a net force on the body, acting against the motion.

Hughes [Hughes (1963), (1965)] proposed that only the term of viscous resistance should be used for modelling the form resistance since until then viscous and wave making resistances were calculated by the Froude method as one. What he observed was that at low Froude numbers,

$$Fn = \frac{V}{\sqrt{gL_{OA}}} \tag{D.7}$$

where g denotes the acceleration of gravity, the wave making resistance will be vanishingly small, and after a certain point the curve of calm water resistance will become approximately parallel to the friction line. Hughes called this the "run–in" point and defined a form factor $1+k_1$ by the expression

$$1 + k_1 = \frac{\text{Viscous Resistance}}{\text{Frictional Resistance}} \tag{D.8}$$

which equivalently defines the form resistance as a function of the frictional resistance

$$R_{Form} = k_1 R_F \tag{D.9}$$

This form factor is independent of the Reynolds number and is the same for all similar models and ships. In this study, the calculation of the form factor of the hull, $1+k_1$, is performed by the formula [Holtrop and Mennen (1982), Holtrop (1984)]

$$1+k_1 = 0.93+0.487118c_{14}(B/L_{OA})^{a_1}(T/L_{OA})^{a_2}(L_{OA}/L_R)^{a_3}(L_{OA}{}^3/\nabla)^{a_4}(1-C_P)^{a_5} \tag{D.10}$$

$$c_{14} = 1+0.011C_{Stern} \tag{D.11}$$

with, $a_1 = 1.06806$, $a_2 = 0.46106$, $a_3 = 0.121563$, $a_4 = 0.36486$, and $a_5 = -0.604247$. In this formula, B and T are the moulded breadth and draught of the ship, respectively, C_P is the prismatic coefficient and ∇ is the moulded displacement volume. The parameter L_R is defined as

$$L_R = L_{OA}\left(1-C_P+\frac{0.06C_P lcb}{4C_P-1}\right) \tag{D.12}$$

where lcb is the longitudinal position at the centre of buoyancy forward of $0.5L$ as a percentage of L. The coefficient c_{14} accounts for the stern shape. It depends on the stern shape coefficient C_{Stern}. Values for C_{Stern} are given in Table D.1.

Table D.1. Stern shape coefficient values.

Afterbody Form	C_{Stern}
Pram with gondola	-25
V-shaped sections	-10
Normal shaped sections	0
U-shaped sections with Hogner stern	10

D.1.3 Model/Ship correlation resistance

The model-ship correlation resistance, R_a, is supposed to primarily describe the effect of the hull roughness. However, it also incorporates the increase in calm water resistance due to the still-air the ship's superstructure "meets" as it sails. The correlation allowance coefficient is used to describe the correlation resistance, and is defined in the same manner as the frictional resistance coefficient:

$$C_a = \frac{R_a}{\frac{1}{2}\rho V^2 S} \tag{D.13}$$

This correlation allowance, once called roughness coefficient, is in essence a correction factor in order to mainly fine–tune model tests with full scale measurements,

since most experimental data, that lead to the construction of all the formulas are based on small scale model tests. Physically, its existence is based on a variety of factors, most notably the difference in roughness characteristics (the model surface is always smoother than the ship) and the laminar flow near the bow of the model (turbulence stimulators are often used on the model to alleviate this phenomenon). Its value, typically in the order of 0.0004, varies for different ship types and model sizes. In this study, the formula by Holtrop and Mennen (1982) is used:

$$C_a = 0.006\left(L_{OA}+100\right)^{-0.16} - 0.00205 + 0.003\sqrt{L_{OA}/7.5}C_B{}^4 c_2\left(0.04 - c_4\right) \tag{D.14}$$

$$c_4 = \begin{cases} T_F/L_{OA} & \text{if} \quad T_F/L_{OA} \le 0.04 \\ 0.04 & \text{if} \quad T_F/L_{OA} > 0.04 \end{cases} \tag{D.15}$$

$$c_2 = \exp(-1.89\sqrt{c_3}) \tag{D.16}$$

$$c_3 = \frac{0.56A_{BT}^{1.5}}{\left\{BT\left(0.31\sqrt{A_{BT}} + T_F - h_B\right)\right\}} \tag{D.17}$$

where A_{BT} is the transverse area of the bulbous bow, h_B denotes the vertical position of the centre of A_{BT} and should not exceed the upper limit of $0.6 \cdot T_F$, with T_F the forward moulded draught. Finally C_B is the ship's block coefficient.

Several expressions for calculating the wetted area of the hull, S, are given in Appendix F.

D.1.4 Wave making/breaking resistance

The wave making resistance of a ship is related to the net force upon the ship due to the normal fluid pressures acting on the hull, just as the frictional resistance is the result of the tangential fluid forces. If the body is travelling on or near the free surface, this pressure variation causes waves which radiate away from the body and carry with them a certain amount of energy that is dissipated in the ocean. The wave making resistance can then be also characterized by the energy expended by the ship that is necessary to maintain the wave system. Purely theoretical determination of the wave making resistance requires knowledge of the wave system generated by a moving ship.

The first serious theoretical attempt towards quantifying the ship wave system, that explained many of its features, was due to Lord Kelvin in the late 19th century [Thomson, (1879)]. In his approach the whole wave pattern moves with the ship and for an observer on the ship the waves appear to be stationary. Kelvin was able to arrive at his model using a general technique in asymptotic analysis, called the method of stationary phase, which he developed precisely for the wave resistance problem. However, to utilize this theory the wave amplitude must be calculated. One way of evaluating it is based on the thin ship theory which was introduced by Michell (1898), as a purely analytic approach for predicting the wave resistance of ships and led to the mathematical formulation of Mitchell integral. Based on this theory, a fairly large number of numerical computations have been carried out both for practical ship geometries and for simplified mathematical forms.

Mitchell's integral is an effective means of comparisons between different theoretical predictions or different hull forms.

More recent numerical studies [Erickson (1990)] of wave making resistance follow the so called panel methods, where the surface of the ship is approximated by a series of panels with distributed sources and sinks and allow for the actual geometry of the hull to be taken into account. Another modern approach [Eggers et al. (1967, Ikehata (1969)] is known as wave pattern analysis, which requires a relatively complex survey of the wake region to determine the amplitude function for all relevant wave angles. These techniques have led to the discovery of an additional drag component associated with *wave breaking*, and to a better understanding of the bulbous bows of supertankers and other ships with low Froude numbers.

In the current work, the wave making and wave-breaking resistance are simultaneously calculated using formulas derived from regression analysis in the work of Holtrop and Mennen (1982) and Holtrop (1984). The formula provides two different predictions of the resistance R_w, one for the high and one for the low speed range.

In the high speed range, $F_n > 0.55$, the wave-making and wave-breaking resistance is calculated as

$$R_{w-B} = c_{17} c_2 c_5 \nabla \rho g \exp\left(m_3 F_n^{-0.9} + m_4 \cos(\lambda F_n^{-2})\right) \tag{D.18}$$

$$c_{17} = 6919.3\left(C_M\right)^{-1.3346}\left(\nabla / {L_{OA}}^3\right)^{2.00977}\left(L_{OA}/B - 2\right)^{1.40692} \tag{D.19}$$

$$m_3 = -7.2035\left(B/L_{OA}\right)^{0.326869}\left(T/B\right)^{0.605375} \tag{D.20}$$

$$m_4 = c_{15} 0.4 \exp\left(-0.034 F_n^{-3.29}\right) \tag{D.21}$$

$$c_5 = \left(1 - \frac{0.8 A_T}{BTC_M}\right) \tag{D.22}$$

$$\lambda = \begin{cases} 1.446 C_P - 0.03 L_{OA}/B & \text{if} \quad L_{OA}/B \le 12 \\ 1.116 C_P - 0.36 & \text{if} \quad L_{OA}/B > 12 \end{cases} \tag{D.23}$$

$$c_{15} = \begin{cases} -1.69385 & \text{if} \quad {L_{OA}}^3/\nabla < 512 \\ -1.69385 + \dfrac{L_{OA}/\nabla^{1/3} - 8}{2.36} & \text{if} \quad 512 < {L_{OA}}^3/\nabla < 1726.91 \\ 0 & \text{if} \quad {L_{OA}}^3/\nabla > 1726.91 \end{cases} \tag{D.24}$$

where C_M is the mid-ship section coefficient, A_T is the transverse immersed transom area at rest, A_{BT} is the transverse area of the bulbous bow, h_B denotes the vertical position of the centre of A_{BT} and should not exceed the upper limit of $0.6 \cdot T_F$, with T_F the forward moulded draught. The coefficient c_2 along with c_3 are given in the previous (model/ship correlation resistance) section by Eqs. (D.16) and (D.17).

Attempts to derive an accurate formula for low and moderate speeds $0.40 < F_n < 0.55$ were not successful, thus a formula up to a Froude number, $F_n < 0.40$, is derived and the wave-making and wave breaking resistance is calculated as

$$R_{w-A} = c_1 c_2 c_5 \nabla \rho g \exp\left(m_1 F_n^{-0.9} + m_4 \cos(\lambda F_n^{-2})\right) \tag{D.25}$$

$$c_1 = 2223105 c_7^{3.78613} \left(T/B\right)^{1.07961} \left(90 - i_E\right)^{-1.37565} \tag{D.26}$$

$$m_1 = 0.0140407\left(L_{OA}/T\right) - 1.75254\left(\nabla^{1/3}/L_{OA}\right) - 4.79323\left(B/T\right) - c_{16} \tag{D.27}$$

$$c_7 = \begin{cases} 0.229577\left(B/L_{OA}\right)^{0.33333} & \text{if} \quad B/L_{OA} < 0.11 \\ B/L_{OA} & \text{if} \quad 0.11 < B/L_{OA} < 0.25 \\ 0.5 - 0.0625 L_{OA}/B & \text{if} \quad {L_{OA}}^3/\nabla > 0.25 \end{cases} \tag{D.28}$$

$$c_{16} = \begin{cases} 8.07981 C_P - 13.8673 {C_P}^2 + 6.984388 {C_P}^3 & \text{if} \quad C_P < 0.8 \\ 1.73014 - 0.7067 C_P & \text{if} \quad C_P > 0.8 \end{cases} \tag{D.29}$$

with i_E the half angle of entrance, which is the angle of the waterline at the bow in degrees with reference to the centre plane, neglecting the local shape at the stern. If i_E is unknown, it can be calculated by the following formula

$$\begin{aligned} i_E = 1 + 89 \exp\Big\{ & -\left(L_{OA}/B\right)^{0.80856} \cdot \left(1 - C_{WP}\right)^{0.30484} \\ & \cdot \left(1 - C_P - 0.0225 lcb\right)^{0.6367} \cdot \left(L_R/B\right)^{0.34574} \\ & \cdot \left(100\nabla/{L_{OA}}^3\right)^{0.16302} \Big\} \end{aligned} \tag{D.30}$$

with C_{WP} the waterplane area coefficient.

For the speed range, $0.40 < F_n < 0.55$, the following interpolation formula is used:

$$R_w = R_{w-A_{0.4}} + (10F_n - 4)(R_{w-B_{0.55}} - R_{w-A_{0.4}})/1.5 \tag{D.31}$$

with $R_{w-A_{0.4}}$ the wave resistance prediction for $F_n = 0.40$ and $R_{w-B_{0.55}}$ the wave resistance prediction for $F_n = 0.55$ according to the respective formulae.

D.1.5 Appendage resistance

The appendage resistance is attributed to the presence of appendages such as bilge keels, rudders, bossings or open shafts and struts in the ship's hull. It can be calculated using the formula proposed by Holtrop and Mennen (1982)

$$R_{APP} = 0.5 \rho V^2 S_{APP} \left(1 + k_2\right)_{eq} C_F \tag{D.32}$$

where S_{APP} is the wetted area of the appendages, $\left(1 + k_2\right)_{eq}$ is the equivalent appendage resistance factor and C_F is the frictional resistance factor (Eq. D.7). The equivalent appendage resistance factor for a combination of appendages is given as:

$$(1+k_2)_{eq} = \frac{\sum(1+k_2)S_{APP}}{\sum S_{APP}} \tag{D.33}$$

where the tentative $(1+k_2)$ values for several types of appendages are given in Table D.2.

Table D.2. Approximate $1+k_2$ values.

Appendage type	$(1+k_2)$
Rudder behind skeg	1.5 - 2.0
Rudder behind stern	1.3 - 1.5
Twin-screw balance rudders	2.8
Shaft brackets	3.0
Skeg	1.5 - 2.0
Strut bossings	3.0
Hull bossings	2.0
Shafts	2.0 - 4.0
Stabilizer fins	2.8
Dome	2.7
Bilge keels	1.4

D.1.6 Bulbous bow resistance

On high speed vessels such as destroyers and passenger liners, a bulbous bow promotes beneficial interference between the waves generated at different points along the length of the hull. Thus, for such vessels, the bulbous bow reduces the wave making resistance. Originally, bulbous bows of a similar form were fitted to supertankers on the basis of experimental measurements indicating significant reductions in the total drag, but these reductions often exceed the total estimated wave resistance. For supertankers and similar vessels, the bulbous bow is effective in reducing the magnitude of the bow wave and thereby in avoiding wave breaking. For naval vessels, this is particularly interesting since it is related to non-acoustic signature and detection considerations.

The bulbous bow itself adds a portion of resistance, R_B, to the total calm water resistance due to pressure phenomena. In this study, this additional portion is calculated by the Holtrop and Mennen (1982) formula

$$R_B = \frac{0.11\exp\left(-3P_B^{-2}\right)F_{ni}^{\ 3}A_{BT}^{\ 1.5}\rho g}{1+F_{ni}^2} \tag{D.34}$$

where the coefficient P_B is a measure for the emergence of the bow

$$P_B = \frac{0.56\sqrt{A_{BT}}}{T_F - 1.5h_B} \tag{D.35}$$

and F_{ni} is the Froude number based on the immersion

$$F_{ni} = \frac{V}{\sqrt{g\left(T_F - h_B - 0.25\sqrt{A_{BT}}\right) + 0.15V^2}} \tag{D.36}$$

with A_{BT} the transverse area of the bulbous bow, h_B the vertical position of the centre of A_{BT}, and T_F the forward moulded draught, as stated previously.

D.1.7 Immersed transom stern resistance

The additional resistance due to pressure phenomena from the immersed transom stern is also modelled using the Holtrop and Mennen (1982) formula:

$$R_{TR} = 0.5\rho V^2 A_T c_6 \tag{D.37}$$

where c_6 is related to the Froude number based on the transom immersion, F_{nT} ,

$$c_6 = \begin{cases} 0.2\left(1 - 0.2F_{nT}\right) & \text{if } F_{nT} < 5 \\ 0 & \text{if } F_{nT} \geq 5 \end{cases} \tag{D.38}$$

while F_{nT} is given by

$$F_{nT} = \frac{V}{\sqrt{2gA_T / \left(B + BC_{WP}\right)}} \tag{D.39}$$

with A_T the transom area and C_{WP} the waterplane area coefficient, as stated above.

In Sections D.2 and D.3, the models used for the calculation of the added resistance due to the weather are presented.

D.2 Added Wind Resistance

A ship sailing on a smooth sea and in still air experiences air resistance but this is usually negligible, and it may become appreciable only in high wind. Although the wind speed and direction are never constant and considerable fluctuations can be expected in a storm, constant –average values– for wind speed and direction are usually assumed. Even in a steady wind, the speed of the wind varies with height above the sea. For consistency therefore the speed is quoted at a datum height of 10 m. Near the sea surface the wind is considerably slower than at and above the datum height. According to Davenport (1982) the variation of speed with height, U_{wind_z}, can be sufficiently represented by

$$\frac{U_{wind_z}}{U_{wind}} = \left(\frac{z}{z_g}\right)^{1/n} \tag{D.40}$$

where z_g is the datum height, U_{wind} is the mean wind speed at the datum height, and n is about 7.5 for the atmosphere (this is like the 7–th power law in turbulent boundary layers).

Since a moving ship has its own non-zero velocity, it experiences the incoming wind differently from a standing still ship. Specifically, it experiences a *relative* or *apparent wind* that is created as a combination of the true wind and the *headwind*, also called oncoming wind, created by the ship's forward motion. The relative wind velocity and direction are both calculated by the vector sum of the true wind and the headwind the ship would experience in still air, as is shown in Fig. D.2. Since the headwind vector in still air is opposing the ship's velocity, the apparent wind can also be defined as a vector subtraction: the velocity vector of the true wind minus the velocity vector of the ship.

Thus, the symbols U_{wind} and ψ_{wind} that are used in this work to describe the wind refer, specifically, to the true wind speed and direction measured during a weather forecast, which is indeed what we are going to use as an input to our problem. However since in the calculations the relative wind also needs to be taken into account, the symbols U_{wind_R} and ψ_{wind_R} are used to describe the relative wind velocity and direction, respectively. Performing the vector subtraction, the following formula for calculating relative wind speed and direction from the true wind speed, direction and ship speed are derived:

$$U_{wind_R} = \sqrt{V^2 + U_{wind}{}^2 + 2VU_{wind}\cos\psi_{wind}} \tag{D.41}$$

$$\psi_{wind_R} = \arctan\left(\frac{U_{wind}\sin\psi_{wind}}{V + U_{wind}\cos\psi_{wind}}\right) \tag{D.42}$$

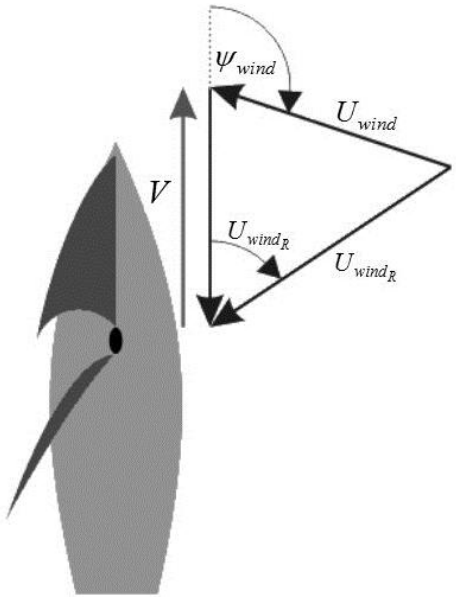

Figure D.2. Real and apparent wind speed and angle.

Figure D.3 defines a Cartesian x-y coordinate reference system for the ship. The origin is located amidship at the intersection of the still water place and on the longitudinal line of ship symmetry. Also, definitions and associated sign conventions for the longitudinal force

X_A , the lateral force Y_A and the yaw moment N_A, which are the three basic forces acted on the ship by the wind, are given.

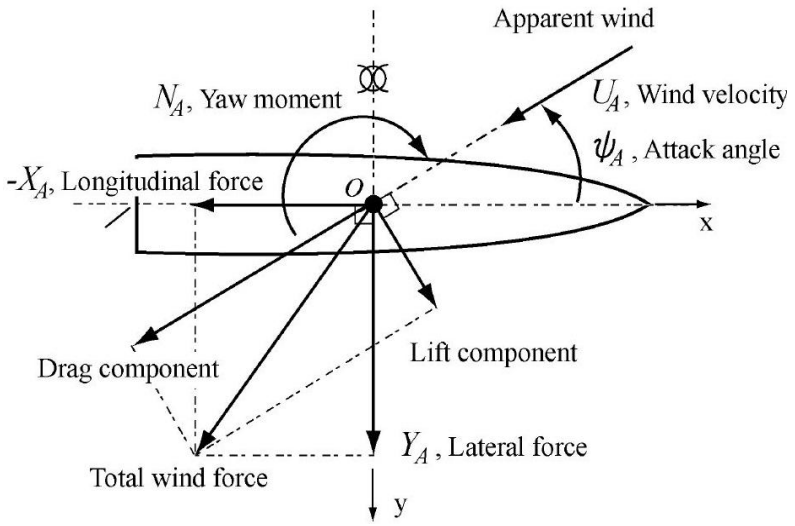

Figure D.3. Coordinate system of wind force coefficients [Fujiwara et al. (2005)].

Since in this study we are only interested in the effects of the wind on the ship's resistance, and not on ship stability, only the longitudinal wind force needs to be taken into account. The longitudinal wind force (resistance) is given in terms of a coefficient C_{XA}, which is called longitudinal wind force coefficient, and is expressed as

$$C_{XA}(\psi_{wind_R}) = \frac{X_A(\psi_{wind\,R})}{1/2\rho_A A_F U_{wind_R}{}^2} \tag{D.43}$$

where A_F is the transverse projected area of the ship and ρ_A is the density of the air. The longitudinal wind force coefficient is a function of the relative wind angle ψ_{wind_R} and typically it varies between ± 0.8 as ψ_{wind_R} from 0 to 180 degrees.

Well known studies for the prediction of the added wind resistance component based on regression of data in the literature are the studies of Isherwood (1973) and Blendermann (1996). In this study, a relatively new method proposed by Fujiwara et al. (2005) is used. The method is based on regression upon multiple data from model tests in wind tunnels in order to calculate the added wind resistance coefficient (or the longitudinal wind force coefficient)

$$\begin{aligned} C_{XA} = {} & C_{LF}\cos\psi_{wind_R} + \\ & C_{XLI}\left(\sin\psi_{wind_R} - \frac{1}{2}\sin\psi_{wind_R}\cos^2\psi_{wind_R}\right)\sin\psi_{wind_R}\cos\psi_{wind_R} + \\ & C_{ALF}\sin\psi_{wind_R}\cos^3\psi_{wind_R} \end{aligned} \tag{D.44}$$

with

$$C_{LF} = \begin{cases} \beta_{10} + \beta_{11}\dfrac{A_{YV}}{L_{OA}B} + \beta_{12}\dfrac{C_{MC}}{L_{OA}} & \text{if} \quad 0 \le \psi_{wind_R} < 90^o \\ \beta_{20} + \beta_{21}\dfrac{B}{L_{OA}} + \beta_{22}\dfrac{H_C}{L_{OA}} + \beta_{23}\dfrac{A_{OD}}{L_{OA}^{\,2}} + \beta_{24}\dfrac{A_{XV}}{B^2} & \text{if} \quad 90^o \le \psi_{wind_R} < 180^o \end{cases} \tag{D.45}$$

$$C_{XLI} = \begin{cases} \delta_{10} + \delta_{11}\dfrac{A_{YV}}{L_{OA}H_{BR}} + \delta_{12}\dfrac{A_{XV}}{BH_{BR}} & \text{if} \quad 0 \le \psi_{wind_R} < 90^o \\ \delta_{20} + \delta_{21}\dfrac{A_{YV}}{L_{OA}H_{BR}} + \delta_{22}\dfrac{A_{XV}}{A_{YV}} + \delta_{23}\dfrac{B}{L_{OA}} + \delta_{24}\dfrac{A_{XV}}{BH_{BR}} & \text{if} \quad 90^o \le \psi_{wind_R} < 180^o \end{cases} \tag{D.46}$$

$$C_{ALF} = \begin{cases} \varepsilon_{10} + \varepsilon_{11}\dfrac{A_{OD}}{A_{YV}} + \varepsilon_{12}\dfrac{B}{L_{OA}} & \text{if} \quad 0 \le \psi_{wind_R} < 90^o \\ \varepsilon_{20} + \varepsilon_{21}\dfrac{A_{OD}}{A_{YV}} & \text{if} \quad 90^o \le \psi_{wind_R} < 180^o \end{cases} \tag{D.47}$$

while for $\psi_{wind_R} = 90^o$ the added wind resistance coefficient is given by

$$C_{AA}\Big|_{\psi_{wind_R}=90^o} = \frac{1}{2}\left(C_{AA}\Big|_{\psi_{wind_R}=90^o-\mu} + C_{AA}\Big|_{\psi_{wind_R}=90^o+\mu} \right) \tag{D.48}$$

where

A_{OD}	lateral projected area of superstructures on deck
A_{XV}	area of maximum transverse section exposed to the winds
A_{YV}	projected lateral area above the waterline
B	ship breadth
C_{MC}	horizontal distance from midship section to centre of lateral projected area A_{YV}
H_{BR}	height of the top of the superstructure
H_C	height from waterline to centre of lateral projected area A_{YV}
L_{OA}	overall ship length
μ	smoothing range, normally $\mu \approx 10^o$.

The non-dimensional coefficients β_{ij}, δ_{ij} and ε_{ij} used in Eqs. (D.45)–(D.47) are given in Table D.3.

Table D.3. Coefficients for the Fujiwara formula.

	i	j				
		0	1	2	3	4
β_{ij}	1	0.922	-0.507	-1.162	-	-
	2	-0.018	5.091	-10.367	3.011	0.341
δ_{ij}	1	-0.458	-3.245	2.313	-	-
	2	1.901	-12.727	-24.407	40.310	5.481
ε_{ij}	1	0.585	0.906	-3.239	-	-
	2	0.314	1.117	-	-	-

D.3 Added Wave Resistance

Most studies of performance of a ship are based primarily on the calm water resistance of the ship hull without considering the sea condition prevailing on the route that the ship is designed to operate. This calm water resistance is used as a first estimation of the power required to drive the ship in a seaway and an allowance, called ‘‘Sea Margin’’ or ‘‘Weather Margin’’, is added to this value of the resistance to consider the effect of the environment on ship behaviour. This value of the Sea Margin is usually stated at the design stage by the ship owner or ship designer (often 15–30% of the ship calm water power), based on experience of similar ships sailing on the same route or tradition. A more accurate value of this Sea Margin can be obtained through theoretical methods that compute the added resistance of a ship based on its motions, that in turn are obtained through numerical calculations or towing tank tests.

A ship moving forward in a wave field generates two kinds of waves: waves associated with forward speed in still water, and waves associated with its motions due to the incident waves. Since both kinds of waves dissipate ship energy, it is expected to conclude that a ship moving in waves will dissipate more energy than one sailing in still water [Arribas (2007)]. This extra-induced loss of energy is called added resistance in waves and is considered to be independent of the calm water -wave making- resistance of a ship [Ström-Tejsen et al. (1973)].

According to the classical sea keeping theories, the energy dissipated of a ship can be attributed to three different components related to the energy supplied from the ship to the water and generated by the ship propulsion plant. These three components are: (i) The drifting force, obtained from the interference between incident waves, which are diffracted when encountering ship hull, and the radiated waves [Alexandersson, (2009)] produced by ship motions, especially those produced by heave and pitch, (ii) The diffraction effect, where incident waves are also reflected in ship hull (Fig. D.4), and also interact with the ship radiated waves, and (iii) A ‘‘viscous’’ effect due to the damping of the vertical motions.

Calculations and measurements indicate that the drifting force, produced by the ship motions radiated waves, would make the largest contribution to the added resistance, whereas diffraction effects would be the least significant, which is more important for short waves. Moreover, only a small part of the energy is consumed by viscous friction, since viscous damping is insignificant compared to hydrodynamic damping of ship motions. From the practical point of view, the added resistance in waves can be considered a non-viscous phenomenon [Ström-Tejsen et al. (1973)], almost produced by potential effects such as inertial and wave phenomena. The radiation induced resistance is dominating when the ship motions are big, while the diffraction induced resistance is dominating for high wave frequencies (Fig. D.4) when the ship motions are small.

On the basis of analytical considerations, in general, the three mentioned effects are considered additive (thus they can be superimposed) and proportional to the squared value of the wave amplitude and –hence– non-linear. The principle of superposition for predicting average resistance was originally stated by Maruo (1957). Rigorous proof was later demonstrated by Vassilopoulos (1967). Also, the assumption of proportionality to the squared value of the wave amplitude was the subject of numerous investigations in the early years of the numerical theories on added resistance [Gerritsma (1961), (1972); Strom-Tejsen et al. (1973); Bhattacharyya (1978); Lloyd (1998)]. Experiments reported in the literature indicate that the linear relationship between added resistance and wave height square at constant speed and wavelength can be considered a good approximation for practical purposes.

Today, it is possible to make analytical predictions of ship motions and sea loads, from the simple but powerful strip theories and time domain calculations, and some commercial codes are available for the designer. Heave and pitch motions in regular waves can be calculated with sufficient accuracy, so that these motion responses can be used with the superposition theory and the sea energy spectrum [Bhattacharyya (1978)] to make practical design predictions for the added resistance in waves. Added resistance in waves can be obtained also from model experiments in regular or irregular head waves with the ship model towed at constant speed, and added resistance measured as the difference between the mean added resistance in waves and the still water resistance measured at the same speed. Several empirical methods widely used are those of Shifrin (1973), Jinkine and Ferdinande (1974), while the analytical methods considered have been developed by Havelock (1937), Gerritsma and Beukelman (1972), Maruo (1957) and Hosoda (1973). The comparison between all the above methods which predict the added resistance as a function of regular wave characteristics is shown in Nabergoj and Prpic-Orsic (2007) for head sea conditions.

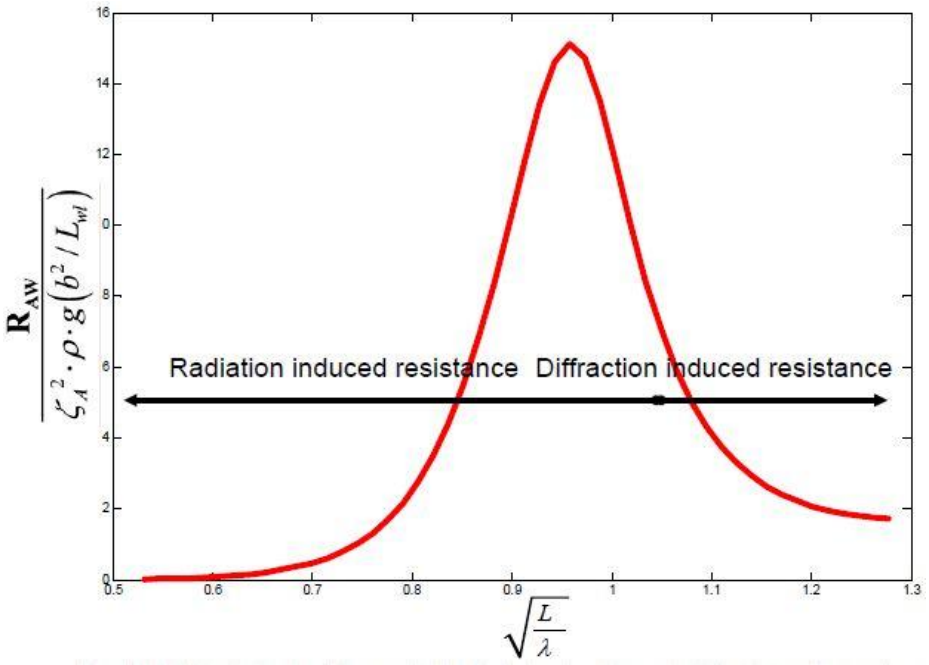

Figure D.4. Radiation and diffraction induced resistance, for different wave frequencies [Alexandersson (2009)].

The calculation of the added resistance in an irregular sea is based on the superposition principle for the components of the wave, motion and resistance spectra as well as on the assumption of linearity for the ship's response. In regular waves the added resistance varies as the square of the wave amplitude. In a wave spectrum the (total) mean added wave resistance would then be calculated from

$$R_{As} = 2\int_0^{2\pi}\int_0^{\infty} \frac{R_{wave}(\omega,\theta,V)}{\zeta_\theta^2} E(\omega,\theta)\, d\omega\, d\theta \qquad \text{(D.49)}$$

where

R_{wave} mean resistance increase in regular waves
ζ_θ wave amplitude
ω circular frequency of regular waves
θ angle between ship heading and regular waves, whereas θ_{wave} which is an input from the weather profile data used before is the primary wave direction
V ship speed
$E(\omega,\theta)$ directional spectrum of the waves:

$$E(\omega,\theta) = S_f(\omega)G(\theta) \tag{D.50}$$

with $S_f(\omega)$ being the frequency spectrum and $G(\theta)$ being the angular distribution spectrum. In this study, the modified Pierson-Moskowitz frequency spectrum of ITTC (1978) is used

$$S_f(\omega) = \frac{A_f}{\omega^{-5}} \exp\left(-\frac{B_f}{\omega^4}\right) \tag{D.51}$$

$$A_f = 173\frac{H_s}{T_1^4} \tag{D.52}$$

$$B_f = \frac{691}{T_1^4} \tag{D.53}$$

$$T_1 = 3.86\sqrt{H_s} \tag{D.54}$$

where H_s denotes the significant wave height defined before as the mean wave height (trough to crest) of the highest third of the waves.

For the angular distribution function the cosine power formula shown next is applied

$$G(\theta) = \frac{2^{2s}}{2\pi}\frac{\Gamma^2(s+1)}{\Gamma(2s+1)}\cos^{2s}\left(\frac{\theta_{wave}-\theta}{2}\right) \tag{D.55}$$

where

s directional spreading parameter (taken equal to 1 for seas and 75 for swells)
Γ Gamma function
θ_{wave} primary wave direction (as stated above).

So, the problem is translated into the calculation of the mean resistance increase in regular waves, R_{wave}. Applying the theoretical considerations examined at the start of this section, the mean resistance in regular waves is decomposed into two terms

$$R_{wave} = R_{wave_M} + R_{wave_R} \tag{D.56}$$

with R_{wave_M} being the mean resistance increase in regular waves induced by ship motion while R_{wave_R} is the mean resistance increase in regular waves induced by wave reflection.

In general the reflection resistance should be calculated with accuracy since the mean resistance increase in short waves is the predominant one.

Ideally the calculation of the mean resistance by ship motion, R_{wave_M}, is based on Maruo's theory [Maruo (1957), (1960)]. However, this involves complicated –computationally heavy– algorithms and requires much information on the geometry of the ship's hull, thus, is out of the scope of this Thesis. Based on the fact that the important term is in fact the term R_{wave_R} and not R_{wave_M}, a simplified empirical method [ITTC (2012)] is used. The method is developed to approximate the transfer function of the mean resistance increase in regular waves by using only main ship dimensions and the ship speed. The formula for the motion resistance is given as

$$R_{wave_M} = \frac{4\rho g \zeta_\theta^{\,2} B^2}{L_{pp} \cdot \overline{raw}(\omega)} \tag{D.57}$$

$$\overline{raw}(\omega) = \bar{\omega}^{b_1} \exp\left(\frac{b_1}{d_1}\left(1-\bar{\omega}^{d_1}\right)\right) a_1 F_n^{\,1.5} \exp\left(-3.5F_n\right) \tag{D.58}$$

$$\bar{\omega} = \frac{\sqrt{\frac{L_{pp}}{g}}\sqrt{k_{yy}}}{1.17F_n^{\,-0.143}}\omega \tag{D.59}$$

$$b_1 = \begin{cases} 11.0 & \text{if} \quad \omega < 1 \\ -8.5 & \text{if} \quad \omega \geq 1 \end{cases} \tag{D.60}$$

$$d_1 = \begin{cases} 14.0 & \text{if} \quad \bar{\omega} < 1 \\ -566\left(\frac{L_{pp}}{B}\right)^{-2.66} & \text{if} \quad \bar{\omega} \geq 1 \end{cases} \tag{D.61}$$

where

k_{yy}	non dimensional radius of gyration in lateral direction
L_{pp}	ship length between perpendiculars
ω	circular frequency of regular waves
θ	angle between ship heading.

Concerning the resistance increase due to reflection, R_{wave_R}, the method given in Tsujimoto et al. (2008) is used:

$$R_{wave_R} = \frac{1}{2}\rho g \zeta_\theta^{\,2} B B_f \alpha_T \left(1 + C_U F_n\right) \tag{D.62}$$

$$\alpha_T = \frac{\pi^2 I_1^{\,2}\left(k_e T\right)}{\pi^2 I_1^{\,2}\left(k_e T\right) + K_1^{\,2}\left(k_e T\right)} \tag{D.63}$$

$$B_f = \frac{1}{B}\left\{\int_I \sin^2(\theta+\beta_w)\sin\beta_w dl + \int_{II} \sin^2(\theta-\beta_w)\sin\beta_w dl\right\} \tag{D.64}$$

$$k_e = k\left(1+\Omega\cos\theta\right) \tag{D.65}$$

$$\Omega = \frac{\omega V}{g} \tag{D.66}$$

where

B_f	bluntness coefficient
C_U	advance speed coefficient
α_T	effect of draught and encounter frequency
I_1	modified Bessel function of the first kind of order 1
K_1	modified Bessel function of the second kind of order 1
k	wave number
T	ship draught
β_w	slope of the line element dl along the water line (Fig. D.5).

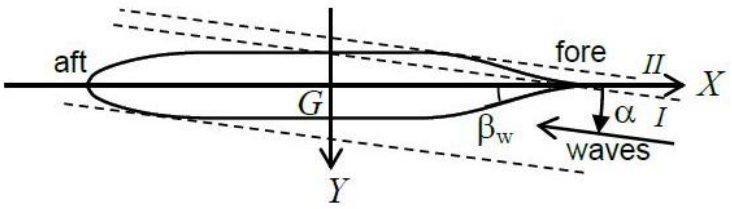

Figure D.5. Domains of integration (I&II) for calculation of bluntness coefficient [Tsujimoto et al. (2008)].

The coefficient of advance speed in oblique waves, C_U, is calculated with the empirical line shown in Fig. D.6, which has been obtained by tank tests of various ship types.

In several cases where not enough information was available about the geometry of the ship's hull, again, a simplified empirical method [ITTC (2012)] was used

$$R_{wave_R} = \frac{1}{2}\rho g \zeta_\theta^{\,2} B a_1(\omega) \tag{D.67}$$

$$a_1(\omega) = \frac{\pi^2 I_1^{\,2}(1.5kT_M)}{\pi^2 I_1^{\,2}(1.5kT_M) + K_1^{\,2}(1.5kT_M)} f_1 \tag{D.68}$$

$$f_1 = 0.692\left(\frac{V}{\sqrt{T_M g}}\right)^{0.769} + 1.81 C_B^{\,6.95} \tag{D.69}$$

where T_M is the draught at midship.

This empirical method is applicable and very accurate, if the following restrictions apply:

(1) $75(m) < Lpp < 350(m)$

(2) $4.0 < \frac{L_{pp}}{B} < 9.0$

(3) $2.2 < \frac{B}{T} < 5.5$

(4) $0.10 < F_n < 0.30$

(5) $0.5 < C_B < 0.90$

(6) the wave direction is heading (within 0 to ±45 degrees).

Since this method applies only to waves in the bow sector (±45 degrees), waves outside this sector are omitted and the angular distribution spectrum loses its meaning. The formula given in Eq. (D.49) for the calculation of the total added wave resistance in irregular seas is then simplified to the following

$$R_{AW} = 2\int_0^\infty \frac{R_{wave}(\omega,V)}{\zeta_A^2} S_f(\omega) d\omega \tag{D.70}$$

with $S_f(\omega)$ being the modified Pierson-Moskowitz frequency spectrum of ITTC (1978) as stated in Eqs. (D.51)-(D.54).

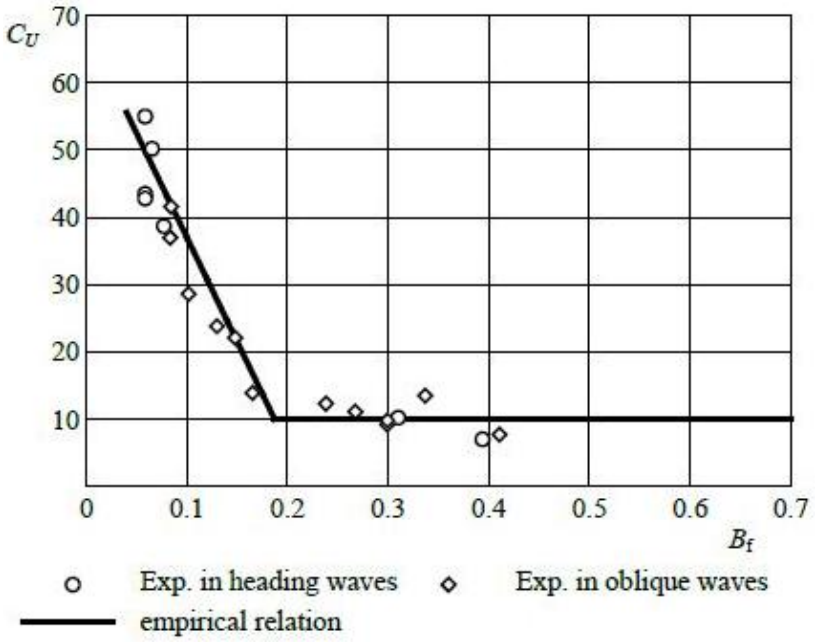

Figure D.6. Relation between the coefficient of advance speed on added resistance due to wave reflection and the bluntness coefficient for conventional hull form above water [Tsujimoto et al. (2008)].

APPENDIX E. SHIP PROPULSION

A moving ship experiences resistance forces from the sea water and the air that must be overcome by a thrust supplied by some kind of a thrust-producing mechanism. In the earliest days this consisted of manually operated oars which in turn gave places to sails and then mechanical devices such as jets, paddle wheels and finally propellers of many different forms. In the following of this section only mechanical means of propulsion will be discussed.

In the scope of finding an appropriate model that can correlate the propulsion engine with the total resistance of the ship, some basic concepts and the corresponding equations of ship powering are described. The basic power terms are schematically depicted in Fig. E.1. The brake power, $\dot{W}_b$, is the power measured at the shaft coupling by means of a mechanical, hydraulic or electrical brake. It is determined by a shop test and is calculated by the formula

$$\dot{W}_b = 2\pi Q n \tag{E.1}$$

where Q is the *brake torque* (kN·m) and n is the revolutions/sec.

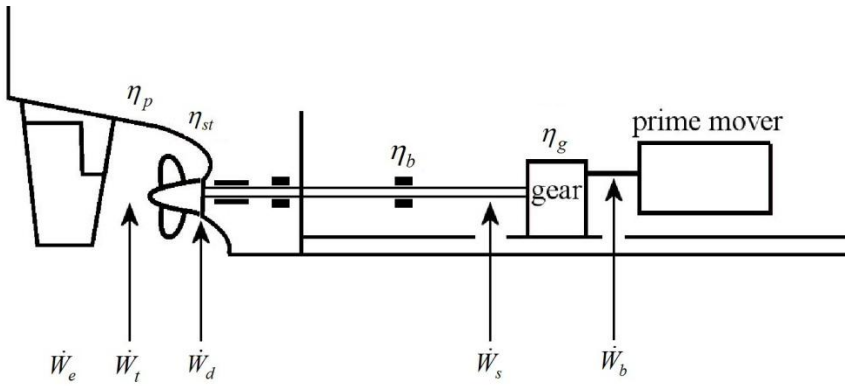

Figure E.1. Ship power definitions.

The *shaft power*, $\dot{W}_s$, is the power transmitted through the shaft and is usually measured aboard the ship by means of a torsion-meter. This instrument measures the angle of twist between two sections of the shaft, which is directly proportional to the torque transmitted. The shaft power is calculated as

$$\dot{W}_s = \dot{W}_b \eta_g \tag{E.2}$$

where η_g is the gearing efficiency. Through the bearing efficiency η_b and the stern-tube efficiency η_{st}, we arrive at the *delivered power*

$$\dot{W}_d = \dot{W}_s \eta_{st} \eta_b = \dot{W}_b \eta_g \eta_{st} \eta_b \tag{E.3}$$

which is the power available to the propeller for the propulsion of the ship.

The corresponding effective/towing power, $\dot{W}_{eff}$, since the ship moves with speed V and experiences total resistance R_T is given as:

$$\dot{W}_{eff} = R_T V \tag{E.4}$$

This effective power is related to the delivered to the propeller power, $\dot{W}_d$, through the quasi–propulsive efficiency

$$\eta_d = \frac{\dot{W}_{eff}}{\dot{W}_d} \tag{E.5}$$

where the coefficient η_d is in the range of 0.5 to 0.7 whereas all other efficiencies are very close to 1. The *total propulsive efficiency* can now be defined as

$$\eta_{prop} = \frac{\dot{W}_{eff}}{\dot{W}_b} = \eta_g \eta_{st} \eta_b \eta_d \tag{E.6}$$

Thus, the problem of correlating the effective power with the brake power, or equivalently calculating the total propulsive efficiency, is reduced to the task of calculating the quasi-propulsive efficiency, η_d. In order to do this, some basic characteristics of the propeller and of the propeller-hull interaction must be taken into account.

As the propeller advances through the water at a *speed of advance* V_A, it delivers a thrust T, and the *thrust power* is

$$\dot{W}_t = TV_A \tag{E.7}$$

The ratio of the work done on the ship to that done by the propeller is called the hull efficiency

$$\eta_h = \frac{\dot{W}_{eff}}{\dot{W}_t} = \frac{R_T V}{TV_A} \tag{E.8}$$

Also, the propeller efficiency is defined based on the torque, Q_d, on the whole propeller, as

$$\eta_p = \frac{\dot{W}_t}{\dot{W}_d} = \frac{TV_A}{2\pi n Q_d} \tag{E.9}$$

The relations between thrust, torque, and rotational speed in open water, where the inflow is uniform, cannot be expected to remain the same behind the hull in the variable flow conditions experienced there. This leads to the possibility of different propeller efficiencies in open water and behind the hull. The propeller in open water, with a uniform inflow velocity at a speed of advance V_A, has an *open water efficiency* given by

$$\eta_o = \frac{\dot{W}_t}{2\pi n Q_0} = \frac{TV_A}{2\pi n Q_0} \tag{E.10}$$

where Q_0 is the torque measured in open water when the propeller is delivering thrust T at rotational speed n. The ratio of propeller to open efficiencies under these conditions is called the *relative rotative efficiency*, being given by

$$\eta_r = \frac{\eta_p}{\eta_o} = \frac{Q_d}{Q} \tag{E.11}$$

The value of the relative rotative efficiency does not, in general, depart significantly from one, being in the range of 0.95 to 1.1 for most twin screw ships, and between 1.0 and 1.05 for single screw. From Eq. (E.5), (E.8), (E.9) and (E.11) we reach to an expression for the quasi-propulsive efficiency expressed as a multiple of hull, rotative and open water efficiencies

$$\eta_d = \frac{\dot{W}_{eff}}{\dot{W}_d} = \frac{\dot{W}_{eff}}{\dot{W}_t}\eta_p = \eta_h \eta_p = \eta_h \eta_r \eta_o \tag{E.12}$$

thus, the total propulsive efficiency, Eq. (E.6) can now be expressed as

$$\eta_{prop} = \frac{\dot{W}_{eff}}{\dot{W}_b} = \eta_g \eta_{st} \eta_b \eta_h \eta_r \eta_o \tag{E.13}$$

The division of the propulsive coefficient into factors in this way is of great assistance both in understanding the propulsion problem as well as in making estimates of propulsive efficiency for design purposes, or even creating a simple and well understood mathematical model of the system. Since the gearing, stern-tube, bearing, rotative and open-water efficiencies are usually in the range of 0.95 - 1, the term that mainly defines the total efficiency is hull efficiency. Thus the task of determining the total propulsive efficiency is reduced to the task of calculating η_h.

The propeller operates while being located behind the model or ship hull. This results in the flow being considerably modified in comparison to when working in open water. The propeller is working in water which has been disturbed by the passage of the hull, and in general the water around the stern has acquired a forward motion in the same direction as the ship. This forward moving water is called the *wake*, w, and one of the results is that the propeller is no longer advancing relatively to the water at the same speed as the ship, V, but at some lower speed, the speed of advance, V_A. This difference between speeds is the *wake speed*. The *wake fraction* is defined as

$$w = \frac{V - V_A}{V} \tag{E.14}$$

Also, when a hull is towed, there is an area of high pressure over the stern which has a resultant forward component reducing the total resistance. With a self-propelled hull, however, the pressure over some of this area is reduced by the action of the propeller in

accelerating the water flowing into it, the forward component is reduced, the resistance is increased and so is the thrust necessary to propel the model or ship. If R_T is the total resistance and T the thrust, we can write for the same ship speed

$$R_T = (1-t)T \tag{E.15}$$

where the expression $(1 - t)$ is called the *thrust deduction factor*.

Combining Eqs. (E.14) and (E.15) with Eq. (E.8) we obtain a new expression for the hull efficiency

$$\eta_h = \frac{1-t}{1-w} \tag{E.16}$$

It is noted that in some ships this is higher than one. At first sight this seems an anomalous situation in that apparently something is being obtained for nothing. It can, however, be explained by the fact that the propeller is making use of the energy which is already in the wake because of its forward velocity.

In this study, the wake and thrust factor are calculated using the formulas of Holtrop and Mennen (1982), Holtrop (1984). For single screw ships with a conventional stern we have for the wake factor

$$\begin{aligned} w = c_9 c_{20} C_V \frac{L_{OA}}{T_A}\left(0.050776 + 0.93405 c_{11}\frac{C_V}{1-C_{P_1}}\right) \\ +0.27915 c_{20}\sqrt{\frac{B}{L_{OA}\cdot\left(1-C_{P_1}\right)}} + c_{19}c_{20} \end{aligned} \tag{E.17}$$

$$c_9 = \begin{cases} c_8 & \text{if} \quad c_8 < 28 \\ 32 - \dfrac{16}{c_8 - 24} & \text{if} \quad c_8 > 28 \end{cases} \tag{E.18}$$

$$c_8 = \begin{cases} \dfrac{BS}{L_{OA}DT_A} & \text{if} \quad B/T_A < 5 \\ \dfrac{S\left(\left(7B/T_A\right)-25\right)}{LD\left(\left(B/T_A\right)-3\right)} & \text{if} \quad B/T_A > 5 \end{cases} \tag{E.19}$$

$$c_{20} = 1 + 0.015 C_{stern} \tag{E.20}$$

$$c_{11} = \begin{cases} \dfrac{T_A}{D} & \text{if} \quad \dfrac{T_A}{D} < 2 \\ 0.0833333\left(\dfrac{T_A}{D}\right)^3 + 1.33333 & \text{if} \quad \dfrac{T_A}{D} > 2 \end{cases} \tag{E.21}$$

$$c_{19} = \begin{cases} \dfrac{0.12997}{0.95-C_B} - \dfrac{0.11056}{0.95-C_P} & \text{if } C_P < 0.7 \\ \dfrac{0.18567}{1.3571-C_M} - 0.71276 + 0.38648 C_P & \text{if } C_P > 0.7 \end{cases} \tag{E.22}$$

$$c_{P_1} = 1.45 C_P - 0.315 - 0.0225 lcb \tag{E.23}$$

$$C_V = \left(1 + k_2\right) C_F + C_a \tag{E.24}$$

where

C_V viscous resistance coefficient (defined in appendix D)
C_F frictional resistance coefficient (defined in appendix D)
C_a allowance resistance coefficient (defined in appendix D)
L_{OA} overall ship length
T_A aft moulded drought
D propeller diameter
S wetted area
B ship breadth
C_{stern} stern shape coefficient (defined in appendix D)
C_P prismatic coefficient on the waterline
C_M midship section coefficient
C_B block coefficient
lcb longitudinal position at the centre of buoyancy forward of $0.5L_{OA}$ as a percentage of L_{OA}.

and for the thrust factor

$$t = \frac{0.25014 \left(\dfrac{B}{L_{OA}} \right)^{0.28956} \left(\dfrac{\sqrt{BT}}{D} \right)^{0.2624}}{\left(1 - C_P + 0.0225 lcb\right)^{0.01762} + 0.0015 C_{stern}} \tag{E.25}$$

In case of multiple screw ships or open-stern single screw, the following formulas are used instead

$$\begin{aligned} w = {} & c_9 C_V \frac{L_{OA}}{T_A} \left(0.0661875 + 1.21756 c_{11} \frac{C_V}{1 - C_{P_1}} \right) \\ & + 0.24558 \sqrt{\frac{B}{L_{OA} \cdot \left(1 - C_{P_1}\right)}} - \frac{0.09726}{0.95 - C_P} + \frac{0.11434}{0.95 - C_B} \\ & + 0.75 C_{stern} C_V + 0.002 C_{stern} \end{aligned} \tag{E.26}$$

with c_9, C_V, c_{11} and C_{P_1} calculated as in the previous formula, and

$$t = \frac{0.001979 L_{OA}}{B - BC_{p_1}} + 1.0585 c_{10} - 0.00524 - \frac{0.1418 D^2}{BT} + 0.0015 C_{stern} \tag{E.27}$$

$$c_{10} = \begin{cases} \dfrac{B}{L_{OA}} & \text{if} \quad \dfrac{L_{OA}}{B} > 5.2 \\ 0.25 - \dfrac{0.003328402}{\dfrac{B}{L_{OA}} - 0.134615385} & \text{if} \quad \dfrac{L_{OA}}{B} < 5.2 \end{cases} \tag{E.28}$$

APPENDIX F. WETTED AREA

The wetted surface is normally calculated by hydrostatic programs. In the work of Kristensen (2012), an analysis of the wetted surface data of 129 ships has been performed. The equations for the wetted surface, which have been deducted from his analysis, are shown in Table F.1, where L_{wl} is the waterline length of the ship hull.

Table F.1. Equation for the wetted surface for several ships [Kristensen (2012)].

Bulk carriers and tankers	$S = 0.99(\frac{\nabla}{T} + 1.9L_{wl}T)$
Container vessels (single screw)	$S = 0.995(\frac{\nabla}{T} + 1.9L_{wl}T)$
Twin screw ships (Ro-Ro ships) with open shaft lines (and twin rudders)	$S = 1.53(\frac{\nabla}{T} + 0.55L_{wl}T)$
Twin skeg ships (Ro-Ro ships with twin rudders)	$S = 1.2(\frac{\nabla}{T} + 1.5L_{wl}T)$
Double ended ferries	$S = 1.11(\frac{\nabla}{T} + 1.7L_{wl}T)$

The formula for calculation of the wetted surface includes the area of rudder(s) skegs and shaft lines. However any additional surfaces, *S'*, from appendages such as bilge keels, stabilizers etc., shall be taken into account by adding the area of these surfaces to the wetted surface of the main hull.

If the wetted surface, S_1, is given for a given draught, T_1, the wetted surface, S_2, for another draught, T_2, can be calculated by using the following formulas, which have been deducted based on an analysis of data for container ships, tankers and bulk carriers:

Container ships: $S_2 = S_1 - 2.4(T_1 - T_2)(L_{wl} + B)$ with $L_{wl} = 1.01L_{pp}$

Tankers and bulk carriers: $S_2 = S_1 - 2.0(T_1 - T_2)(L_{wl} + B)$ with $L_{wl} = 1.02L_{pp}$

The corresponding formula proposed by Holtrop and Mennen (1982) is

$$\begin{aligned} S = {} & L_{OA}\left(2T + B\right)\sqrt{C_M} \cdot \left(0.453 + 0.4425C_B \right. \\ & \left. - 0.2862C_M - 0.003467\,B/T + 0.3696C_{WP}\right) \\ & + 2.38\,A_{BT}/C_B \end{aligned} \tag{F.1}$$

where C_M is the midship section coefficient, C_B the block coefficient on the waterline length, C_{WP} the waterplane area coefficient and A_{BT} the transverse sectional area of the bulb at the position where the still water surface intersects the stern.

Formulas from both Kristensen and Holtrop and Mennen are adopted for the case studies of this work, depending on the quantity of available information considering the specific vessel of each case study.

APPENDIX G. BEAUFORT SCALE

The Beaufort scale is an empirical measure that relates wind speed to observed conditions at sea or on land. Its full name is the Beaufort wind force scale, although it is a measure of wind speed and not of force in the scientific sense.

In the early 19th century, naval officers made regular weather observations, but there was no standard scale and so they could be very subjective. Beaufort succeeded in standardizing the scale that went through a long and complex evolution from the previous work of others. Then it was adopted officially and first used during the voyage of HMS Beagle under Captain Robert FitzRoy, later to set up the first Meteorological Office (Met Office) in Britain giving regular weather forecasts.

Specifications and equivalent speeds									
Beaufort wind scale	Mean Wind Speed		Limits of wind speed		Wind descriptive terms	Probable wave height in metres*	Probable maximum wave height in metres*	Seastate	Sea descriptive terms
	Knots	ms^{-1}	Knots	ms^{-1}					
0	0	0	<1	<1	Calm	-	-	**0**	Calm (glassy)
1	2	1	1–3	1-2	Light air	0.1	0.1	**1**	Calm (rippled)
2	5	3	4–6	2-3	Light breeze	0.2	0.3	**2**	Smooth (wavelets)
3	9	5	7–10	4-5	Gentle breeze	0.6	1.0	**3**	Slight
4	13	7	11–16	6-8	Moderate breeze	1.0	1.5	**3–4**	Slight–Moderate
5	19	10	17–21	9-11	Fresh breeze	2.0	2.5	**4**	Moderate
6	24	12	22–27	11-14	Strong breeze	3.0	4.0	**5**	Rough
7	30	15	28–33	14-17	Near gale	4.0	5.5	**5–6**	Rough–Very rough
8	37	19	34–40	17-21	Gale	5.5	7.5	**6–7**	Very rough–High
9	44	23	41–47	21-24	Severe gale	7.0	10.0	**7**	High
10	52	27	48–55	25-28	Storm	9.0	12.5	**8**	Very High
11	60	31	56–63	29-32	Violent storm	11.5	16.0	**8**	Very High
12	-	-	64+	33+	Hurricane	14+	-	**9**	Phenomenal

Figure G.1. The Beaufort Scale [Met office (2011)].

The initial scale had thirteen classes (zero to twelve) and did not include wind speed numbers but related qualitative wind conditions to effects on the sails of a frigate. The scale was made a standard for ship's log entries on Royal Navy vessels in the late 1830s and was adapted to non-naval use from the 1850s, with scale numbers corresponding to cup anemometer rotations. In 1916, to accommodate the growth of steam power, the descriptions were changed to how the sea, not the sails, behaved and extended to land observations. Rotations to scale numbers were standardized only in 1923. The scale was extended in 1946, when forces 13 to 17 were added, intended to apply only to special

cases, such as tropical cyclones. Nowadays, the extended scale is only used in Taiwan and mainland China, which are often affected by typhoons. Internationally, WMO Manual on Marine Meteorological Services (2012 edition) defined the Beaufort scale only up to Force 12 and there was no recommendation on the use of the extended scale. A typical Beaufort scale is given in Fig. G.1.

Wind speed on the 1946 Beaufort scale is based on the empirical relationship:

$$U_{wind} = 0.836 \cdot B^{3/2} \tag{G.1}$$

where U_{wind} is the equivalent real wind speed (in m/sec) at 10 meters above the sea surface and B is the Beaufort scale number. Note that wave heights in the scale are for conditions in the open ocean, not along the shore, and that these values refer to well-developed winds.

The important, for our study, characteristic of the widely used Beaufort scale is that it provides an empirical correlation of the wind above the sea and the corresponding wave effect at the sea. As discussed earlier, in order to fully describe the weather state and use it as input to the problems, four parameters must be known: the wind speed and direction and the significant wave height and wave direction. However, in essence, only three inputs are required, since the significant wave height can be deduced from the wind speed using the Beaufort scale. Thus, in order to efficiently use the scale, interpolation is performed based on the data given in Fig. G.1 and the significant wave height is stated as a function of the wind speed. More specifically, a seventh order polynomial is used and the significant wave height (in meters) is given by the equation

$$H_s = \sum_{j=0}^{7} b_j \cdot \left(U_{wind}\right)^j \tag{G.2}$$

where the b_i coefficients are given in Table G.1.

Table G.1. Coefficients for the wave height - wind speed interpolation polynomial.

b_7	$3.61600798 \cdot 10^{-9}$	b_3	0.00732495739
b_6	$-4.513220943 \cdot 10^{-7}$	b_2	-0.0186024963
b_5	$2.330232355 \cdot 10^{-5}$	b_1	0.1433105708
b_4	-0.0006007757097	b_0	-0.01933157561

REFERENCES

Abramowitz M., Stegun I.A. (1965), "*Handbook of Mathematical Functions with Formulas, Graphs and Mathematical Tables*," New York, Dover.

Alexandersson M. (2009), "*A Study of Methods to Predict Added Resistance in Waves*", Master Thesis, KTH Centre for Naval Architecture, Stockholm, January.

Allgor R.J., Barton P.I. (1997), "Mixed Integer Dynamic Optimization," *Computers and Chemical Engineering*, Vol. 21, pp. 451-456.

Androulakis I., Venkatasubramanian V. (1991), "A Genetic Algorithm: Framework for process design and optimization," *Computers and Chemical Engineering*, Vol. 15, pp. 217-228.

Annaratone D. (2008), "*Steam Generators, Description and Design"*, Berlin, Heidelberg: Springer–Verlag; 2008.

Arcuri P., Beraldi P., Florio F., Fragiacomo P. (2015), "Optimal Design of a Small Size Trigeneration Plant in Civil Users: A MINLP (Mixed Integer Non Linear Programming) Model", *Energy*, Vol. 80, pp. 628−641.

Arribas F.P. (2007), "Some Methods to Obtain the Added Resistance of a Ship Advancing in Waves," *Ocean Engineering*, Vol. 34, pp. 946-955.

Ascher U.M., Mattheij R.M.M., Russell R.D. (1995), "*Numerical Solution of Boundary Value Problems for Ordinary Differential Equations*," Classics in Appl. Math. 13, SIAM, Philadelphia.

ATTC (1947), "Report of the Seakeeping Committee", *Proceedings of the 7th International Towing Tank Conference*.

Bader G., Ascher U. (1987), "A New Basis Implementation for Mixed Order Boundary Value ODE Solver," *SIAM Journal of Scientific Computing*, Vol. 8, pp. 483–500.

Balsa-Canto E., Vassiliadis V.S., Banga J.R. (2005), "Dynamic Optimization of Single- and Multi- Stage Systems Using a Hybrid Stochastic-Deterministic Method," *Industrial and Engineering Chemistry Research*, Vol. 44, pp. 1514–1523.

Balsa-Canto M-S.G.E., Banga J.R., Alonso A.A., Vassiliadis V.S. (2001), "Dynamic Optimization of Chemical and Biochemical Processes using Restricted Second-Order Information," *Computers and Chemical Engineering*, Vol. 25, pp. 539–546.

Banga J.R., Irizarry-Rivera R., Seider W.D. (1998), "Stochastic Optimization for Optimal and Model-Predictive Control," *Computers and Chemical Engineering*, Vol 22, No. 10, pp. 603–612.

Barberis S., Rivarolo M., Traverso A., Massardo A.F. (2016), "Thermo−economic Optimization of a Real Polygenerative District", *Applied Thermal Engineering*, Vol. 97, pp. 1−12.

Bard Y. (1974), "*Nonlinear Parameter Estimation*", Academic Press, New York.

Barton P.I., Allgor R.J., Feehery W.F., Galan S. (1998), "Dynamic Optimization in a Discontinuous World," *Industrial and Engineering Chemistry Research*, Vol. 37, pp. 966-981.

Bausa J., Tsatsaronis G. (2001), "Dynamic Optimization of Startup and Load-Increasing Processes in Power Plants" - "Part I: Method," *ASME Journal of Engineering for Gas Turbines and Power*, Vol. 123, pp. 246-250. - "Part II: Application," pp. 251-254.

Bell M.L., Limebeer D.J.N., Sargent R.W.H. (1996), "Robust Receding Horizon Optimal Control," *Computers and Chemical Engineering*, Vol. 20, pp. 781-786.

Bellman R.E. (1957), "*Dynamic Programming*," Princeton University Press, Princeton, NJ., Republished 2003, Dover.

Betts J.T. (2010), "*Practical Methods for Optimal Control and Estimation Using Nonlinear Programming*," 2nd ed., Advances in Design and Control 19, SIAM, Philadelphia.

Bhattacharyya R. (1978), "*Dynamics of Marine Vehicles*", Wiley, New York, pp. 220–227.

Biegler L.T. (1984), "Solution of Dynamic Optimization Problems by Successive Quadratic Programming and Orthogonal Collocation," *Computers and Chemical Engineering*, Vol. 8, pp. 243-248.

Biegler L.T. (2010), "*Nonlinear Programming, concepts, algorithms and application to chemical processes*," MOS-SIAM Series on Optimization.

Biegler L.T., Cervantes A.M., Wachter M.A. (2002), "Advances in Simultaneous Strategies for Dynamic Process Optimization," *Chemical Engineering Science*, Vol. 57, pp. 575-593.

Biegler L.T., Grossman I.E. (2004), "Retrospective on Optimization," *Computers and Chemical Engineering*, Vol. 28, pp. 1169–1192.

Blendermann, W. (1996), "Wind Loading on Ships-collected Data from Wind Tunnel Tests in Uniform Wind", *Institut für Schiffbau der Universität Hamburg*, Report 574.

Bock H.G., Platt, K.J. (1984), "A Multiple Shooting Algorithm for Direct Solution of Optimal Control Problems," *In 9th IFAC world congress*, pp. 242-247, Budapest.

Branke J. (2001). "*Evolutionary Optimization in Dynamic Environments*," Kluwer Academic Publishers, Norwell, MA, USA, 2001.

Bryson A.E. (1999), "*Dynamic Optimization,"* Addison Wesley Longman, Inc.

Bryson A.E., Ho Y.C. (1969), "*Applied Optimal Control*," Blaisdell Publishing Company, Blaisdell, Waltham, MA, 1969.

Bu Z., Zheng B. (2010), "Perspectives in Dynamic Optimization Evolutionary Algorithm," *Advances in Computation and Intelligence*, Vol. 6382 of Lecture Notes in Computer Science, pp. 338–348. Springer Berlin / Heidelberg, 2010.

Buoro D., Casisi M., Pinamonti P., Reini M. (2012), "Optimal Synthesis and Operation of Advanced Energy Supply Systems for Standard and Domotic Home", *Energy Conversion and Management,* Vol. 60, pp. 96-105.

Calise F., Dentice d' Accadia M., Vanoli L., Von Spakovsky M.R. (2007), "Full Load Synthesis/Design Optimization of a Hybrid SOFC–GT Power Plant", *Energy* Vol. 32, pp. 446–458.

Caputo M.R. (2005), "*Foundations of Dynamic Economic Analysis: Optimal Control Theory and Applications*," Cambridge University Press.

Cardona E., Piacentino A. (2007), "Optimal Design of CHCP Plants in the Civil Sector by Thermoeconomics," *Applied Energy*, Vol. 84, pp. 729-748.

Carey G.F., Finlayson B.A. (1974), "Orthogonal Collocation on Finite Elements," *Chemical Engineering Science*, Vol. 30, pp. 587–596.

Carvalho M., Serra L.M., Lozano M.A. (2011), "Optimal Synthesis of Trigeneration Systems Subject to Environmental Constraints," *Energy*, Vol. 34, pp. 261-273.

Cervantes A., Biegler L.T. (1998), "Large-scale DAE Optimization using a Simultaneous NLP Formulation," *American Institute of Chemical Engineers Journal*, Vol. 44, No. 5, pp. 1038-1050.

Chachuat B. (2009), "Optimal Control Lectures 19-20: Direct Solution Methods," *Department of Chemical Engineering, McMaster University, downloaded from*: "http://la.epfl.ch/files/content/sites/la/files/shared/import/migration/IC_32/Slides19-21.pdf", (last access date 25/7/2012).

Chen H.J., Wang D.W.P., Chen S.L. (2005), "Optimization of an Ice-Storage Air Conditioning System using Dynamic Programming Method," *Applied Thermal Engineering*, Vol. 25, pp. 461-472.

Chen M.W., Zalzala A.M.S. (1997), "Dynamic Modelling and Genetic-Based Trajectory Generation for Non-Holonomic Mobile Manipulators," *Control Engineering Practice*, Vol. 5, pp. 39–48.

Chen S.Y., Wu C.H., Hung Y.H., Chung C.T. (2018), "Optimal Strategies of Energy Management Integrated with Transmission Control for a Hybrid Electric Vehicle using Particle Swarm Optimization", *accepted for publication in Energy*, Vol. 155, *doi: 10.1016/j.energy.2018.06.023*.

Cheng C., Liao S., Tang Z.T., Zhao M.Y. (2009), "Comparison of Particle Swarm Optimization and Dynamic Programming for Large Scale Hydro Unit Load Dispatch," *Energy Conversion and Management*, Vol. 50, pp. 3007-3014.

Crescitelli S., Nicoletti S. (1973), "Near Optimal Control of Batch Reactors," *Chemical Engineering Science*, Vol. 28, pp. 463–471.

Cuthrell J.E., Biegler L.T. (1987), "On the Optimization of Differential-Algebraic Process Systems," *American Institute of Chemical Engineers Journal*, Vol. 33, pp. 1257-1270.

Cuthrell J.E., Biegler L.T. (1989), "Simultaneous Optimization Methods for Batch Reactor Control Profiles," *Computers and Chemical Engineering*, Vol. 13, pp. 49-62.

Dadebo S.A., McAuley K.B. (1995), "Dynamic Optimization of Constrained Chemical Engineering Problems using Dynamic Programming," *Computers and Chemical Enineering.*, Vol. 19, pp. 513–525.

Dakev N.V., Chipperfield A.J., Whidborne J.F., Fleming P.J. (1996), "An Evolutionary Algorithm Approach for Solving Optimal Control Problems," *IFAC 13th Triennial World Congress*, pp. 321–326, San Francisco, USA.

Davenport A. G., "The Interaction of Wind and Structures," in: *E. Plate(Ed.), Engineering Meteorology*, Elsevier Scientific Publishing Company, Amsterdam, pp. 557-572 (Chapter 12).

Dimopoulos G. (2009), "*Synthesis, Design and Operation Optimization of Marine Energy Systems*," Ph.D. Thesis, National Technical University of Athens, School of Naval Architecture and Marine Engineering.

Dimopoulos G.G., Frangopoulos C.A. (2008), "Synthesis, Design and Operation Optimization of the Marine Energy System for a Liquefied Natural Gas Carrier," *International Journal of Thermodynamics*, Vol. 11, No. 4, pp. 203-211.

Dimopoulos G.G., Kougioufas A.V. and Frangopoulos C.A. (2008), "Synthesis, Design and Operation Optimization of a Marine Energy System," *Energy*, Vol. 33, pp. 180–188.

Du H., Xiong W., Jiang Z., Wang L. (2018), "Energy Efficiency Control of Pneumatic Actuator Systems Through Nonlinear Dynamic Optimization", *Journal of Cleaner Production*, Vol 184, pp. 511-519.

Edgar T.F., Himmelblau D.M. (1988), "*Optimization of Chemical Processes*," New York, McGraw-Hill.

Eggers K.W.H., Sharrna S.D., Ward L.W. (1967),"An Assessment of Some Experimental Methods for Determining the Wavemaking Characteristics of a Ship Form", *Transactions SNAME*, Vol. 75, pp. 112–144.

EPA U.S. Environmental Protection Agency: Characterization of Combined Heat and Power Technologies, http://www.epa.gov/CHP/ (visited: 2014).

Erickson L.L. (1990), "Panel Methods: An Introduction", *NASA Technical Paper 2995*, NASA, 1990.

Evins R. (2015), "Multi−level Optimization of Building Design, Energy System Sizing and Operation." Energy 2015, Vol. 90, pp. 1775−1789.

Feehery W. F. (1998), "Dynamic Optimisation with Path Constraints," Ph.D thesis, MIT.

Feehery W.F., Barton P.I. (1998), "Dynamic Optimization with State Variable Path Constraints," *Computers and Chemical Engineering*, Vol. 22, No. 9, pp. 1241–1256.

Feehery W.F., Tolsma J.E, Barton P.I. (1997), "Efficient Sensitivity Analysis of Large-Scale Differential-Algebraic Systems," *Applied Numerical Mathematics*, Vol. 25, No 1, pp. 41–54.

Fikar M., Latifi M.A. (2002), "User's Guide for FORTRAN Dynamic Optimisation Code DYNO," *Technical Report mf0201, LSGC CNRS*, Nancy, France; STU Bratislava, Slovak Republic.

Frangopoulos C.A. (1991a), "Intelligent Functional Approach: A Method for Analysis and Optimal Synthesis−Design−Operation of Complex Systems", *International Journal of Energy, Environment and Economics*, Vol. 1, pp. 267−274.

Frangopoulos C.A. (1991b), "Optimization of Synthesis−Design−Operation of a Cogeneration System by the Intelligent Functional Approach", *International Journal of Energy, Environment and Economics*, Vol. 1, pp. 275−287.

Frangopoulos C.A. (1992), "Optimal Synthesis and Operation of Thermal Systems by the Thermoeconomic Functional Approach", *Journal of Engineering for Gas Turbines and Power*, Vol. 114, pp. 707−714.

Frangopoulos C.A., Lygeros A.I., Markou C.T., Kaloritis P. (1996), "Thermoeconomic Operation Optimization of the Hellenic Aspropyrgos Refinery Combined-cycle Cogeneration System", *Applied Thermal Engineering*, Vol. 16, No. 12, pp. 949-958.

Frangopoulos C.A., Von Spakovsky M.R., Sciubba E. (2002), "A Brief Review of Methods for the Design and Synthesis Optimization of Energy Systems", *International Journal of Applied Thermodynamics*, Vol. 5, No. 4, pp. 151–160.

Frangopoulos, C.A. (1990), "Intelligent Functional Approach: a Method for Analysis and Optimal Synthesis-Design-Operation of Complex Systems," *A Future for Energy*, S. S. Stecco and M. J. Moran, Eds., Florence World Energy Re-search Symposium, Florence, Italy, May 28-June 1, pp. 805-815, Pergamon Press, Oxford.

Froude W. (1872), "Experiments on the Surface-friction Experienced by a Plane Moving Through Water", *42nd Report of the British Association for the Advancement of Science*, Brighton, 1872.

Froude, W. (1874), "Report to the Lords Commissioners of the Admiralty on Experiments for the Determination of the Frictional Resistance of Water on a Surface, Under Various Conditions", *44th Report by the British Association for the Advancement of Science*, performed at Chelston Cross, under the Authority of their Lordships, Belfast, 1874.

Fuentes−Cortés L.F., Ponce−Ortega J.M., Nápoles−Rivera F., Serna−González M., El−Halwagi M. (2015), "Optimal Design of Integrated CHP Systems for Housing Complexes", *Energy Conversion and Management*, Vol. 99, pp. 252–263.

Fujiwara T., Ueno M., Ikeda Y. (2005), "A New Estimation Method of Wind Forces and Moments acting on Ships on the basis of Physical Component Models", *Journal of Japan Society of Naval Architects and Ocean Engineers*, Vol. 2. pp. 243–255.

Furlonge H.I., Pantelides C.C., Sorensen E. (1999), "Optimal Operation of Multivessel Batch Distillation Columns," *American Institute of Chemical Engineers Journal*, Vol. 45, No. 4, pp. 781-800.

Garg D., Patterson M., Hagera W.W., Raoa A.V., Bensonb D.A., Huntington G.T. (2010), "A Unified Framework for the Numerical Solution of Optimal Control Problems using Pseudospectral Methods," *Automatica, doi: 10.1016 / Journal of.Automatica*. 2010.06.048.

Gelfand I.M, Fomin S.V., Silverman R.A. (1963), "*Calculus of Variations*," Courier Dover Publications, 1963.

Georgopoulos N.G., von Spakovsky M.R., Muñoz J.R. (2002), "A Decomposition Strategy Based on Thermoeconomic Isolation Applied to the Optimal Synthesis/Design and Operation of a Fuel Cell Based Total Energy System", *Proceedings of the IMECE 2002, ASME International Mechanical Engineering Congress & Exposition* November 17–22, 2002, New Orleans, Louisiana.

Gerritsma J., Beukelman W. (1972), "Analysis of the Resistance Increase in Waves of a Fast Cargo Ship", *International Shipbuilding Progress*, Vol. 19, No. 217.

Gerritsma J., Van der Bosch J.J., Beukelman W. (1961), "Propulsion in Regular and Irregular Waves", *International Shipbuilding Progress*, Vol. 8, No. 82, pp. 285–293.

Gill P.E, Murray W., Wright M.H. (1981), "*Practical Optimization*," Academic Press Inc., London, 1981.

Gill P.E., Murray, W., Saunders, M.A. (1997), ‘‘SNOPT: An SQP Algorithm for Large-Scale constrained Optimization,’’ *Tech. Rep. NA 97-2*, Department of Mathematics, University of California, San Diego.

Goderbauer S., Bahl B., Voll P., Lübbeckeb M., Bardow A., Koster A.M.C.A. (2016), “An Adaptive Discretization MINLP Algorithm for Optimal Synthesis of Decentralized Energy Supply Systems”, *Computers and Chemical Engineering*, Vol. 95, pp. 38–48.

gPROMS, 2016, User Guide, Version 4.1.1, Process Systems Enterprise Ltd., London, United Kingdom.

GTW (2010), *Gas Turbine World Handbook*, Pequot Publishing, Southport CT.

Gutin, G., Punnen, A.P. (2006), "*The Traveling Salesman Problem and Its Variations*," Springer.

Havelock T.H. (1942), "Drifting Force on a Ship among Waves", *Philosophical Magazine*, Vol. 33.

Hazewinkel M. (2001), "*Lagrange interpolation formula*," Encyclopedia of Mathematics, Springer.

Holtrop J. (1984), "A Statistical Re-Analysis of Resistance and Propulsion Data", *International Shipbuilding Progress*, Vol. 28, No. 363, pp. 272–276.

Holtrop J., Mennen G.G.J. (1982), "An Approximate Power Prediction Method", *International Shipbuilding Progress*, Vol. 29, No. 335, pp. 166–170.

Hosoda, R. (1973), "The Added Resistance of Ships in Regular Oblique Waves", *Japanese Society of Naval Architects*, Vol. 133, pp. 1-20.

Hughes G. (1963), "Correlation of Model Resistance and Application to Ship", R.I.N.A.

Hughes G. (1965), "Ship Model Viscous Resistance Coefficients ", *NPL Ship TM*, Vol. 80.

Ikehata M. (1969), "On Experimental Determination of Wave-Making Resistance of A Ship", *Japan Shipbuilding & Marine Engineering*, Vol. 4, No. 5 p. 5–14.

Isherwood R.M. (1973), "Wind Resistance on Merchant Ships", *Transactions of R.I.N.A.*, Vol. 115.

ITTC (1987), "Report of the Seakeeping Committee", *Proceedings of the 18th International Towing Tank Conference*, Vol. 1, pp. 401–468.

ITTC (2012), "Recommended Procedures and Guidelines", *Speed and Power Trials, Part 2*, 7.5-04-01-01.2, pp. 1–25.

Jacobson D.H., Speyer J.L., Lele M.M. (1971), "New Necessary Conditions of Optimality for Control Problems with State-Variable Inequality Constraints," *Journal of Mathematical Analysis and Applications*, Vol. 35, No. 2, pp. 255–284.

Jinkine V., Ferdinande V. (1974), "A Method for Predicting the Added Resistance of Fast Cargo Ships in Head Waves", *International Shipbuilding Progress*, Vol. 21, pp. 149-167.

Kalikatzarakis M., Frangopoulos C.A. (2017), “Thermo-economic Optimization of Synthesis, Design and Operation of a Marine Organic Rankine Cycle System”, *Proc IMechE Part M: J. Engineering for the Maritime Environment*, Vol. 231, No. 1, pp. 137–152.

Kavvadias K.C., Maroulis Z.B. (2010), "Multi-Objective Optimization of a Trigeneration Plant," *Energy Policy*, Vol. 38, pp. 945-954.

Kehlhofer R. (1997), *Combined-Cycle Gas & Steam Turbine Power Plants*, PennWell Publishing, Tulsa, 1997.

Kendall A.A. (1989), "*An Introduction to Numerical Analysis* (2nd ed.), "New York, John Wiley & Sons.

Kikkinides E.S., Georgiadis M.C., Stubos A.K. (2006), "Dynamic Modeling and Optimization of Hydrogen Storage in Metal Hydride Beds," *Energy*, Vol. 31, pp. 2428-2446.

Kim K., von Spakovsky M.R., Wang M., Nelson D.J. (2011), "A Hybrid Multi-level Optimization Approach for the Dynamic Synthesis/Design and Operation/Control Under Uncertainty of a Fuel Cell System", *Energy*, Vol. 36, pp. 3933–3943.

Kim K., Wang M., von Spakovsky M.R., Nelson D.J. (2008), "Dynamic Synthesis/Design and Operation/Control Optimization Under Uncertainty of a PEMFC System", In: *Proceedings of IMECE 2008 ASME International Mechanical Engineering Congress and Exposition*, Boston, Massachusetts, USA, October 31–November 6 2008, paper no. 68070, pp. 679-689, New York: ASME.

Ko D., Lee M., Jang W.H., Krewer U. (2008), "Non-Isothermal Dynamic Modelling and Optimization of a Direct Methanol Fuel Cell," *Journal of Power Sources*, Vol. 180, pp. 71-83.

Kougioufas A. (2005), "*Marine Energy System Optimization with Reliability and Availability Considerations*", Diploma Thesis, National Technical University of Athens, Athens, Greece.

Kraft D. (1994), "Algorithm 733: TOMPs Fortran Modules for Optimal Control Calculations," *ACM Transactions on Mathematical Software*, Vol. 20, pp. 262-281.

Kristensten H. O. (2012), "Prediction of Resistance and Propulsion Power of Ships," *Project no. 2010-56, Emissionsbeslutningsstøttesystem Work Package 2, Report no. 4*, Technical University of Denmark, October 2012.

Krupiczka R., Rotkegel A., Walczyk H., Dobner L. (2003), "An Experimental Study of Convective Heat Transfer from Extruded Type Helical Finned Tubes", *Chemical Engineering and Processing*, Vol. 42, pp. 29–38.

Laurie D.P. (2001), "Computation of Gauss-type Quadrature Formulas," *Journal of Computational and Applied Mathematics*, Vol. 127, pp. 201-217.

Lawler E.L., Lenstra J.K., Rinnooy K.A.H.G., Shmoys D.B. (1985), "*The Traveling Salesman Problem: A Guided Tour of Combinatorial Optimization*," John Wiley & Sons.

Lloyd A.R.J.M. (1998), "Ship Behaviour in Rough Weather", *ARJM Lloyd*, UK, pp. 150–151.

Logsdon J.S., Biegler L.T. (1989), "Accurate Solution of Differential-Algebraic Optimization Problems," *Industrial and Engineering Chemistry Research*, Vol. 28, No. 11, pp. 1628-1639.

Logsdon J.S., Biegler L.T. (1992), "Decomposition Strategies for Large Scale Dynamic Optimization Problems," *Chemical Engineering Science*, Vol. 47, No. 4, pp. 851–864.

Luus R. (1990), "Application of Dynamic Programming to High-Dimensional Non-Linear Optimal Control Problems," *International Journal of Control*, Vol. 52, pp. 239–250.

MacRosty D.M.R., Swartz L.E. (2007), "Dynamic Optimization of Electric Arc Furnace Operation," *American Institute of Chemical Engineers Journal*, Vol. 53, No. 3, pp. 640-653.

MAN, Computerized Engine Application System (CEAS). Last accessed 20/09/2017. http://marine.mandieselturbo.com/two-stroke/ceas.

Marano V., Rizzo G., Tiano F.A. (2012), "Application of Dynamic Programming to the Optimal Management of a Hybrid Power Plant with Wind Turbines, Photovoltaic Panels and Compressed Air Energy Storage," *Applied Energy*,Vol. 97, pp. 849–859.

Martelli E., Carpa F., Consonni S. (2015) "Numerical Optimization of Combined Heat and Power Organic Rankine Cycles – Part B: Simultaneous Design & Part−load Optimization", *Energy*, Vol. 90, pp. 329−343.

Maruo H. (1957), "The Excess Resistance of a Ship in Rough Seas", *International Shipbuilding Progress*, Vol. 4, No. 35, pp. 337–345.

Maruo H. (1960), "The Drift of a Body Floating on Waves", *Journal of Ship Research*, Vol. 4, No. 3, pp. 1−10.

McKay B., Willis M., Barton G. (1997), "Steady-State Modelling of Chemical Process Systems Using Genetic Programming," *Computers & Chemical Engineering*, Vol. 21, pp. 981–996.

Mehnen J., Wagner T., Rudolph G. (2006), "Evolutionary Optimization of Dynamic Multi-Objective Test Functions," In *Proceedings of the Second Italian Workshop on Evolutionary Computation (GSICE2)*, Collegio S. Chiarra, CD-ROM proceedings, September 2006.

Met Office (2011), "National Meteorological Library and Archive Fact sheet 6 — The Beaufort Scale", Met Office. Retrieved 2011-05-13.

Michalewicz Z., Dasgupta D., Le Riche R.G., Schoenauer M. (1996), "Evolutionary Algorithms for Constrained Engineering Problems," *Computers & Industrial Engineering Journal*, Vol. 30, No. 2, pp. 851-870.

Mitchell J.H. (1898), "The Wave Resistance of a Ship", *Philosophical Magazine*, Vol. 45, Ser. 5, pp.106–123.

Miyatake M., Ko H. (2010), "Optimization of Train Speed Profile for Minimum Energy Consumption," *IEEJ Transactions on Electrical and Electronic Engineering*, Vol. 5, pp. 263-269.

Mohideen M.J., Perkins J.D., Pistikopoulos E.N. (1996), "Optimal Synthesis and Design of Dynamic Systems Under Uncertainty", *Computers and Chemical Engineering*, Vol. 20, pp 895–900.

Moiseiwitsch, B.L. (1966), "*Variational Principles*," Interscience Publishers, London and New York, 1966.

Morimoto T., Hatou K., Hashimoto Y. (1996), "Intelligent Control for a Plant Production System", *Control Engineering Practice*, Vol. 4, pp. 773–784.

Moros R., Kalies H., Rex H.G., Schaffarczyk S. (1996), "A Genetic Algorithm for Generating Initial Parameter Estimations for Kinetic Models of Catalytic Processes," *Computers & Chemical Engineering*, Vol. 20, pp. 1257–1270.

Munoz J.R., Von Spakovsky M.R. (2001a), "A Decomposition Approach for the Large Scale Synthesis/Design Optimization of Highly Coupled, Highly Dynamic Energy Systems", *International Journal of Applied Thermodynamics*, Vol. 4, No. 1, pp. 19-33.

Munoz J.R., Von Spakovsky M.R. (2001b), "The Application of Decomposition to the Large Scale Synthesis/Design Optimization of Aircraft Energy Systems", *International Journal of Applied Thermodynamics*, Vol. 4, No. 2, pp. 61-76.

Munoz J.R., Von Spakovsky M.R. (2003), "Decomposition in Energy System Synthesis/Design Optimization for Stationary and Aerospace Applications", *Journal of Aircraft*, Vol. 40, No. 1, pp. 35–42.

Mussati S.F., Aguirre P.A., Scenna N.J. (2004), "A Rigorous, Mixed-integer, Nonlineal Programming Model (MINLP) for Synthesis and Optimal Operation of Cogeneration Seawater Desalination Plants", *Desalination* Vol. 166, pp. 339–345.

Nabergoj R., Prpic-Oršic J. (2007), "A Comparison of Different Methods for Added Resistance Prediction", 22nd IWWWFB, Plitvice, Croatia.

Neuman C.P., Sen A. (1973), "A Suboptimal Control Algorithm for Constrained Problems Using Cubic Splines," *Automatica*, Vol. 9, pp. 601-613.

Norstad I., Fagerholt K., Laporte G. (2011), "Tramp Ship Routing and Scheduling With Speed Optimization", Transportation Research Part C, Vol. 19, pp. 853-865.

NTC, (2018), Nye Thermodynamics Corporation, Last access date: December 2017. http://nyethermodynamics.com/trader/manprice.htm.

Olsommer B. (1998), "Time-dependent Thermoeconomic Modeling and Optimization of the Synthesis, Design and Operation of a Waste Incineration Cogeneration Power Plant (Méthode d'optimisation thermoéconomique appliquée aux centrales d'incinération d'ordures à cogénération avec appoint énergétique)", Ph.D Thesis, EPFL, Lausanne.

Olsommer B., Favrat D., Von Spakovsky M.R. (1999), "An Approach for the Time-dependent Thermoeconomic Modeling and Optimization of Energy System Synthesis, Design and Operation Part I: Methodology and Results", *International Journal of Applied Thermodynamics* Vol. 2, No. 3, pp. 97–114.

Ondeck A., Edgar T.F., Baldea M. (2017), "A Multi−scale Framework for Simultaneous Optimization of the Design and Operating Strategy of Residential CHP Systems", *Applied Energy*, Vol. 205, pp. 1498−1511.

Oyarzabal B., Von Spakovsky M.R., Ellis M.W. (2004), "Optimal Synthesis/Design of a PEM Fuel Cell Cogeneration System for Multi-unit Residential Applications– Application of a Decomposition Strategy", *Journal of Energy Resources Technology*, Vol. 126, pp 30–39.

Papanikolaou A. (2010), "Holistic ship design optimization", *Computer-Aided Design*, Vol. 42, pp. 1028–1044.

Pelster S. (1998), "Environomic Modeling and Optimization of Advanced Combined Cycle Cogeneration Power Plants Including CO_2 Separation Options", PhD Thesis, EPFL, Lausanne.

Pelster S., Favrat D., Von Spakovsky M.R. (2001), "The Thermoeconomic and Environomic Modeling and Optimization of the Synthesis, Design, and Operation of Combined Cycles with Advanced Options", *Journal of Engineering for Gas Turbines and Power* Vol. 123, pp. 717–726.

Petruschke P., Gasparovic G., Voll P., Krajacic G., Duic N., Bardow A. (2014), "A Hybrid Approach for the Efficient Synthesis of Renewable Energy Systems", *Applied Energy*, Vol. 135, pp. 625–633.

Phillips C.A., Drake J.C. (2000), "Trajectory Optimization for a Missile Using a Multitier Approach," *Journal of Spacecraft and Rockets*, Vol. 37, No. 5, September–October

Phillips, C.A. (1988), "Energy Management for a Multiple Pulse Missile", *American Institute of Aeronautics and Astronautics Paper 88-0334*, January.

Politis G.K. (2018), "*Ship Resistance and Propulsion*," 5th edition, National Technical University of Athens, Athens, 2018, (available for dowlload in: "https://1drv.ms/b/s!AuhmkWH18AWoiDXr-F9dA0_CO2v8").

Politis G.K., Skamnelis F.A. (2007), "*Ship Resistance*," 2nd edition, National Technical University of Athens, Athens, 2007.

Pontryagin L.S., Boltyanskii V.G., Gamkrelidze R.V., Mishchenko E.F. (1962), "*The Mathematical Theory of Optimal Processes*," Interscience, New York.

Powell K.M., Hedengren J.D., Edgar T.F. (2013), "Dynamic Optimization of a Solar Thermal Energy Storage System over a 24 Hour Period using Weather Forecasts," *American Control Conference Proceedings, 2013*.

Powell K.M., Hedengren J.D., Edgar T.F. (2014), "Dynamic Optimization of a Hybrid Solar Thermal and Fossil Fuel System", *Solar Energy*, Vol. 108, pp. 210–218.

Prata A., Oldenburg J., Kroll A., Marquardt W. (2008), "Integrated Scheduling and Dynamic Optimization of Grade Transitions for a Continuous Polymerization Reactor," *Computers and Chemical Engineering*, Vol. 32, pp. 463-476.

Psaraftis H.N. (1988), "Dynamic Vehicle Routing Problems," *Vehicle Routing: Methods and Studies*, Vol. 16, pp. 223–248.

Rajesh J., Gupta K., Kusumakar H.S., Jayaraman V.K., Kulkarni B.D. (2001), "Dynamic Optimization of Chemical Processes using Ant Colony Framework," *Computers and Chemistry*, Vol. 25, pp. 583–595.

Rancruel D.F. (2005), "Dynamic Synthesis/Design and Operational/Control Optimization Approach Applied to a Solid Oxide Fuel Cell Based Auxiliary Power Unit Under Transient Conditions", Ph.D. Dissertation, Virginia Polytechnic Institute and State University, Blacksburg, VA.

Rancruel D.F., Von Spakovsky M.R. (2003), "Decomposition with Thermoeconomic Isolation Applied to the Optimal Synthesis/Design of an Advanced Tactical Aircraft System", *International Journal of Thermodynamics*, Vol. 6, No. 3, pp. 93–105.

Rancruel D.F., Von Spakovsky M.R. (2005), "Development and Application of a Dynamic Decomposition Strategy for the Optimal Synthesis/Design and Operational/Control of a SOFC Based APU Under Transient Conditions", In: *Proceedings of the*

International Mechanical Engineering Congress and Exposition—IMECE, Orlando, Florida, USA, November 5-11 2005, paper No. 82986. New York: ASME.

Rao S.S. (1996), "*Engineering Optimization: Theory and Practice,"* 3rd ed., John Wiley & Sons, New York.

Ray W.H. (1981), "*Advanced Process Control,*" McGraw-Hill, New York.

Renfro J.G., Morshedi A.M., Asbjornsen A. (1987), "Simultaneous Optimization and Solution of Systems Described by Differential/Algebraic Equations," *Computers and Chemical Engineering*, Vol. 11, No. 5, pp. 503-517.

Reynolds O. (1883), "An Experimental Investigation of the Circumstances which Determine Whether the Motion of Water Shall be Direct or Sinuous, and the Law of Resistance in Parallel Channels", *Philosophical Transactions of the Royal Society*, Vol. 174, pp. 935–982.

Rodriguez M., Diaz M.S. (2006a), "Large-Scale Dynamic Optimization of an Integrated Cryogenic Process," *Computer Aided Chemical Engineering*, Vol. 21, pp. 1477-1482.

Rodriguez M., Diaz M.S. (2006b), "Dynamic Modeling and Optimization of Cryogenic Systems," *Applied Thermal Engineering*, Vol. 27, pp. 1182-1190.

Rund H. (1966), "*The Hamilton-Jacobi Theory in the Calculus of Variations: Its Role in Mathematics and Physics,"* Van Nostrand, London and New York, 1966.

Saerens B., Vandersteen J., Persoons T., Swevers J., Diehl M., Van der Bulck E. (2009), "Minimization of the Fuel Consumption of a Gasoline Engine using Dynamic Optimization," *Applied Energy*, Vol. 86, pp. 1582-1588.

Sargent R.W.H., Sullivan G. R. (1979). "Development of Feed Change-Over Policies for Refinery Distillation Units," *Industrial & Engineering Chemistry Process Design and Development*, Vol. 18, pp. 113-124.

Schoenherr K.E. (1932), "Resistance of Flat Surfaces Moving Through a Fluid", *Transactions of the Society of Naval Architects and Marine Engineers*, Vol. 40.

Schulz V.H., Bock H.G., Steinbach M.C. (1998), "Exploiting Invariants in the Numerical Solution of Multipoint Boundary Value Problems for DAE", *SIAM Journal on Scientific Computing*, Vol. 19, No 2, pp. 440-467.

Schweiger G., Larsson P., Magnusson F., Lauenburg P., Velut S., (2017), "District Heating and Cooling Systems – Framework for Modelica-based Simulation and Dynamic Optimization", *Energy*, Vol. 137, pp. 566-578.

Shah R., Sekulic D. (2003), "*Fundamentals of heat exchanger design*", New Jersey: John Wiley & Sons; 2003, p.111.

Shifrin L.S. (1973), "Priblizennyj rascet dopolnitel'nogo soprotivlenija sudna na regularnom volnenii", *Sudostroenie*, Vol. 12, pp. 5-7.

SNAME (1973), *Marine Steam Power Plant Heat Balance Practices*, Society of Naval Architects and Marine Engineers, Jersey City, NJ.

Software MarineGTs (2015), Laboratory of Thermal Turbomachines, NTUA, https://www.ltt.ntua.gr/index.php/en/softwaremn/marine-gts.

Sorensen E., Macchietto S., Stuart G., Skogestad S. (1996), "Optimal Control and On-Line Operation of Reactive Batch Distillation," *Computers and Chemical Engineering* Vol. 20, No. 12, pp. 1491-1498.

Srinivasan B., Bonvin D., Visser E., Palanki S. (2003b), "Dynamic Optimization of Batch Processes: II. Role of Measurements in Handling Uncertainty," *Computers and Chemical Engineering*, Vol. 27, No. 1, pp. 27-44.

Srinivasan, B., Myszkorowski P., Bonvin D. (1995), "A Multicriteria Approach to Dynamic Optimization," *In American Control Conference*, pp. 1767-1771, Seattle, WA.

Srinivasan, B., Palanki S., Bonvin D. (2003a), "Dynamic Optimization of Batch Processes I. Characterization of the Nominal Solution," *Computers and Chemical Engineering*, Vol. 27, pp. 1-26.

Stoer J. and Bulirsch R. (2002), "*Introduction to Numerical Analysis*," 3rd ed., Springer.

Strom-Tejsen J., Yeh H.Y.H., Moran D. (1973), "Added Resistance in Waves", *Transactions of the SNAME*, Vol. 81, pp. 109–143.

Süli E., Mayers D. (2003), "*An Introduction to Numerical Analysis*," Cambridge University Press.

Sun L., Gai L., Smith R. (2017), "Site Utility System Optimization with Operation Adjustment Under Uncertainty", *Applied Energy*, Vol. 186, pp. 450–456.

Tanartkit P., Biegler L.T. (1995), "Stable Decomposition for Dynamic Optimization," *Industrial and Engineering Chemical Research*, Vol. 34, pp. 1253-1266.

Tantar A.A., Tantar E., Bouvry P. (2010), "Design and Classification of Dynamic Multi-Objective Optimization Problems," *GECCO '11 Proceedings of the 13th Annual Conference Companion on Genetic and Evolutionary Computation*, Dublin, Ireland.

Tantar A.A., Tantar E., Bouvry P. (2011), "A Classification of Dynamic Multi-Objective Optimization Problems," *GECCO '11 July 12-16, 2011*, Dublin, Ireland.

Thomson W. (Lord Kelvin) (1879), "On Gravitational Oscillations of Rotating Water", *Proceedings of Royal Society*, Edinburgh, Vol. 10, pp. 92–100.

Toffolo A. (2014), "A Synthesis/Design Optimization Algorithm for Rankine Cycle Based Energy Systems", *Energy*, Vol. 66, pp. 115-127.

Toth P., Vigo D. (2001), "*The Vehicle Routing Problem*," SIAM Monographs on Discrete Mathematics and Applications, Philadelphia.

Tsang T.H., Himmelblau D.M., Edgar T.F. (1975), "Optimal Control via Collocation and Nonlinear Programming," *International Journal of Control*, Vol. 21, No. 5, pp. 763-768.

Tsujimoto M., Shibata K., Kuroda M., Takagi K. (2008), "A Practical Correction Method for Added Resistance in Waves", *Japan Society of Naval Architects and Ocean Engineers*, Vol. 8, pp. 177–184.

Vallianou V.A. (2009), "*Dynamic Operation Optimization of a Cogeneration System,*" Diploma Thesis, School of Naval Architecture and Marine Engineering, National Technical University of Athens (in Greek).

Vallianou V.A., Frangopoulos C.A. (2012), "Dynamic Operation Optimization of a Trigeneration System," *International Journal of Thermodynamics*, Vol. 15, No. 4, pp. 239-247.

Vassiliadis V.S. (1993), "*Computational Solution of Dynamic Optimization Problems with General Differential-Algebraic Constraints*," Ph.D thesis, University of London.

Vassiliadis V.S., Sargent R.W.H., Pantelides C.C. (1994a), "Solution of a Class of Multistage Dynamic Optimization Problems. 1. Problems without Path Constraints," *Industrial and Engineering Chemistry Research*, Vol. 33, No. 9, pp. 2111-2122.

Vassiliadis V.S., Sargent R.W.H., Pantelides C.C. (1994b), "Solution of a Class of Multistage Dynamic Optimization Problems. 2. Problems with Path Constraints," *Industrial and Engineering Chemistry Research*, Vol. 33, No. 9, pp. 2123-2133.

Vassilopoulos L.A. (1967), "The Application of Statistical Theory of Nonlinear Systems to Ship Motion Performance in Random Seas", *International Shipbuilding Progress*, Vol. 14, No 150.

Wang K., Yan X., Yan Y., Jiang X., Lin X., Negenborn R.R. (2018), "Dynamic Optimization of Ship Efficiency Considering Time-varying Environmental Factors", *Transportation Research*, Vol. 62, Part D, pp 685-698.

Wang M., Kim K.,von Spakovsky M., Nelson D. (2008), "Multi- versus Single- level of Dynamic Synthesis/Design and Operation/Control Optimizations of a PEMFC System", *Proceeding of IMECE2008, 2008 ASME International Mechanical Engineering Congress and Exposition*, October 31–November 6, 2008, Boston, Massachusetts.

Wang Z., Guo B. (2012), "Legendre-Gauss-Radau Collocation Method for Solving Initial Value Problems of First Order Ordinary Differential Equations," *Journal of Scientific Computing*, Vol. 52, pp. 226–255.

Wartsila (2014), Last accessed 2014. https://www.wartsila.com/products/.

Weicker, K. (2002), "Performance Measures for Dynamic Environments," *Parallel Problem Solving from Nature – PPSN*, Vol. II, pp. 64–73, Berlin: Springer.

Wozny G., Li P. (2000), "Planning and Optimization of Dynamic Plant Operation," *Applied Thermal Engineering*, Vol. 20, pp. 1393-1407.

Xin Y., Yaochu J., Ke T., Xin Yao (2010), "Robust Optimization Over Time – A New Perspective on Dynamic Optimization Problems," *WCCI 2010 IEEE World Congress on Computational Intelligence*, Barcelona, Spain.

Yourgrau W., Mandelstam S. (1968), "*Variational Principles in Dynamics and Quantum Theory*," Saunders, Philadelphia, 1968.

Yu Y.B., Wang Q.N., Min H.T., Wang P.Y., Hao C.G. (2009), "Control Strategy Optimization using Dynamic Programming Method for Synergetic Electric System on Hybrid Electric Vehicle," *Natural Science*, Vol. 1, No. 3, pp. 222-228.

Zaccone R., Ottaviani E., Figari M., Alosole M. (2018), "Ship Voyage Optimization for Safe and Energy-efficient Navigation: A Dynamic Programming Approach", *Ocean Engineering*, Vol. 153, pp. 215-224.

Zeng Q., Zhang B., Fang J., Chen Z. (2017), "A bi−level Programming for Multistage Co−expansion Planning of the Integrated Gas and Electricity System", *Applied Energy*, Vol. 200, pp. 192−203.

Zhen L., Wang S., Zhuge D. (2017), "Dynamic Programming for Optimal Ship Refueling Decision", *Transportation Research*, Vol. 100, Part E, pp. 63-74.

Zhu Q., Luo X., Zhang B., Chen Y. (2017), "Mathematical Modeling and Optimization of a Large−scale Combined Cooling, Heat and Power System that Incorporates Unit Changeover and Time−of−use Electricity Price", *Energy Conversion and Management*, Vol. 133, pp. 385−398.

PUBLICATIONS

Frangopoulos C.A., Tzortzis G.J. (2012), "Types of Problems and Corresponding Solution Methods for Dynamic Optimization of Energy Systems", *3rd International Conference on Contemporary Problems of Thermal Engineering*, CPOTE 2012, 18-20 September 2012, Gliwice, Poland.

Tzortzis G.J., Frangopoulos C.A. (2015), "Optimization of ship speed profile along a route under variable weather conditions", *28th International Conference on Efficiency, Cost, Optimization, Simulation and Environmental Impact*, ECOS 2015, 29 June-3 July, 2015, Pau, France.

Frangopoulos C.A., Sakalis G.N., Tzortzis G.J. (2016), "Intertemporal and Dynamic Optimization of Synthesis, Design and Operation of Energy Systems", *4th International Conference on Contemporary Problems of Thermal Engineering*, CPOTE 2016, 14−16 October, 2016, Katowice, Poland.

Tzortzis G.J., Frangopoulos C.A. (2018), "Dynamic Optimization of Synthesis, Design and Operation of Marine Energy Systems", *Proceedings of the Institution of Mechanical Engineers, Part M: Journal of Engineering for the Maritime Environment*, pp. 1–20. DOI:10.1177/1475090217749370.